WASM: Minerals, Energy, and Chemical Engineering

Recovery of Gold and Copper from Alkaline Cyanide-Starved Glycine Solutions Using Sulfide Precipitation and Ion-Exchange

Zixian Deng
0000-0001-5079-5487

This thesis is presented for the Degree of
Doctor of Philosophy (Mining and Metallurgical Engineering)
of
Curtin University

February 2021

Author's Declaration

I, the undersigned, hereby declare that all the research outcomes contained in this thesis are my original work and all the materials are not previously published by any other person or university for a degree.

Name: …Zixian Deng……

Signature: ……

Date: …21/11/2020……

Abstract

As the cyanide leachable free-milling resources are depleted, a large portion of gold is now produced from complex gold ores accompanied by reactive copper minerals. Those copper-bearing gold ores have become important resources for gold and copper and they are reserved in a great number of deposits over the world. To extract gold from these resources, the traditional cyanidation process suffers to be an economic and effective approach, mainly because the reactive copper minerals significantly increase the cyanide consumption and a large amount of cyanide have to be used to achieve an acceptable level of gold extraction. Although there are other alternative techniques specifically designed for gold extraction from copper-gold ores such as the ammonia-cyanide, ammonia-thiosulfate leach system, these methods were not commonly applied in the industry due to the issues such as the complex chemistry and complicated process control.

A novel glycine-based leach system was recently developed and patented at Curtin University, Western Australia. Glycine leaching process has been proved to be effective for copper and gold extraction. The synergistic glycine-cyanide system that can be used in traditional tank leach operations is particularly effective for treating copper-gold resources. To further improve this process and pave the way to scale-up the process from bench-scale to pilot-scale testing, the feasibilities of downstream metals recovery technologies were studied and evaluated. Sulfide precipitation and ion-exchange resins were used for gold and copper recovery from the cyanide-starved glycine solutions.

From the sulfide precipitation study, it was found that sulfide precipitation can effectively recover 100% of Cu^{2+} from the cyanide-starved glycine solutions using NaHS. The precipitation behaviours were stable with no or a very small amount of Cu^{+} and Au being co-precipitated at most of the precipitation conditions tested. Pre-oxidation of Cu^{+} to Cu^{2+} using peroxide confirmed the effects of oxidation state on copper precipitation and a high total Cu recovery of about 96.5% was achieved after pre-oxidation. No gold co-precipitation and no significant glycine oxidation was observed after peroxide pre-oxidation.

The sulfide precipitate characteristics study revealed that additions of Ca^{2+} or increase of solution ionic strength can enhance the formation of coarse and settable particles. The lower supersaturation level has insignificant effects on the particle

size distributions (PSD). Relatively large particle size is generated at medium stirring speed with fast addition rate. No significant effects of ageing, heating, and seeding on the PSD, but these factors can affect the morphologies of the individual particles based on the SEM images. XRD results implied that a more mature and crystalline copper sulfide precipitates can be produced by ageing, heating, or seeding.

The Cu adsorption by ion-exchange resins studies indicated that the Puromet MTS9300 resin is more efficient than the other types of chelating resins, due to its high selectivity towards Cu^{2+} over Cu^{+} and Au. Over 99% of Cu^{2+} recovery with almost zero Cu^{+} and Au recovery was achieved by using the MTS9300 resin. The copper results were fitted well to both the empirical Freundlich and Langmuir isotherm models, while the Langmuir model shows a better correlation coefficient. The adsorption kinetic data of Cu^{2+} is well fitted to the pseudo-second-order model. Alkaline glycine solutions in the presence of NaCl or HCl can be used for the resin elution. The multi-cycle tests demonstrated that the loading capacity, regeneration efficiency and desorption efficiency were not significantly changed after regeneration. From the SEM images, no significant changes of resin's shape and surface morphology was observed, although more cracks and rifts were found after the multi-cycle tests.

The adsorption behaviours of gold using gold-selective resin were studied. A novel molecularly imprinted resin (IXOS-AuC) with a better selectivity towards gold against copper was chosen for further investigations. It was found that the factors such as cyanide to total copper ($[CN^-]$:$[Cu_T]$) and glycine to total copper ([Gly]: $[Cu_T]$) molar ratios have insignificant effects on the adsorption of gold and copper. Increasing the initial gold concentration decreased with the copper co-adsorption on the resin. The equilibrium and kinetics studies were carried out with the experimental adsorption data being fitted to the Freundlich model and pseudo-second-order model. The copper can be selectively pre-eluted over gold from the loaded resin by 0.4M NaCN at pH 11.5, while gold can be effectively eluted by either acidic thiourea or alkaline thiocyanate. The multi-cycle adsorption/elution tests showed that the resin can be effectively regenerated in both acidic thiourea and alkaline thiocyanate system. The change of surface morphology of the resin was not significant after adsorption/regeneration according to the SEM analysis.

Acknowledgements

I would like to express my gratefulness to many people who have given me academic and mental support during the three-year PhD candidacy. Without their assistance, this research work could not be progressed so smoothly and successfully.

Firstly, I would like to express my sincere gratitude to my supervisors Prof. Jacques Eksteen and Dr Elsayed Oraby for the continuous support of my PhD study and related research, for their patience and encouragement. I appreciate their guidance, mentorship and insightful comments in planning experiments, and analysing the results and comments during the compilation of journal papers.

My sincere gratitude would go to the staff working in the Gold Technology Group for their assistance and support, particularly Mr Jim Cupitt, for his guidance regarding health and safety, Ms Karen Barbetti, for her support in calibrating the AAS at the time and Ms Irlina Winata, for her guidance and help in laboratory work.

I would like to thank my fellow doctoral students, Mr Huan Li, Ms Ndagha Mkandawire and Dr Peo Tauetsile and Dr Mojtaba Saba for their feedback, cooperation and of course friendship.

I would acknowledge with thanks the financial support from Curtin University, Newcrest Mining, Mining and Process Solutions Pty Ltd (MPS) and Australian Research Council (ARC). The research was predominantly funded through the ARC Linkage Grant, supported by Newcrest Mining and MPS, through the grant no. LP160101121.

Lastly, I would like to express my deepest appreciation to my families, my mom and my dad who love me so much with selfless dedications for my life. I am particularly grateful to my beloved and supportive wife Shushu Zhang who is always by my side and always loves me with heart and soul, and my adorable cat, Romeo, who always comforts me with his purr.

List of Publication included as part of the thesis

All the tests were conducted and all the manuscripts were written by the PhD student. The main body thesis has consisted of the following peer-reviewed published paper:

Deng, Z., Oraby, E. A., & Eksteen, J. J. (2019). The sulfide precipitation behaviour of Cu and Au from their aqueous alkaline glycinate and cyanide complexes. *Separation and Purification Technology, 218*, 181-190.

Deng, Z., Oraby, E. A., & Eksteen, J. J. (2020). Sulfide precipitation of copper from alkaline glycine-cyanide solutions: Precipitate characterisation. *Minerals Engineering, 145*, 106102.

Deng, Z., Oraby, E. A., & Eksteen, J. J. (2020). Cu adsorption behaviours onto chelating resins from glycine-cyanide solutions: Isotherms, kinetics and regeneration studies. *Separation and Purification Technology, 236*, 116280.

Deng, Z., Oraby, E.A., Eksteen, J.J. (2020). Gold recovery from cyanide-starved glycine solutions in the presence of Cu using a molecularly imprinted resin (IXOS-AuC). *Hydrometallurgy, 196*,105425

Statement of contributions of others

The PhD candidate conceived, planned and conducted all the experiments, collected, organised, processed and interpreted all the experimental data and is the primary author of the manuscript of all four journal articles which form the main body of this thesis. Prof. Jacques Eksteen and Dr Elsayed Oraby provided insightful comments and constructive feedback throughout the research, assisting in results analysis and interpretation, edition and revision of the manuscripts. Co-authors have permitted the published papers to be included in this thesis. A signed statement of the contributions of each co-author to the published works arising from this thesis is attached in Appendix A at the back of this volume.

Dedication

This work is dedicated to my beautiful wife, Shushu Zhang, my mom, my dad, my mother-in-law, my father-in-law, my cat, Romeo and my coming son who mean so much to me. I love you all and I appreciate that you are all being with me and always support and love me wholeheartedly.

Table of Contents

List of Figures

List of Tables

Chapter 1: Introduction and overview

1. 1 General background

Gold, the most valuable metal in history, was first leached from its ores using Aqua Regia (a mixture of nitric and hydrochloric acids), where the mechanism is due to chlorine and nitrosyl chloride. In 1851, Karl Friedrich Plattner first used aqueous solutions of chlorine to leach and recover gold from its ores. This process was known as chlorination which was later introduced in gold mines in America and Australia (Adams, 2016).

In the 1880s, cyanidation process was patented and employed in gold mining industry and it superseded other processes for gold extraction worldwide as it is relatively simple, efficient and economic (La Brooy et al., 1994). Cyanide is an effective lixiviant for gold dissolution owing to the strong bond between cyanide and gold, creating high stability of gold cyanide complexes. The oxidant of cyanidation is dissolved oxygen from the air, contributing to a great attractiveness of cyanidation process (Marsden & House, 2009). Annually, approximately one billion tons of gold sources are treated in the world using cyanidation process to extract gold, it is also the largest tonnage of any kind of ore that is treated chemically (Adams, 2016).

Although cyanide can effectively leach gold from a wide range of ores, some kind of ores may not respond well to the conventional cyanidation process. In some cases, reactive minerals especially copper minerals can consume cyanide in side reactions, thus increasing the consumption of cyanide/or oxygen to extract gold (La Brooy et al., 1994). It is estimated that a large portion of gold extracted in the 21st century will be recovered from cyanide soluble copper minerals due to the declining resources of free milling cyanide extractable gold deposits (Dai et al., 2011). It is reported that a majority of the copper minerals are highly soluble by cyanide including copper oxides, carbonates, sulfides (except for chalcopyrite), and native copper. The dissolution of reactive copper in cyanide solutions can incur an extra consumption of cyanide by forming copper cyanide complexes with high stability such as $Cu(CN)_2^-$, $Cu(CN)_3^{2-}$, and $Cu(CN)_4^{3-}$, with the sulfide sulfur component leading to the formation of thiocyanate (CNS^-) and iron (in copper sulfides such as chalcopyrite leading to ferrocyanide ($Fe(CN)_6^{4-}$), leading to high cyanide

consumption. It is reported that different kinds of copper minerals associated with gold can be dissolved by cyanide to different degree from 5% –10% for chalcopyrite to over 90% for most oxide minerals; around 30kg/t NaCN is required to leach 1% of reactive copper minerals which leads to conventional cyanidation to extract gold-copper ores uneconomic (Muir, 2011). Also, the Weak Acid Dissociable (WAD) cyanide are required to be detoxified at a significant expense (Marsden & House, 2009), all these factors can make the processes uneconomic. Besides, the presence of copper in the leachate can cause problems for the recovery processes such as co-absorption with gold onto the activated carbon or ion-exchange, reduction of gold electrowinning cell efficiency and gold losses onto copper minerals by cementation (Dai et al., 2011).

To selectively leach gold from gold-copper ores, an ammonia-cyanide leaching system which was first discovered and patented by Hunt has been intensively studied since 1901 (Adams et al., 2008; Costello et al., 1992; La Brooy et al., 1991). This technique was further studied and optimised with typical results of around 70% –80% gold and 3% copper recovery using 2.5 – 5 kg/t NaCN and 1.1 kg/t NH_3 (Muir, 2011). In the 1990s, it was developed further and two commercial plants operated to treat oxidized copper tailings for a few years in Western Australia and Mauritania (Costello et al., 1992; Ruane, 1991). However, this process is not suitable for treating sulfidic ores where higher reagents concentrations are required and poorer gold recovery is usually obtained. Also, ammonia is volatile and toxic which may generate environmental concerns.

A thiosulfate-copper-ammonia leaching system which is more advantageous than that of cyanide in terms of lower toxicity and higher gold leaching rate was also considered as a feasible alternative process to treat gold-copper ores. However, as the difficulty in maintaining it stable under variable Eh/pH environments, the application becomes expensive and uneconomic in the gold industry (Breuer & Jeffrey, 2000).

Recently, Gold Technology Group from Curtin University developed and patented a novel leaching method using an environmental-benign glycine as the alternative lixiviant to leaching copper and gold from its ores and flotation concentrates. Glycine, the simplest type of amino acid, has a number of advantages over cyanide. For example, it is a colourless sweet-tasting crystalline solid without toxicity and volatility which is environmentally friendly; it is accessible and economically

effective that can be manufactured industrially or derived as a by-product from different micro-organisms (González-López et al., 2005); the gold and copper glycinate complexes have good stability (Ksp = 18) over a wide pH-Eh range that can be regenerated after leaching (Eksteen & Oraby, 2015). Glycine as the only lixiviant is effective in leaching copper including metallic copper, copper oxides (e.g. azurite, cuprite, malachite) and copper sulfide (e.g. chalcocite) (Eksteen, et al., 2017; Tanda, et al., 2017). Gold can be also leached by the glycine as the only lixiviant, but the leaching rate is significantly slower than that of cyanide even at elevated temperatures of around 50℃ – 60 ℃, which is application may only be suitable for in-situ or heap leaching (Oraby & Eksteen, 2015b), unless other catalysts or oxidants are used, where the suitability depends upon the ore treated.

A synergistic leaching system was also developed using glycine as the main lixiviant with a small portion of cyanide (i.e. cyanide is at "starvation" conditions and no free cyanide is present in the leachate at any time) at alkaline conditions is shown high efficiency and effectiveness in leaching gold from gold-copper ores and flotation concentrates at room temperature with a fast gold dissolution rate and a significant reduction of cyanide consumption (Oraby & Eksteen, 2015; Oraby et al., 2017). The typical final leaching solutions from the synergistic leaching system contain gold cyanide and gold glycinate compounds with mostly cupric glycinate, a small amount of cuprous cyanide species and zero free cyanide, which in some extend simplifies the detox process. This technique has attracted many attentions from the industry, it is, therefore, important to explore different recovery methods for the glycine-cyanide synergistic leaching system and further improve the process.

Carbon adsorption as the most commonly used gold recovery method in the gold industry, its application has been proved to be feasible and effective for gold recovery from both the glycine only and glycine-cyanide leaching system and its adsorption isotherms and kinetics were studied in detail (Tauetsile et al., 2018a, 2018b, 2019a, 2019b). However, co-adsorption of copper may have an adverse effect on the gold adsorption capacity of the activated carbon, a copper removal/recovery process is required prior to the carbon adsorption.

Studies conducted by Tanda(2017) and Eksteen et al. (2018) pointed out that copper can be precipitated effectively from the non-cyanide cupric glycinate leachate by adding NaHS powders. This implies that sulfide precipitation could be a feasible

method to recover the copper from the glycine-cyanide leachate containing cupric glycinate and cuprous cyanide.

Tanda et al. (2017) successfully used solvent extraction technique to recover the copper from cupric glycinate in the glycine only leaching system. This provides another approach which is using ion-exchange resins to recover the metal ions from the glycine-cyanide leachate, as ion exchange is usually compared with solvent extraction (Kim et al., 2016; Li et al., 2013).

1.2 Objective and significance of the study

The leaching side of the novel glycine technology has been intensively studied, however the downstream of metals recovery from solutions has not been addressed. Therefore, this project aims to explore and investigate the downstream options of copper and gold recovery from starved-cyanide glycine solutions. Sulfide precipitation and ion exchange resins as two promising and well-known methods for copper and gold are deeply studied and evaluated in this research project. To be more specific, the study aims to:

- Investigate the effectiveness of sulfide precipitation for the copper recovery and gain insight into the precipitation chemistry;
- Study the precipitates characteristics and understand the factors that affect the final size of the precipitates and its purity;
- Explore the feasible ion-exchange resins including chelating resins and novel molecularly imprinted resin for copper and gold recovery and conduct adsorption isotherm and kinetic studies;
- Propose effective eluting agents for the selected resins and verify their reusability through multi-cycle adsorption/desorption tests.

This project is a linkage study for the synergetic glycine-cyanide leaching system which is highly significant for some mining companies which require innovative solutions to minimize the cyanide consumption and mitigate the production of Weak Acid Dissociable (WAD) cyanide which can impose threats to health and the environment. Successfully achieving the above aims could impose constructive and meaningful influences on the gold industry. Specifically, it would gain a deeper understanding and provide a theoretical basis for the application of sulfide precipitation and ion-exchange adsorption from the synergetic glycine-cyanide leaching system; expand more recovery methods and provide more clear ideas for

designing process flowsheets; eventually, improve the performance of the leaching system; pave the way to scale-up from bench-scale to pilot-scale testing and eventually accelerate the process to be commercialised.

1.3 Scope of the study

This project mainly included a range of fundamental studies related to the discipline of hydrometallurgy. The first part of the study focused on the copper recovery by sulfidation, the effects of various factors on the precipitation chemistry were investigated. The second part addressed how different chemical and operational conditions influence the size of the precipitates as well as the setting performance. Scan Electron Microscope (SEM) and X-ray Diffraction (XRD) analysis were conducted to understand how crystals evolved and transformed under different operational conditions. The third/fourth part of the study investigated the adsorption behaviours of copper/gold by using different types of ion-exchange resins and selected the most selective resins for further investigations. The adsorption isotherms and kinetics studies were covered for both the selected copper-selective and gold-selective resins. Elution and regenerated studies were included for both resins. The surface morphology of the resin before and after adsorption/regeneration were visualised by SEM.

It should be noted that demonstrations of the recovery methods for copper and gold are limited to the hydrometallurgy performance obtained from the synthetic glycine-cyanide leachates. The recovery performance from the real leachates is out of the scope of this study.

1.4 Thesis overview

This thesis is written in compliance with the specific guidelines for the thesis by publication and copyright policies of Curtin University. The experimental design including materials and methods for the study were demonstrated and explained in the attached published papers. The thesis consists of 7 Chapters. The overview of each chapter is given below:

Chapter 1: Introduction and overview

Chapter 1 covers an introduction and overview of the study. It includes general background, objective and significance, scope and thesis overview. The chapter

points out the research gaps in scientific knowledge and gives the readers a general outline of the research.

Chapter 2: Literature review

Chapter 2 provides the literature review of the hydrometallurgical approaches for gold/copper extraction/recovery from copper-gold ores. It highlighted the copper-gold deposits are essential resources for either copper or gold and mentioned the significance of the applications of copper and gold to human societies. Different current techniques for leaching gold from copper-gold resources were discussed. This was followed by a review of an innovative glycine-based leach system including glycine-only and synergetic glycine-cyanide system. The last section of chapter 2 introduced a variety of techniques for copper and gold recovery (i.e. solvent extraction, sulfide precipitation, zinc cementation, carbon adsorption, and ion-exchange resin adsorption).

Chapter 3: Sulfide precipitation behaviour of copper and gold

Chapter 3 (Published paper 1, Deng et al., 2019) demonstrates the sulfide precipitation behaviour of copper and gold from the alkaline glycine-cyanide solutions. Effects of reaction time, pH, temperature, $[HS^-]$: $[Cu_T]$, [Gly]:$[Cu_T]$, $[CN^-]$: $[Cu_T]$ molar ratios on the Cu_T recovery were studied. Pre-oxidation of Cu^+ to Cu^{2+} was also studied, and the precipitation behaviours of Cu_T at different levels of dissolved oxygen, $[HS^-]$: $[Cu_T]$ molar ratios and reaction time after precipitation were investigated. Glycine analysis was conducted to verify whether the glycine was oxidised during the pre-oxidation stage or not.

Chapter 4: Sulfide precipitates characteristics

Chapter 4 (Published paper 2, (Deng et al., 2020b)) elaborates the effects of different chemical and operational conditions on the precipitate particle characteristics particularly the particle size distributions (PSD). Factors affecting on settling characteristics, particle morphologies and particle structure were also studied.

Chapter 5: Copper adsorption using ion-exchange chelating resins

Chapter 5 (Published paper 3, (Deng et al., 2020a)) presents a copper recovery method from glycine-cyanide solutions by using chelating resins. The chapter covers how different factors (i.e. [Gly]:[Cu], $[CN^-]$: [Cu] molar ratios and resin dosage) effect on the resin adsorption of copper and gold. In this chapter, the

adsorption isotherms and kinetics of the copper adsorbed onto the resin were studied and their experimental data were fitted to commonly used isotherm (Freundlich and Langmuir models) and kinetic (pseudo-first-order, pseudo-second-order and intra-particle) models. Elution tests using alkaline glycine as the eluent were conducted and compared to the conventional acid elution method. Regeneration studies were carried out to confirm whether the resin can be effectively reused or not.

Chapter 6: Gold adsorption and regeneration studies using a molecularly imprinted resin (IXOS-AuC)

Chapter 6 (Published paper 4, Deng et al., 2020c) investigates the copper and gold adsorption behaviours of a type of molecularly imprinted resin (IXOS-AuC). The effects of different [Gly]:[Cu], [CN^-]:[Cu] molar ratios and initial gold concentration on the adsorption of gold and copper on the resin were investigated. Adsorption isotherms and kinetics tests were carried out, with their experimental data being fitted with commonly used adsorption isotherm (Freundlich and Langmuir models) and kinetic (pseudo-first-order and pseudo-second-order) models. Two-stage elution tests were conducted, where cyanide was used at the first stage for copper elution and acidic thiourea or alkaline thiocyanate were used for the second stage for gold elution. Regeneration studies for both the acidic thiourea and alkaline thiocyanate elution system were carried out.

Chapter 7 Conclusions and recommendations

Chapter 7 gives the overall and enumerated conclusions based on the results obtained in this research study. Recommendations for future research studies are also outlined at the end of the chapter.

1.5 Reference

Adams, M., D. (2016). Gold ore processing: project development and operations / edited by Mike D. Adams (2nd ed.): Amsterdam, [Netherlands]: Elsevier.

Adams, M., Lawrence, R., & Bratty, M. (2008). Biogenic sulphide for cyanide recycle and copper recovery in gold–copper ore processing. *Minerals Engineering, 21*(6), 509-517. https://doi.org/10.1016/j.mineng.2008.02.001

Breuer, P. L., & Jeffrey, M. I. (2000). Thiosulfate leaching kinetics of gold in the presence of copper and ammonia. *Minerals Engineering, 13*(10), 1071-1081. https://doi.org/10.1016/S0892-6875(00)00091-1

Costello, M. C., Ritchie, I. C., & Lunt, D. J. (1992). Use of the ammonia cyanide leach system for gold copper ores with reference to the retreatment of the torco tailings. *Minerals Engineering, 5*(10), 1421-1429. https://doi.org/10.1016/0892-6875(92)90176-A

Dai, X., Simons, A., & Breuer, P. (2011). A review of copper cyanide recovery technologies for the cyanidation of copper containing gold ores. *Minerals Engineering*. doi:10.1016/j.mineng.2011.10.002

Deng, Z., Oraby, E. A., & Eksteen, J. J. (2019). The sulfide precipitation behaviour of Cu and Au from their aqueous alkaline glycinate and cyanide complexes. *Separation and Purification Technology, 218*, 181-190. https://doi.org/10.1016/j.seppur.2019.02.056

Deng, Z., Oraby, E. A., & Eksteen, J. J. (2020a). Cu adsorption behaviours onto chelating resins from glycine-cyanide solutions: Isotherms, kinetics and regeneration studies. *Separation and Purification Technology, 236*, 116280. https://doi.org/10.1016/j.seppur.2019.116280

Deng, Z., Oraby, E. A., & Eksteen, J. J. (2020b). Sulfide precipitation of copper from alkaline glycine-cyanide solutions: Precipitate characterisation. *Minerals Engineering, 145*, 106102. https://doi.org/10.1016/j.mineng.2019.106102

Deng, Z., Oraby, E.A., Eksteen, J.J. (2020c). Gold recovery from cyanide-starved glycine solutions in the presence of Cu using a molecularly imprinted resin (IXOS-AuC). *Hydrometallurgy, 196*,105425

Eksteen, J. J., & Oraby, E. A. (2015). The leaching and adsorption of gold using low concentration amino acids and hydrogen peroxide: Effect of catalytic ions, sulphide minerals and amino acid type. *Minerals Engineering, 70*, 36-42. https://doi.org/10.1016/j.mineng.2014.08.020

Eksteen, J. J., Oraby, E. A., & Tanda, B. C. (2017). A conceptual process for copper extraction from chalcopyrite in alkaline glycinate solutions. *Minerals Engineering, 108*, 53-66. https://doi.org/10.1016/j.mineng.2017.02.001

Eksteen, J. J., Oraby, E. A., Tanda, B. C., Tauetsile, P. J., Bezuidenhout, G. A., Newton, T., Bryan, I. (2018). Towards industrial implementation of glycine-based leach and adsorption technologies for gold-copper ores. *Canadian Metallurgical Quarterly, 57*(4), 390-398. https://doi.org/10.1080/00084433.2017.1391736

González-López, J., Rodelas, B., Pozo, C., Salmerón-López, V., Martínez-Toledo, M. V., & Salmerón, V. (2005). Liberation of amino acids by heterotrophic nitrogen fixing bacteria. *Amino Acids, 28*(4), 363-367. doi:10.1007/s00726-005-0178-9

Kim, H., G. Eggert, R., W. Carlsen, B., & W. Dixon, B. (2016). Potential uranium supply from phosphoric acid: A U.S. analysis comparing solvent

extraction and Ion exchange recovery. *Resources Policy, 49*(C), 222-231. https://doi.org/10.1016/j.resourpol.2016.06.004

La Brooy, S. R., Komosa, T., & Muir, D. M. (1991). Selective leaching of gold from copper-gold ores using ammonia-cyanide mixtures. Paper presented at the 5th Extractive Metallurgy Conference - AusIMM 1991, Perth.

La Brooy, S. R., Linge, H. G., & Walker, G. S. (1994). Review of gold extraction from ores. *Minerals Engineering, 7*(10), 1213-1241. doi:10.1016/0892-6875(94)90114-7

Li, W., Zhang, Y., Liu, T., Huang, J., & Wang, Y. (2013). Comparison of ion exchange and solvent extraction in recovering vanadium from sulfuric acid leach solutions of stone coal. *Hydrometallurgy, 131-132*, 1-7. https://doi.org/10.1016/j.hydromet.2012.09.009

Marsden, J. O. (2009). Chemistry of Gold Extraction (2nd ed.), Littleton: SME.

Muir, D. M. (2011). A review of the selective leaching of gold from oxidised copper–gold ores with ammonia–cyanide and new insights for plant control and operation. *Minerals Engineering, 24*(6), 576-582. https://doi.org/10.1016/j.mineng.2010.08.022

Oraby, E. A., & Eksteen, J. J. (2015). The leaching of gold, silver and their alloys in alkaline glycine–peroxide solutions and their adsorption on carbon. *Hydrometallurgy, 152*(C), 199-203. https://doi.org/10.1016/j.hydromet.2014.12.015

Ruane, M. (1991). Gold recovery from the Paris mine tailings using ammoniacal cyanide leachant. Paper presented at the Processing of Gold–Copper Ores Colloquium, Perth.

Tanda, B. C., Eksteen, J. J., & Oraby, E. A. (2017). An investigation into the leaching behaviour of copper oxide minerals in aqueous alkaline glycine solutions. *Hydrometallurgy, 167*, 153-162. https://doi.org/10.1016/j.hydromet.2016.11.011

Tanda, B. C., Oraby, E. A., & Eksteen, J. J. (2017). Recovery of copper from alkaline glycine leach solution using solvent extraction. *Separation and Purification Technology, 187*, 389-396. https://doi.org/10.1016/j.seppur.2017.06.075

Tauetsile, P. J., Oraby, E. A., & Eksteen, J. J. (2018a). Adsorption behaviour of copper and gold glycinates in alkaline media onto activated carbon. Part 1: Isotherms. *Hydrometallurgy, 178*, 202-208. https://doi.org/10.1016/j.hydromet.2018.04.015

Tauetsile, P. J., Oraby, E. A., & Eksteen, J. J. (2018b). Adsorption behaviour of copper and gold Glycinates in alkaline media onto activated carbon. Part 2: Kinetics. *Hydrometallurgy, 178*, 195-201. https://doi.org/10.1016/j.hydromet.2018.04.016

Tauetsile, P. J., Oraby, E. A., & Eksteen, J. J. (2019a). Activated carbon adsorption of gold from cyanide-starved glycine solutions containing copper. Part 1: Isotherms. *Separation and Purification Technology, 211*, 594-601. https://doi.org/10.1016/j.seppur.2018.09.024

Tauetsile, P. J., Oraby, E. A., & Eksteen, J. J. (2019b). Activated carbon adsorption of gold from cyanide-starved glycine solutions containing copper. Part 2: Kinetics. *Separation and Purification Technology, 211*, 290-297. https://doi.org/10.1016/j.seppur.2018.09.022

Chapter 2: Literature review

2.1 Gold-copper resources

2.1.1 Background

Free-milling (easily extracted through cyanidation) gold ores are nearly exhausted, occupying only 18% of the global gold deposits (Adams, 2016). Nowadays, much of the gold is produced from the refractory gold ores, many of which are accompanied by reactive copper minerals. A portion of the gold (14%) is also produced as a by-product from the smelting of copper concentrates (Adams, 2016). While due to the stricter regulations of sulfur dioxide and other toxic emissions from the smelting of copper sulfides, the application of hydrometallurgy is a now preferential option for the mining industry (Lakshmanan et al., 2016).

Porphyry deposits and iron-oxide-copper-gold (IOCG) deposits are the two main gold-copper resources in the world. The porphyry deposits are the major source of copper, accounting for nearly three-quarters of the world's copper and it is an important resource of gold which contains about one-fifth of the gold production worldwide (Sillitoe & Meinert, 2010). It is estimated that, according to the 2014 United State Geographical Survey (USGS), the discovered global copper deposits contain around 2.1 billion tons of copper (1.8 billion tons of those are porphyry copper deposits), while the undiscovered copper is about 3.5 billion tons. The survey also reported that about one-quarter of the unidentified gold resources were estimated to be contained in the porphyry copper deposits. Typical porphyry copper deposits contain about 0.5 to 1.5% of Cu, and 0.01 to 1.5g/t Au, although a few of them contain high grade of gold ranging from 0.9 to 1.5g/t with less than 0.1% of copper (Kesler, et al., 2002; Sillitoe & Meinert, 2010).

Alongside with porphyry deposit, iron-oxide-copper-gold deposits are also important resources of copper and gold, which have become the third producer of copper and a significant producer of gold since the discovery of supergiant Olympic Dam deposit in Australia in 1975 (Zhu, 2016). These types of deposits associated with copper minerals such as chalcopyrite, chalcocite and bornite and the gold is usually present in native gold, electrum and gold-bismuth-antimony-tellurium alloy. The copper grades of the IOCG deposits are similar to those of porphyry copper deposits, which are generally low, usually under 1%, with the gold grade at a low value (mostly below 1g/t) (Shaofeng & Shuixing, 2016; Zhu, 2016).

Fig. 2.1 shows the worldwide locations of major porphyry copper-gold and IOCG deposits which are modified based on several studies (Kesler et al., 2002; Pian & Santosh, 2019; Shaofeng & Shuixing, 2016; Sillitoe & Meinert, 2010; Zhu, 2016).

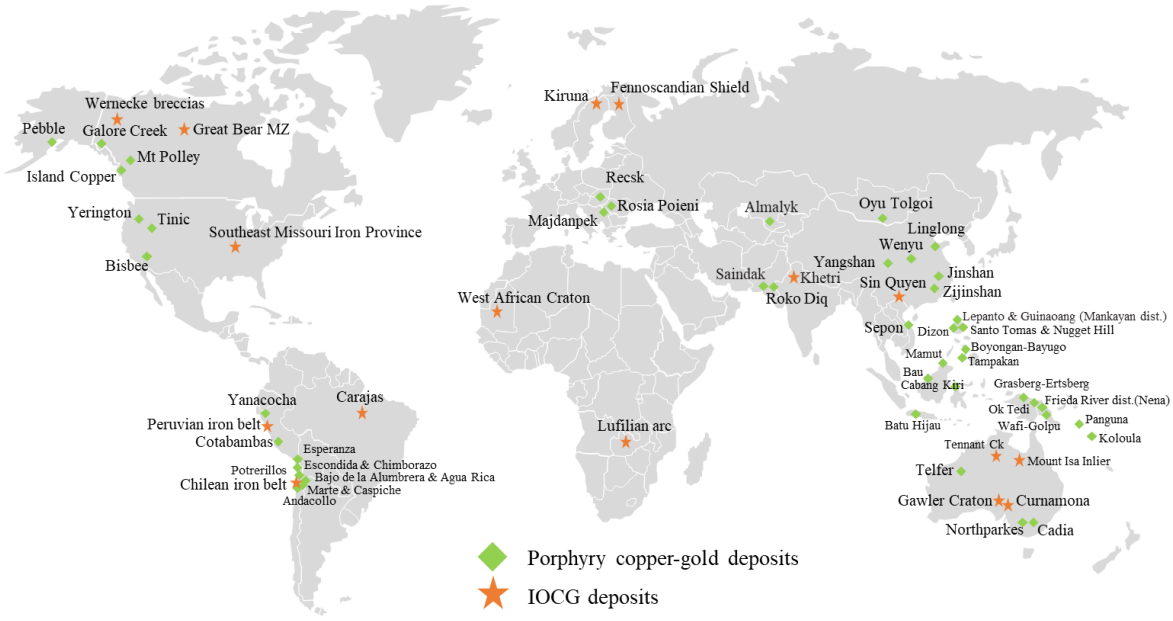

Figure 2.1 Geographical distribution of porphyry copper-gold ore and IOCG deposits worldwide modified based on Kesler et al. (2002); Pian and Santosh (2019); Shaofeng and Shuixing (2016); Sillitoe and Meinert (2010); Zhu (2016).

2.1.2 Significance of gold and copper

Gold has been valued by human beings from ancient times to the present days due to its beauty, usefulness and rarity. The market price of gold has risen significantly in the past two decades from about 300 USD/oz in 2000 to its highest point 1800 USD/oz in 2011, and the price fluctuated and ranged between 1,700 and 1,900 USD/oz in 2020 (peaking at nearly 2,050 USD /oz in early August 2020). The rising gold price has driven many mining companies to exploit more gold mines which were deemed to be difficult or expensive to mine and process.

Due to its lustrous colour and its resistance to tarnishing, gold was widely used as a currency before paper money was introduced. Gold is usually used as jewellery and other decorative ornaments due to its softness. It's the excellent conductivity and general resistance to oxidation and corrosion of gold leads to about 10% of the new gold produced worldwide goes to the industry for the manufacture of corrosion-free electrical connectors in electronic devices (Adams, 2016). Some recent technologies revealed that the application of gold nanoparticles can be extended to many other fields such as medicine, photonics and chemistry (Herb, 2013).

On the other hand, as the most common base metal, copper is one of the first metals that ever exploited and used by humans. Although the price of copper is much cheaper than gold, the consumption/demand of copper has increased significantly in the past two decades as large developing countries (e.g. China and India) entered the global market, seeking more mineral commodities for their infrastructure. The copper price has been rising consistently from about 0.6 USD per pound in 2000 to about 2.6 USD per pound in 2020.

Copper is an essential contributor to the progress and development of the societies since the dawn of civilisation. Since copper is easily stretched, moulded and shaped and due to its good resistance to corrosion, heat conductivity and electricity conductivity, copper is always important to people for a variety of domestic, industrial and high-technology applications. Copper is commonly used in building construction, power generation, transmission and distribution, electrical equipment and electronic circuitry, industrial machinery, transportation equipment, etc. Copper wiring and plumbing are the essential components for heating and cooling system, and telecommunications links in homes and business. Copper's outstanding conductivity improves the efficiency of electrical motors. Copper is used throughout the electric vehicles, charging stations and supporting infrastructure. It is foreseen that the consumption of copper will increase dramatically due to the energy challenges in terms of coal, oil and gas (Anonymous, 2016).

2.2 Current leaching processes for gold-copper ores

2.2.1 Cyanidation

Cyanide is the most commonly used lixiviant in the gold industry, mainly because of its relatively low cost, and superior effectiveness and efficiency for gold dissolution. Despite its toxicity and the risk of health and environmental concerns, it has been used for gold leaching for over a hundred year. Oxygen supplied from the air is used as the oxidant in cyanidation which is another attractiveness of the process. Eq. 1 is the most common equation for the dissolution of gold in the presence of cyanide and oxygen, which is also known as Elsner's Equation (Marsden & House, 2009).

$$4Au + 8NaCN + O_2 + 2H_2O \rightarrow 4NaAu(CN)_2 + 4NaOH \quad (1)$$

However, cyanidation is not economic when gold is associated with the copper mineralisation such as azurite, malachite, chalcocite, chalcopyrite, enargite,

covellite, cuprite and bornite as these reactive copper minerals can cause side reaction which consumes an extra amount of free cyanide and oxygen required for gold leaching (Sceresini & Breuer, 2016). Research has shown every 1% of reactive copper minerals consume around 30kg/t NaCN, leading to conventional cyanidation for extracting gold-copper ores uneconomic (Muir, 2011). If copper sulfide is present such as covellite, the consumption of cyanide can reach 51 kg/t, because of the formation of cyanate and thiocyanate (Sceresini, 2005). Statistical analysis has shown that gold recovery and copper consumption are linearly related to reactive copper content (i.e. metallic copper, copper oxides and secondary copper sulfides) (Jiang et al., 2001). The cyanide soluble copper minerals can form a series of copper cyanide complexes (CuCN, $Cu(CN)_2^-$, $Cu(CN)_3^{2-}$ and $Cu(CN)_4^{3-}$), depending on the cyanide to copper ratios pH and temperature (Wang & Forssberg, 1990). Their equilibria in cyanide solution are shown in Eq. 2 - 5 (Marsden & House, 2009).

$$Cu^+ + CN^- \leftrightarrow CuCN_{(s)} \quad (2)$$

$$CuCN + CN^- \leftrightarrow Cu(CN)_2^- \quad (3)$$

$$Cu(CN)_2^- + CN^- \leftrightarrow Cu(CN)_3^{2-} \quad (4)$$

$$Cu(CN)_3^{2-} + CN^- \leftrightarrow Cu(CN)_4^{3-} \quad (5)$$

According to the Eh-pH diagram shown in Figure 2.2, $Cu(CN)_3^{2-}$ is the most common cuprous cyanide species present under the typical cyanide leaching conditions. Thus, it may consume more cyanide if copper was not removed from the leach circuit, since the natural degradation of $Cu(CN)_3^{2-}$ to $Cu(CN)_2^-$, may deplete the free cyanide or weakly bond cyanide to form $Cu(CN)_3^{2-}$ and $Cu(CN)_4^{3-}$ (Marsden & House, 2009).

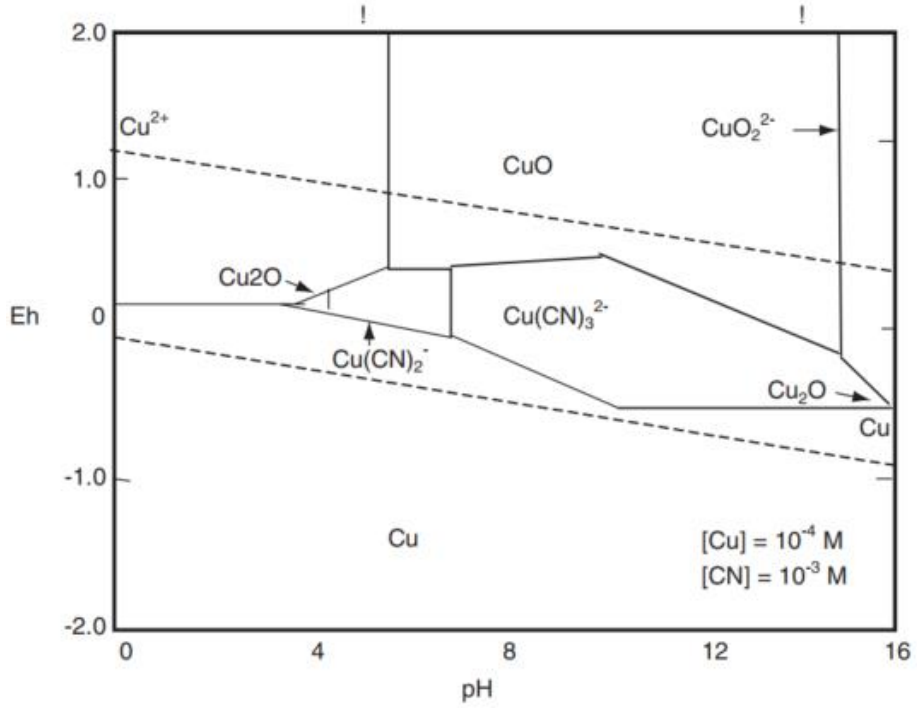

Figure 2.2 Eh-pH diagram of Cu-CN-H_2O system (CuCN is ignored) (Sceresini, 2005).

2.2.2 Ammonia-cyanide leaching

The typical copper-gold deposits can be either the copper deposits with significant levels of gold or the gold deposits contain a small amount of copper mineralisation which is normally present at nuisance levels to the gold deposits. For those copper dominated deposits, gold can be economically recovered as a by-product (slime) from the smelting and refining process. However, when copper present at nuisance levels, it can impose many adverse effects on the cyanide leaching process and the downstream recovery process (Jiang et al., 2001). To selectively leach gold from the copper-gold ores, an alkaline ammonia-cyanide leaching system was developed. Additionally, selective mining, flotation and pre-leaching of copper can also be effective methods to reduce the soluble copper before the leaching process.

The ammonia-cyanide leaching method which has been first developed and patented by Hunt (1901) for over a hundred year can leach the oxidised copper-gold ores selectively using ammonia to suppress the copper interference with up to 90% of Au recovery and less than 1 % of Cu recovery. This leaching process was revived by La Brooy et al. (1991), and it verified that the gold in oxidised ores can be selectively leached with a gold recovery between 80 and 90% at low reagent addition, while it was not effective to treat transition or sulfidic ores with poor gold recovery, even using higher reagent concentrations.

There are three important roles of ammonia in the ammoniacal cyanide leaching system. Firstly, a mixed copper-ammonia-cyanide complex ($Cu(NH_3)_2(CN)_2$) formed by the complexation between copper (I) ammonia and cyanide can leach gold. Secondly, copper (I) ammine can be rapidly oxidised by oxygen to copper (II), which provides extra oxidant for gold leaching, its effect is more apparent particularly in highly saline solutions where the dissolved oxygen (DO) concentration is very low. Thirdly, the ammonia promotes the precipitation of copper in the ammonia-cyanide solution by forming solid CuCN, $Cu(OH)_2$ or $Cu(NH_3)_2(CN)_4$. Eq. 6 shows the overall equation of gold leaching in the ammoniacal cyanide leaching system was a redox reaction which oxygen is not needed (Sceresini & Breuer, 2016).

$$Cu(NH_3)_2(CN)_2 + Au \rightarrow Cu(NH_3)_2^+ + Au(CN)_2^- \quad (6)$$

The optimum conditions are quite sensitive to the solution composition and reagent mixture. A study conducted by Muir et al. (1995) found that gold recovery can reach maximum value with the increasing concentration of NaCN and NH_3 at a fixed ratio of NaCN:NH_3, but this can also increase the copper recovery, which means a decrease in selectivity. Typically, about 1 – 2 kg/t NaCN and 1 – 2 kg/t NH_3 at pH between 10.5 and 11.0 and Eh between 350 – 400 mV (nHe) with 50% w/w solid ratio are deemed to be optimum (Dai et al., 2011).

During leaching, solid CuCN or $Cu(OH)_2$ can be slowly formed from the oxidation and precipitation of $Cu(CN)_2^-$ species, which may lead to a significant gold loss as the AuCN•CuCN precipitation, which was observed by Muir et al. (1989). Therefore, the Cu^{2+} concentration should be controlled at around 30 to 60 mg/L by controlling the ammonia concentration. Also, a solid-liquid separation stage is required to filter the precipitation of CuCN or $Cu(OH)_2$ before the gold recovery using activated carbon. Moreover, ammonia can be adsorbed by activated carbon, which may result in a loss in reagent during the circuit (Dai et al., 2011). To control the optimum conditions and speciation, it is important to monitor and control Eh, pH, or total NH_3 addition, Cu^{2+}, total Cu and total CN^- using electrodes and spectrophotometric, electrochemical or auto-titration methods (Dai et al., 2011). For example, constant incremental addition of ammonia is required to make up for the volatile loss; pre-oxidation of the reactive sulfide minerals is usually required to maintain the Cu^{2+} concentration.

In a word, the ammonia-cyanide system can selectively leach gold from the copper-gold ores, but the application of this process remains uncommon mainly due to its complicated chemistry and complexity in process control.

2.2.3 Non-cyanide leaching methods

The environmental hazards posed by the toxicity of cyanide have driven many researchers to seek alternative non-cyanide lixiviant for gold leaching, while most of the studies focused on thiocyanate, thiourea and halide-leaching (Aylmore, 2005). A few of the studies have investigated the leaching performance of using these alternative lixiviants to treat copper-gold ores.

2.2.3.1 Thiosulfate leaching

According to the literature review conducted by Aylmore and Muir (2001), researchers started their interests in the treatment of carbonaceous and copper-gold ores using thiosulfate since the 1980s due to the cyanidation is not effective for treating these kinds of ores. The early studies used a high concentration of thiosulfate (up to 40kg/t) to reach reasonable gold recovery, but it was found that it was essential to control the copper concentration as the Cu(II) in the solutions lead to a degradation of thiosulfate, thus increasing the consumption of thiosulfate. Later, Langhans et al. (1992) identified the catalytic role of copper and established a comparable leaching method using dilute ammoniacal thiosulfate solutions.

The equations of dissolution of metallic gold in ammoniacal thiosulfate solutions in the presence of Cu(II) at Eh about 0V are represented in Eq. 7 and 8 (Aylmore, 2016a).

$$Au + 5S_2O_3^{2-} + Cu(NH_3)_4^{2+} \rightarrow Au(S_2O_3)_2^{3-} + 4NH_3 + Cu(S_2O_3)_3^{5-} \quad (7)$$

$$4Cu(S_2O_3)_3^{5-} + 16NH_3 + O_2 + 2H_2O \rightarrow 4Cu(NH_3)_4^{2+} + 4OH^- + 12S_2O_3^{2-} \quad (8)$$

Many studies have investigated the leaching performance of thiosulfate for copper-gold ores with the typical 50 – 85% of gold extraction and 20 – 50% copper extraction using 10 – 40 kg/t thiosulfate (Aylmore, 2016b). Freitas et al. (2001) carried out studies on three different copper-gold ores from Brazil, and different leaching performances were identified for each ore using different leaching conditions. Also, they found a portion of copper was precipitated in some cases and the maximum gold recoveries obtained after 8h of leaching in a range between 70 to 90%. Xia et al. (2003) recognised that lowing dissolved oxygen (DO)

concentration, increasing pulp densities, adding strong chelating agent (EDTA or NTA) in a ratio of 1:1 (EDTA:Cu), reducing copper sulfate addition or replacing copper sulfate with nickel sulfate can reduce the consumption of thiosulfate when treating a mild-refractory copper-gold ore, where the DO concentration and pulp density play the most significant role. Dai et al. (2013) compared the metal extractions using cyanide and ammoniacal-thiosulfate for treating a suite of copper sulfide concentrates. The ammoniacal-thiosulfate leaching system showed a better selectivity for gold than that with cyanidation. Comparable gold recovery was achieved in the case of treating pyrite flotation concentrate and better gold recovery was obtained for the leaching of gravity gold concentrate, however, the reagent consumptions were about twice larger than those with cyanidation.

The ammoniacal-thiosulfate system is generally effective for leaching copper-gold ores, but issues such as the complex chemistry, reagent degradation, unstable gold recovery (fluctuated from samples to samples) and high reagent consumption hinder its further application in the gold industry.

2.2.3.2 Thiourea leaching

Thiourea has been proven effective in gold leaching at acidic conditions; its reaction is rapid and the gold recovery of up to 99% can be achieved (Aylmore, 2016a; Hilson & Monhemius, 2006). In practice, thiourea has to be used under relatively restricted conditions at thiourea concentration of 10 g/L, ferric ion concentration of 5 g/L, pH of 1 – 3 and at potentials from 0.42 to 0.45V (vs. SHE) (Aylmore, 2016a). Ferric is the most common oxidant, other oxidants which have been examined include hydrogen peroxide, manganese dioxide, mono-per-oxysulfate compounds and ozone (Sparrow & Woodcock, 1995). The leaching of gold using thiourea is sensitive to pH as decomposition of thiourea is intrinsically unstable and the decomposed substances have no effect on gold dissolution. Besides, the Eh should be maintained carefully between 0.42 and 0.45V (vs. SHE) to minimise the decomposition of thiourea (Tremblay et al., 1996). The overall reaction of gold in thiourea and ferric ion solutions is described in Eq .9.

$$Au + 2NH_2CSNH_2 + Fe^{3+} \rightarrow [Au(NH_2CSNH_2)_2]^+ + Fe^{2+} \quad (9)$$

The application of thiourea for copper-gold ore leaching is feasible. Although strong copper thiourea complex can be formed, which can increase the reagent consumption (Alodan & Smyrl, 1998), the dissolution of copper in acidic thiourea

is much less than that in cyanide solutions (Fang & Muhammed, 1992). A lab-based study undertaken by Lacoste-Bouchet et al. (1998) showed that after an acid wash pre-treatment, a copper-bearing gold ore containing 0.4% Cu and 5.6 g/t Au can be leached at a condition of 3.9 kg/t thiourea, pH 3 and Eh from 0.41 to 0.45V, the 89% of final gold extraction was obtained.

Despite the effectiveness of thiourea as the alternative gold lixiviant, its commercial adoption is still limited. That is mainly because it is more expensive than cyanide; suffers from high reagents consumption; it is labelled as a potential carcinogen; the leaching conditions are sensitive and its gold recovery requires further investigations and development (Aylmore, 2016a).

2.2.3.3 Halide leaching

Halide leaching using chlorine, bromine or iodine as the lixiviant for gold leaching. This technique especially chlorination was applied in the gold industry before the introduction of cyanide in the late 19th century. The application of bromine/iodine was reported as early as 1846 (Aylmore, 2016a). This leaching method revived in the 1990s after several bromine/bromide systems were lodged and patented (Tran, 1998). In recent decades, the increasing refractory nature of gold ores and the rising gold price became the incentive for the resurgence of the application of halide leaching.

High-oxidation conditions are required for the halide leaching for gold. The general halogen-based reaction of gold with chloride or bromine is shown in Eq. 10.

$$2Au + 3X_2 + 2X^- \rightarrow 2AuX_4^- \text{ , where X = Cl or Br} \quad (10)$$

The $AuCl_2^-$ is formed initially and is rapidly oxidised to $AuCl_4^-$. For the iodine leaching system, iodine reacts with iodide to form I_3^- ions to for Au(I) iodide rather than. That is due to E^o for $AuI_2^- < AuI_4^-$. Au(III) iodide complex is unstable which can be reduced to Au(I) iodide by iodine (Tran, 1998). The iodine gold leaching reaction is described in Eq. 11.

$$2Au + I_3 + I^- \rightarrow 2AuI_2^- \quad (11)$$

The gold halide complex is not very stable compared to gold cyanide, its stability depends on the halide concentration, solution pH and potential and the presence of reductants (e.g. metals and sulfidic minerals) in the ores (Tran, 1998). In order to

prevent the precipitation of metallic gold from solution, it is necessary to add oxidant to maintain a high Eh of the solution. Halide leaching is more rapid than cyanidation. The rate of reaction is in the order of Cl > Br > I, whereas the stability is in the order of I > Br > Cl (Aylmore, 2016a).

The typical leaching conditions for chlorine, bromine, iodine as the lixiviants were shown in Table 2.1.

Table 2.1 Typical conditions for gold leaching using halides (Aylmore, 2016a).

Reagent	Ligand	Oxidant	Gold complex	Typical leaching conditions	pH
Chlorine	Cl^-	Cl_2	$AuCl_4^-$	5 – 10 g/L Cl_2, 5 – 10 g/L NaCl	<3
Bromine	Br^-	Br_2	$AuBr_4^-$	2 – 5 g/L Br_2, 0 – 10 g/L NaNr	5 – 8
Iodine	I^-	I_2	AuI_2^-	1 g/L I_2, 9 g/L NaI	5 – 9

Research on the application of halide leaching for copper-gold ores is also limited since the gold halide complex can be reduced and precipitated by sulfidic minerals. Stace (1984) found that flotation collectors can be used as a coating which reduces the reactivity of metal sulfides (e.g. copper sulfides) in the chloride-chlorine system without reducing the reaction rate of gold dissolution. On the other hand, the iodine-iodide leaching system does not oxidise metal sulfides such as chalcocite, thus avoiding extra reagent consumption during the leaching (Hiskey & Qi, 1991). However, high leaching cost is the main challenge for the iodine-iodide system which hinder and restrict its development. Also, the recovery system for gold and the regeneration of iodine from the solutions remain unsolved, thus deeper studies are required in the future (Liang & Li, 2019).

2.3 Novel glycine leaching process

2.3.1 Glycine leaching system

A novel alkaline glycine-based leaching system which uses a glycine as a type of amino acids, as the main lixiviant for copper and gold leaching, was originally developed and patented by Curtin University. Glycine (NH_2-CH_2-COOH) as the alternative lixiviant for gold leaching has several advantages over cyanide. It is the simplest possible amino acid, has a carboxylic group and amine group, which is non-toxic and is prevalent in food, pharmaceutical, medicine, agronomy and nutrition industries. It is colourless, odourless, sweet-tasting, biodegradable and non-volatile. Glycine is the cheapest of the amino acids which can be manufactured industrially (sold at a lower cost than sodium cyanide) from chloroacetic acid (itself

produced from trichloroethylene, i.e. the petrochemical industry) or derived as a by-product from different micro-organisms (González-López et al., 2005). The gold and copper glycine complexes in the solution have high stability over a wide pH-E_h range, thus the glycine can be recovered and reused after leaching instead of losing in leach residue during solid/liquid separation.

The original idea of using glycine as the lixiviant was derived from bioleaching which uses complexing chemicals such as amino acids secreted by bacteria for gold dissolution in the presence of oxidising agents such as peroxide and potassium permanganate. This innovative leaching method was intensively studied since 2014 and over 30 research items including journal papers and conference papers have been published based on this leaching system.

This alkaline glycine-only leaching system is effective to leach metallic copper, copper minerals and concentrates including copper oxides (e.g. azurite, cuprite, malachite and bornite) and copper sulfide (e.g. chalcocite and chalcopyrite) (Eksteen et al., 2017; Oraby & Eksteen, 2014; Tanda et al., 2017; Tanda et al., 2019; Tanda, et al., 2018a,2018b). Gold can be leached in the presence of peroxide at moderately elevated temperature (Eksteen & Oraby, 2015; Oraby & Eksteen, 2015b) or a high pH level of 12.5 (Oraby et al., 2019), while the leaching rate is too low that may only be feasible for heap, vat and in-situ leaching as glycine can be a serious contender to cyanide due to its non-toxicity. Glycine mixed with a small amount of cyanide can significantly increase the gold dissolution rate, which is suitable for traditional agitated tank leaching (Oraby & Eksteen, 2015a; Oraby et al., 2017). Different recovery methods for the glycine leaching process were studied. It was found that the traditional carbon adsorption is still feasible for both the glycine only and glycine-cyanide leaching system (Tauetsile et al., 2018a, 2018b, 2019a, 2019b). On the other hand, copper can be recovered by solvent extraction or sulfide precipitation from their glycinate complex (Tanda, 2017; Tanda, et al., 2017). Additionally, its application has now been extended to recycle the base and precious metals from the electric and electronic wastes (Li et al., 2020; Oraby et al., 2019). A high-level cost/economic impact estimation indicated that by using the glycine-based leaching system, the margin of operation can be more than double through the potential saving of reagent cost, and the glycine-cyanide synergetic leach system has potential to enable those complex ore bodies particularly copper-gold ores economically viable for exploitation (Eksteen et al., 2018).

2.3.1.1 Glycine leaching of copper

Du et al. (2004) investigated the mechanism of copper dissolution in glycine solutions in the presence of peroxide, and it is suggested that copper is oxidised by peroxide and then the soluble copper glycinate complex was formed by the oxidised copper and the glycine in solutions. Aksu and Doyle (2001) reported that copper dissolution increased with the increasing glycine concentration in both acidic and alkaline conditions, while a decrease in copper dissolution was observed when the peroxide concentration was over 0.25 wt %, indicating that the glycine can be oxidised by peroxide. According to O'Connor et al. (2018), the Cu (II) glycinate species in solutions can exist as $Cu(H_2NCH_2COO)_2$, $Cu(H_3NCH_2COO)^{2+}$ and $Cu(H_2NCH_2COO)^{+}$, while the predominant Cu (I) glycinate is $Cu(H_2NCH_2COO)^{2-}$, depending on the solution pH. Their stability as indicated the stability constants is shown in Table 2.2. The copper glycinate complex is stable over a wide range of Eh-pH range from 2.6 to 12 and the neutral copper glycinate complex ($Cu(H_2NCH_2COO)_2$) is the dominant species at alkaline conditions, as indicated in Fig. 2.3. On the other hand, the solubility of copper glycinate in alkaline conditions is dependent on temperature, concentration of the components and pH. It was reported that precipitation of cupric glycinate was observed several hours or days when NaOH or KOH is used for pH modification (Gylienė, 2001).

Table 2.2 Stability of the copper glycinate complexes (Aksu & Doyle, 2001).

Copper ion	**Cu glycianate complex**	**Stability log*K***
Cu^{2+}	$Cu(H_2NCH_2COO)_2$	15.6
Cu^{+}	$Cu(H_2NCH_2COO)^{2-}$	10.1
Cu^{2+}	$Cu(H_2NCH_2COO)^{+}$	8.6

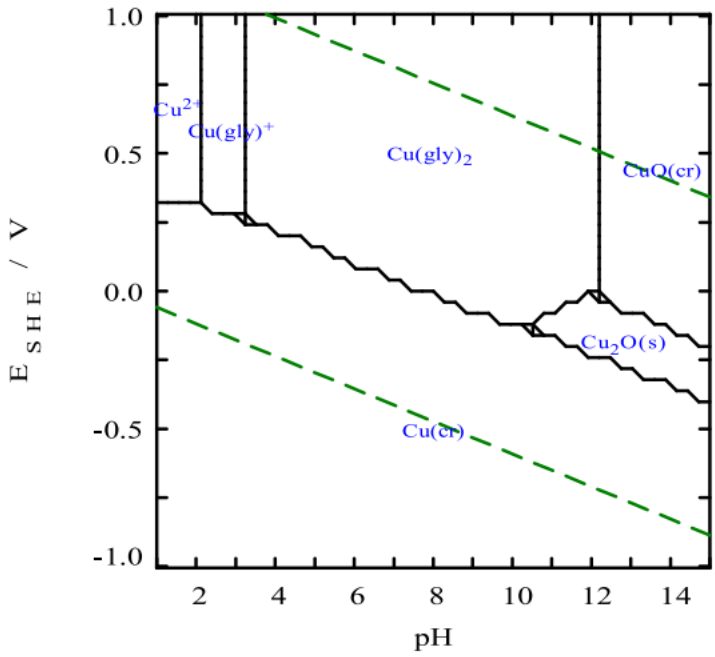

Figure 2.3 Eh-pH diagram of copper glycine system at 0.5M glycine, 0.05M Cu at 25 ℃ (H. Li et al., 2020)

Oraby and Eksteen (2014) proposed a leaching process to selectively leach copper from a copper-gold gravity concentrate (3.75% Cu, 11.6% Fe, 11.4% S and 0.213% Au) using alkaline glycine solutions. This process was conducted in two stages using identical leaching conditions (0.3M glycine, 1% H_2O_2, pH 11 and ambient temperature). The results showed high effectiveness in selective leaching of reactive copper before gold, with 98% of total copper recovery (100% recovery of metallic copper and chalcocite and about 80% recovery of chalcopyrite). The schematic diagram of the process is shown in Fig. 2.4. This process is advantageous over the conventional acid-base leaching for copper, where the dissolution of gangue minerals particularly pyrite and the cyanide consumption can be significantly reduced. Also, as the process is conducted under alkaline conditions, the leach residues can be directly leached by cyanidation or the glycine-cyanide process.

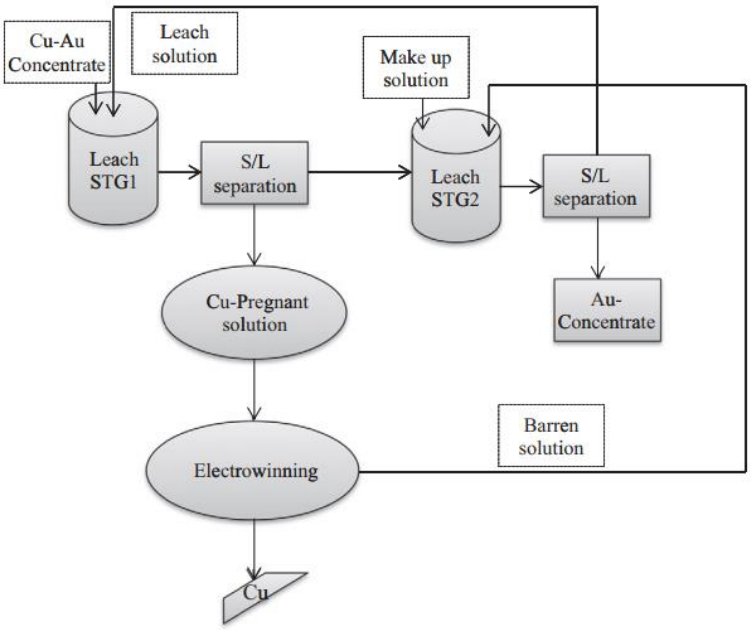

Figure 2.4 Schematic diagram of the two-stage counter-current Cu leach process (Oraby and Eksteen, 2014)).

The leaching behaviours of metallic copper and individual copper minerals including oxide ores (i.e. azurite, malachite, chrysocolla and cuprite) and sulfide ores (i.e. chalcocite and chalcopyrite) were detailly studied by Tanda (2017). Fundamental studies for the leaching kinetics for malachite (Tanda et al., 2018b), chalcocite (Tanda et al., 2018a) and chalcopyrite (Tanda et al., 2019) were performed. It was found that, for copper oxide minerals, chrysocolla was the most difficult mineral to dissolve in the glycine leach system, while a high copper extraction from azurite, cuprite and malachite can be achieved easily in 24h of leaching (Tanda et al., 2017). Copper sulfide minerals, on the other hand, are relatively difficult to leach compared with oxide minerals and require a high Gly:Cu molar ratio with prolonged leaching period. For chalcopyrite, a copper extraction of 71% was obtained at a Gly:Cu molar ratio of 8:1, pH of 11 and a leaching time of 800h (Tanda, 2017). Alternatively, pre-treatment such as ultrafine grinding and pre-oxidation of the sulfide minerals can be used to improve the copper extraction. Around 92% of copper extraction from chalcopyrite was achieved within 17h at 60 after ultrafine grinding and alkaline pre-oxidation (Eksteen et al., 2017). For copper leaching in the glycine leach system, glycine concentration and solution pH are considered to be the important factors, while temperature, stirring speed, particle size and DO levels can also affect the rate and extent of copper extraction.

2.3.1.2 Glycine leaching of gold

The interaction of amino acids with gold was first discussed by Kharaka et al. (1986) who look ed at the system from a geohydrological perspective, as follows: (1) they provide H^+, thus control the pH of subsurface waters; (2) they behave as reducing agents, thus determine the Eh and the oxidation state of the solutions; (3) they can be de-carboxylated into carbon dioxide and hydrocarbon gases; and (4) they can form soluble complexes with metals and other inorganic species. Groudev et al. (1995) utilised amino-acid generating bacteria and attributed the bioleaching of the gold to a mixture of amino acids present in the biomass, in the presence of oxidants such as oxygen, peroxide or permanganate. It was postulated by Pakiari and Jamshidi (2007) using the density functional theory (DFT) that the interaction between gold and glycine is dominated by two principle bonding factors which are the anchoring N-Au and O-Au bonds and the nonconventional N-H-Au hydrogen bonds. The gold glycinate complex with the Au-NH_3 anchoring bond is more stable with the sole pair of electrons being transferred to the antibonding orbitals of gold (Xiao-Hua & Bing, 2013). The stability constant of gold complexed with glycine at pH 9 is 18.0 which is higher than $AuCl^-_2$ (9.1), $AuBr^-_2$ (12.0), $Au(SCN)^-_2$ (17.1) and $Au(SO_3)^{-3}_2$ (Aylmore, 2005).

Eksteen and Oraby (2015) performed a batch study on the dissolution of metallic gold in an alkaline amino acids-hydrogen peroxide solution. They found that gold can be dissolved by this lixiviant system under alkaline conditions at ambient temperature to moderately elevated temperature (23 – 60°C), where the gold dissolution rate increased with increasing temperate, pH and concentration of amino acids. Glycine, amongst a range of amino acids, showed the highest gold dissolution as a single amino acid compared to histidine and alanine. Also, it was reported that the presence of cupric ions can enhance the gold dissolution. Oraby and Eksteen (2015b) performed further investigations on this lixiviant system for gold/silver dissolution and found that the gold leaching rate was 0.322 μmol/m^2 s in solutions containing 0.5M glycine, 1% H_2O_2 at pH 11, 60°C and the reaction rate was found to be chemically controlled as it is sensitive to the change of temperature. Also, they found that the gold-glycinate complex can be effectively adsorbed by activated carbon with the adsorption rate up to 13.2g/kg in 4h. The gold dissolution rate was much slower than cyanide leaching, therefore, it was considered to apply this glycine-based lixiviant system for those leach modes such as in-situ, vat or heap

leaching approaches where their leach rates are determined by bulk or particle diffusion processes. Oraby et al. (2019) conducted a study using the alkaline glycine system to leach gold from a Western Australia paleochannel ores (free-milling ores). The study showed good amenability for the application of in-situ, vat and heap leaching, and above 85% of gold was leached from ores using an aerated solution containing 15 g/L glycine in the absence of peroxide at pH 12.5 and a temperature of 55℃ in 336 hours. They also suggested that the temperature of 55℃ is not difficult to achieve for in-situ or heap leaching, particularly in Australia where the solar thermal heating can be easily obtained in appropriate climates.

2.3.2 Cyanide-starved glycine leaching system for gold-copper ores

Another type of glycine-based leaching method developed by Oraby and Eksteen (2015a) use a synthetic cyanide-starved glycine solution at ambient temperature to enhance the dissolution rate of the pure gold. Cyanide-starved is referred to the cyanide present as cuprous cyanide running at starvation levels and is insufficient for the dissolution of any cyanide soluble copper minerals and that no free cyanide is present as either HCN or the CN^- anion. It was observed that in the presence and absence of glycine, the gold dissolution rates increased significantly from 0.65 μmol/m^2 s to 11.1 μmol/m^2 s in a solution containing 10mM copper cyanide species, which is about 6.5 times higher than the dissolution rate in the conventional cyanidation at the same pH conditions and temperature. Also, it was found that increasing the glycine concentration, initial Cu concentration, pH and [CN]:[Cu] molar ratio can increase the gold dissolution rate.

Oraby et al. (2017) performed a study for three types of copper-gold sources including a Cu-Au-Ag gravity concentrate with complex copper mineralogy, a Cu-Au oxide ore with nuisance Cu and a Cu-Au sulfide ore with recoverable Cu using the synergetic glycine-cyanide lixiviant. They found that a small amount of cyanide used in conjunction with glycine has a better gold recovery and faster gold dissolution rate than those obtained from cyanidation at room temperature and the same pH conditions. Their leaching performance in terms of gold and copper recoveries were compared with those in cyanidation as can be seen in Table 3.

The mechanism and the role of the cyanide-starved glycine system to dissolve gold and copper from ores were expected as follows (Oraby & Eksteen, 2015a; Oraby et al., 2017):

- Glycine dissolves the copper minerals and complexes with copper ions to form either Cu(I) or Cu(II) glycinate. According to Eh-pH diagram (Fig. 3) and the stability of the copper glycinate (Table 2), the neutral $Cu(H_2NCH_2COO)_2$ is the dominant species, as shown in Eq. 12.

$$Cu^{2+} + 2NH_2CH_2COO^- \rightarrow Cu(NH_2CH_2COO)_2 \quad (12)$$

- Copper was initially dissolved by cyanide to form cuprous cyanide.
- The cuprous cyanide species were then oxidized to cupric glycinate with time in the presence of glycine and oxidants (e.g. oxygen), thus reducing the levels of WAD cyanide and releasing more free cyanide to leach and complex with gold (as shown in Eq. 1). The oxidising reactions of cuprous cyanide are indicated in Eq. 13 and 14.

$$8CuCN + 8(NH_2CH_2COO^-) + O_2 + 2H_2O \rightarrow 4Cu(NH_2CH_2COO)_2 + 4Cu(CN)_2^- + 4OH^- \quad (13)$$

$$4Cu(CN)_2^- + 8(NH_2CH_2COO^-) + O_2 + 2H_2O \rightarrow 4Cu(NH_2CH_2COO)_2 + 8CN^- + 4OH^- \quad (14)$$

- Glycine acts as an additional lixiviant for gold leaching, as described by Eq. 15.

$$4Au + 8NH_2CH_2COOH + O_2 + 4NaOH \rightarrow 4NaAu(NH_2CH_2COO)_2 + 6H_2O \quad (15)$$

The synergetic glycine-cyanide lixiviant system is advantageous over cyanide, it can be concluded as follows (Oraby et al., 2017):

- Significantly lower cyanide consumption with normally one-tenth of the use in cyanidation.
- The formation of cupric glycinate provides Cu^{2+} as the extra oxidants for the leaching.
- Gold dissolution rate is almost three times faster than the traditional cyanidation process.
- The leachate contains dominate amount of cupric glycinate and a small amount of cuprous cyanide (mainly cuprous dicyanide) with zero free cyanide.

- The weak acid dissoluble (WAD) cyanide can be maintained at below the limits for disposal described by the International Cyanide Management Code, thus avoiding costly detoxification.
- The soluble copper can be reduced from 50% to less than 10% compared to cyanidation.

This process using glycine as main lixiviant mixing with a small amount of cyanide and the Cu^{2+} as the additional oxidants, significantly reduce the cyanide consumption and increase the gold leaching rate and recovery. Glycine also maximises the cyanide leaching efficiency by oxidising the Cu^{+} and releasing CN^{-} from the cuprous cyanide, meanwhile, reduces the toxicity of the final leachate i.e. lower WAD cyanide concentration. In short, if the downstream processes can be successfully demonstrated, this process can be implemented for those metallurgical plants originally designed for cyanidation, while seeking innovative methods to reduce the consumption of cyanide and the environmental impacts of the use of cyanide.

2.4 Options of gold and copper recovery (from alkaline solutions containing them)

In hydrometallurgy plants, copper extracted from the copper-gold resources is usually recovered by solvent extraction, sulfide precipitation or ion-exchange resin adsorption; while gold is usually recovered by zinc cementation, carbon adsorption or resin adsorption (Sceresini & Breuer, 2016). Different techniques for recovering copper and gold were detailedly reviewed in this section.

2.4.1 Solvent extraction

Solvent extraction (SX) is a fundamental separation process which is commonly used in hydrometallurgical processes for metal extraction, separation and purification. SX refers to a two-phase distribution of a solute (e.g. molecular, ions), i.e. a distribution between two immiscible liquid phases in contact with each other, one that is generally an aqueous solution (polar) and the other usually an organic solvent (non-polar) (Rydberg, 2004). The distribution of a solute is determined by its preference (solubility) in one or the other liquid. A transfer of a solute from one into the other liquid, generally from aqueous to organic, is driven by chemical potential, which means once the transfer is complete, the overall chemical system of the components that include the solutes and the solvents are at more stable

configuration i.e. lower free energy (Godfrey & Slater, 1994). The enriched solvent is called extract, while the depleted feed solution is called raffinate.

From hydrometallurgical perspectives, SX is advantageous in being able to selectively separating very similar metals, where its application is prevalent in the separation and purification of rare earth elements, uranium/plutonium, zirconium/hafnium, niobium/tantalum, nickel/cobalt, etc. Its operation was confined to a rather small scale at its first introduction to hydrometallurgy in the 1940s. After the development of selective chelating acidic reagents in the 1960s, SX was seen to be a commercially feasible process for hydrometallurgical plants and an alternative process such as cementation (Rydberg, 2004). It should be noted that SX requires solid/liquid separation which can be quite costly.

In the traditional cyanidation for copper-gold ores, SX integrated with electrowinning can be used to recover both copper and cyanide as cuprous cyanide species. Copper and cyanide recovery processes involved SX have been investigated based on different solvent extraction reagents, e.g. LIX® 7820 (Davis et al., 1998; Xie & Dreisinger, 2009a) and LIX® 7950 (Dreisinger et al., 1995; Xie & Dreisinger, 2009b). Copper cyanide complexes loaded in the organic solvents are stripped from LIX® 7820 by a strong caustic solution, while a high-pH copper-cyanide-rich spent electrolyte is used for copper stripping from LIX® 7950 (Sceresini & Breuer, 2016). The copper cyanide extraction and stripping can be represented as Eq. 16 and 17.

$$Cu(CN)_{3(aq)}^{2-} + 2R + 2H_2O \rightarrow Cu(CN)_3(RH)_{2(org)} + 2OH^- \quad (16)$$

$$Cu(CN)_3(RH)_{2(org)} + 2OH^- \rightarrow Cu(CN)_{3(aq)}^{2-} + 2R + 2H_2O \quad (17)$$

Further investigations conducted by Xie and Dreisinger (2009a, 2009b) found that the extraction efficiency of both LIX® 7820 and LIX® 7950 reduces significantly with increasing cyanide concentration, while a low cyanide concentration may lead to CuCN precipitation in the organic phase. Additionally, the presence of thiocyanate dramatically depresses the extraction of copper. Issues such as the potential contamination of the raffinate by the organics and the degradation of expensive organic solvents also hinder the applications of SX technology, thus the application of SX receives little attention from the gold-copper industry.

Recently, Tanda et al. (2017) presented a study on SX for Cu recovery from the alkaline glycinate leachates using Mextral 84H and Mextral 54-100 in kerosene as diluent. They found that Cu was effectively recovered from the alkaline glycinate media. An extraction efficiency over 99.9% was achieved with 5% Mextral 54-100 at an aqueous-to-organic (A:O) ratio of 2:1 at room temperature. Under similar conditions, 95.87% of Cu recovery was obtained by 10% Mextral 84H. Cu can be stripped from the organic phases by acidic solutions, about 97% of Cu stripping efficiency was achieved at 120 g/L of sulfuric acid. According to the HPLC analysis for free glycine concentration, the extraction of copper into the organic phase happened via copper ions only, neither the complex nor any glycinate dissolved into the organic phase, which implies that most of the glycine can be recovered and recycled to the leach circuit. The loading and stripping for cupric ions can be described by the following reactions, as shown in Eq. 18 and 19:

$$2RH_{(org)} + Cu(H_2NCH_2COO)_{2(aq)} \rightarrow R_2Cu_{(org)} + 2H_2NCH_2COOH_{(aq)} \quad (18)$$

$$R_2Cu_{(org)} + 2H^+_{(aq)} \rightarrow 2RH_{(org)} + Cu^{2+}_{(aq)} \quad (19)$$

2.4.2 Sulfide precipitation

Precipitation is a process that has been widely applied in the field of chemistry, medicine and metallurgy. Precipitation is similar to crystallization, both of these two processes first experience supersaturation, then nucleation and finally crystal growth. However, due to the consequence of the high supersaturation at which it occurs, precipitation has much faster kinetics compared with crystallization (Söhnel & Garside, 1992). In hydrometallurgy, precipitation processes can be effective by using either solid (FeS, CaS), aqueous (Na_2S, NaHS, NH_4S) or gaseous (H_2S) sulfide sources to recover metals (e.g. Zn, Cu, Ni, Mg, Pd, Fe, Co, Cd, Mo and V) as saleable metal sulfide precipitates.

Sulfide precipitation has several advantages over hydroxide precipitation, including lower solubility of metal sulfide precipitates, potential for selective metal removal, fast reaction rates, better settling properties and potential for re-use of sulfide precipitates by smelting (A. Lewis, 2010). Due to the low solubility of the metal sulfide precipitates, a lower effluent concentration (<0.01mg/L) can be achieved, compared with the concentration in a range of 0.5 – 2mg/L normally obtained from hydroxide precipitation (Veeken et al., 2003). Sulfide also gives a possibility of selective precipitation according to the different solubility of the different metal

sulfides. A sulfide selective electrode (pS-electrode) was used to control the sulfide addition i.e. pS (-log(S^{2-})) at different levels to achieve selective precipitation (Sampaio et al., 2009; Veeken et al., 2003).

2.4.2.1 SART process

In traditional cyanidation process, there are several processes have been developed based on sulfide precipitation for Cu and cyanide recovery. Among these, the sulfidisation-acidification-recycling-thickening (SART) process is the most common ones, with seven SART plants currently being operated over the world (Estay, 2018). SART process is a relatively advanced technology with regards to safety and equipment size. It includes thickening and recycling stages instead of only using filtration to separate the metal sulfide precipitates like the MNR process (Fleming 2005, Estay 2018).

The principle of the SART process based on the protonation of cyanide at a low pH by adding acid, releasing cyanide from the copper cyanide complexes through reactions Eq. 20 to 23 (Dai et al 2011):

$$Cu(CN)_4^{3-} \leftrightarrow Cu(CN)_3^{2-} + CN^- \quad (20)$$

$$Cu(CN)_3^{2-} \leftrightarrow Cu(CN)_2^- + CN^- \quad (21)$$

$$Cu(CN)_2^- \leftrightarrow CuCN + CN^- \quad (22)$$

$$CuCN_{(s)} \leftrightarrow Cu^+ + CN^- \quad (23)$$

After acidification, adding bisulfide (HS^-) ion to the copper cyanide solutions leads to the copper precipitation as chalcocite as shown in Eq 24. (Estay, 2018).

$$2Cu(CN)_3^{2-} + HS^- + 5H^+ \rightarrow Cu_2S + 6HCN_{(g)} \quad (24)$$

After precipitation, the slurry is transferred to the thickener to separate the chalcocite from the hydrocyanic acid solutions. Also, the SART process recycled a portion of the thickening underflow slurry as seed during precipitation for promotion of crystal growth. The hydrocyanic acid solution is then neutralised by lime to covert the hydrocyanic acid back to cyanide.

During the reaction, toxic hydrogen cyanide (HCN) gas can be emitted where an effective gas extraction and scrubbing system is required, giving rise to higher capital and operational costs. Generally, the entire process is covered and

maintained under a slight negative pressure to avoid leakage of hydrogen cyanide gas. HCN and water are soluble in each other in all proportions and HCN has a strong water affinity, making it quite hard (high gas flows required with its associated blower costs and relatively large equipment) to effectively strip HCN from aqueous solutions for reabsorption into caustic solutions. Also, the use of sulfuric acid during acidification can lead to the formation of scale when lime is used for pH modification, which is due to the reaction between sulfate and calcium to form gypsum which should be removed periodically (Dai et al., 2011).

2.4.2.2 Precipitate characteristics

Products from the sulfide precipitation are generally difficult to control owing to the sparingly soluble nature i.e. extremely low solubility of the sulfide precipitates and very high supersaturation level which can reach to 10^{35} or higher (A. Lewis & van Hille, 2006). Extremely fine sulfide precipitates were usually formed during the traditional sulfide precipitation process where the precipitates were too fine to filter (< 0.45μm) (Simons & Breuer, 2011). Sceresini and Breuer (2016) point out that synthetic Cu_2S tends to be finely divided and not easily filterable in the MNR process, even with recycling a portion of underflow precipitates as seed material. It is reported that the copper is difficult to crystallise via sulfidation as the formation of fine particles (ca. 100 nm) without proper control measures (Chung et al., 2015; Mokone et al., 2010). Several factors significantly affecting supersaturation and crystal growth during the precipitation reaction determine the precipitate characteristics such as particle size distribution (PSD), filtering or settling performance and crystal morphology and structure.

Supersaturation

The level of supersaturation is a critical factor for any precipitation that can govern the rates of nucleation and final particle size and (PSD). For sulfide precipitation, the level of supersaturation is usually very high as the extremely low solubility of the precipitated products, for example, the K_{sp} of CuS is 6.3×10^{-36} (Dean, 1990). Primary nucleation rates are usually very high at the high supersaturation, resulting in a large number of primary nuclei that limits the average size to which the crystal can grow (Mersmann, 1999; Patel & Anderson, 2013). A study performed by (Sampaio et al., 2010) illustrated that decreasing the levels of supersaturation (i.e. lower sulfide concentrations) was beneficial to form larger particle during the precipitation of Zn using Na_2S. Similarly, Lewis and van Hille (2006) suggested

that controlling the supersaturation by a reduction of metal and sulfide concentrations and an increase of flowrate of H_2S gas can reduce spontaneous homogeneous nucleation, and eventually mitigate the formation of fine precipitates. However, it was also reported that a lower initial concentration caused wider PSD and has no significant effects on the average particle size (Farahani et al., 2014). Besides, supersaturation can be affected by the intensity of mixing i.e. stirring speed, as supersaturation may exhibit spatial variations in the reactor and the level of variations may be affected by the mixing conditions (Söhnel & Garside, 1992). It was observed that an increase of stirring speed can lead to a decrease in mean particle size (Eksteen et al., 2008; Marcant & David, 1991). Whereas, contradictory results obtained by Farahani et al. (2014), Houcine et al. (1997) and Torbacke & Rasmuson (2001) show that larger particle size was achieved by increasing agitation speed. Several studies observed that the average particle size initially increased with higher energy dissipation rate, reached a maximum point at optimum stirring speed and then decreased with increasing mixing rate (Torbacke & Rasmuson, 2001, Marcant & David, 1991). In the case of the effect of agitation on precipitation, it is not purely the agitation speed or mixing energy but the power dissipation at the macro, meso and micro levels that have to be optimised (Söhnel & Garside, 1992).

Factors affecting crystal growth

Typically, the final particle size distributions of precipitates are significantly influenced by the stage of crystal growth which involves secondary nucleation and secondary change. Secondary nucleation occurs in the presence of parent crystal i.e. seed crystal and interaction with the environment such as other crystals, crystallizer walls and impeller (Wong et al., 2013). For the precipitation of sparingly soluble solids (e.g. CuS), the extent of secondary nucleation may be insignificant at the extremely high level of supersaturation (Söhnel & Garside, 1992), given the extreme insolubility of CuS. Introduction of seed crystals may be an effective approach for precipitation of sparingly soluble substances. Seeding is a technique usually applied as templates for secondary nucleation to avoid spontaneous homogeneous nucleation in metastable solutions and control the particle polymorphism and particle size distribution (Donnet et al., 2005; Linga, 2017). It allows to crystal growth from seeds occur in the metastable zone, while spontaneous nucleation cannot occur. Seed materials are normally obtained from

the same materials as it to be precipitated, but other substances can also be introduced as seeds (Beckmann, 2013). In a typical SART process, a portion of the thickener underflow served as seeds are recycled into the precipitation tank for enhancing the crystal growth of the Cu_2S precipitates (Estay, 2018).

Secondary changes such as ageing and agglomeration can play critical roles in increasing the crystal size of particles. Ageing refers to contact of the solid precipitates with the mother liquor, involving recrystallization of non-equilibrium shapes of primary particles (i.e. needles and dendrites) to form more compact shapes of secondary particles. It can also involve the transformation of meta-stable polymorph to stable modifications, for example, an amorphous phase could transform into a crystalline phase during ageing (Söhnel & Garside, 1992). As illustrated by Söhnel and Garside (1992), a transformation of original $SrSO_4$ amorphous particle size (~0.02µm) to crystalline particles (~0.16µm) occurred at 5 minutes of ageing and further growth of particle size to 4.5 µm was observed after 3 minutes of ageing. Agglomeration is the predominant particle size enlargement mechanism for insoluble/low solubility precipitates that determines the final particle size distribution (Ilievski & White, 1994). Agglomerates are referred to the secondary particles (cluster of separate particles) held together by crystalline bridges but also sometimes physical forces. Minute amounts of additives present in the system can greatly influence the crystal growth, the particle size and the degree of agglomeration. It was reported that divalent cation such as Ca^{2+} can be used as cross-linking agents to facilitate the growth of CuS crystals during sulfidation, much denser and larger aggregations of particles were observed (Chung et al., 2015).

2.4.2.3 Sulfide precipitation for glycine-based leach system

The Cu from the cupric glycinate produced in the glycine leaching system can also be recovered by sulfide precipitation at alkaline conditions. Tanda (2017) carried out a batch-scale sulfide precipitation study based on the glycine leach system. It was found that copper can be effectively precipitated as fast settling, coarse-grained, covellite (CuS) from the alkaline cyanide-free cupric glycinate leachates by adding NaHS powder. A Cu:S molar ratio of 1:1.2 and a reaction time of 10 minutes gave a copper recovery of about 99% from a synthetic cupric glycinate solution. The solution pH from 8 to 11 did not pose a significant effect on the Cu recovery and the precipitated product was indicated as 100% CuS according to the XRD results. Eksteen et al. (2017) performed a sulfide precipitation test from real cupric

glycinate leachates from chalcopyrite extraction, a copper recovery of 99.1% was obtained at a Cu:S molar ratio of 1:1. They also proposed a conceptual flowsheet for copper extraction by alkaline glycine solutions, where copper is recovered as CuS using NaHS addition, as shown in Figure 2.5. It is noted that in the flowsheet, lime is added for sulfur removal (as sulfate) and it is also used for the removal of any solubilised silicate, phosphate, aluminate or carbonate as the calcium precipitates, which acts as a polishing step for the barren aqueous glycinate solutions before recycling back to the leach circuit.

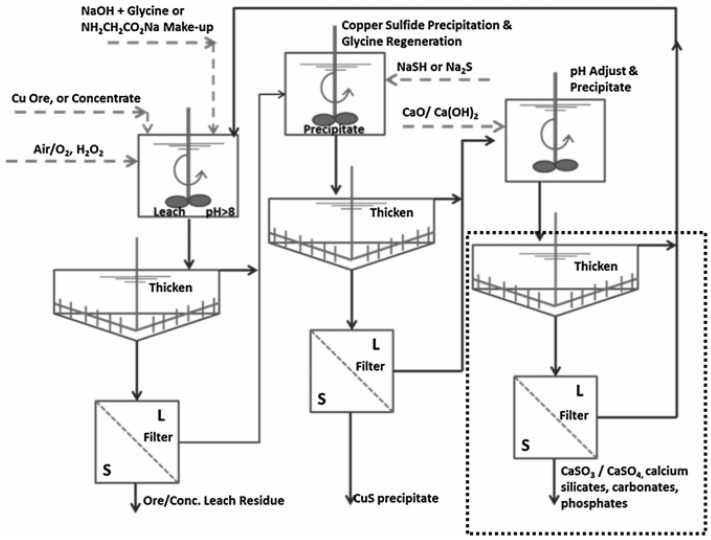

Figure 2.5. A conceptual flowsheet for copper leaching and recovery by sulfide precipitation from the glycine leach system (Eksteen et al., 2017)

For the cyanide-starved glycine leaching system, it is predicted that cupric glycinate can be recovered by sulfide precipitation at alkaline conditions, which mitigates the risks of toxic HCN emissions. In terms of the cuprous cyanide, it is possible to use oxidants such as hydrogen peroxide to pre-oxidise the cuprous ions to cupric ions to achieve a high level of copper recovery. Alternatively, the cuprous cyanide remaining in the solutions can be recycled back to the leach circuit.

2.4.3 Zinc cementation

Zinc cementation, or zinc precipitation, is a well-known component of the Merrill-Crowe process for gold and silver recovery from the pregnant solutions since 1888 (Walton, 2016). During the process, gold is precipitated/cemented by adding zinc powders or shavings, which is a classic electrochemical reaction involving oxidation and reduction. The Typical chemical reaction for zinc cementation of gold cyanide is described as Eq. 25.

$$2Au(CN)_2^- + Zn \rightarrow 2Au + Zn(CN)_4^{2-} \quad (25)$$

Zinc cementation is typically applied to pregnant solutions from a solid-liquid separation stage after leaching, directly from heap leaching or the eluates from elution process. The application of zinc precipitation has been largely replaced by CIP/CIL following by electrowinning process as it required costly solid-liquid separation stage. However, the zinc cementation process is still favourable in some situations, for example, it is suitable when a high amount of organics are present; it is also useful when it follows a heap leach where the heap serves as a deep bed filter and solid-liquid separation is not required; it is preferential when the Ag:Au ratio in the leach solution is high as the presence of soluble Ag lowers the gold loading capacity; it is suitable for leachates containing a high level of mercury which its cyanide complex can be adsorbed onto the activated carbon and further contaminate the various processes after elution (Marsden & House, 2009).

There are four main steps of the Merrill-Crowe process i.e. clarification, deaeration, zinc cementation and filtration, as indicated in Figure 2.6 (Walton, 2016). The pregnant solutions from a heap-leach or tank-leach operation after solid-liquid separation have to be clarified to about 1 ppm suspended solids for effective cementation. After clarification, the solution is pulped to the deaeration or Crowe tower, where the dissolved oxygen level can be reduced to below 1 ppm by applying vacuum to this tower. During the zinc cementation, a stream of barren solutions containing zinc powders or shavings enters the piping suction ahead of the pump from the zinc cone, with the precipitated gold and silver as well as excess zinc being collected by a precipitate filter. The precipitates may be retorted, dried or calcinated before refining, depending on the base-metal and mercury levels.

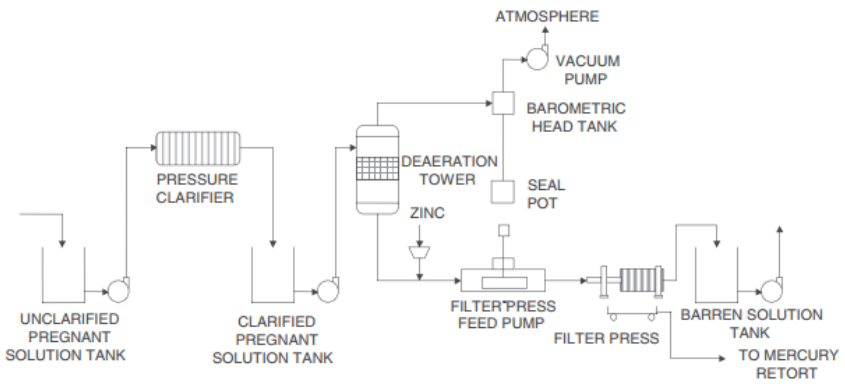

Figure 2.6 Classic flowsheet of the Merrill-Crowe process (Walton, 2016)

Nowadays, the use of basic Merrill-Crowe process has been now expanded to the gold recovery from the carbon-stripping eluates and solutions from the intensive cyanidation of gravity concentrates, where the chemistry of these solutions is similar. For those eluates from carbon elution, deaeration is not necessary as their dissolved oxygen level is low. Also, the eluates subjected to zinc precipitation require a bleed to reduce the concentration of soluble zinc, which is different from those subjected to electrowinning that is generally recycled for reducing overall reagent consumption.

The limitation of zinc cementation, however, may not be economically suitable for gold recovery from the copper-bearing gold ores that copper co-precipitation will occur when treating copper-gold ore, increasing the complexity of downstream processes and the amount of zinc used in the process. Copper co-precipitation with gold can result in high consumption of zinc and the copper must be separated from the gold slimes by sulfuric acid digestion before smelting (Sceresini & Breuer, 2016). Given the cost of zinc (around 2,750 USD per tonne at the time of writing) versus copper (7,180 USD per tonne at the time of writing), cementation is not an economic alternative for copper recovery and gold recovery in the presence of significant copper will lead to excessive zinc consumption.

2.4.4 Activated carbon adsorption

2.4.4.1 Activated carbon

Activated carbon has slightly disordered graphitic structure with a large internal surface area and a high degree of surface reactivity which is an ideal adsorbent. It can be made from materials containing amorphous carbon such as wood, coal, peat and coconut shell, and is formed through a thermal process, where the volatile components are removed. Activated carbon is widely used in the removal of undesirable odour, colour, taste, organic and inorganic impurities from wastewater; air purification for food and chemical industries; colour removal from various syrups and pharmaceutical products; air filter in gas mask and respirators; filter in compressed air; teeth whitening, etc. (Bansal & Goyal, 2005). In the field of hydrometallurgy, activated carbon is well known for its use for precious metal recovery.

The adsorption mechanism of gold on activated carbons is not yet clearly understood. There are several possible mechanisms have been proposed, the more

important being (1) the ion pair theory, (2) the reduction theory and (3) the aurocyanide anion adsorption theory. Amongst these theories, it seems that the ion pair theory is the most acceptable one in gold adsorption studies (Jia et al., 1998). This theory proposed that gold is adsorbed on the activated carbons as an ion pair $Me^{n+}[Au(CN)2]_n$ (Me is metal ions), which is based on the observation of the spectator cations such as Ca^{2+} and Na^{+}, i.e. spectator cations were adsorbed only when they were present along with $Au(CN)_2^-$, while not when with CN^- (Davidson, 1974). Further studies suggested that the $Au(CN)_2^-$ ions were not experienced chemical changes such as a reduction of $Au(CN)_2^-$ to AuCN or metallic Au using different analytical methods such as Fourier transform infrared spectroscopy (FTIR) and X-Ray photoelectron spectroscopy (XPS) (McDougall et al., 1980).

2.4.4.2 CIL/CIP process

The use of activated carbon has been recognised as the dominant recovery method in the gold industry. According to a detailed review conducted by Staunton (2016), the earliest application of activated carbon for gold recovery can be traced back to the early 1890s, where gold was recovered from the chlorination leachates. Soon after, it was reported that activated carbon was used for the recovery of gold from cyanide leach solutions in the late 19th century. The development of the carbon-in-pulp (CIP) process had attracted many attentions from the gold industry, since its first development in the early 1950s by Zadra et al. (1952). However, activated carbon was not widely used in cyanidation for gold recovery until the 1980s. Nowadays, carbon-in-leach and carbon-in-pulp (CIL/CIP) process is the modern application of activated carbon as a substitution of the Merrill-Crowe process, where its application has now become the dominant gold recovery process. By 2000, hundreds of CIL/CIP plants had been built and operated (Staunton, 2016).

The CIL/CIP process is advantageous over the Merrill-Crowe process (Bansal & Goyal, 2005; Marsh, 2006):

- The adsorption of gold and silver is not significantly affected by the presence of other metals such as copper, nickel and antimony in solutions.
- The activated carbon is added directly into the cyanide pulp, thus preventing the clarification, deaeration and filtration stages of the Merrill-Crowe process and making the CIL/CIP process more economical.

- The activated carbon can be effectively eluted, and the regenerated carbon can be recycled to the adsorption circuit.
- Activated carbon can be applied for the solutions even at a very small concentration of gold (0.2 mg/L or even less)

The CIP process is a well-established technology which is more common compared with the CIL process. The typical CIP process incorporated with Electrowinning is shown in Figure 2.7. The screened cyanide leach slurry is being pulped to the adsorption tanks, the purpose of the screening is to remove any oversize materials such as woodchips that may block the interstage screen (Bailey, 1987). The slurry passes through several stages during the carbon adsorption, and the number of stages ranging from 4 to 10, with 5 or 6 most common, depending principally on the tank size, carbon concentration, and the amount of gold to be adsorbed. Interstage screens with apertures slightly smaller than that of the carbon, while large enough for a free flow of slurry between the stages are used to retain the carbon during the adsorption stage. The carbon and pulp move in a counter-current flow where the fresh and regenerated carbons are introduced at the last adsorption tank and transferred continuously to the upper adsorption stages, while the pulp moves in an opposite direction but at a much slower rate, that is due to the slurry flows by gravity from one stage to the next, while carbon is transferred by pumping. Therefore, the carbon in the first stage with the highest gold loading is then transferred to the elution circuit and the pulp in the last stage with depleted gold in solution is transfer to the tailing dam.

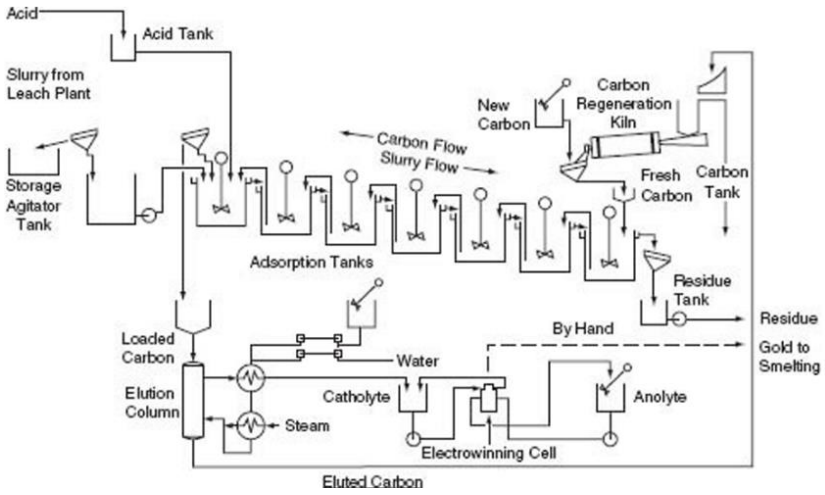

Figure 2.7 A classical CIP process (Marsden & House, 2009)

During the elution process, a hot strong alkaline cyanide solution is used to strip the gold from the loaded carbon, the concentration of solutions depends on the method used for elution. The Zadra process and the Anglo American Research Laboratories (AARL) process are the most common ones (Figure 2.7 shows a Zadra process). Zadra process can be operated at either ambient pressure or high pressure (400 to 500 kPa) using a solution containing about 1% to 2% of sodium hydroxide, and 0.1% of sodium cyanide. The pressure Zadra process can reach a temperature from135℃ to 140℃, which has a much faster elution time (8h to 14h) than the atmospheric Zadra process which normally operates at 95℃ with an elution time between 36h and 72h (Marsden & House, 2009). In the AARL process, carbon is acid washed by a dilute mineral acid and then preconditioned in 1% to 2% of sodium hydroxide and 3% of sodium cyanide solutions for 30 minutes. Thereafter, the carbon is eluted with 6 to 10 bed volume (BV) of deionised water at a flow rate of 2BV/h, a temperature from 110℃ to 120℃ and a pressure from 70 to 100 kpa. The elution time of the AARL process is normally in 8h to 14 h. The major difference between these two processes is that the AARL process requires an acid wash and a preconditioning stage, where the elution column with a butyl rubber-lined is required to withstand acid and alkaline media.

Electrowinning is usually incorporated with elution for the treatment of high-grade gold eluates to produce gold loaded cathodes which require further refining. The reduction reaction occurs at the cathode is shown in Eq. 26 (Marsden & House, 2009).

$$Au(CN)_2^- + e^- \rightarrow Au + 2CN^- \quad (26)$$

In the case of the Zadra process, electrowinning cells are in series with the elution column. The eluents are circulated between the elution column and the electrowinning cell until the gold content of the eluted carbon is less than 100g/t so that the carbon can be sent to regeneration process and then to the adsorption circuit. As for the AARL process, electrowinning is carried out on a batch of eluate that produced by a single pass through the elution column. The eluate is then recirculated through the cell until the gold concentration in solutions is low enough to be returned to the adsorption circuit (Costello, 2016).

A variety of organic and inorganic substances can be adsorbed on the carbon along with gold, resulting in a loss of activity of the carbon by blocking the active sites.

Carbon regeneration, or carbon reactivity, is, therefore, an important component in a CIP process as the average carbon activity in a circuit which is highly related to the gold recovery and gold loading kinetics is a function of the efficiency of the carbon regeneration process (Staunton, 2016). Effective carbon regeneration can be done thermally in a kiln, by heating the carbon to about 750 – 850℃ (measured in carbon bed) at a non-oxidising environment for 15 to 30 minutes to vaporise and burn off the volatile and non-volatile adsorbates (Claflin et al., 2015). However, due to a lack of focus in this area, e.g. underinvestment in good equipment, poor operating practices, and poor maintenance, the average regenerated carbon often has a kinetic activity no better than 50% (usually 20 – 40%) of the fresh carbon (Staunton, 2016).

The CIL process, on the other hand, is often an attractive option from a capital cost point of view as the carbon is added during the leaching, reducing the numbers of the agitated tanks in the gold processing plant. However, the CIL process is also problematic compared with the traditional CIP process, such as higher gold and carbon inventory (high carbon concentration), higher carbon loss due to carbon breakage and greater risk of carbon fouling and lower gold extraction owing to a reduction of residence time (Nicol et al., 1984).

2.3.3.3 Copper co-adsorption on activated carbon

The presence of copper in a cyanide leach solution can be problematic as copper can be readily adsorbed onto activated carbon and compete with gold under certain conditions, thus a higher carbon addition and a more complicated elution stage (Cu pre-elution stage) are required to maintain a high gold recovery (Sceresini & Breuer, 2016). To achieve a low Cu co-adsorption onto the carbon, high pH and high free-cyanide concentrations are required to stabilise the copper cyanide species in solution in the form of $Cu(CN)_3^{2-,}$ and $Cu(CN)_4^{3-}$ (Sceresini & Staunton, 1991). However, operating at pH > 10 is sometimes impractical when the process water is hypersaline, which means a high alkali consumption occurred owing to the buffering effect of magnesium precipitation (Staunton, 2016). If severe copper co-adsorption occurs, copper must be eluted by cyanide at ambient temperature before the hot elution of the gold, otherwise, it will result in a significant copper deposition along with gold at the cathode during electrowinning and production of high-copper gold bullion.

2.3.3.4 Carbon adsorption and elution from a glycine-based leach system

Detailed research conducted by Tauetsile (2019) investigated the feasibility of carbon adsorption to be used for the gold recovery from the glycine-based leach system. Fundamental studies based on the adsorption equilibrium isotherms and kinetics were undertaken on the glycine-only system (Tauetsile et al., 2018a, 2018b) and the synergetic glycine-cyanide system (Tauetsile et al., 2019a, 2019b). It was reported that activated carbon is an effective adsorbent for gold for both the glycine-based leach system, while it is also sensitive to the changing operating conditions e.g. glycine concentration, solution pH, ionic strength and initial gold and copper in solutions, and Cu:CN molar ratio in case of the cyanide-starved glycine solutions.

Tauetsile et al. (2018a, 2019a) conducted the adsorption isotherm studies of gold and copper onto the activated carbon from the alkaline glycine-based leach system using an empirical Freundlich model. It was reported that increasing the glycine concentration up to 10 g/L increased the gold loading capacity on the carbon, while reduced the copper co-adsorption due to an increasing force between copper and glycinate to keep copper in solution. The optimum solution pH was about 10, and the increasing pH lowered the gold adsorption capacity, mainly because of the formation of $Cu(OH)_2$ precipitates at high pH conditions, thus fouling the carbon by blocking the active sites. When Cu concentration was less than 20 ppm, the gold loading capacity increased more than doubled compared with that with no Cu present. While the gold loading capacity slightly decreased with the increasing Cu concentration when [Cu] > 20 ppm, resulting from the competition for active sites of the carbon between gold and copper. It was found that the addition of Ca^{2+} ions increased the gold loading significantly. Also, the higher Ca^{2+} concentration (i.e. higher ionic strength) resulted in an enhancement in gold adsorption.

As for the kinetic studies, the Fleming k, n adsorption model was used to analyse the adsorption data for the glycine-based leachates (Tauetsile et al., 2018b, 2019b). It was observed that over 99% of gold was adsorbed on the carbon in 24h for both glycine-based systems with more than 95% of gold recovery within 6h. For both systems, less than 50% of copper was co-adsorbed on the carbon with gold in 24h with the copper adsorption kinetics being significantly slower than that of gold. Process conditions such as solution pH, carbon additions and initial copper concentration can affect the rate of adsorption of gold but not the overall recovery, whereas those factors can affect both the adsorption rate and the recovery of copper.

In the case of cyanide-starved glycine system, the increase of CN:Cu molar ratio enhanced the initial adsorption rate of both gold and copper.

Tauetsile (2019) also investigated the elution of gold glycinate from the activated carbon using an AARL technique. Carbon was pre-loaded in an alkaline glycine-only system in the presence of Au with no Cu present. The loaded carbon was then washed by DI water and dried in an oven. The dry carbon was pre-treated by an acid wash using 3% HCl for 30 mins at 80℃ and then was soaked in a bed volume of solution containing 3% NaCN and 1% NaOH for 30 mins at 110℃ before being transferred into a stainless steel column with a bed volume of 20 cm^3. An elution efficiency of 87.68% was achieved by using 20BV of DI water at 130℃ and a pressure of 50 psi.

2.4.5 Ion-exchange resin adsorption

2.4.5.1 Ion-exchange (IX)

Ion exchange refers to a reaction that involves a reversible interchange of ions between a solid phase (normally ion-exchange resin) and a solution phase. Ion exchange a phenomenon of adsorption and the adsorption mechanism of ion exchange based on electrostatic can be either cation exchange or anion exchange (Harland, 1994). The basic cation exchange reaction may be represented by the following Eq. 27, where M^-A^+ represents the cation-exchanger carrying cation A^+, and B^+ is the cations in an aqueous solution phase.

$$M^-A^+ + B^+ \leftrightarrow M^-B^+ + A^+ \quad (27)$$

In the same way, anion (B^-) can be exchanged by an anion-receptive ion-exchanger (M^+A^-), the anion exchange reaction is described as Eq. 28.

$$M^+A^- + B^- \leftrightarrow M^+B^- + A^- \quad (28)$$

The ion-exchange technology is widely used in a variety of industries, including food and beverage, industrial water treatment, pharmaceuticals, chemicals, and hydrometallurgy. In hydrometallurgy, the primary applications are for gold and uranium recovery, while it is also employed in the recovery of rhenium, nickel, cobalt, copper and other valuable metals (van Deventer, 2011).

2.4.5.2 Type of IX resin

An ion-exchange resin is an insoluble cross-linked porous polymer substance consisting of ionogenic groups (or functional group) with mobile ions, which is the

most commonly used medium for ion exchange. According to (Horie et al., 2010), typical ion-exchange resins are fabricated based on crosslinked polystyrene i.e. copolymerisation of styrene and different levels of cross-linking agent (divinylbenzene). Activation of the copolymer is carried out by introducing the active ion-exchanging sites (functional groups) by polymerisation which is a process of reacting the monomers together in a chemical reaction to form polymer chains or three-dimensional networks.

Ion-exchange resin is described as being cationic or anionic, weak or strong and acidic or basic (Harland, 1994). The first classification refers to the charge on the counter-ion concern i.e. the cationic or anionic nature of the fix ions on the functional groups. The term strong base or strong acid has nothing at all related to the physical strength of the resin but is associated with their electrolyte chemistry sense meaning that they are highly ionised like the strong bases or acids with complete deionisation of OH^- or H^+. Strong base resins contain quaternary ammonium groups (e.g. $–CH_2N(CH_3)_3^+Cl^-$), while strong acid resins contain sulfonic acid groups (e.g. $–SO_3^-H^+$ or $–SO_3^-Na^+$). Weak acid resin typified by carboxylic acid functional groups (e.g. $–COO^-H^+$) which in their acid forms are only weakly ionised i.e. pK_a is from 4 to 6. Weak base resins containing primary, secondary or tertiary ammonium groups (e.g. $–CH_2NH(CH_3)_2^+Cl^-$) behave similarly to the weal acid resins that the degree of ionisation is pH-independent. Typically, weak acid resins are used for treating the solutions at less than pH 6, while weak base resins exhibit a minimum exchange capacity above a pH of 7. The strong base and strong acid resins can be used over the entire pH range.

The development of ion-exchange resin is on-going with different functional groups being polymerised on to the copolymers to enhance specific ion selectivity. A type of specific ion-exchange resins called chelating resins incorporated with a certain class of chemical reagents (e.g. iminodiacetate, amino-phosphonate, thiol, benzyl-triethylammonium and phenol) that form strong complexes with either cations or anions by chelation, usually exhibit a high affinity for specific ions (Oshita & Motomizu, 2008). The type of chelate structure to be expected in a resin is similar to that of the ethylenediaminetetraacetic acid (EDTA) complex. It should be noted that this type of resin does not necessarily mean an affinity to a specific ion, but commonly with relative affinities to several chemically similar ions compared with the conventional ion-exchange resins. For example, the amino-phosphonic

functionalised chelating resins have high selectivity towards divalent alkaline earth cations over monovalent ions (Harland, 1994).

A more recent ion-exchange resin developed based on a 'lock and key' chemistry called molecularly imprinted polymer (MIP) may exhibit an even higher selectivity towards specific ions, which has potential to be applied for metal recovery in hydrometallurgy, although this field is still small and not well recognised (Cheong et al., 2013). Molecular imprinted is a concept of preparing substrate-selective recognition sites in a matrix with a molecular template in a casting procedure. Molecular imprinted described as a way of making an artificial lock for a molecular key, the molecular imprinting procedure can be simplified as Fig. 2.8. During the synthesis, the molecular template (key) is first allowed to be polymerised with several types of functional monomers to form a polymer matrix. The molecular template is then washed from the matrix, leaving behind a complementary cavity (lock) which has a high selectivity to the original template molecule (Yan & Ramström, 2004).

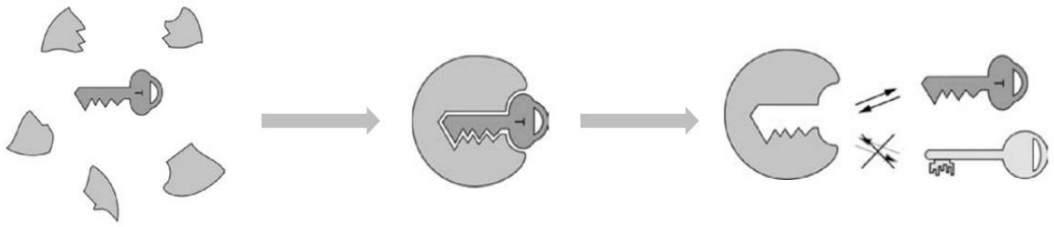

Figure 2.8 A simplified procedure of molecular imprinting (Yan & Ramström, 2004).

2.4.5.3 IX Resin for gold recovery

In the past decades, the significant development of gold-selective ion exchange resins which can selectively adsorb gold over base metal, have enabled the process such as resin-in-pulp (RIP) or resin-in-leach (RIL) as alternatives to CIP/CIL process for recovering gold from pregnant leach solution (Kotze et al., 2016). Although the significant advantages of using ion-exchange resin are well recognised, CIP/CIL process is still the preferred route for gold recovery in the Western World excluding Russia. Specifically, the advantages of using ion-exchange resins over activated carbon include (Fleming, 1998):

- Faster adsorption kinetics and higher gold loading capacity
- More suitable for gold recovery from carbonaceous ores
- Less likely to be poisoned by organics species

- The ability to be eluted at ambient temperature
- Do not require expensive thermal regeneration process
- Selectivity against Ca, Mg and silica
- Capability to minimise attrition and breakage
- Resistivity against blinding by fine clay particles

The major disadvantages to applying this technology would be the higher unit cost of resins, more complex elution processes, smaller particles size and lower densities than carbon that may lead to engineering challenges (Ben et al., 2017).

The RIP/RIL process is similar to the CIP/CIL process, while the elution circuit for the RIP/RIL process varies depending on one the type of the resins and mineralogy. There are several types of commercially available gold-selective resins and their elution methods have been well demonstrated. Most of them are demonstrated at a laboratory scale, while some of them have been successfully applied in RIP/RIL processes in commercial plants, for example, the Minix/Dowex® XZ-91419 resin was used at Penjom Gold Mine in Malaysia (G, Lewis, 2000) and Barbrook Gold Mine in South Africa (Anonymous, 2003); AM2B is the conventional strong-base resin which was widely used in the former Union of Soviet Socialist Republics (Lakshmanan et al., 2016).

Minix/Dowex® XZ-91419 resin

The Minix resin originally developed by Mintek is now commercialised by Dow Chemicals under a name Dowex® XZ-91419. The Minix resin is a type of strong-base resin, functionalised by tributylamine where its selective towards gold was based on lowering the functional group content. The Minix resin is particularly selective towards gold against cobalt and iron with a high gold adsorption capacity (~36300 g/t) (Fleming & Hancock, 1979; van Deventer, 2011).

Due to a strong affinity of the Minix resin for metal cyanide, gold is commonly eluted by acidic thiourea, while the base metals such as nickel, zinc and copper were removed by an acid wash. The elution can be improved by increasing the thiourea concentration, the acid concentration and the temperature. An elution recovery of 99.6% was achieved by using an eluent with 0.5M sulfuric acid and 1M thiourea at 60℃ (Conradie et al., 1995). However, HCN gas will be emitted during the acidic thiourea elution of the loaded resin, an effective gas extraction and scrubbing system is required regarding health and safety.

The Minix resin was successfully implemented in a RIL circuit which was converted from a CIL circuit, due to the preg-robbing nature of the ore containing 0.2% – 1.5% organic carbon. G. Lewis (2000) demonstrated that the Minix resin had been proved to have a good selectivity over base metals compared with the conventional strong-base resin such as AM2B. It was further reported that resin regeneration was simple and effective with an insignificant resin loss at below 5g/t in this plant and a residual gold at below 50 g/t (G. Lewis, 2000). Similarly, the Barbrook Gold Mine used Minix in a RIL circuit for gold recovery from a pre-robbing ore, but very little information is available about this plant (Anonymous, 2003).

Medium-base resin

The main advantage of using the medium-base resin is the elimination the risk of toxic HCN gas formation as they can be eluted at alkaline conditions. Representative examples of medium-base resins are S992 (Purolite) and Aurix® 100 (Congis).

A) S992 resin

The S992 resin contains a mixture of quaternary, tertiary, secondary, and primary amine groups. It can be used at pH values between 9 and 11, but a reduction of gold loading capacity occurs above pH 10.5 (van Deventer, 2011). It was reported that the S992 resin exhibited high selectivity towards gold against copper from a synthetic cyanide solution containing Au, Cu, Ni and Zn, that no copper adsorption was detected (Van et al., 2012). They also investigated the elution characteristics of S992 resin, and it was found that the resin can be effectively eluted under alkaline conditions, using a solution containing 20g/L NaCN and 10g/L NaOH at a flowrate of 2BV/h and 60℃. Complete elution of Au and other metals such as Fe, Ni and Zn was achieved within 8 BV, and the barren resin contained only 32g/t of gold. No pilot-scale or commercial-scale test work based on the S992 resin was recorded.

B) Aurix® 100

The Aurix® 100 resin developed by Congis has a guanidine functional group (A. Gray et al., 2005). S. Gray et al., (1999) performed a study using 200 g/L of Aurix® 100 resin to recover gold from intensive cyanidation leachate containing 4000 ppm gold and 11000 ppm copper at a very high pH of 13.1. The results showed that above 95% of gold was adsorbed with only about 1% of copper being co-adsorbed,

indicating a high selectivity of Aurix® 100 resin towards gold over copper at high pH. A. Gray et al. (2005) carried out a bench-scale test to investigate adsorption behaviour of Aurix® 100 using a synthetic solution containing 2 ppm Au, 300 ppm Ag and 100 ppm Cu and 1% of cyanide at pH values from 9.6 to 12. They found that the gold and silver recoveries were typically high at 100% and above 90% over the pH range tested, respectively. Whereas copper recovery was about 90% at pH 11, then the recovery dropped to zero at pH 12, implying that a cold alkaline solution may be able to elute the copper from the resin. Typical eluent for Aurix® 100 contains 40 g/L NaOH, 70 g/L sodium benzoate and 100 – 200 mg/l free cyanide. The addition of sodium benzoate is not necessary as it only affects the rate of elution but not the overall efficiency (A. Gray et al., 2005). The elution process is operated with electrowinning at a temperature of 60°C with single-pass efficiency from 66.5 – 91.7% and an overall gold recovery of 94.5 – 99.8% (Kotze et al., 2016). Pilot-scale tests were once conducted based on the Aurix® 100 resin (A. Gray et al., 2005; Fisher et al., 2000), but no commercial-scale application was recorded.

IXOS-AuC resin

A recent developed IXOS-AuC resin is a type of molecularly imprinted polymer (MIP) and a branch of nanotechnology which is specifically targeting aurocyanide. According to Ritz et.al. (2018), unlike the regular ion-exchange resin, the adsorption of gold cyanide onto the IXOS-AuC resin is based on a complementary charge and a physical imprint for aurocyanide, allowing the co-adsorption of other metals to be minimised. Also, the synthesis of the IXOS-AuC resin is different from that of the typical ion-exchange resins which are merely functionalised to allow metal ions to exchange with a donor ion. This kind of resin is synthesised using a combination of polystyrene and other monomers bound together by a functionalised ligand that imprints the shape of the $Au(CN)_2^-$ molecule during the polymerisation stage (Ritz et al., 2018). The physical imprint for aurocyanide which mitigates the formation of strong bonds between other metal cyanide complexes allows the target aurocyanide to be adsorbed preferentially and to displace the less boned metal cyanide during the adsorption. Ritz et al. (2018) stated that the IXOS-AuC resin can be eluted by thiocyanate or acidic thiourea, however, the elution conditions were not described. The application of this type of resin is still at a very early stage, further investigations are required.

2.4.5.4 IX resin for copper recovery

Sceresini and Breuer (2016) reviewed several processes using IX resins for copper and cyanide recovery. All of the processes used conventional strong-base resins such as Purolite A500, Vitrokele 912, Ameberite IRA900 and Dowex MSA1. It was noted by the authors that those resins performed in similar manners as they are all quaternary amine functionalised. These strong-base resins are usually characterised as low selectivity and tend to recover all the metal cyanide complexes in solution. Additionally, the anion metal cyanide complexes are strongly bonded with the strong-base resin, thus intensive elution conditions (e.g. acidic thiourea) are usually required.

For the glycine-based leach system, all copper is present as cupric glycinate in a glycine-only system, while most of the copper is present as cupric glycinate in a cyanide-starved glycine system. Thus, it will be not feasible to recover Cu using the anion strong-base/medium-base resin, since the cupric glycinate is a neutral species. The neutral cupric glycinate is expected to undergo an equilibrium reaction as shown in Eq 29. It is predicted that the copper dissociated from the cupric glycinate can be recovered by the cation ion-exchangers.

$$Cu(NH_2CH_2COO)_2 \leftrightarrow Cu^{2+} + 2(NH_2CH_2COO)^- \quad (29)$$

Several types of chelating resins which exhibit an affinity to copper ion are reviewed in the following section.

A) Puromet MTS9300

Puromet MTS9300 is a weak base/acid cation resin possessing an iminodiacetic functional group with Na^+ as the mobile ion. It is generally used for base metal removals such as Cu, Co, Ni and Zn and wastewater treatment. Riley et al., (2018) reported that the MTS9300 resin showed high selectivity towards Cu^{2+} and Fe^{3+} at low H^+ concentration i.e. high pH conditions, indicating that it may be suitable for the alkaline glycine-based system. Similar chelating resins (e.g. Chelax 100, Amberlite IRC – 718) with the same functional groups (H^+ form) also showed high selectivity on the adsorption of divalent transition metal ions, particularly copper and nickel (Lehto et al., 1994; Leinonen & Lehto, 2000). The anion iminodiacetate can act as a tridentate ligand to complex with metal ions, particularly divalent metal ions, and form stronger metal complexes than the bidentate ligand glycine (Krishnamurthy, 2009; Schwarzenbach, 1952), implying the dominant Cu^{2+} from

the cupric glycinate in the cyanide-starved glycine solutions can be adsorbed by this type of chelating resin.

B) Puromet MTS9600

The Puromet MTS9600 resin is a weak base resin with the bis-picolylamine functional group, which has three nitrogen donor atoms and two of them are in the aromatic pyridyl groups (tertiary amine). Similar commercially available bis-picolylamine functionalised resins include Dowex M4195 and Lewatit MonoPlus TP-220. The application of this type of resin can be considered for removal, separation and purification of metal ions from water, solid waste and wastewater (Diniz et al., 2005; Wołowicz & Hubicki, 2010). Some research studies indicated that the bis-picolylamine functionalised resin showed a very high Cu affinity (99% recovery) compared to other metals such as Al, Fe, Pb, Sn, Ni, Zn, Au and Ag in an acidic environment (Neto et al. 2016; Riley et al. 2018; Wołowicz & Hubicki, 2012). It should be noted that due to the cationic nature of ammonium functional groups, this type of resin can also adsorb anion species (Wołowicz & Hubicki, 2012), thus this type of resin may be able to load the anion cuprous cyanide, gold cyanide and gold glycinate from the cyanide-starved glycine system.

C) Puromet MTS9850

The Puromet MTS9850 is polyamine functionalised weak base resin with the deprotonated form of amines and is used for heavy metal removal and purification from wastewater. Kononova et al. (2014) investigated the adsorption behaviours of Cu and Zn from acidic chloride solutions and they found that MTS9850 resin showed the greatest affinity to Cu^{2+} compared with a strong-based resin Purolit A500. However, it was observed that the MTS9850 exhibited poor selectivity towards divalent transition elements e.g. Cu, Ni, Co and Zn (Riley et al., 2018). Again, similar to the MTS9600 resin, it is expected that a co-adsorption Cu^{2+} with other anion species from the cyanide-starved glycine solutions may occur due to the anionic nature of the MTS9850 resin.

Such types of resins are normally stripping in a concentrated acidic solution, usually between 1 to 2M using either HCl or HNO_3 (Kononova et al., 2014; Malla et al., 2002; J. Wang et al., 2012; Wołowicz & Hubicki, 2012). It is noted that for the alkaline glycine-based system, particularly the cyanide-starved glycine system, the eluted resin by acid should be regenerated in a high concentration alkali solution, otherwise, it may cause health and safety risks as toxic HCN gases can be evolved.

Therefore, it is better to explore an effective alkaline-based eluent for Cu elution for the alkaline cyanide-starved glycine system.

2.5 Summary

This chapter of the thesis summarised that copper-gold ores deposits are important resources for both gold and copper. There is a huge reserve of copper-gold resources in the form of porphyry deposits and iron-oxide-copper-gold deposits distributed over the world. The significance of gold and copper regarding their value and applications in different fields were highlighted. The chemistry and operations of the current leaching technologies such as cyanidation, ammonia-cyanide leaching, and non-cyanide leaching for gold extraction from copper-gold ores were reviewed. A review of glycine-based leach system including the glycine-only and the synergetic glycine-cyanide system was given. Different recovery techniques i.e. solvent extraction, sulfide precipitation, zinc cementation, carbon adsorption and ion-exchange adsorption for gold and copper were discussed. Among these approaches, sulfide precipitation and ion-exchange resin adsorption were particularly emphasised as both techniques are innovative options for metals recovery from glycine solutions. The application of sulfide precipitation and ion-exchange resins are the main focuses of this study.

2.6 References

Adams, M., D. (2016). *Gold ore processing: project development and operations / edited by Mike D. Adams* (2nd ed.): Amsterdam, [Netherlands]: Elsevier.

Aksu, S., & Doyle, F. (2001). Electrochemistry of copper in aqueous glycine solutions. *J. Electrochem. Soc., 148*(1), B51-B57.

Anonymous, 2003. Caledonia shows multi-commodity promise. Mining Mirror September, 10-15.

Alodan, M., & Smyrl, W. (1998). Effect of thiourea on copper dissolution and deposition. *Electrochimica Acta, 44*(2), 299-309. https://doi.org/10.1016/S0013-4686(98)00060-7

Anonymous. (2016). Green vehicles could drive copper boom; Electric vehicles require more copper. *Mining Engineering, 68*(12), 18.

Aylmore, M. (2016a). Alternative lixiviants to cyanide for leaching gold ores. In M.D Adams (Ed.), *Gold Ore Processing* (2nd ed., pp 447-484). Elsevier B.V.

Aylmore, M. (2016b). Thiosulfate as an alternative lixiviant to cyanide for gold ores. In M.D Adams (Ed.), *Gold Ore Processing* (2nd ed., pp 485-523). Elsevier B.V.

Aylmore, M. G. (2005). Alternative lixiviants to cyanide for leaching gold ores. In M.D Adams (Ed.), *Gold Ore Processing* (1st ed., pp 501-539). Elsevier B.V.

Aylmore, M. G., & Muir, D. M. (2001). Thiosulfate leaching of gold—A review. *Minerals Engineering, 14*(2), 135-174. https://doi.org/10.1016/S0892-6875(00)00172-2

Bailey, P. (1987). Application of Activated Carbon to Gold Recovery. (Retroactive Coverage). *South African Institute of Mining and Metallurgy, The Extractive Metallurgy of Gold in South Africa. Vol. 1, pp. 379-614, 1987, 1*, 379-614.

Bansal, R. C., & Goyal, M. (2005). Activated carbon adsorption / Roop Chand Bansal, Meenakshi Goyal: Boca Raton : Taylor & Francis.

Beckmann, W. (2013). Crystallization: Basic Concepts and Industrial Applications (1. Aufl.1st ed.). Weinheim: Weinheim: Wiley-VCH.

Ben, S., Jeff, B., & Stephen, L., Brooy. (2017). Gold recovery via ion exchange resins. In ALTA 2017, Gold-PM Proceedings, Perth, Australia.

Cheong, W. J., Yang, S. H., & Ali, F. (2013). Molecular imprinted polymers for separation science: A review of reviews. *Journal of Separation Science, 36*(3), 609-628. https://doi.org/10.1002/jssc.201200784

Chung, J., Jeong, E., Choi, J. W., Yun, S. T., Maeng, S. K., & Hong, S. W. (2015). Factors affecting crystallization of copper sulfide in fed-batch fluidized bed reactor. *Hydrometallurgy, 152*, 107-112. https://doi.org/10.1016/j.hydromet.2014.12.014

Claflin, J.K., La Brooy, S.R., Preedy, D.R., Slater, A., Urutia, F., 2015. Fast pay-back reactivation of carbon from a flotation tails CIL circuit. In: Proceedings of the World Gold Conference 2015 (SAIMM Symposium Series S85). SAIMM, Johannesburg, 337-348.

Conradie, P. J., Johns, M. W., & Fowles, R. J. (1995). Elution and electrowinning of gold from gold-selective strong-base resins. *Hydrometallurgy, 37*(3), 349-366. doi:https://doi.org/10.1016/0304-386X(94)00032-X

Costello, M. (2016). Chapter 33 - Electrowinning. In M. D. Adams (Ed.), *Gold Ore Processing (2nd Edition)* (pp. 585-594): Elsevier.

Dai, X., Breuer, P., Hewitt, D., & Bergamin, A. (2013). *Thiosulfate process for treating gold concentrates*. Paper presented at the World Gold 2013, Brisbane, Queensland, Australia.

Dai, X., Simons, A., & Breuer, P. (2011). A review of copper cyanide recovery technologies for the cyanidation of copper containing gold ores. *Minerals Engineering*. https://doi.org/10.1016/j.mineng.2011.10.002

Davidson, R. J. (1974). The mechanism of gold adsorption on activated charcoal. Journal of the South African Institute of Mining and Metallurgy, 75(4), 67-76.

Davis, M., Sole, K., Mackenzie, J., & Virnig, M. (1998). A proposed solvent extraction route for the treatment of copper cyanide solutions produced in leaching of gold ores. In M. Davis (Ed.), (pp. 2/1-2/44).

Dean, J. A. (1990). LANGE'S HANDBOOK OF CHEMISTRY. *Materials and Manufacturing Processes, 5*(4), 687-688. https://doi.org/10.1080/10426919008953291

Diniz, C. V., Ciminelli, V. S. T., & Doyle, F. M. (2005). The use of the chelating resin Dowex M-4195 in the adsorption of selected heavy metal ions from manganese solutions. *Hydrometallurgy, 78*(3), 147-155. https://doi.org/10.1016/j.hydromet.2004.12.007

Donnet, M., Bowen, P., Jongen, N., Lemaître, J., & Hofmann, H. (2005). Use of Seeds to Control Precipitation of Calcium Carbonate and Determination of Seed Nature. *Langmuir, 21*(1), 100-108. https://doi.org/10.1021/la048525i

Dreisinger, D., Ji, J., & Wassink, B. (1995). The solvent extraction and electrowinning recovery of copper and cyanide using XI7950 extractant and membrane cell electrolysis. *Randol Gold Forum '95*, 239-244.

Du, T., Vijayakumar, A., & Desai, V. (2004). Effect of hydrogen peroxide on oxidation of copper in CMP slurries containing glycine and Cu ions. *Electrochimica Acta, 49*(25), 4505-4512. https://doi.org/10.1016/j.electacta.2004.05.008

Eksteen, J. J., & Oraby, E. A. (2015). The leaching and adsorption of gold using low concentration amino acids and hydrogen peroxide: Effect of catalytic ions, sulphide minerals and amino acid type. *Minerals Engineering, 70*, 36-42. https://doi.org/10.1016/j.mineng.2014.08.020

Eksteen, J. J., Oraby, E. A., & Tanda, B. C. (2017). A conceptual process for copper extraction from chalcopyrite in alkaline glycinate solutions. *Minerals Engineering, 108*, 53-66. https://doi.org/10.1016/j.mineng.2017.02.001

Eksteen, J. J., Oraby, E. A., Tanda, B. C., Tauetsile, P. J., Bezuidenhout, G. A., Newton, T., Bryan, I. (2018). Towards industrial implementation of glycine-based leach and adsorption technologies for gold-copper ores. *Canadian Metallurgical Quarterly, 57*(4), 390-398. https://doi.org/10.1080/00084433.2017.1391736

Eksteen, J. J., Pelser, M., Onyango, M. S., Lorenzen, L., Aldrich, C., & Georgalli, G. A. (2008). Effects of residence time and mixing regimes on the precipitation characteristics of CaF 2 and MgF 2 from high ionic strength sulphate solutions. *Hydrometallurgy, 91*(1), 104-112. https://doi.org/10.1016/j.hydromet.2007.12.002

Estay, H. (2018). Designing the SART process – A review. *Hydrometallurgy, 176*, 147-165. https://doi.org/10.1016/j.hydromet.2018.01.011

Fang, Z., & Muhammed, M. (1992). Leaching of Precious Metals from Complex Sulphide Ores. On the Chemistry of Gold Lixiviation by Thiourea. *Mineral Processing and Extractive Metallurgy Review, 11*(1-2), 39-60. https://doi.org/10.1080/08827509208914213

Farahani, B. V., Rajabi, F. H., Bahmani, M., Ghelichkhani, M., & Sahebdelfar, S. (2014). Influence of precipitation conditions on precursor particle size distribution and activity of Cu/ZnO methanol synthesis catalyst. *Applied Catalysis A, General, 482*, 237-244. https://doi.org/10.1016/j.apcata.2014.05.034

Fisher, G.T., Lewis, R.G., Virnig, M.J., Mackenzie, J.M.W., Davis, M.R., 2000. Cognis AuRIX 100 resin for gold extraction, engineering cost study and pilot plant investigations. In: ALTA 2000 SX/IX-1. ALTA Metallurgical Services, Melbourne.

Fleming, C. A. (1998). *The potential role of anion exchange resins in the gold industry*. In EPD Congress 1998 (pp. 95-117).

Fleming, C. A., & Hancock, R. D. (1979). The mechanism in the poisoning of anion-exchange resins by cobalt cyanide. *Journal of the South African Institute of Mining and Metallurgy, 79*(11), 334-341.

Freitas, L. R., Trindade, R. B. E., & Carageorgos, T. (2001). *Thiosulfate leaching of gold-copper ores from Igarape Bahia mine (CVRD).* Paper presented at the Proceedings of the Sixth Southern Hemisphere Meeting on Mineral Technology.

Godfrey, J. C., & Slater, M. J. (1994). *Liquid-liquid extraction equipment / edited by J.C. Godfrey and M.J. Slater*. Chichester

González-López, J., Rodelas, B., Pozo, C., Salmerón-López, V., Martínez-Toledo, M. V., & Salmerón, V. (2005). Liberation of amino acids by heterotrophic nitrogen fixing bacteria. *Amino Acids, 28*(4), 363-367. https://doi.org/10.1007/s00726-005-0178-9

Gray, A., Hughes, T., & Abols, J. (2005). The Use of AuRIX®100 Resin for the Selective Recovery of Gold and Silver From Copper, Gold and Silver Solutions. *Australasian Institute of Mining and Metallurgy Publication Series*.

Gray, S., Katsikaros, N., & Fallon, P. (1999). Gold recovery from gold-copper gravity concentrates using the InLine Leach Reactor and weak-base resin. In S. Gray (Ed.), (pp. 67-79).

Groudev, S. N., Ivanov, I. M., Spasova, I. I., & Groudeva, V. I. (1995). Pilot-scale microbial leaching of gold and silver from an oxide ore in Elshitza Mine, Bulgaria. In (pp. 135-144).

Gylienė, O. (2001). Insoluble compounds of heavy metal complexes. Paper presented at the XVI-th ARS SEPARATORIA, Borówno, Poland.

Harland, C. E. (1994). *Ion-exchange: theory and practice / C. E. Harland* (2nd ed.). London: Royal Society of Chemistry.

Herb, B. (2013). Gold. *Nature, 495*(7440), S1. https://doi.org/10.1038/495S1a

Hilson, G., & Monhemius, A. J. (2006). Alternatives to cyanide in the gold mining industry: what prospects for the future? *Journal of Cleaner Production, 14*(12-13), 1158-1167. https://doi.org/10.1016/j.jclepro.2004.09.005

Hiskey, J. B., & Qi, P. H. (1991). *Leaching behaviour of gold in iodide solutions*. Paper presented at the World Gold ’91, Melbourne.

Horie, K., Barón, M., Fox, R., Hess, M., Kahovec, J., Kitayama, T., Work, W. (2010). Definitions of terms relating to reactions of polymers and to functional polymeric materials (IUPAC Recommendations 2003). *Pure and Applied Chemistry. Chimie Pure et Appliquee, 76*(4), 889-906. https://doi.org/10.1351/pac200476040889

Houcine, I., Plasari, E., David, R., & Villermaux, J. (1997). Influence of mixing characteristics on the quality and size of precipitated calcium oxalate in a pilot scale reactor. *Chemical Engineering Research and Design, 75*(2), 252-256. https://doi.org/10.1205/026387697523534

Hunt, B., 1901. U.S. Patent 689190.

Jia, Y. F., Steele, C. J., Hayward, I. P., & Thomas, K. M. (1998). Mechanism of adsorption of gold and silver species on activated carbons. *Carbon, 36*(9), 1299-1308. https://doi.org/10.1016/S0008-6223(98)00091-8

Jiang, T., Zhang, Y.-z., Yang, Y.-b., & Huang, Z.-c. (2001). Influence of copper minerals on cyanide leaching of gold. *Science & Technology of Mining and Metallurgy, 8*(1), 24-28. https://doi.org/10.1007/s11771-001-0019-2

Kesler, S. E., Chryssoulis, S. L., & Simon, G. (2002). Gold in porphyry copper deposits: its abundance and fate. *Ore Geology Reviews, 21*(1), 103-124. https://doi.org/10.1016/S0169-1368(02)00084-7

Kharaka, Y. K., Law, L. M., Carothers, W. W., & Goerlitz, C. F. (1986). Role of organic species dissolved in formation waters from sedimentary basins in mineral digenesis. from The Society of Economic Paleontologists and Mineralogists (SEPM), U.S. Geological Survey

Kononova, O., Kuznetsova, M., Mel'nikov, A., Karplyakova, N., & Kononov, Y. (2014). Sorption recovery of copper (II) and zinc (II) from chloride aqueous solutions. *Journal of the Serbian Chemical Society, 79*, 1037-1049. https://doi.org/10.2298/JSC130911033K

Kotze, M., Green, B., Mackenzie, J., & Virnig, M. (2016). Chapter 32 - Resin-in-Pulp and Resin-in-Solution. In M. D. Adams (Ed.), *Gold Ore Processing (2nd Edition)* (pp. 561-583): Elsevier.

Krishnamurthy, G. T. (2009). *Nuclear Hepatology : A Textbook of Hepatobiliary Diseases / by Gerbail T. Krishnamurthy, S. Krishnamurthy*. Berlin, Heidelberg: Berlin, Heidelberg : Springer Berlin Heidelberg.

La Brooy, S. R., Komosa, T., & Muir, D. M. (1991). *Selective leaching of gold from copper-gold ores using ammonia-cyanide mixtures*. Paper presented at the 5th Extractive Metallurgy Conference - AusIMM 1991, Perth.

Lacoste-Bouchet, P., Deschênes, G., & Ghali, E. (1998). Thiourea leaching of a copper-gold ore using statistical design. *Hydrometallurgy, 47*(2), 189-203. https://doi.org/10.1016/S0304-386X(97)00043-1

Lakshmanan, V. I. e., Roy, R. e., & Ramachandran, V. e. (2016). *Innovative Process Development in Metallurgical Industry: Concept to Commission / edited by Vaikuntam Iyer Lakshmanan, Raja Roy, V. Ramachandran* (1st ed. 2016.. ed.): Cham: Springer International Publishing : Imprint: Springer.

Langhans, J. W., Lei, K. P. V., & Carnahan, T. G. (1992). Copper-catalyzed thiosulfate leaching of low-grade gold ores. *Hydrometallurgy, 29*(1-3), 191-203. https://doi.org/10.1016/0304-386X(92)90013-P

Lehto, J., Paajanen, A., Harjula, R., & Leinonen, H. (1994). Hydrolysis and H + Na + exchange by Chelex 100 chelating resin. *Reactive Polymers, 23*(2), 135-140. https://doi.org/10.1016/0923-1137(94)90013-2

Lewis, G.V., (2000). *"The Penjom Process" an innovative approach to extracting gold from carbonaceous ore.* Gold Processing in the 21st Century, An International Forum. AJ Parker Cooperative Research Centre for Hydrometallurgy, Perth, Australia.

Leinonen, H., & Lehto, J. (2000). Ion-exchange of nickel by iminodiacetic acid chelating resin Chelex 100. *Reactive and Functional Polymers, 43*(1), 1-6. https://doi.org/10.1016/S1381-5148(98)00082-0

Lewis, A., & van Hille, R. (2006). An exploration into the sulphide precipitation method and its effect on metal sulphide removal. *Hydrometallurgy, 81*(3), 197-204. https://doi.org/10.1016/j.hydromet.2005.12.009

Lewis, A. E. (2010). Review of metal sulphide precipitation. *Hydrometallurgy, 104*(2), 222-234. https://doi.org/10.1016/j.hydromet.2010.06.010

Li, H., Oraby, E., & Eksteen, J. (2020). Extraction of copper and the co-leaching behaviour of other metals from waste printed circuit boards using alkaline glycine solutions. *Resources, Conservation & Recycling, 154*. https://doi.org/10.1016/j.resconrec.2019.104624

Liang, C. J., & Li, J. Y. (2019). Recovery of gold in iodine-iodide system - a review. *Separation Science and Technology, 54*(6), 1055-1066. doi:10.1080/01496395.2018.1523931

Linga, Å. (2017). Effects of Seeding on the Crystallization Behaviour and Filtration Abilities of an Aromatic Amine. [Master's thesis, NTNU]. https://ntnuopen.ntnu.no/ntnu-xmlui/handle/11250/2461109

Malla, M. E., Alvarez, M. B., & Batistoni, D. A. (2002). Evaluation of sorption and desorption characteristics of cadmium, lead and zinc on Amberlite IRC-718 iminodiacetate chelating ion exchanger. *Talanta, 57*(2), 277-287. https://doi.org/10.1016/S0039-9140(02)00034-6

Marcant, B., & David, R. (1991). Experimental evidence for and prediction of micromixing effects in precipitation. *AIChE Journal, 37*(11), 1698-1710. https://doi.org/10.1002/aic.690371113

Marsden, J. O., & House, C. I. (2009). *Chemistry of Gold Extraction* (2nd ed.). Littleton: SME.

Marsh, H. (2006). *Activated carbon / Harry Marsh, Francisco Rodríguez-Reinoso* (1st ed.). Amsterdam: Elsevier.

McDougall, G. J. H. R. D. N. M. J. W. O. L., & Copperthwaite, R. G. (1980). The mechanism of the adsorption of gold cyanide on activated carbon. *Journal of the South African Institute of Mining and Metallurgy, 80*(9), 344-356.

Mersmann, A. (1999). Crystallization and precipitation. *Chemical Engineering & Processing: Process Intensification, 38*(4), 345-353. https://doi.org/10.1016/S0255-2701(99)00025-2

Mokone, T. P., van Hille, R. P., & Lewis, A. E. (2010). Effect of solution chemistry on particle characteristics during metal sulfide precipitation. *Journal of Colloid And Interface Science, 351*(1), 10-18. https://doi.org/10.1016/j.jcis.2010.06.027

Muir, D. M. (2011). A review of the selective leaching of gold from oxidised copper–gold ores with ammonia–cyanide and new insights for plant control and operation. *Minerals Engineering, 24*(6), 576-582. https://doi.org/10.1016/j.mineng.2010.08.022

Muir, D. M., La Brooy, S. R., & Cao, C. (1989). *Recovery of copper from copper bearing ores*. Paper presented at the World Gold '89, Warrendale.

Muir, D. M., Vukcevic, S., & Shuttleworth, J. (1995). *Optimising the ammonia–cyanide process for copper–gold ores.* Paper presented at the Proceedings Randol Gold Forum, Perth.

Nicol, M. J., Fleming, C.A., amp, & Cromberge, G. (1984). The absorption of gold cyanide onto activated carbon. II. Application of the kinetic model to multistage absorption circuits. *84*(3), 70-78.

O'Connor, G. M., Lepkova, K., Eksteen, J. J., & Oraby, E. A. (2018). Electrochemical behaviour of copper in alkaline glycine solutions. *Hydrometallurgy, 181*, 221-229. https://doi.org/10.1016/j.hydromet.2018.10.001

Oraby, E. A., & Eksteen, J. J. (2014). The selective leaching of copper from a gold–copper concentrate in glycine solutions. *Hydrometallurgy, 150*, 14-19. https://doi.org/10.1016/j.hydromet.2014.09.005

Oraby, E. A., & Eksteen, J. J. (2015a). Gold leaching in cyanide-starved copper solutions in the presence of glycine. *Hydrometallurgy, 156*, 81-88. https://doi.org/10.1016/j.hydromet.2015.05.012

Oraby, E. A., & Eksteen, J. J. (2015b). The leaching of gold, silver and their alloys in alkaline glycine–peroxide solutions and their adsorption on carbon. *Hydrometallurgy, 152*(C), 199-203. https://doi.org/10.1016/j.hydromet.2014.12.015

Oraby, E. A., Eksteen, J. J., Karrech, A., & Attar, M. (2019). Gold extraction from paleochannel ores using an aerated alkaline glycine lixiviant for consideration in heap and in-situ leaching applications. *Minerals Engineering, 138*, 112-118. https://doi.org/10.1016/j.mineng.2019.04.023

Oraby, E. A., Eksteen, J. J., & Tanda, B. C. (2017). Gold and copper leaching from gold-copper ores and concentrates using a synergistic lixiviant mixture of glycine and cyanide. *Hydrometallurgy, 169*, 339-345. https://doi.org/10.1016/j.hydromet.2017.02.019

Oraby, E. A., Li, H., & Eksteen, J. J. (2019). An Alkaline Glycine-Based Leach Process of Base and Precious Metals from Powdered Waste Printed Circuit Boards. *Waste and Biomass Valorization*. https://doi.org/10.1007/s12649-019-00780-0

Oshita, K., & Motomizu, S. (2008). Development of chelating resins and their ability of collection and separation for metal ions. In *Bunseki Kagaku* (Vol. 57, pp. 291-311).

Pakiari, A. H., & Jamshidi, Z. (2007). Interaction of amino acids with gold and silver clusters. *The journal of physical chemistry. A, 111*(20), 4391-4396. https://doi.org/10.1021/jp070306t

Patel, D. D., & Anderson, B. D. (2013). Maintenance of supersaturation II: Indomethacin crystal growth kinetics versus degree of supersaturation. *Journal of Pharmaceutical Sciences, 102*(5), 1544-1553. https://doi.org/10.1002/jps.23498

Pian, H., & Santosh, M. (2019). Gold deposits of China: Resources, economics, environmental issues, and future perspectives. *Geological Journal*. 1-12. https://doi.org/10.1002/gj.3531

Riley, A. L., Pepper, S. E., Canner, A. J., Brown, S. F., & Ogden, M. D. (2018). Metal recovery from jarosite waste – A resin screening study. *Separation Science and Technology, 53*(1), 22-35. https://doi.org/10.1080/01496395.2017.1378679

Ritz, S., Gluckman, J., Southard, G., Maull, B., & Kim, D. J. (2018). *Imprinted Resin—The 21st Century Adsorbent.* Extraction 2018, Proceedings of the 1st Global Conference on Extactive Metallurgy, Ottawa, Canada.

Rydberg, J. (2004). *Solvent extraction principles and practice / edited by Jan Rydberg .[et al.]* (2nd ed.). New York: M. Dekker.

Sampaio, R. M. M., Timmers, R. A., Kocks, N., André, V., Duarte, M. T., van Hullebusch, E. D., Lens, P. N. L. (2010). Zn–Ni sulfide selective precipitation: The role of supersaturation. *Separation and Purification Technology, 74*(1), 108-118. https://doi.org/10.1016/j.seppur.2010.05.013

Sampaio, R. M. M., Timmers, R. A., Xu, Y., Keesman, K. J., & Lens, P. N. L. (2009). Selective precipitation of Cu from Zn in a pS controlled continuously stirred tank reactor. *Journal of Hazardous Materials, 165*(1), 256-265. https://doi.org/10.1016/j.jhazmat.2008.09.117

Sceresini, B. (2005). Gold-Copper Ores. In D. A. M. B. A. Wills (Ed.), *Developments in Mineral Processing* (Vol. 15, pp. 789-824): Elsevier.

Sceresini, B., & Breuer, P. (2016). Chapter 43 - Gold-Copper Ores. In M. D. Adams (Ed.), *Gold Ore Processing (2nd Edition)* (pp. 771-801): Elsevier.

Sceresini, B., & Staunton, W. P. (1991). Copper/cyanide in the treatment of high copper gold ores. In (pp. 123-125).

Schwarzenbach, G. (1952). Der Chelateffekt. *35*(7), 2344-2359. https://doi.org/10.1002/hlca.19520350721

Shaofeng, L., & Shuixing, F. (2016). A Research Review of Iron Oxide Copper-Gold Deposits. *Acta Geologica Sinica - English Edition, 90*(4), 1341-1352. https://doi.org/10.1111/1755-6724.12773

Sillitoe, R. H., & Meinert, L. D. (2010). Porphyry copper systems. *Economic Geology and the Bulletin of the Society of Economic Geologists, 105*(1), 3-41. https://doi.org/10.2113/gsecongeo.105.1.3

Simons, A., & Breuer, P. (2011). *The effect of process variables on cyanide and copper recovery using SART*. ALTA 2011, Gold Procceedings, Perth, Australia.

Söhnel, O., & Garside, J. (1992). *Precipitation: basic principles and industrial applications / Otakar Söhnel and John Garside*. Oxford [England]

Sparrow, G. J., & Woodcock, J. T. (1995). Cyanide and Other Lixiviant Leaching Systems for Gold with Some Practical Applications. *Mineral Processing and Extractive Metallurgy Review, 14*(3-4), 193-247. https://doi.org/10.1080/08827509508914125

Stace, C. R. (1984). *Selective Passivation of Sulfides*. Technical report, No R84/043, CRA Services Ltd Research, Cockle Creek.

Staunton, W. P. (2016). Chapter 30 - Carbon-in-Pulp. In M. D. Adams (Ed.), *Gold Ore Processing (2nd Edition)* (pp. 535-552): Elsevier.

Tanda, B. C, Eksteen, J., & Oraby, E. (2018). Kinetics of chalcocite leaching in oxygenated alkaline glycine solutions. *Hydrometallurgy, 178*, 264-273. https://doi.org/10.1016/j.hydromet.2018.05.005

Tanda, B. C. (2017). *Glycine as a lixiviant for the leaching of low grade copper-gold ores* [Dotoral thesis, Curtin University].

Tanda, B. C., Eksteen, J. J., & Oraby, E. A. (2017). An investigation into the leaching behaviour of copper oxide minerals in aqueous alkaline glycine solutions. *Hydrometallurgy, 167*, 153-162. https://doi.org/10.1016/j.hydromet.2016.11.011

Tanda, B. C., Eksteen, J. J., Oraby, E. A., & O'Connor, G. M. (2019). The kinetics of chalcopyrite leaching in alkaline glycine/glycinate solutions. *Minerals Engineering, 135*, 118-128. https://doi.org/10.1016/j.mineng.2019.02.035

Tanda, B. C., Oraby, E. A., & Eksteen, J. J. (2017). Recovery of copper from alkaline glycine leach solution using solvent extraction. *Separation and Purification Technology, 187*, 389-396. https://doi.org/10.1016/j.seppur.2017.06.075

Tanda, B. C., Oraby, E. A., & Eksteen, J. J. (2018). Kinetics of malachite leaching in alkaline glycine solutions. *Mineral Processing and Extractive Metallurgy: Transactions of the Institute of Mining and Metallurgy*, 128(1). https://doi.org/10.1080/25726641.2018.1505211

Tauetsile, P. J. (2019). *Adsorption of Gold and Copper from Alkaline Glycine-based Leach Solutions using Activated Carbon* [Dotoral thesis, Curtin University].

Tauetsile, P. J., Oraby, E. A., & Eksteen, J. J. (2018a). Adsorption behaviour of copper and gold glycinates in alkaline media onto activated carbon. Part 1: Isotherms. *Hydrometallurgy, 178*, 202-208. https://doi.org/10.1016/j.hydromet.2018.04.015

Tauetsile, P. J., Oraby, E. A., & Eksteen, J. J. (2018b). Adsorption behaviour of copper and gold Glycinates in alkaline media onto activated carbon. Part 2: Kinetics. *Hydrometallurgy, 178*, 195-201. https://doi.org/10.1016/j.hydromet.2018.04.016

Tauetsile, P. J., Oraby, E. A., & Eksteen, J. J. (2019a). Activated carbon adsorption of gold from cyanide-starved glycine solutions containing copper. Part 1: Isotherms. *Separation and Purification Technology, 211*, 594-601. https://doi.org/10.1016/j.seppur.2018.09.024

Tauetsile, P. J., Oraby, E. A., & Eksteen, J. J. (2019b). Activated carbon adsorption of gold from cyanide-starved glycine solutions containing copper. Part 2: Kinetics. *Separation and Purification Technology, 211*, 290-297. https://doi.org/10.1016/j.seppur.2018.09.022

Torbacke, M., & Rasmuson, Å. C. (2001). Influence of different scales of mixing in reaction crystallization. *Chemical Engineering Science, 56*(7), 2459-2473. https://doi.org/10.1016/S0009-2509(00)00452-8

Tran, T., Lee, K., & Fernando, K. (2001). Halide as an alternative lixiviant for gold processing - an update. In (pp. 501-508).

Tremblay, L., Deschênes, G., Ghali, E., McMullen, J., & Lanouette, M. (1996). Gold recovery from a sulphide bearing gold ore by percolation leaching with thiourea. *International Journal of Mineral Processing, 48*(3-4), 225-244. https://doi.org/10.1016/S0301-7516(96)00029-4

Van, D., Yahorava, V., & Kotze, M. (2012). *Gold Recovery from Copper-rich Ores Employing the Purolite S992 Gold Selective Ion Exchange Resin*: Mintek.

van Deventer, J. (2011). Selected Ion Exchange Applications in the Hydrometallurgical Industry. *Solvent Extraction and Ion Exchange, 29*(5-6), 695-718. https://doi.org/10.1080/07366299.2011.595626

Veeken, A. H. M., de Vries, S., van Der Mark, A., & Rulkens, W. H. (2003). Selective Precipitation of Heavy Metals as Controlled by a Sulfide-Selective Electrode. *Separation Science and Technology, 38*(1), 1-19. https://doi.org/10.1081/SS-120016695

Walton, R. (2016). Chapter 31 - Zinc Cementation. In M. D. Adams (Ed.), *Gold Ore Processing (2n Edition)* (pp. 553-560): Elsevier.

Wang, J., Xu, L., Cheng, C., Meng, Y., & Li, A. (2012). Preparation of new chelating fiber with waste PET as adsorbent for fast removal of Cu2+ and Ni2+ from water: Kinetic and equilibrium adsorption studies. *Chemical Engineering Journal, 193-194*, 31-38. https://doi.org/10.1016/j.cej.2012.03.070

Wang, X., & Forssberg, K. S. E. (1990). The Chemistry of Cyanide-Metal Complexes in Relation to Hydrometallurgical Processes of Precious Metals. *Mineral Processing and Extractive Metallurgy Review, 6*(1-4), 81-125. https://doi.org/10.1080/08827509008952658

Wołowicz, A., & Hubicki, Z. (2010). Selective Adsorption of Palladium(II) Complexes onto the Chelating Ion Exchange Resin Dowex M 4195 - Kinetic Studies. *Solvent Extraction and Ion Exchange, 28*(1), 124-159. https://doi.org/10.1080/07366290903408953

Wołowicz, A., & Hubicki, Z. (2012). The use of the chelating resin of a new generation Lewatit MonoPlus TP-220 with the bis-picolylamine functional groups in the removal of selected metal ions from acidic solutions. *Chemical Engineering Journal, 197*, 493-508. https://doi.org/10.1016/j.cej.2012.05.047

Wong, S. Y., Myerson, A. S., & Cui, Y. (2013). Contact secondary nucleation as a means of creating seeds for continuous tubular crystallizers. *Crystal Growth and Design, 13*(6), 2514-2521. https://doi.org/10.1021/cg4002303

Xia, C., Yen, W., & Deschenes, G. (2003). Improvement of thiosulfate stability in gold leaching. *An Official International Peer-reviewed Journal of the Society, 20*(2), 68-72. https://doi.org/10.1007/BF03403135

Xiao-Hua, C., & Bing, X. (2013). Recent advances on asymmetric Strecker reactions. *Arkivoc, 2014*(1), 205. https://doi.org/10.3998/ark.5550190.p008.487

Xie, F., & Dreisinger, D. (2009a). Copper Solvent Extraction from Waste Cyanide Solution with LIX 7820. *Solvent Extraction and Ion Exchange, 27*(4), 459-473. https://doi.org/10.1080/07366290902966829

Xie, F., & Dreisinger, D. (2009b). Recovery of copper cyanide from waste cyanide solution by LIX 7950. *Minerals Engineering, 22*(2), 190-195. https://doi.org/10.1016/j.mineng.2008.07.001

Yan, M., & Ramström, O. (2004). *Molecularly Imprinted Materials: Science and Technology*. Baton Rouge: Baton Rouge: CRC Press.

Zadra, J. B., Engel, A. L., Heinen, H. J., & United States. (1952). *Process for recovering gold and silver from activated carbon by leaching and*

electrolysis. Washington, D.C.: U.S. Department of the Interior, Bureau of Mines.

Zhu, Z. (2016). Gold in iron oxide copper–gold deposits. *Ore Geology Reviews, 72*(1), 37-42. https://doi.org/10.1016/j.oregeorev.2015.07.001

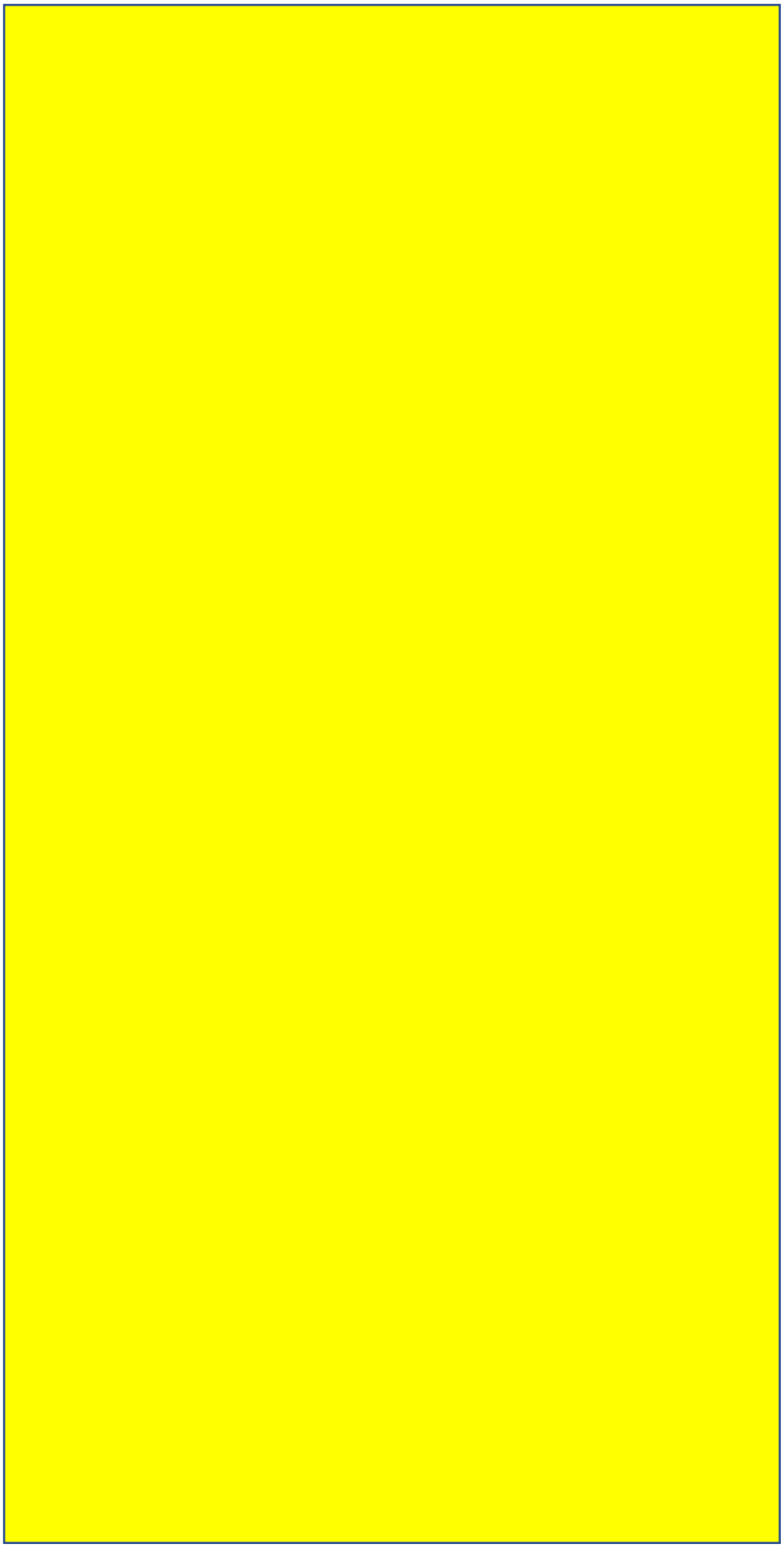

Chapter 3: The sulfide precipitation behaviour of Cu and Au from cyanide-starved glycine solutions

Submitted for publication as:

The sulfide precipitation behaviour of Cu and Au from their aqueous alkaline glycinate and cyanide complexes

Deng, Z. Oraby, E.A. and Eksteen, J.J., 2019.

Separation and Purification Technology, 218, pp.181-190.

Accepted for publication on 28 February 2019.

© 2019 Elsevier Ltd.

Reprinted with permission from the publisher.

DOI: https://doi.org/10.1016/j.seppur.2019.02.056

Separation and Purification Technology 218 (2019) 181–190

Contents lists available at ScienceDirect

Separation and Purification Technology

journal homepage: www.elsevier.com/locate/seppur

The sulfide precipitation behaviour of Cu and Au from their aqueous alkaline glycinate and cyanide complexes

Z. Deng[a], E.A. Oraby[a,b], J.J. Eksteen[a,*]

[a] Western Australian School of Mines: Minerals Energy and Chemical Engineering, Curtin University, GPO Box U1987, Perth, Western Australia, 6845, Australia
[b] Faculty of Engineering, Assiut University, Egypt

ARTICLE INFO

Keywords:
Sulfide precipitation
Glycine
Cyanide
Copper
Gold

ABSTRACT

Recently, a novel leach process for treating gold-copper ores and concentrates by glycine in the presence of starved cyanide in solutions were investigated where the Cu species are present as cuprous cyanide and cupric glycinate. Often Cu-levels in these gold ores are insufficient to economically justify solvent extraction with electrowinning, and sulfide precipitation is often preferred. This research reports the precipitation behaviour of Cu and Au from glycine-cyanide solutions by adding NaHS. Contrary to conventional cyanide-only systems, where all the copper is present as cuprous cyanide and alkaline precipitation of copper by sulfide addition is not feasible, the synergistic lixiviant system leads to a cupric-dominant system where copper can be precipitated. As the leach solution mainly contains glycine(Gly), cyanide(CN^-) and copper in alkaline environment, the effect of glycine concentration [Gly], [HS^-]: [Cu_T] and [CN^-]: [Cu_T] molar concentration ratios, pH, temperature and reaction time on the Cu and Au precipitation have been studied, where [Cu_T] = [Cu^+] + [Cu^{2+}]. The results show that CuS precipitation (covelite) increased slightly with moderately elevated temperature, but decreased significantly with increasing [CN^-]:[Cu_T] molar ratio. CuS precipitation was found to be insensitive to [HS^-]: [Cu_T] molar ratio, glycine concentrations, pH and reaction time. Pre-oxidation of cuprous Cu^+ to cupric Cu^{2+} was carried out using H_2O_2 to confirm the effect of oxidation state on copper precipitation. The kinetics of pre-oxidation was fast and above 95% of Cu^+ were oxidized to Cu^{2+} in 5 min. The optimal [H_2O_2]:[Cu^+] molar ratio was found to be 5:1 and 4:1 at [CN^-]:[Cu_T] molar ratio of 2:1 and 1:1 respectively, implying significant reagent consumption to complete the reaction. With pre-oxidation and oxygen removal by nitrogen gas stripping, a Cu recovery as high as 96.5% was achieved with the addition of 1.4 mol of sulfide per mole Cu_T for 5 min at [Cu]:[CN^-]:[Gly] molar ratio of 1:2:3 and pH 10.5. No Au co-precipitation was observed after precipitation for most of tested conditions. This study showed that a high level of Cu and Au separation can be obtained by sulphide precipitation with H_2O_2 pre-oxidation from CN-starved glycine solutions and allowing Au to be subsequently removed by activated carbon.

1. Introduction

Due to the decrease in high grade and free milling gold resources, a great proportion of gold deposits in the 21st century are now processing complex gold ores that contain soluble copper minerals. One of the options to recover the dissolved copper from the leachate is to precipitate the copper using sulfide such as sodium sulfide (Na_2S), sodium hydrosulphide (NaHS), or hydrogen sulfide (H_2S). Sulfide precipitation plays an important part in hydrometallurgical processes with the several merits over hydroxide precipitation, including lower solubility of precipitate, higher selectivity for metal removal, faster reaction rates, better settling properties and the copper can be easily recovered by smelting [12].

In the process of extracting gold from gold-copper ores by traditional cyanidation, copper can also be recovered as a by-product, and cyanide can be recycled by processes such as Metallgesellschaft Natural Resources (MNR) [19] or the Sulfurisation-Acidification-Recycle-Thickening (SART) process [1,10,11]. SART process is a relatively advanced technology compared with the MNR process in terms of safety and equipment size that includes thickening and recycling stages instead of only using filtration to separate the solid precipitates [10,11]. These two processes are based on the protonation of cyanide by adding acid to achieve low pH, releasing cyanide in copper cyanide complexes through reactions Eq. (1)–(4) [5]:

$$Cu(CN)_4^{3-} \leftrightarrow Cu(CN)_3^{2-} + CN^- \quad (1)$$

* Corresponding author.
E-mail address: jacques.eksteen@curtin.edu.au (J.J. Eksteen).

https://doi.org/10.1016/j.seppur.2019.02.056
Received 6 October 2018; Received in revised form 22 February 2019; Accepted 28 February 2019
Available online 01 March 2019
1383-5866/ © 2019 Elsevier B.V. All rights reserved.

$$Cu(CN)_3^{2-} \leftrightarrow Cu(CN)_2^- + CN^- \quad (2)$$

$$Cu(CN)_2^- \leftrightarrow CuCN + CN^- \quad (3)$$

$$CuCN_{(s)} \leftrightarrow Cu^+ + CN^- \quad (4)$$

After acidification, adding bisulfide (HS^-) ion to the copper cyanide solutions leads to the copper precipitation as chalcocite as shown in Eq. (5) [10]. A recent study have cast doubt upon the existence of free "S^{2-}·" in aqueous solutions based off the recent analytical and instrumental chemistry using a new Raman spectra [14]. This does not particularly influence our analysis, although previous sulfide precipitation papers may have used the free sulfide anion. For the SART system, the following reaction can therefore be proposed (historically this would have been written as free sulfide (S^{2-})) and

$$2Cu(CN)_3^{2-} + HS^- + 5H^+ \rightarrow Cu_2S + 6HCN_{(g)} \quad (5)$$

During the reaction, toxic hydrogen cyanide (HCN) gas is generated where an effective gas extraction and scrubbing system is required, giving rise to higher capital and operational costs. HCN and water are soluble in each other in all proportions and HCN has a strong water affinity, making it quite hard (high gas flows required with its associated blower costs and relatively large equipment) to effectively strip HCN from aqueous solutions for reabsorption into caustic solutions. Also, the use of sulfuric acid during acidification can lead to the formation of scale when lime is used for pH modification [5]. That is due to the reaction between sulfate and calcium to form gypsum which should be removed periodically.

Recently, a new process using glycine as an alternative lixiviant in alkaline medium for gold and copper extraction has been invented and published [7,9,15,17,16,22,24,25]. Glycine has many advantages for its non-toxicity, ease of handling, non-volatility, cost-efficacy, and high stability over a wide range of pH-E_h and non-reactivity towards most ubiquitous gangue minerals. It was found that gold foils can be dissolved in alkaline glycine condition at a moderately elevated temperature in the presence of oxidants such as hydrogen peroxide and activated carbon can be an effective adsorbent for gold removal from the alkaline glycine solutions. [7,17,26,27]. Tanda et al. [23] has shown how copper can be removed from is alkaline glycinate leachates using solvent extraction, and Tauetsile et al. [28,29] has studied the adsorption of gold and copper from glycinate-cyanide solutions.

In a cyanide-starved glycine system with cyanide (11 mM) and glycine (13 mM), the gold dissolution rate was about 6.5 higher than that in the conventional cyanidation with the same amount of cyanide (11 mM) [16]. At the end of the leaching, the amount of cyanide is too small and is not measurable by traditional titration with silver nitrate. Thus all of the cyanide complex with Cu to form cuprous cyanide (with higher forms of complexation when more cyanide is present). Also, it was indicated that a glycine-cyanide synergistic (GCS) leaching process has a better gold, silver and copper recovery and faster dissolution rates compared to traditional cyanidation; in the presence of glycine, the cyanide consumption can be reduced by at least 75% [18] with commensurate savings in cyanide detoxification, whereas glycine can predominantly be recycled. It was reported that 99.5% gold extraction and 95.5% copper extraction were obtained when treating gold-copper gravity concentrate at ambient temperature in a solution with 800 ppm NaCN and 5 g/L glycine [18]. The authors have shown that in the GCS system, the copper minerals were complexed with cyanide and form different cuprous cyanide species (CuCN, $Cu(CN)_2^-$, $Cu(CN)_3^{2-}$ and $Cu(CN)_4^{3-}$), depending on the cyanide to copper ratio in solution. The CuCN, and $Cu(CN)_2^-$ can be oxidized to cupric glycinate in the presence of glycine and oxidants, thus reducing the levels of WAD cyanide and releasing more free cyanide to leach and complex with gold. Additionally, most of the copper present are in form of cupric glycinate at the end of the leaching, although a low level of copper cyanide species may remain; the reactions are indicated in Eqs. (6) and (7).

$$8CuCN + 8(NH_2CH_2COO)^- + O_2 + 2H_2O \rightarrow 4Cu(NH_2CH_2COO)_2 + 4Cu(CN)2^- + 4OH^- \quad (6)$$

$$4Cu(CN)_2^- + 8(NH_2CH_2COO)^- + O_2 + 2H_2O \rightarrow 4Cu(NH_2CH_2COO)_2 + 8CN^- + 4OH^- \quad (7)$$

A study carried out by Eksteen et al. [8,9] pointed out that copper can be effectively precipitated as fast settling, coarse grained, covelite from cyanide-free cupric glycinate leachates by adding NaHS powder. Their results showed that 99.1% of copper can be precipitated at a bisulde (HS^-) to total copper (Cu_T) molar ratio of 1:1 in a cyanide-free system, where total the molar concentration total copper equates to the sum of the cupric and cuprous molar concentrations, i.e., $[Cu_T] = [Cu^+] + [Cu^{2+}]$. The study was conducted on a leachate derived from chalcopyrite using glycine as the only lixiviant at pH of 11. The XRD pattern data indicated that the copper sulphide precipitate is pure covellite (CuS).

However, alkaline cyanide systems behave quite different to their alkaline glycinate counterparts. A study carried out by Simons [20] illustrated that zero copper recovery was obtained by adding Na_2S from a solution containing 2000 mg/L copper with a $[CN^-]$:$[Cu_T]$ ratio of 3:1 and $[HS^-]$:$[Cu_T]$ ratio of 0.5:1 at pH 10. Tauetsile et al. [26,27] illustrated that the dicyanocuprate $[Cu(CN)_2^-]$ complex has a higher affinity to adsorb onto activated carbon than the cupric glycinate equivalent (both having two moles of ligand coordinated with the copper). It is, therefore, proposed to oxidize the cuprous ions to cupric ions by the use of an oxidant such as hydrogen peroxide (H_2O_2) before precipitation·H_2O_2 is particularly favorable as it does not introduce any additional pollutant. According to Chen et al. [3], copper cyanide species ($Cu(CN)_3^{2-}$ and $Cu(CN)_2^-$) can be destroyed progressively by H_2O_2 as own in Eqs. (8)–(10). During the reactions, cyanide was oxidized to cyanate and consequently Cu^+ was released and then oxidized to Cu^{2+} by H_2O_2 through a Fenton-like reaction. In the presence of glycine, Cu^{2+} will be complexed with glycine to form cupric glycinate instead of $Cu(OH)_2$ in alkaline conditions, as shown in Eq. (11).

$$Cu(CN)_3^{2-} + H_2O_2 \rightarrow Cu(CN)_2^- + CNO^- + H_2O \quad (8)$$

$$Cu(CN)_2^- + 2H_2O_2 \rightarrow Cu^+ + 2(CNO)^- + 2H_2O \quad (9)$$

$$Cu^+ + H_2O_2 \rightarrow Cu^{2+} + {}^{\cdot}OH + OH^- \quad (10)$$

$$Cu^{2+} + 2NH_2CH_2COO^- \rightarrow Cu(NH_2CH_2COO)_2 \quad (11)$$

In terms of gold, it is expected that the precipitation will not occur, although some literature focused on SART process demonstrates that a small amount of gold ranging from about 1.5% to 30% was precipitated at different acidic pH values from 2.5 to 6 [20,13,6]. As for an alkaline glycine system, a gold loss of 16% and 24% was also reported after precipitation by adding NaHS from a leachate containing 784 mg/L $[Cu_T]$ and 0.241 mg/L gold at $[HS^-]$:$[Cu_T]$ molar ratio of 1:1 and 1.1:1 [21]. It is suggested by Simons [20] that the gold loss might be attributed to the adsorption of copper precipitates instead of precipitation of gold as a sulfide due to the slight recovery of gold. Nevertheless, the behaviour of gold from cyanide-starved solutions by sulfide precipitation remains unknown.

The main aim of this study is to evaluate the behavior of copper and gold during sulfide precipitation in a synthetic glycine-cyanide solutions. The effects of pre-oxidation of Cu^+ to Cu^{2+} using hydrogen peroxide as an oxidant were also evaluated. For the precipitation tests without pre-oxidation, parameters which may affect the precipitation process were investigated, including $[HS^-]$:$[Cu_T]$ molar ratio, [Gly]:$[Cu_T]$ molar ratio, $[CN^-]$:$[Cu_T]$ molar ratio, reaction time, pH and temperature. Regarding the pre-oxidation tests, the kinetics of the oxidation with different $[H_2O_2]$:$[Cu^+]$ molar ratio at different $[CN^-]$:$[Cu_T]$ molar ratios were investigated. The effects of different parameters, including dissolved oxygen, $[HS^-]$:$[Cu_T]$ molar ratio, reaction

time and gold concentration on the copper precipitation with pre-oxidation were also studied. Free glycine analysis before and after oxidation and precipitation by titration was also performed to establish if the oxidation led to any measureable glycine destruction.

2. Experimental design

2.1. Synthetic solutions

All tests in this study were conducted using synthetic solutions, and analytical grade reagents and deionized water were used throughout the tests. A stock cyanide-starved glycine solution containing gold and copper was first prepared. Gold powders (99.998%, spherical, −200 mesh, Alfar Aesar – Thermo Fisher Scientific) were dissolved in deionized water contained glycine (> 99%, Sigma-Aldrich) and CuCN (95%, Ajax, Finechem). The pH of the solutions were buffered at pH 10 using sodium hydroxide (NaOH), and then the pH was adjusted to 10.5 using $Ca(OH)_2$ (Chem-Supply Pty Ltd) with a pH meter (Model AQUA-PH Meter). The solution was agitated with a magnetic stirrer and Teflon magnetic stirrer bars at 350 rpm. The solution was filtered with a Supor® 0.45 µm membrane disc filter (Pall Corporation) prior to the tests. A standard solution of glycine in the presence of starved cyanide containing 300 mg/L Cu_T, 1 mg/L Au at $[Cu_T]$:$[CN^-]$:[Gly] molar ratio of 1:1:3 was obtained by diluting the stock solution accordingly.

2.2. Pre-oxidation

Pre-oxidation tests were performed in a 500 ml beaker agitated with a magnetic stirrer at 350 rpm. Various concentrations of hydrogen peroxide (30% w/v, Rowe Scientific) were added based on the Cu^+ concentration which was determined by the differences between $[Cu^{2+}]$ and $[Cu_T]$ using a UV–Vis and an atomic adsorption spectrometer (AAS, Agilent 55B AAS model), respectively. Samples were taken by a 10 ml syringe up to 4 h and the DO level was measured by a Syland M6000 DO meter.

2.3. Precipitation

Small-scale batch precipitation tests were conducted in a 200 ml beaker equipped with magnetic stirring facilities. A fresh high concentration of NaHS (0.5 g/ml) solution was used to avoid the effect of solution volume changes. The NaHS solution was added in relation to the moles of total copper in the leach solution. The precipitates were filtered by a vacuum filter and a Supor® 0.45 µm membrane disc filter paper (Pall Corporation). The solution samples before and after precipitation were analyzed for copper and gold by AAS tests to calculate the recovery of copper and gold. A UV–Vis spectrum was used to measure the concentration of Cu^{2+}. The concentration of Cu^+ in solutions was calculated by the differences between the total copper and the cupric ions. Zeta potential (Eh) was measured before and after precipitation using an Ionode platinum electrode with a Ag/AgCl reference. Free glycine concentration was measured by an acid-based titration method.

3. Results and discussions

3.1. Precipitation without pre-oxidation

3.1.1. Effects of $[HS^-]$:$[Cu_T]$ molar ratio

For a typical SART process, stoichiometric sulfide dosage values varied between 95 and 120% were used to achieve copper recovery higher than 85% [10]. The effects of different $[HS^-]$:$[Cu_T]$ molar ratio ranging from 1:1 to 3:1 on the metals precipitation from a solution containing 300 mg/L Cu_T, 1 mg/L Au, in the presence of glycine and cyanide $[Cu_T]$:$[CN^-]$:[Gly] = 1:1:3) were investigated and the results are shown in Table 1. It is clear from Table 1 that the copper removals peaked at 69.1% with $[HS^-]$:$[Cu_T]$ molar ratio of 1.3:1, and a decrease of copper removal was observed with the increasing $[HS^-]$:$[Cu_T]$ molar ratio. It is illustrated that the excess amount of sulfide tend to re-dissolve the copper precipitates by forming soluble copper polysulphide species in solutions [12,30], thus lowering the copper removal. No Cu^{2+} was present after the precipitation at $[HS^-]$:$[Cu_T]$ molar ratio ranging from 1.1:1 to 3:1. The remaining copper in solutions was cuprous cyanide which cannot be further precipitated with the increasing $[HS^-]$:$[Cu_T]$ molar ratio. A $[HS^-]$:$[Cu_T]$ molar ratio of 1:1 could not precipitate all the cupric ions that around 30 mg/L of Cu^{2+} remained in the filtrate.

Table 1
Metals removal and Cu^{2+} concentration after precipitation as different $[HS^-]$:$[Cu_T]$. Experimental conditions: 300 mg/L Cu_T, 1 mg/L Au, $[Cu_T]$:$[CN^-]$:[Gly] molar ratio = 1:1:3, pH = 10.5 and 5 min reaction time.

$[HS^-]$:$[Cu_T]$	$[Cu^{2+}]$ after precipitation	pH after precipitation	Cu_T removal	Au Removal
	mg/l		%	%
1:1	30	10.41	62.8	0.0
1:1.1	0	10.23	68.1	0.0
1.3:1	0	10.20	69.1	0.0
1.6:1	0	10.31	68.0	0.0
2:1	0	10.34	66.1	0.0
3:1	0	10.35	68.3	0.0

The pH values after bisulfide precipitation were shown in Table 1, it can be seen that the pH bottomed at a $[HS^-]$:$[Cu_T]$ ratio of 1.3:1 and then increased slightly with the increasing sulfide additions. It is proposed that bisulfide in solutions was first consumed by the cupric ions to produce covellite (CuS) and hydrogen ions (H^+) that decreased the pH, as shown in Eq. (12) [4].

$$Cu^{2+} + HS^- \rightarrow CuS_{(s)} + H^+ \quad (12)$$

The remaining HS^- in aqueous solutions underwent hydrolysis (equilibria shown in Eq. (13) [2], producing hydrogen sulfide (H_2S) and hydroxide (OH^-) that increased the solution pH.

$$HS^- + H_2O \leftrightarrow H_2S + OH^- \quad (13)$$

The change of pH indicated that a complete precipitation of Cu^{2+} was achieved at a $[HS^-]$:$[Cu_T]$ molar ratio of 1.3:1 and the excess sulfide addition influenced the equilibrium (Eq. (13)) that produced more OH^- and increased the solution pH.

Redox potential (E_h), usually used as an indicator for sulphide dosage, was also measured after the precipitation. As can be seen in Fig. 1, the results show that a more reducing E_h were observed with the increasing $[HS^-]$:$[Cu_T]$ molar ratio. This indicates that an E_h range from −200 to −300 mV (relative to a Ag/AgCl electrode) is optimum for the precipitation. It can also be seen from Table 1, no gold precipitation was observed, despite the presence of excess bisulphide. This implies that it is possible to achieve a high level of gold and copper separation if most of the copper can be precipitated.

3.1.2. Effects of reaction time

The effects of reaction time were also evaluated and the results are shown in Fig. 2. It is obvious that the reaction rate of the precipitation was fast, as 69.1% copper removal was achieved in 5 min, followed by a minor increase up to 72.8% at 30 min. The copper precipitation decreased slightly at 60 min, which might be owing to the re-dissolution of the copper sulfide precipitates in the presence of glycine. Similar experimental data were also obtained from the Telfer SART plant where a re-dissolution of copper sulfide precipitates (i.e.Cu_2S) was observed due to the prolonged residence time during the thickening process [20]. Moreover, it is noted that a small portion of gold (2.2%) were co-precipitated at 60 min, which agrees with the previous studies that report a small portion of gold loss occur during SART process [20,13,6]. It was

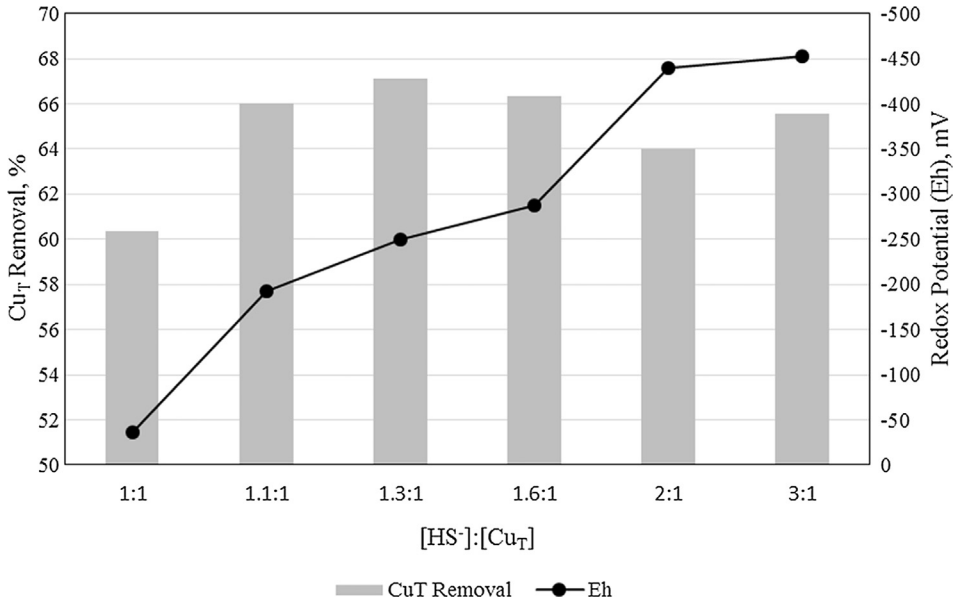

Fig. 1. Copper removal and Eh as a function of [HS^-]:[Cu_T]. Experimental conditions: 300 mg/L Cu_T, 1 mg/L Au, [Cu_T]:[CN^-]:[Gly] molar ratio = 1:1:3, pH = 10.5 and 5 mins reaction time.

also observed that the particle settling was being faster and larger particles were retained on the filter paper with time. This may be ascribed to the effects of aging that involves recrystallization of non-equilibrium shapes of primary particles to more compact shapes [31].

3.1.3. Effects of [Gly]:[CuT] molar ratio

An increase of [Gly]:[Cu_T] molar ratio up to (2.2:1) is favorable to higher gold and copper extractions during the GCS leaching process, further increase of the glycine concentration in the system have no evident effects on gold and copper extractions [18]. To evaluate the effects of glycine concentration on the metals precipitation, tests were performed at different [Gly]:[Cu_T] molar ratio ranged from 3:1 to 8:1. As can be observed from Table 2, there is no obvious variation in terms of metals removal (no gold precipitation). In addition, with the increasing [Gly]:[Cu_T] molar ratio, there are no noticeable changes in Cu^{2+} concentration in solutions after 4 h mixing. A reasonable explanation is that the transformation from cuprous cyanide to cupric glycinate is a slow redox reaction where sufficient oxidants are

Table 2
Metals removal and initial Cu^{2+} concentration at different [Gly]: [Cu_T] molar ratio. Experimental conditions: 300 mg/L Cu_T, 1 mg/L Au, [CN^-]:[Cu_T] = 1:1, pH = 10.5, [HS^-]:[Cu_T] = 1.3:1 and 5 min reaction time.

[Gly]:[Cu_T]	Initial [Cu^{2+}]	Cu_T removal	Au removal
	mg/L	%	%
3:1	200	68.8	0.0
4:1	202	69.4	0.0
6:1	202	69.4	0.0
8:1	203	69.9	0.0

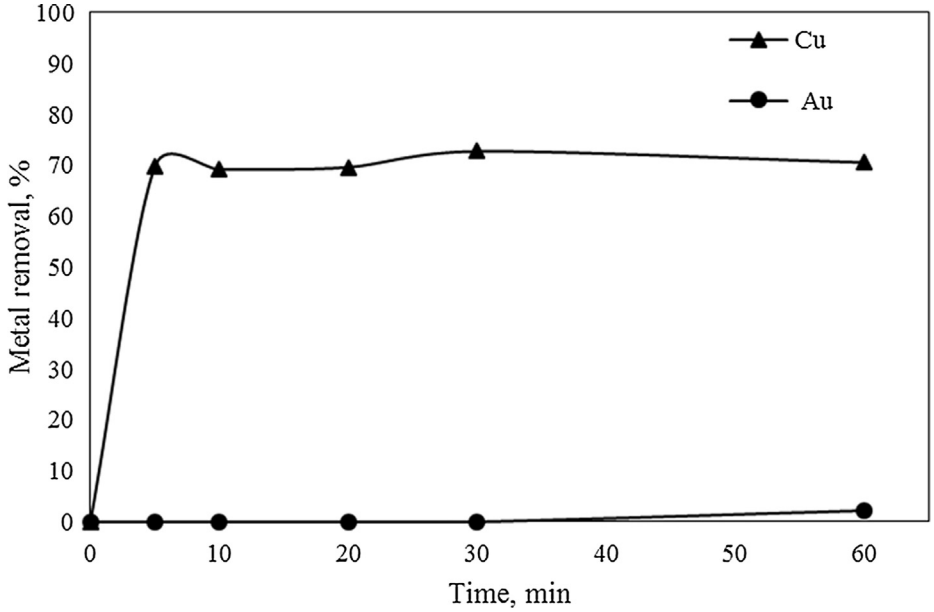

Fig. 2. Copper and gold removal as a function of reaction time. Experimental conditions: 300 mg/L Cu_T, 1 mg/L Au, [Cu_T]:[CN^-]:[Gly] molar ratio = 1:1:3, pH = 10.5 and [HS^-]:[Cu_T] = 1.3:1.

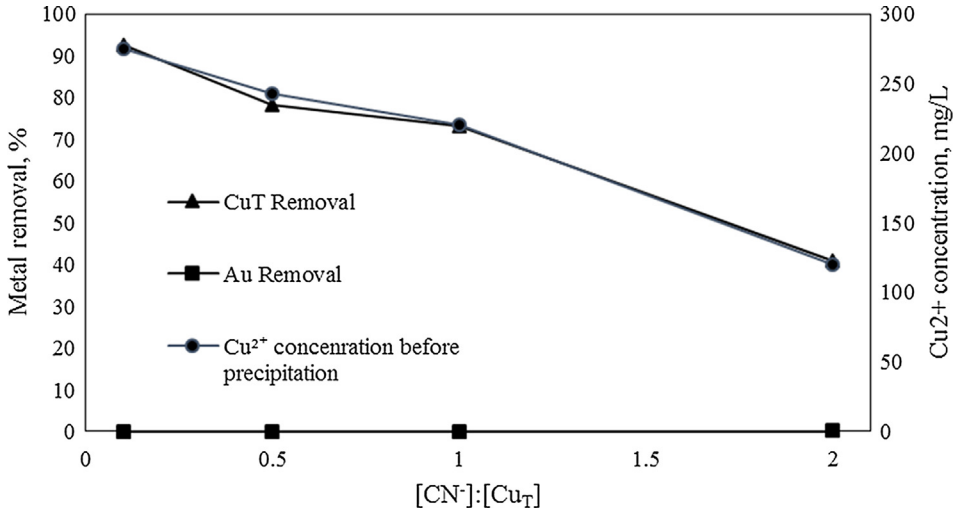

Fig. 3. Metal removal and Cu^{2+} concentration at different levels of $[CN^-]$:$[Cu_T]$ molar ratio. Other conditions: 300 mg/L Cu_T, 1 mg/L Au, [Gly]:$[Cu_T]$ = 3:1, pH = 10.5, $[HS^-]$:$[Cu_T]$ = 1.3:1 and 5 min reaction time.

required. Also, this phenomenon demonstrates that the dissolutions of copper sulfide precipitates were insignificant in the presence of excess amount of free glycine.

3.1.4. Effects of $[CN^-]$:$[Cu_T]$ molar ratio

Precipitation tests at four levels of $[CN^-]$:$[Cu_T]$ molar ratio and fixed glycine concentration ([Gly]:$[Cu_T]$ molar ratio of 3:1) were carried out to investigate the effects of cyanide concentration on the copper and gold removal. Solid CuCN was dissolved in glycine solutions and then $CuSO_4{\cdot}5H_2O$ powders were added accordingly to achieve the required total copper concentration (i.e. 300 mg/L) and low $[CN^-]$:$[Cu_T]$ molar ratio (0.1:1 and 0.5:1). In order to obtain high $[CN^-]$:$[Cu_T]$ molar ratio, CuCN and sodium cyanide (NaCN) was were added stoichiometrically to achieve the target cyanide concentration (i.e. $[CN^-]$:$[Cu_T]$ molar ratio of 2:1). It can be observed from Fig. 3, the effect of $[CN^-]$:$[Cu_T]$ molar ratio is significant on copper precipitation that copper removal decreased dramatically as the $[CN^-]$:$[Cu_T]$ molar ratio increased, 92.7% of copper removal was achieved at $[CN^-]$:$[Cu_T]$ ratio of 0.1:1, while only 40.8% of copper removal was obtained at $[CN^-]$:$[Cu_T]$ molar ratio of 2:1. The concentrations of Cu^{2+} at different $[CN^-]$:$[Cu_T]$ molar ratio are also indicated in Fig. 3, it appears that the initial Cu^{2+} concentration in solutions were determined by the $[CN^-]$:$[Cu_T]$ molar ratio, indicating the $[Cu^{2+}]$ to $[Cu_T]$ ratio determines the copper removal. Again it confirmed that the remaining copper in form of cuprous cyanide cannot precipitate by using sulfide in alkaline conditions. During the precipitation, no gold precipitation was observed even at low $[CN^-]$:$[Cu_T]$ molar ratio.

3.1.5. Effects of pH

Previous studies revealed that a pH range from 10.5 to 11 is optimal for gold extraction in a glycine-cyanide synergistic system [18]. The effects of pH were investigated in the range from 8 to 12; results are shown in Table 3. It can be seen that increasing the pH from 8 to 12 has marginal effects on the copper removal which ranges between 65.3% and 69%. Again, no gold precipitation was observed at different pH conditions. This phenomenon implies that no pH adjustment may be required at the end of the leaching where pH usually declines. Moreover, it is interesting to notice that the pH increased at pH 8 and 9 while pH decreased at pH 10.5 and 12 after precipitation. A more likely explanation is the different extent of hydrolysis of HS^- (shown in Eq. (13)) at different pH that more OH^- was generated at lower pH (i.e. pH 8 and 9), while the equilibrium may move backward in the presence of higher concentration of OH^- at higher pH values. This phenomenon can be beneficial if filtrates with low pH are recycled during the process as fewer pH modifiers will be required to reach the optimal pH for leaching.

Table 3
Metals removal and pH before and after precipitation. Experimental conditions: 300 mg/L Cu_T, 1 mg/L Au, $[Cu_T]$:$[CN^-]$:[Gly] molar ratio = 1:1:3, $[HS^-]$:$[Cu_T]$ = 1.3:1, 5 min reaction time.

pH before precipitation	pH After precipitation	Cu removal	Au removal
		%	%
8.10	9.50	65.3	0.0
9.04	9.58	69.0	0.0
10.55	10.38	67.6	0.0
12.00	11.79	68.8	0.0

3.1.6. Effects of temperature

To evaluate the effects of temperature on the performance of precipitation, three levels of temperature (25, 35 and 55 °C) were selected in a solution containing 300 mg/L Cu_T, 1 mg/L Au, $[Cu_T]$:$[CN^-]$:[Gly] molar ratio of 1:1:3. A hot plate equipped with a temperature probe was used to heat the solutions to the target temperature before and during the precipitation tests. As can be seen from Table 4, it can be observed that elevated temperature appears to increase the copper removal by around 10% from 25 to 55 °C. The changes in concentrations of Cu^{2+} after heating were marginal, indicating a portion of Cu^+ precipitated with the increasing temperature. This observation contradicts to some works for SART process, showing elevated temperature has an insignificant effect on copper recovery [13]. Also, it can be seen that gold remained stable in the solutions even at higher levels of temperature.

3.2. Pre-oxidation of Cu^+ to Cu^{2+}

It was obvious that the NaHS and glycine concentrations, pH and

Table 4
Metal removal and Cu^{2+} after heating for 4 h at different temperature. Experimental conditions 300 mg/L Cu_T, 1 mg/L Au, $[Cu_T]$:$[CN^-]$:[Gly] = 1:1:3, pH = 10.5, $[HS^-]$:$[Cu_T]$ = 1.3:1 and 5 min reaction time.

Temperature	Cu_T removal	Au removal	Cu^{2+} after heating for 4 h
°C	%	%	mg/L
25	65.8	0.0	204
35	69.2	0.0	205
55	75.9	0.0	208

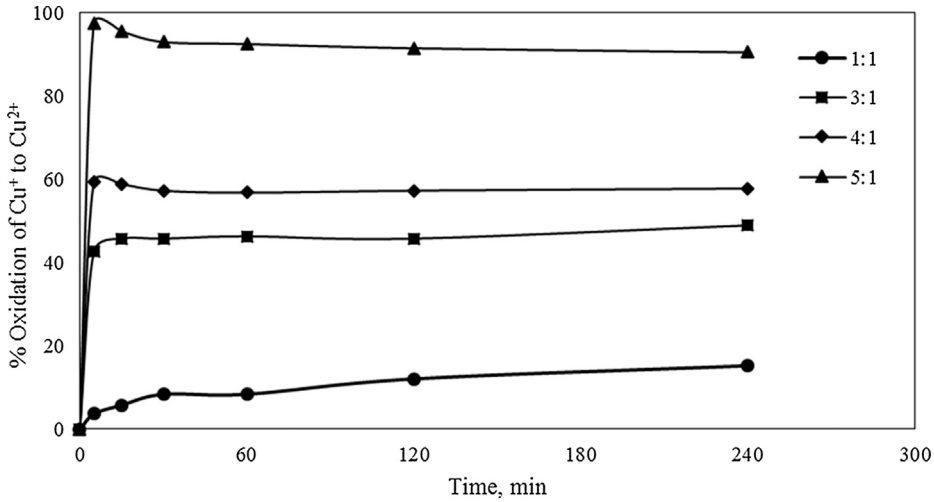

Fig. 4. Cu^{+} oxidisation to Cu^{2+} as a function of time at different $[H_2O_2]$:$[Cu^{+}]$ molar ratio. Experimental conditions: 300 mg/L Cu_T, 1 mg/L Au, $[Cu_T]$:$[CN^{-}]$:[Gly] = 1:2:3, pH = 10.5 and room temperature.

time have minor effects on the copper and gold removal. It appears that the precipitation of copper is dominated by the $[Cu^{2+}]/[Cu^{+}]$ratio in solutions. Therefore, it is essential to oxidize the Cu^{+} to Cu^{2+} before the precipitation to achieve maximum copper removal.

In order to evaluate the effects of pre-oxidation on precipitation using H_2O_2 as the oxidant, a $[CN^{-}]$:$[Cu_T]$ molar ratio of 2:1 was selected for the pre-oxidation tests. The other conditions were as follows: 300 mg/L Cu_T (100 mg/L Cu^{2+}), 1 mg/L Au, [Gly]: $[Cu_T]$ molar ratio of 3:1, pH 10.5 and room temperature. The amount of H_2O_2 was added stoichiometrically according to the amount of Cu^{+} present in solutions.

3.2.1. Pre-oxidation at different $[H_2O_2]$:$[Cu^{+}]$ molar ratio

Pre-oxidation at four levels of $[H_2O_2]$:$[Cu^{+}]$ molar ratio were investigated. As it can be observed from Fig. 4, the level of oxidation was enhanced by the increasing $[H_2O_2]$:$[Cu^{+}]$ molar ratio; 97.49% of Cu^{+} was oxidized to Cu^{2+} in 5 min. Also, it appears that the levels of oxidation decreased slightly over time at higher $[H_2O_2]$:$[Cu^{+}]$ molar ratio (i.e. 5:1 and 4:1), but increased gradually at lower level of $[H_2O_2]$:$[Cu^{+}]$ molar ratio (i.e. 1:1 and 3:1). Based on the above observations, 5 mins of pre-oxidation with a $[H_2O_2]$:$[Cu^{+}]$ molar ratio of 5:1 was chosen as optimal conditions for oxidizing Cu^{+} to Cu^{2+} when the $[CN^{-}]$:$[Cu_T]$ molar ratio is 2:1.

3.2.2. Effects of $[CN]^{-}$:$[Cu_T]$ molar ratio on H_2O_2 dosage

The formation of cuprous cyanide species (i.e. CuCN, $Cu(CN)_2^{-}$, $Cu(CN)_3^{2-}$ and $Cu(CN)_4^{3-}$) in solutions are dependent on the $[CN^{-}]$:$[Cu_T]$ molar ratio that can affect the dosage of H_2O_2 for the oxidation from Cu^{+} to Cu^{2+}. As can be seen Fig. 5, a H_2O_2:Cu^{+} molar ratio of 4:1 was adequate when $[CN^{-}]$:$[Cu_T]$ molar ratio is 1:1, where around 96% of Cu^{+} were oxidized to Cu^{2+} in 5 min. Further increase in $[H_2O_2]$:$[Cu^{+}]$ molar ratio to 5:1 only enhanced the oxidation Cu^{+} to Cu^{2+} by about 2%. This observation reveals that the optimal $[H_2O_2]$:$[Cu^{+}]$ molar ratio is determined by the $[CN^{-}]$:$[Cu_T]$ molar ratio that lower $[CN^{-}]$:$[Cu_T]$ molar ratio may require lower $[H_2O_2]$:$[Cu^{+}]$ molar ratio to reach complete oxidation of Cu^{+} to Cu^{2+}.

3.3. Precipitation after pre-oxidation

3.3.1. Effects of dissolved oxygen

As reported by Chen et al. [3] that the decomposition of H_2O_2 to O_2 occurred after the oxidation of Cu^{+} to Cu^{2+} using a $[H_2O_2]$:$[Cu^{+}]$ ratio of 12:1 and the DO concentration reached the peak after 15 min at 45 ppm and then dramatically decreased to 12.5 ppm in 10 min. The concentrations of dissolved oxygen (DO) were measured during the pre-oxidation and Fig. 6 shows the relationships between the DO concentration and the reaction time. It is clear that at any $[H_2O_2]$:$[Cu^{+}]$ molar ratio, the DO concentration reached the peak at 5 min, followed by a significant decline, the DO concentration kept constant after 60 min. It appears that the H_2O_2 decomposition occurred in 5 min of reaction, implying the rate oxidation of Cu^{+} to Cu^{2+} completed in 5 min.

Precipitation tests were undertaken to investigate the effects of different initial DO concentrations at 22, 4.5 and 0 ppm. Solutions with 4.5 and 0 ppm DO were obtained by injecting nitrogen gas for 15 min and 30mins, respectively, after 5 min of pre-oxidation. The results are shown in Fig. 7, it can be seen that the copper removals levelled off at about 94% from 0 to 4.5 ppm, and then decreased to 86.9% at 22 ppm DO. After the precipitation, almost most of the copper left in the solution was in the form of Cu^{2+} and the concentration of Cu^{2+} increased by the increasing DO concentration. A reasonable explanation is that a small portion of HS^{-} in solutions were oxidized by the high level of DO or by any H_2O_2 left in solutions thus negatively affecting on the Cu removal. It is, therefore, recommended to inject nitrogen gas to remove most of dissolved oxygen before starting the precipitation.

It should be noted no gold precipitation was detected at all levels of DO concentration and no cyanide can be detected by titration after the precipitation which suggests that the copper cyanide species may be oxidized to cyanate as indicated in Eqs. (8) and (9).

3.3.2. Effects of $[HS^{-}]$:$[Cu_T]$ molar ratio

It was observed that around 10% of copper as Cu^{2+} remained unreacted after precipitation by adding NaHS with a $[HS^{-}]$:$[Cu_T]$ molar ratio of 1.3:1, implying the dosage of NaHS might not be sufficient as HS^{-} can be oxidized by any H_2O_2 left in the system. The effects of four levels of $[HS^{-}]$:$[Cu_T]$ molar ratio on precipitation were evaluated in a pre-oxidized solution at a zero DO level. Table 5 shows that the copper removals were enhanced by the increasing $[HS^{-}]$:$[Cu_T]$ molar ratio up to 1.4:1 at 96.5%. However, a subsequent reduction in copper removal was observed at a $[HS^{-}]$:$[Cu_T]$ molar ratio of 1.6:1. Again, this observation can be explained by the formation of soluble copper polysulfide species as the re-dissolution of copper precipitates. Also, in such conditions, no gold precipitation was observed. Based on the results, a $[HS^{-}]$:$[Cu_T]$ molar ratio of 1.4:1 was selected to evaluate the other effects on copper and gold removal.

3.3.3. Effects of contact time during precipitation

The effects of extended precipitation time after the pre-oxidation were investigated at conditions of 0 ppm DO and $[HS^{-}]$:$[Cu_T]$ molar

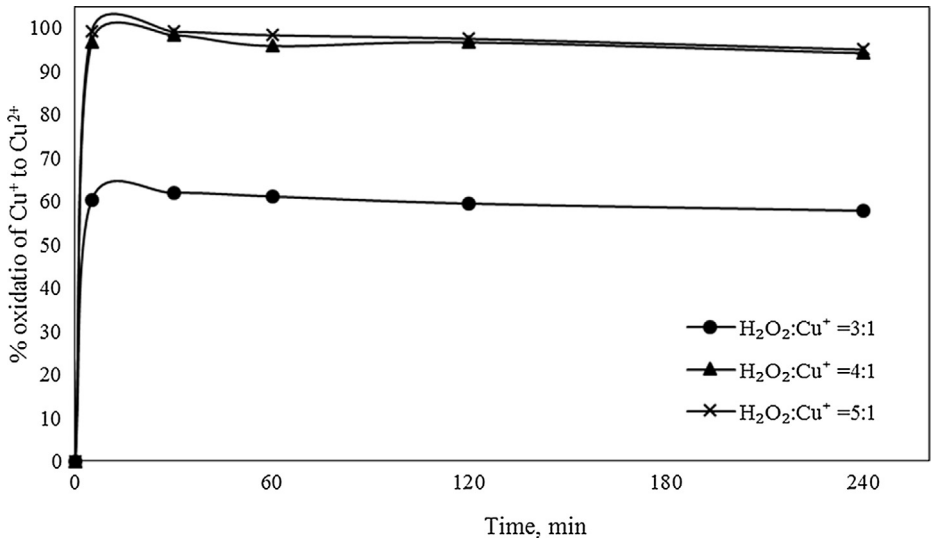

Fig. 5. Cu^{+} oxidisation to Cu^{2+} as a function of time at different $[H_2O_2]$:$[Cu^{+}]$ molar ratio. Experimental conditions: 300 mg/L Cu_T, 1 mg/L Au, $[Cu_T]$:$[CN^{-}]$:[Gly] = 1:1:3, pH = 10.5 and room temperature.

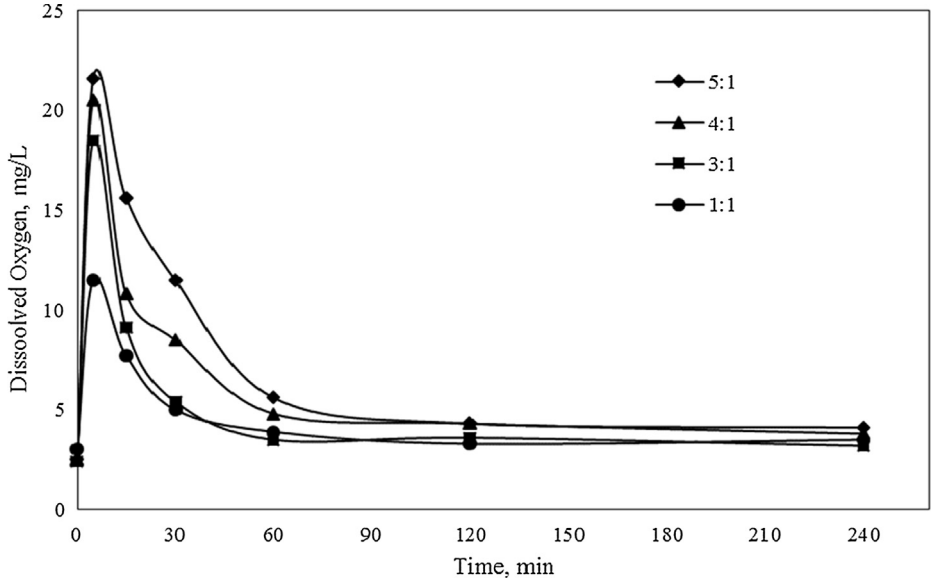

Fig. 6. DO concentration as a function of time at different $[H_2O_2]$:$[Cu^{+}]$ molar ratio. Experimental conditions: 300 mg/L Cu_T, 1 mg/L Au, $[Cu_T]$:$[CN^{-}]$:[Gly] = 1:2:3, and pH = 10.5.

ratio of 1.4:1. As has been shown in Fig. 8, the copper removal declines gradually with the time from 96.5% at 5 min to 89.8% at 60 min, indicating the precipitation completed at 5 min. Similar to the results of precipitation without pre-oxidation, gold precipitation was observed at 60 min, but with larger amount of precipitation. This implied that the co-precipitation of gold may occur at an extended reaction time through adsorption onto the CuS particles. In order to achieve a maximum gold/copper separation and prevent any gold precipitation, a short reaction time (i.e. 5 min) was considered as the optimal reaction time.

3.3.4. Effects of pre-oxidation on gold precipitation

Precipitation tests were conducted to evaluate the effects of pre-oxidation and precipitation on metals recovery at higher gold concentration. The conditions of pre-oxidation and precipitation were as follows: 5 min of pre-oxidation using $[H_2O_2]$:$[Cu^{+}]$ molar ratio of 5:1 and 5 min of precipitation at 0 ppm DO and $[HS^{-}]$:$[Cu_T]$ molar ratio of 1.4:1. As indicated in Table 6, no gold precipitation was monitored at any gold concentration level with or without pre-oxidation. And it is obvious that effects of initial gold concentration is negligible on the copper removal and it is clear that the copper removal increased significantly from 40.8% without pre-oxidisation to 96.1% with pre-oxidation.

Followed copper precipitation, gold can be recovered by the conventional active carbon adsorption. Studies done by Tauetsile et al. [28,29] revealed that in the glycine-cyanide system, activated carbon could adsorb gold effectively at a wide range of pH from 9 to 12 and carbon has a higher selectivity of gold over copper in the presence of low concentration of free cyanide. The gold adsorption on carbon can be a feasible option to recover gold after the pre-oxidation and precipitation processes as cyanide oxidised by H_2O_2 and any copper left in solution is present in the cupric form Cu^{2+} which has less affinity to activated carbon.

3.3.5. Free glycine analysis by titration

An acid-based glycine titration method developed using a Metrohm

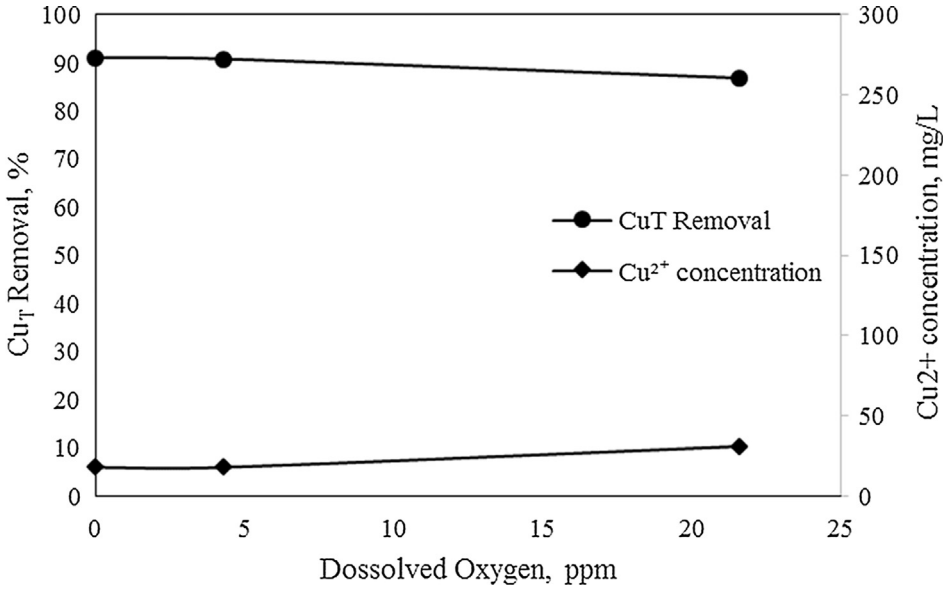

Fig. 7. Cu removal and Cu^{2+} concentration after precipitation as a function of DO concentration. Experimental conditions: 300 mg/L Cu_T, 1 mg/L Au, $[Cu_T]$:$[CN^-]$:[Gly] = 1:2:3, and pH = 10.5, $[HS^-]$:$[Cu_T]$ = 1.3:1, 5 min reaction time.

Table 5
Cu and Au removal at different $[HS^-]$:$[Cu_T]$ molar ratio. Experimental conditions: 300 mg/L Cu_T, 1 mg/L Au, $[Cu_T]$:$[CN^-]$:[Gly] = 1:2:3, and pH = 10.5, 0 ppm Do, 5 min reaction time.

$[HS^-]$:$[Cu_T]$	Cu_T removal	Au removal	$[Cu^{2+}]$ after precipitation
	%	%	mg/L
1:1	71.2	0	86
1.3:1	91.1	0	27
1.4:1	96.5	0	12
1.6:1	91.4	0	26

Table 6
Gold and copper removal at different concentrations of gold with or without pre-oxidation.

Initial [Au] mg/L	Cu_T removal %	Au removal %
4 (With pre-oxidation)	96.1	0.0
1 (With pre-oxidation)	96.4	0.0
4 (Without pre-oxidation)	40.8	0.0

716 DMS Titrino was undertaken to investigate the effects of pre-oxidation on the free glycine concentration. Solutions from the tests for evaluating the effects of $[HS^-]$:$[Cu_T]$ molar ratio after pre-oxidation and precipitation were selected for free glycine titration, the conditions can be seen in Table 5. The results of experimental and theoretical free glycine concentration (assuming no glycine oxidation) are shown in Table 7. The free glycine concentration of the original solution was 0.965 g/L as around 0.1 g/L Cu^{2+} were complexed with glycine. The free glycine concentration reduced to 0.657 g/L after the pre-oxidation. This reduction is mainly because the cuprous cyanide was oxidized and Cu^{2+} were released and then complexed with glycine in solutions, resulting in a decline of free glycine concentration (but not in glycine

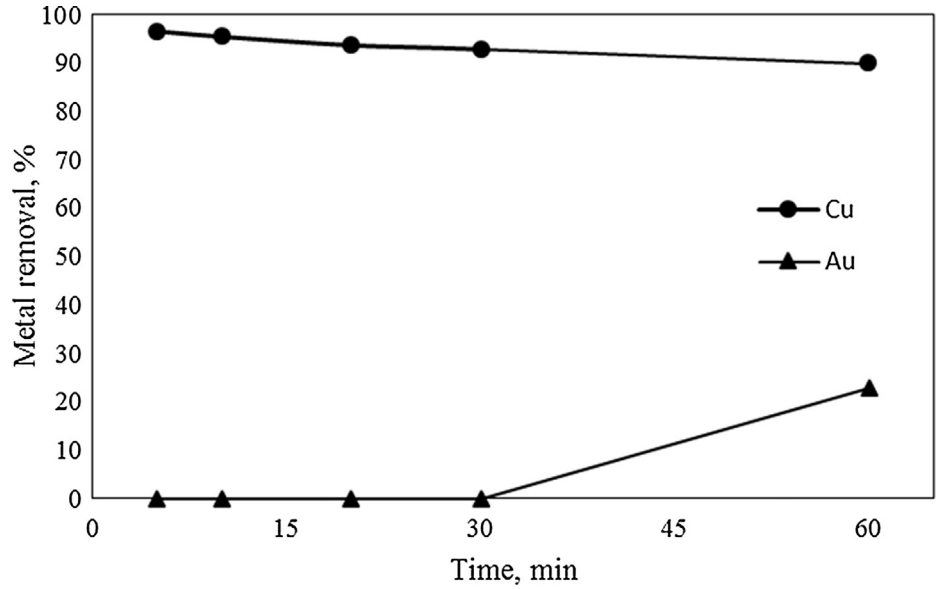

Fig. 8. Cu and Au removal as a function of time after the H_2O_2 pre-oxidation for 5 min, at 0 ppm DO, $[Cu_T]$:$[CN^-]$:[Gly] = 1:2:3, $[HS^-]$:$[Cu_T]$ molar ratio of 1.4:1, 5 min of precipitation.

Table 7
Experimental and theoretical glycine concentration of different solutions.

Solutions	Experimental glycine concentration g/L	Theoretical glycine concentration g/L
Before pre-oxidation ($[Cu_T]$:$[CN^-]$:[Gly] = 1:2:3)	0.965	0.949
After pre-oxidation ($[H_2O_2]$:$[Cu^+]$ = 5:1)	0.657	0.749
After precipitation ($[HS^-]$:$[Cu_T]$ = 1:1)	0.878	0.963
After precipitation ($[HS^-]$:$[Cu_T]$ = 1.3:1)	0.953	1.022
After precipitation ($[HS^-]$:$[Cu_T]$ = 1.4:1)	0.986	1.037
After precipitation ($[HS^-]$:$[Cu_T]$ = 1.6:1)	0.958	1.023
After precipitation ($[HS^-]$:$[Cu_T]$ = 1.6:1, without pre-oxidation)	1.007	1.049

destruction) to form the cupric glycinate complex. It can be observed that the free glycine concentration increased after precipitation as the cupric glycinate were precipitated by bisulfide, thus glycine was released. However, it can also be seen that there are around 0.1–0.05 g/L differences between the experimental and theoretical results, which might be attributed to analytical errors or a small portion of glycine oxidation. Therefore, it can be concluded that the effect of H_2O_2 on free glycine concentration is insignificant.

4. Conclusion

The behaviour of copper precipitation derived from bisulfide (HS^-) addition to glycine-starved cyanide solutions has been studied at different conditions and the effects of pre-oxidation using H_2O_2 as the oxidant has also been evaluated. From the results that have been shown, the following can be concluded:

- The effects of $[HS^-]$:$[Cu_T]$, [Gly]:$[Cu_T]$, pH and time are insignificant on the copper precipitation
- A noticeable improvement in copper removal was observed when temperature was raised to 55 °C.
- Copper removal is dominantly controlled by $[CN^-]$:$[Cu_T]$ molar ratio (which impacts the $[Cu^+]$:$[Cu^{2+}]$ molar ratio) in solutions and higher copper removal as CuS precipitate can be achieved in the presence of higher amount of Cu^{2+}.
- All gold tend to remain in solutions, but a small portion of gold precipitated at 60 min of contacting time which may be ascribed to surface adsorption of gold onto CuS.
- When the $[CN^-]$:$[Cu_T]$ molar ratio was 1:1 and 2:1, the optimal $[H_2O_2]$:$[Cu^+]$ molar ratios for pre-oxidation of Cu^{2+} to Cu^+ were 4:1 and 5:1, respectively.
- Copper redissolution can be decreased slightly by decreasing the DO concentration by nitrogen gas injection.
- There are no observable effects of pre-oxidation on the behavior of gold and the results confirmed that gold remained in solutions at different initial gold concentrations.
- Copper removal increased significantly after pre-oxidation, confirming that cupric glycinate participates in the precipitation reaction.
- The total glycine remained constant, within experimental error, during pre-oxidation.
- A high level of copper precipitation can be achieved after pre-oxidation and sulphide precipitation at the conditions of low concentration of DO, 5 min of reaction time and $[HS^-]$:$[Cu_T]$ molar ratio of 1.4:1 where the copper removal reached to ~96.5% without any gold precipitation.

Acknowledgements

The authors would like to acknowledge the financial support from Curtin University, and Australian Research Council (ARC) Grant No. LP160101121.

Appendix A. Supplementary material

Supplementary data to this article can be found online at https://doi.org/10.1016/j.seppur.2019.02.056.

References

[1] O. Alonso-González, F. Nava-Alonso, C. Jimenez-Velasco, A. Uribe-Salas, Copper cyanide removal by precipitation with quaternary ammonium salts, Miner. Eng. (2012), https://doi.org/10.1016/j.mineng.2012.11.013.
[2] William Bleam, Chapter 5 – Water Chemistry, in: William Bleam (Ed.), Soil and Environmental Chemistry, Second Ed., Academic Press, 2017, pp. 189–251.
[3] Fayuan Chen, Xu Zhao, Huijuan Liu, Qu Jiuhui, Reaction of $Cu(CN)_3^{2-}$ with H_2O_2 in water under alkaline conditions: cyanide oxidation, Cu^+/Cu^{2+} catalysis and H_2O_2 decomposition, Appl. Catal. B 158–159 (C) (2014) 85–90, https://doi.org/10.1016/j.apcatb.2014.04.010.
[4] Irena Ciglenečki, Damir Krznarić, George R. Helz, Voltammetry of copper sulfide particles and nanoparticles: investigation of the cluster hypothesis, Environ. Sci. Technol. 39 (19) (2005) 7492–7498, https://doi.org/10.1021/es050586v.
[5] Xianwen Dai, Andrew Simons, Paul Breuer, A review of copper cyanide recovery technologies for the cyanidation of copper containing gold ores, Miner. Eng. 25 (1) (2011), https://doi.org/10.1016/j.mineng.2011.10.002.
[6] David Dreisinger, James Vaughan, Lu Jianming, Berend Wassink, Paul West-Sells, Treatment of the Carmacks copper-gold ore by acid leaching and cyanide leaching with sart recovery of copper and cyanide from barren cyanide solution, in: C.A. Young, P.R. Taylor, C.G. Anderson, Y. Choi (Eds.), Hydrometallurgy 2008, Proceedings of the 6th International Symposium, SME, Littleton (CO), 2008, pp. 740–749.
[7] J.J. Eksteen, E.A. Oraby, The leaching and adsorption of gold using low concentration amino acids and hydrogen peroxide: effect of catalytic ions, sulphide minerals and amino acid type, Miner. Eng. 70 (2015) 36–42, https://doi.org/10.1016/j.mineng.2014.08.020.
[8] J.J. Eksteen, E.A. Oraby, B.C. Tanda, A conceptual process for copper extraction from chalcopyrite in alkaline glycinate solutions, Miner. Eng. 108 (2017) 53–66, https://doi.org/10.1016/j.mineng.2017.02.001.
[9] J.J. Eksteen, E.A. Oraby, B.C. Tanda, P.J. Tauetsile, G.A. Bezuidenhout, T. Newton, F. Trask, I. Bryan, Towards industrial implementation of glycine-based leach and adsorption technologies for gold-copper ores, Can. Metall. Q. 57 (4) (2017) 390–398, https://doi.org/10.1080/00084433.2017.1391736.
[10] Humberto Estay, Designing the SART process – a review, Hydrometallurgy 176 (2018) 147–165, https://doi.org/10.1016/j.hydromet.2018.01.011.
[11] C.A. Fleming, Cyanide recovery, Dev. Miner. Process. 15 (C) (2005) 703–727, https://doi.org/10.1016/S0167-4528(05)15029-7.
[12] Alison Emslie Lewis, Review of metal sulphide precipitation, Hydrometallurgy 104 (2) (2010) 222–234, https://doi.org/10.1016/j.hydromet.2010.06.010.
[13] P. Littlejohn, D. Kratochvil, A. Hall, Sulfidisation-acidification-recycling-thickening (SART) for complex gold ores, Publication Series 9/2013, Proceedings of *World Gold 2013*, AusIMM, Brisbane (QLD), 2013, pp. 149–155.
[14] P.M. May, D. Batka, G. Hefter, E. Knigsberger, D. Rowland, Goodbye to S2 in aqueous solution, Chem. Commun. 54 (16) (2018) 1980–1983, https://doi.org/10.1039/c8cc00187a.
[15] E.A. Oraby, J.J. Eksteen, The selective leaching of copper from a gold–copper concentrate in glycine solutions, Hydrometallurgy 150 (2014) 14–19, https://doi.org/10.1016/j.hydromet.2014.09.005.
[16] E.A. Oraby, J.J. Eksteen, Gold leaching in cyanide-starved copper solutions in the presence of glycine, Hydrometallurgy 156 (2015) 81–88, https://doi.org/10.1016/j.hydromet.2015.05.012.
[17] E.A. Oraby, J.J. Eksteen, The leaching of gold, silver and their alloys in alkaline glycine–peroxide solutions and their adsorption on carbon, Hydrometallurgy 152 (2015) 199–203, https://doi.org/10.1016/j.hydromet.2014.12.015.
[18] E.A. Oraby, J.J. Eksteen, B.C. Tanda, Gold and copper leaching from gold-copper ores and concentrates using a synergistic lixiviant mixture of glycine and cyanide, Hydrometallurgy 169 (2017) 339–345, https://doi.org/10.1016/j.hydromet.2017.02.019.
[19] G. Potter, A. Bergmann, U. Haidlen, Process of recovering copper and of optionally recovering silver and gold by a leaching of oxide- and sulfide-containing materials with water-soluble cyanides, Conserv. Recycl. 9 (1986) 371–372, https://doi.org/

10.1016/0361-3658(86)90099-8.
[20] Andrew Murray Simons, A Fundamental Study of Copper and Cyanide Recovery from Gold Tailings by Sulfidisation, Ph.D. Western Australian School of Mines, Department of Metallurgical and Minerals Engineering., Curtin University, 2015.
[21] Bennson Chemuta Tanda, Glycine as a Lixiviant for the Leaching of Low Grade Copper-Gold Ores, Ph.D Western Australian School of Mines, Curtin University, 2017.
[22] B.C. Tanda, J.J. Eksteen, E.A. Oraby, An investigation into the leaching behaviour of copper oxide minerals in aqueous alkaline glycine solutions, Hydrometallurgy 167 (2017) 153–162.
[23] B.C. Tanda, J.J. Eksteen, E.A. Oraby, Recovery of copper from alkaline glycine leach solution using solvent extraction, Sep. Purif. Technol. 187 (2017) 389–396.
[24] B.C. Tanda, E.A. Oraby, J.J. Eksteen, Kinetics of chalcocite leaching in oxygenated alkaline glycine solutions, Hydrometallurgy 178 (2018) 264–273.
[25] B.C. Tanda, E.A. Oraby, J.J. Eksteen, Kinetics of malachite leaching in alkaline glycine solution, Miner. Process. Extract. Metall. (TIMM C). 1–10 (2018), https://doi.org/10.1080/25726641.2018.1505211.
[26] P. Tauetsile, Elsayed Oraby, Jacques Eksteen, Adsorption behaviour of copper and gold Glycinates in alkaline media onto activated carbon. Part 2: isotherms, Hydrometallurgy 178 (178) (2018) 202–208.
[27] P. Tauetsile, Elsayed Oraby, Jacques Eksteen, Adsorption behaviour of copper and gold Glycinates in alkaline media onto activated carbon. Part 2: kinetics, Hydrometallurgy 178 (2018) 195–201, https://doi.org/10.1016/j.hydromet.2018.04.016.
[28] P.J. Tauetsile, E.A. Oraby, J.J. Eksteen, Activated carbon adsorption of gold from cyanide-starved glycine solutions containing copper. Part 1: isotherms, Separat. Purifi. Technol. (2019) In Press.
[29] P.J. Tauetsile, E.A. Oraby, J.J. Eksteen, Activated carbon adsorption of gold from cyanide-starved glycine solutions containing copper. Part 2: kinetics, Separat. Purifi. Technol. (2019) In Press.
[30] Van Hille, P. Robert, Karen A. Peterson, Alison E. Lewis, Copper sulphide precipitation in a fluidised bed reactor, Chem. Eng. Sci. 60 (10) (2005) 2571–2578, https://doi.org/10.1016/j.ces.2004.11.052.
[31] Otakar Söhnel. Precipitation: Basic Principles and Industrial Applications/Otakar Söhnel and John Garside, John Garside (Ed.), Oxford, UK, 1992.

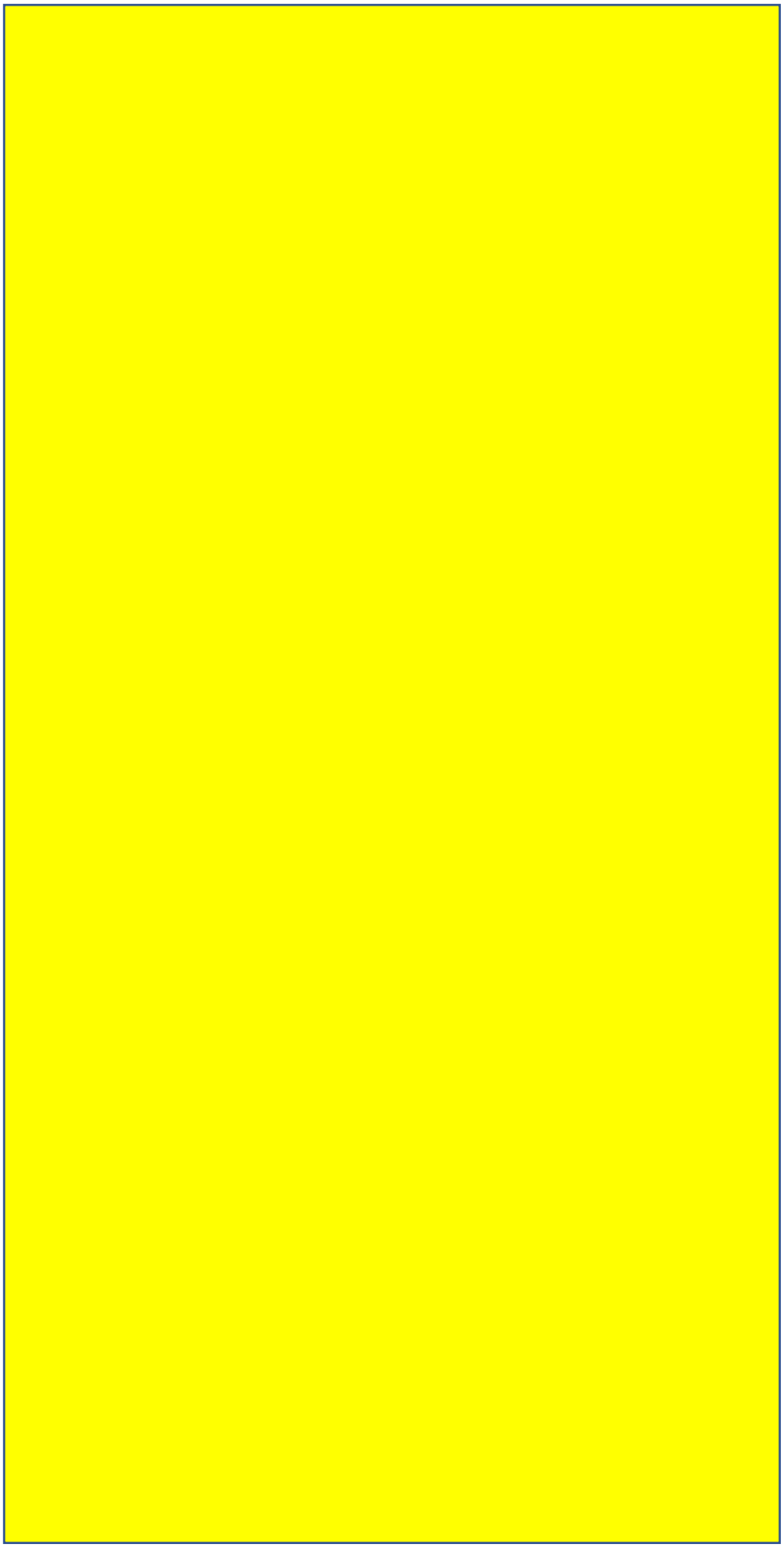

Chapter 4: The sulfide precipitate characterisation from cyanide-starved glycine solutions

Submitted for publication as:

Sulfide precipitation of copper from alkaline glycine-cyanide solutions:

Precipitate characterisation

Deng, Z. Oraby, E.A. and Eksteen, J.J., 2020.

Minerals Engineering, 145, 106102.

Accepted for publication on 21 October 2019.

© 2019 Elsevier Ltd.

Reprinted with permission from the publisher.

DOI: https://doi.org/10.1016/j.mineng.2019.106102

Minerals Engineering 145 (2020) 106102

Contents lists available at ScienceDirect

Minerals Engineering

journal homepage: www.elsevier.com/locate/mineng

Sulfide precipitation of copper from alkaline glycine-cyanide solutions: Precipitate characterisation

Z. Deng[a], E.A. Oraby[a,b], J.J. Eksteen[a,*]

[a] Faculty of Science and Engineering, Western Australian School of Mines: Minerals, Energy and Chemical Engineering, Curtin University, GPO Box U1987, Perth, WA 6845, Australia

[b] Mining and Metallurgical Engineering, Faculty of Engineering, Assiut University, Egypt

ARTICLE INFO

Keywords:
Precipitation
Glycine
Copper
Gold
Particle size distribution
Morphology

ABSTRACT

A synergistic leaching system using glycine containing starvation levels of cyanide as lixiviants has been shown to be an effective approach to leach gold-copper ores, allowing the consumption of cyanide to be reduced significantly while glycine is recycled. Sulfide precipitation to remove the bulk of the copper was studied. The previous study on the precipitation behaviour of Cu and Au from the alkaline glycine-cyanide solution shows that the cupric (Cu^{2+}) glycinate can be easily precipitated, while the gold and cuprous (Cu^{+}) cyanide species remain stable in the solution. Due to the sparingly soluble nature of metal sulfides, colloidal and poorly settling particles are usually formed without control methods, which create challenges for solid-liquid separation processes such as thickening and filtration. This study investigated the effects of chemical and operational conditions on particle characteristics particularly particle size distributions (PSD). Settling characteristics, particle morphologies and particle structure were also studied. In the presence of divalent cations such as Ca^{2+} and Mg^{2+}, particularly Ca^{2+}, large and fast settling particle agglomerates were generated. Increasing ionic strength of the solution was also noted to enlarge the particles. The high supersaturation level has insignificant effects on the PSD as long as Ca^{2+} is present. A relatively large particle size is generated at a medium stirring speed with fast addition rate. There are no significant effects of aging, heating, and seeding on the PSD, but these factors profoundly influenced the morphologies of the individual particles according to the SEM results. SEM and XRD analysis illustrate that a more mature and crystalline copper sulfide precipitates were produced after aging, heating, or seeding.

1. Introduction

A synergistic glycine-cyanide leaching system has been studied and reported by numerous authors Oraby & Eksteen (2015) and Oraby et al. (2017) indicating that it is a possible alternative leaching process to conventional cyanidation for processing gold-copper ores, which are normally excessive cyanide consuming ores. In the presence of glycine, the cyanide consumption can be significantly reduced, e.g. by at least 75% (and often > 90%) compared to conventional cyanidation whilst allowing glycine recycle. In this leaching system, the pregnant leach solutions contain Au and Cu which mostly presents as cupric glycinate and a small portion of cuprous cyanide species. In a synthetic glycine-cyanide solution, the Cu^{2+}/Cu^{+} ratios are controlled by the $[Cu_T]$:[Gly]:$[CN^{-}]$ ratio in the system by adding CuCN, glycine and NaCN accordingly (Deng et al., 2019; Tauetsile et al., 2019a,b). The carbon adsorption tests specific to the glycine-cyanide system in the presence of gold and copper carried out by Tauetsile et al. (2019a,b) elaborate that gold can effectively adsorb onto activated carbon. However, it was also illustrated that the competing adsorption of copper onto activated carbon cannot be avoided and the cuprous cyanide species in solutions have higher affinity onto the activated carbon than their cupric glycinate counterparts.

In order to explore the feasibility of other downstream processes for the novel glycine-cyanide leaching system, a conventional sulfide precipitation for the recovery of Cu was studied (Deng et al., 2019). The authors found that the cupric glycinate in the system can be easily precipitated in 5 min by adding concentrated NaHS solutions. The copper recovery was found to be dominated by the Cu^{2+}/Cu^{+} ratio, as the cuprous cyanide species cannot be precipitated under alkaline conditions. Pre-oxidation tests of Cu^{+} to Cu^{2+} using hydrogen peroxide was conducted; with basically all cupric glycinate in solutions, a high copper removal (~96.5%) was achieved with a $[HS^{-}]$:$[Cu_T]$ ratio of

* Corresponding author.
E-mail address: jacques.eksteen@curtin.edu.au (J.J. Eksteen).

https://doi.org/10.1016/j.mineng.2019.106102
Received 24 July 2019; Received in revised form 13 October 2019; Accepted 21 October 2019
0892-6875/ © 2019 Elsevier Ltd. All rights reserved.

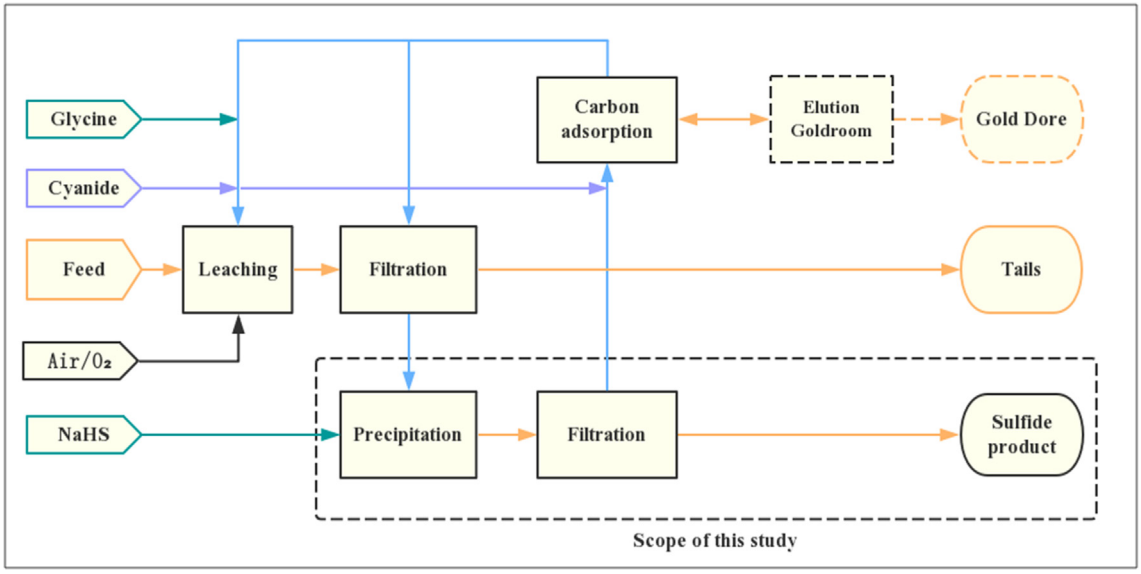

Fig. 1. Block diagram flowsheet of glycine leaching process utilising cyanide at starvation levels with copper removal by sulfide precipitation and carbon adsorption (Seaman et al., 2019).

1.4:1. The authors showed that a high level of gold and copper separation can be achieved by H_2O_2 oxidation followed by sulfide precipitation where no gold precipitation was observed. By this means, copper can be effectively removed under alkaline conditions without intensive pH modification before traditional carbon adsorption for gold recovery, minimizing the competitive effects of copper onto the activated carbon.

A recent pilot plant campaign (Seaman et al., 2019) was conducted to demonstrate the metallurgical performance of the alkaline glycine leaching system under starved cyanide conditions in a continuous, closed-circuit operation, as applied to low-grade copper-gold flotation (rougher) concentrates. A flowsheet including copper recovery by sulfide precipitation and gold recovery by carbon adsorption is illustrated in Fig. 1 (Seaman et al., 2019). The results demonstrated that almost all Cu^{2+} was successfully removed as covellite with no Cu^{+} and Au precipitation.

However, metal sulfide precipitation reactions are usually difficult to control due to the sparingly soluble nature of sulfide precipitates (very low solubilities) and high supersaturation levels (up to 10^{35} and higher) (Lewis & van Hille, 2006; Mokone et al., 2010), which lead to very fine and highly dispersed particles usually being generated. This can result in significant technical difficulties regarding solid-liquid separation and the downstream recovery processes. Therefore, the PSD should be optimized to an acceptable level for solid-liquid separation processes.

Similar difficulty was noted by the authors that extremely fine precipitates (highly dispersed particles) were generated after adding NaHS solutions at the preliminary stage of a previous study focusing on sulfide precipitation chemistry, where the pH of the synthetic solutions was only adjusted by NaOH (Deng et al., 2019). It was observed that the particles were very fine and a large portion of fines cannot be filtered by the 0.45 μm membrane filter paper. It was found that if the pH of the synthetic solutions were adjusted by NaOH and $Ca(OH)_2$, large and filterable precipitates were generated. This phenomenon implied that the addition of Ca^{2+} or other cations can be a critical factor for the formation of large precipitates (Deng et al., 2019).

There are many studies which addressed the issues of the formation of fines through controlling the chemical conditions such as sulfide and initial metal concentrations (Al-Tarazi et al., 2005; Farahani et al., 2014; Lewis & van Hille, 2006; Sampaio et al., 2010) and operational conditions such as stirring speed (Eksteen et al., 2008; Farahani et al., 2014; Houcine et al., 1997; Marcant & David, 1991; Torbacke & Rasmuson, 2001), aging time (Eksteen et al., 2008; Söhnel & Garside, 1992), temperature (Roy & Srivastava, 2007) and adding seed materials (Agrawal et al., 2018; Donnet et al., 2005). However, few of them have investigated the copper sulfide precipitation under alkaline conditions since $Cu(OH)_2$ precipitation will be the dominant species in the precursor aqueous system. None of the studies have investigated the sulfide precipitate characteristics from an alkaline glycine-cyanide solution in the presence of Cu and Au which is mainly a mixture of cupric glycinate, cuprous dicyanide, gold cyanide and free glycine.

To minimise the production of very fine precipitates, a more detailed investigation on the effects of different processing conditions on the copper sulfide precipitates characteristics from the glycine-cyanide solutions was conducted. The main objective of the current study is to investigate the effects of different chemical conditions (i.e. addition of cations, dosage of cations, sulfide concentrations, copper concentrations and ionic strength) and operational conditions (i.e. stirring speed, sulfide addition rate, aging time, temperature, and addition of seeds) on particle characteristics. The settling performance of the precipitates were also investigated as the supplementary evidence for the PSD results. The morphologies of individual particles which may be influenced by aging, heating, or seeding was visualised by Scanning Electron Microscope (SEM). The phase and crystal structure of the precipitated product was identified by means of X-ray Powder Diffraction (XRD). Fig. 2 shows a typical precipitation process with the potential impact factors on each step based on the literatures (Agrawal et al., 2018; Al-Tarazi et al., 2005; Donnet et al., 2005; Eksteen et al., 2008; Farahani et al., 2014; Houcine et al., 1997; Lewis & van Hille, 2006; Marcant & David, 1991; Sampaio et al., 2010; Söhnel & Garside, 1992; Torbacke & Rasmuson, 2001).

2. Experimental design

2.1. NaHS solutions

A 50 g of NaHS solid (Sigma-Aldrich) was dissolved in 100 ml deionised water to make a very concentrated NaHS stock solutions. The sulfide concentration of the stock solution was 5 M which was determined by the concentration of Na and S measured by Inductively Coupled Plasma Optical Emission Spectrometry (ICP-OES). This ICP-OES confirmation is important due to the hygroscopic nature of the

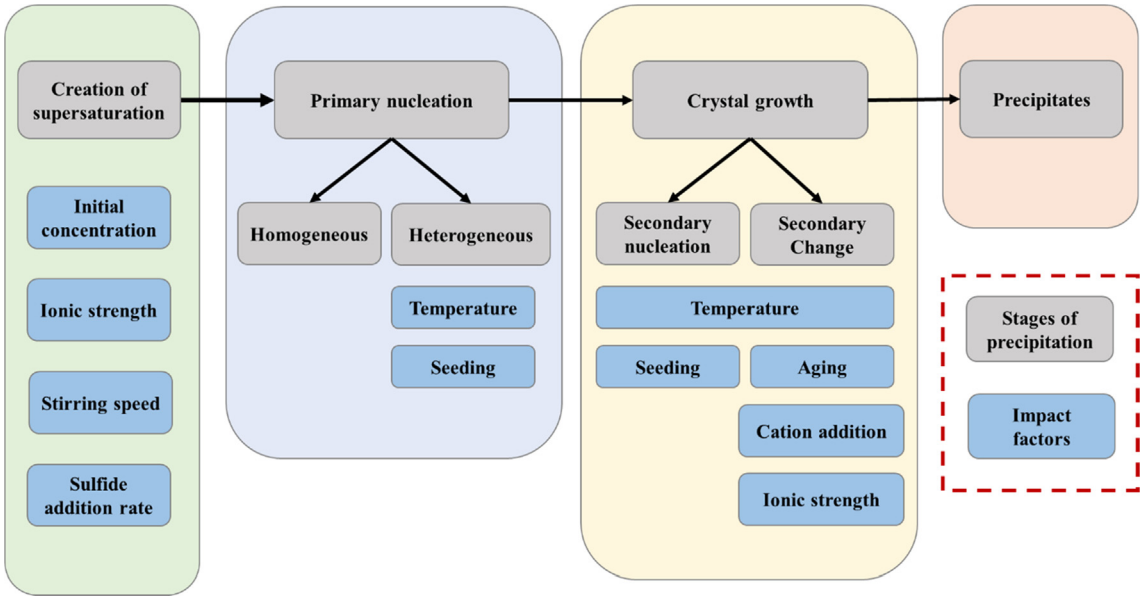

Fig. 2. Process of precipitation and the possible impact factors on each step.

crystals. Lower sulfide concentrations (i.e. 0.25 M and 0.05 M) were prepared by diluting the 5 M NaHS solution accordingly in de-ionised water.

2.2. Synthetic solutions

All the tests in this study were conducted using synthetic solutions. Analytical grade reagents and deionized water were used throughout the tests. A stock cyanide-starved glycine solution containing gold and copper was first prepared. Gold powder (99.998%, spherical, −200 mesh, Alfa Aesar – Thermo Fisher Scientific) were dissolved in deionized water contained glycine (> 99%, Sigma-Aldrich) and CuCN (95%, Ajax, Finechem) for 24 h. The concentration of Au was measured by ICP-OES. The pH of the solutions was adjusted using sodium hydroxide (NaOH, Chem-Supply Pty Ltd) and measured by a pH meter Model AQUA-PH Meter. The solution was agitated with a magnetic stirrer and Teflon magnetic stirrer bars at 200 rpm. The solution was filtered with a Supor® 0.45 μm membrane disc filter (Pall Corporation) prior to the tests. A standard cyanide-starved glycine solution containing 300 mg/L total copper (Cu_T), 1 mg/L Au at [Cu_T]:[CN^-]:[Gly] molar ratio of 1:1:3 was obtained by diluting the stock solution accordingly. It should be noted that the [Cu_T], [CN^-] and [Gly] refer to the total copper, cyanide and glycine concentrations present and not their "free" species in solution.

2.3. Precipitation procedure

Batch precipitation tests were conducted in a 1L glass reactor equipped with four equally spaced baffles and a RW 20 digital overhead stirrer with a metallic blade impeller. The NaHS solution was added into 500 ml synthetic solutions at a [HS^-]: [Cu] molar ratio of 1.3:1 and mixed by the overhead stirrer (the stirring speed for each test was specified in each caption of the figure). After 5 min of reaction, the stirrer was turned off and the yielded precipitates were transferred to an imoff settling cone to record the settling behaviour for 20 min. The supernatant was then decanted, and the precipitates were washed by DI water several times. The precipitates with DI water were stored in a 50 ml sampling tube and ready for PSD analysis. Due to dry samples were required for XRD and SEM analysis, duplicate tests were conducted and the precipitates were collected by the filtration with a Supor® 0.45 μm membrane disc filter (Pall Corporation) and washed by DI water several times before drying in an oven at 70 °C for 24 h.

2.4. Analytical methods

The particle size analysis was conducted using laser diffraction sizing technology with a Malvern Mastersizer 2000. The particle morphology study was undertaken using a scanning electron microscopy, a Zeiss Neon 40Esb Cross-Beam FESEM model. The phase and crystal structure of the precipitates were analysed by a D8-Advance Bruker X-ray spectrometer with DIFFRAC.SUIT for qualitative analysis and TOPAS for quantitative analysis with the assistance of the staff in Microscopy and Microanalysis Facility, Curtin University.

3. Results and discussions

3.1. Effects of chemical conditions

3.1.1. Effects of cation addition

It was noted by observation from the previous study focusing on solution chemistry that if the pH of the synthetic solutions was first buffered to 10 by NaOH and then adjusted to 10.5 by $Ca(OH)_2$, much larger particles were generated and the precipitates can be easily filtered (Deng et al., 2019).

Based on the previous experience, the presence of Ca^{2+} seems to be the main contributor for the formation of large precipitates. Two kind of divalent cations Ca^{2+} and Mg^{2+} and one kind of trivalent cation Al^{3+} were selected to investigate their effects on the PSDs and settling performance. The Ca^{2+}, Mg^{2+} and Al^{3+} used in this study were added as $CaCl_2$, $MgCl_2$ and $AlCl_3$ solutions respectively. To compare the cations effects, similar molar concentration of these cations (0.5 mM) were added to the synthetic solutions. A plot using a base 10 logarithmic scale (i.e. particle size in log) showed the volume-based PSDs (Fig. 3A) and a base 2 semi-log (i.e. time in log) plot demonstrated the settling performances of the yielded precipitates (Fig. 3B). It was observed that the addition of Al^{3+} has no effects on the formation of large particles and highly dispersed particles were still generated. For those fine and colloidal precipitates, their PSDs were not shown as a complete solid-liquid separation was not achieved. The size of the precipitates increases due to the effect of aging, thus an accurate PSD analysis cannot be obtained. As shown in Fig. 3A, the addition of Ca^{2+} has better results, where its yielded mean particle size (44.3 μm) is about 2

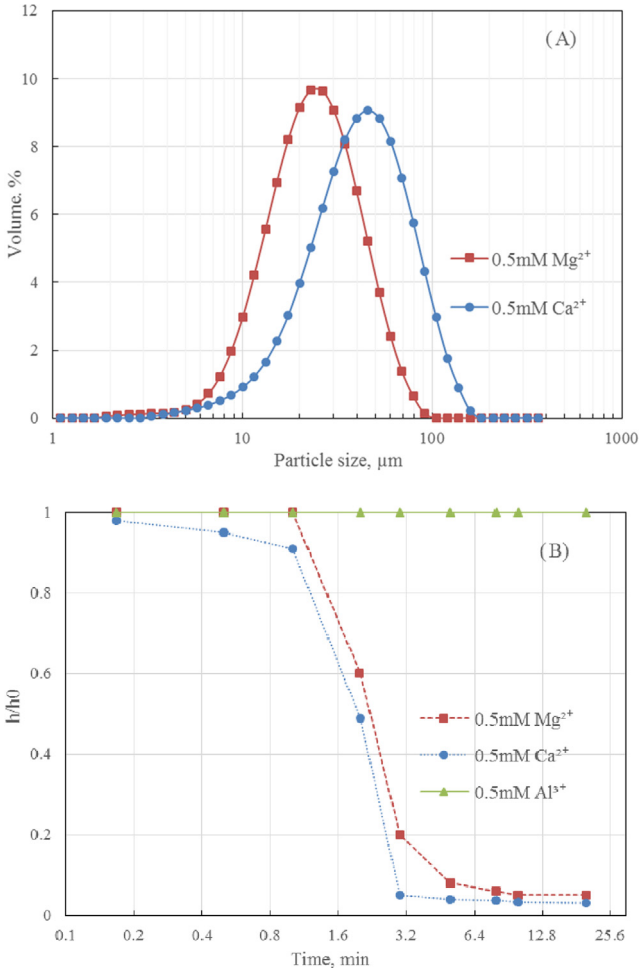

Fig. 3. Effects of different divalent cations on (A) PSDs and (B) settling performance. Experimental conditions: $[Cu_T]$ = 300 mg/L, $[Cu_T]$:$[CN^-]$:[Gly] = 1:1:3, pH = 10.5, room temperature, $[HS^-]$ = 5 M, $[HS^-]$:[Cu] = 1.3:1, reaction time = 5 min, stirring speed = 200 rpm.

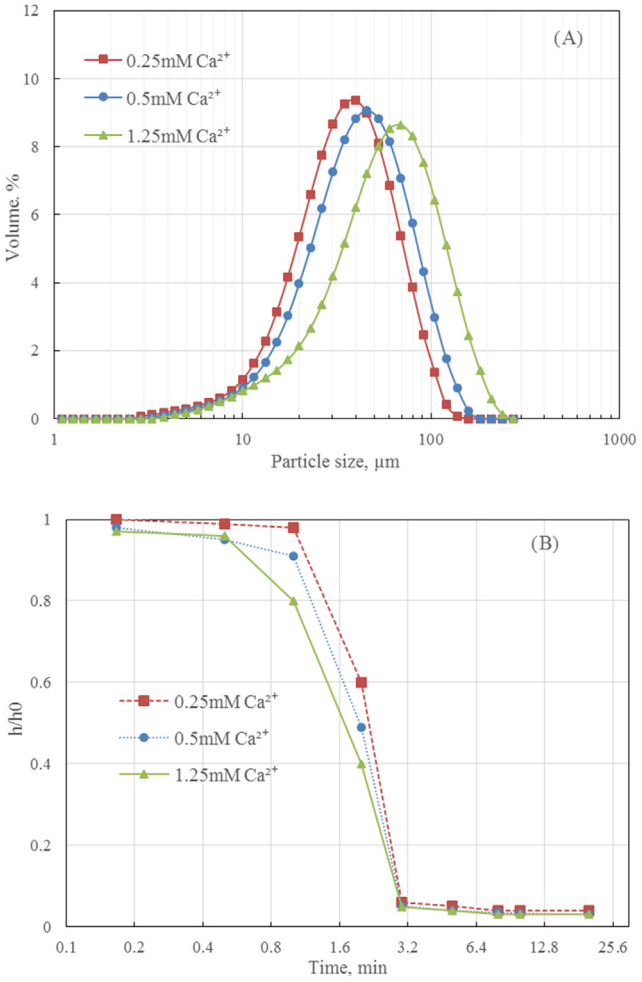

Fig. 4. Effects of different Ca^{2+} dosage on (A) PSD and (B) settling performance. Experimental conditions: $[Cu_T]$ = 300 mg/L, $[Cu_T]$:$[CN^-]$:[Gly] = 1:1:3, pH = 10.5, room temperature, $[HS^-]$ = 5 M, $[HS^-]$:$[Cu_T]$ = 1.3:1, reaction time = 5 min, stirring speed = 200 rpm.

times larger than that with Mg^{2+} addition (21.7 μm). The settling behaviour of the precipitated particles are shown in Fig. 3B. It is clear that the addition of Ca^{2+} and Mg^{2+} significantly enhanced the settling performance, and the addition of Ca^{2+} shows a faster settling rate. The differences obtained from the results for the tested cations can be explained by the available free cations in the aqueous alkaline environment. The total concentrations of cations were presented however these concentrations are not represent the free cations available in the system. All these cations will form metal hydroxide precipitates at pH 10.5 (the tested pH condition), but their solubilities are different, where the solubility (K_{sp}) of $Ca(OH)_2 = 5.5 \times 10^{-6}$, $Mg(OH)_2 = 5.6 \times 10^{-12}$ and $Al(OH)_3 = 1.3 \times 10^{-33}$ (Dean, 1990). According to their solubilities, $Ca(OH)_2$ appears to dissociate the most free cations (Ca^{2+}), while $Al(OH)_3$ dissociates the least free cations (Al^{3+}), resulting in very limited effects of adding Al^{3+} into the alkaline glycine-cyanide solutions. It was found that of the effect of cation ions on the copper precipitation from e glycine-cyanide system is followed the order: $Ca^{2+} > Mg^{2+} > Al^{3+}$.

During the precipitation reaction, it was observed that visible particles were generated at around 1 min after adding Ca^{2+} and about one and a half minutes after adding Mg^{2+}. The agglomeration of particles then became obvious during the setting processes. Park et al. (2008) revealed that divalent cations such as Ca^{2+} and Mg^{2+} have the ability to bind to the crystal surface and enhance the mechanical properties via chemical cross-linking. Chung et al. (2015) used Ca^{2+} as a cross-linking agent for bridging the fine copper sulfide precipitation, enhancing the crystal growth and agglomeration of precipitation. Therefore, the hypothesis is that the lower solubility of the metal hydroxide precipitation leads to lower concentration of free cations in the solutions, thus affecting the cross-linking effects of the divalent cations on the surface of crystals. Based on the PSD results and settling performance, calcium ion was selected for further investigation as $Ca(OH)_2$ is also commonly used as a pH modifier.

3.1.2. Effects of Ca^{2+} dosage

The effects of Ca^{2+} dosage on the PSDs and the settling performances were investigated. From Fig. 4A, with the increasing dosage of Ca^{2+}, the mean particle size increased from 37.1 μm at 0.25 mM to 62.1 μm at 1.25 mM. The results support the hypothesis drawn from the above section that higher concentration of free cations has positive effects on enlarging the final particle size by cross-linking effects as higher dosage of Ca^{2+} means higher concentration of free Ca^{2+} available in the solutions. It can also be observed that higher Ca^{2+} concentration appears to result in a wider PSD. This can be explained by the formation of highly incompact and loose agglomerates, where a sponge-like morphology in Fig. 5. As shown in Fig. 4B, despite the differences in the mean particle size, similar settling characteristics were observed at different dosage of Ca^{2+}.

3.1.3. Effects of supersaturation

The supersaturation level or supersaturation ratio (S) is calculated

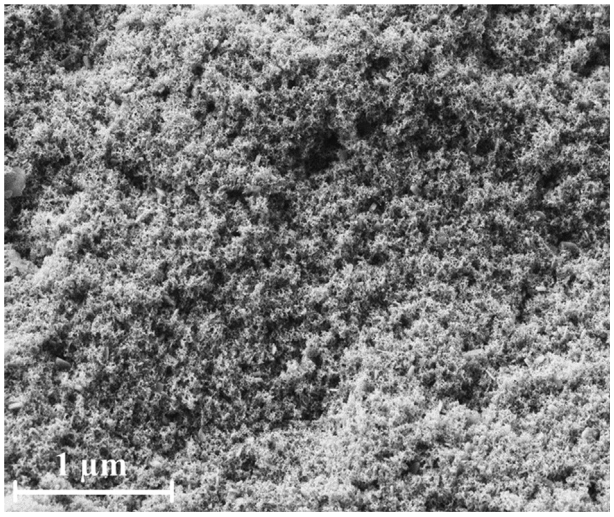

Fig. 5. SEM images of the precipitates produced at Ca^{2+} dosage of 0.5 mM.

by Eq. (1) (Eksteen et al., 2008; Söhnel and Garside, 1992):

$$S = \left(\frac{[M_+^{Z_1}][X_-^{Z_2}]}{K_{sp}} \right)^{\frac{1}{Z_1+Z_2}} \quad (1)$$

where the solubility of the compound $M_{Z_1}^{+}X_{Z_2}^{-}$, $K_{sp} = [M_{+,eq}^{Z_1}] \bullet [X_{-,eq}^{Z_2}]$.

From Eq. (1), the supersaturation level is influenced by the metal and sulfide concentrations. At high supersaturation, primary nucleation rates are usually very high, resulting in a large number of nuclei which further limits crystal growth (Söhnel & Garside, 1992). Many researchers have reported that larger copper sulfide particles were obtained at lower supersaturation level i.e. lower sulfide or metal concentration (Lewis & van Hille, 2006; Sampaio et al., 2009). The effects of sulfide concentrations and total copper concentrations on the PSD and settling performance were studied and the results were summarized in Fig. 6. As it can be seen in Fig. 6A, the width of the PSD for all the tests are quite similar. The mean particle size slightly increased from 44.3 μm at $[HS^-]$ of 5 M to 52.8 μm at $[HS^-]$ of 0.05 M. At higher Cu concentration of 1000 mg/L, the mean particle size decreased slightly to 39.4 μm. It should be noted that without the presence of Ca^{2+}, colloidal particles were generated at all the tested sulfide and Cu concentrations, implying the effects of supersaturation were not significant.

The settling characteristics (in Fig. 6B) were also compared; no evident variation of settling performance was observed. The insignificant effects of supersaturation on PSD and settling can be attributed to the sparingly soluble nature of CuS ($K_{sp} = 6.3 \times 10^{-36}$) (Dean, 1990), the calculated values of initial supersaturation (S) of the lowest levels sulfide and Cu concentrations in this study is 8.7×10^{15} which is very high as $S > 1 \times 10^3$ is considered as high supersaturation level (Söhnel & Garside, 1992). To achieve a significant lower level of the supersaturation, a huge dilution factor of the NaHS solution would be required, which is unrealistic from a processing perspective. These results are consistent with previous studies which were indicated the size of copper sulfide precipitates barely changed with the concentration of copper (Al-Tarazi et al., 2005; Farahani et al., 2014).

3.1.4. Effects of ionic strength

The ionic strength of the solutions can vary during the process circuit due to the water quality and the addition of chemicals such as NaOH, NaHS, and NaCN. It is important to consider the effect of ionic strength on the size of the precipitates and its effect was barely studied in the literatures. According to DLVO theory (named after Derjaguin, Landau, Verwey and Overbeek), when the ionic strength of the solution increases to a certain level that van der Waals attraction is greater than the electrostatic repulsion, the stability of colloidal particles suspension

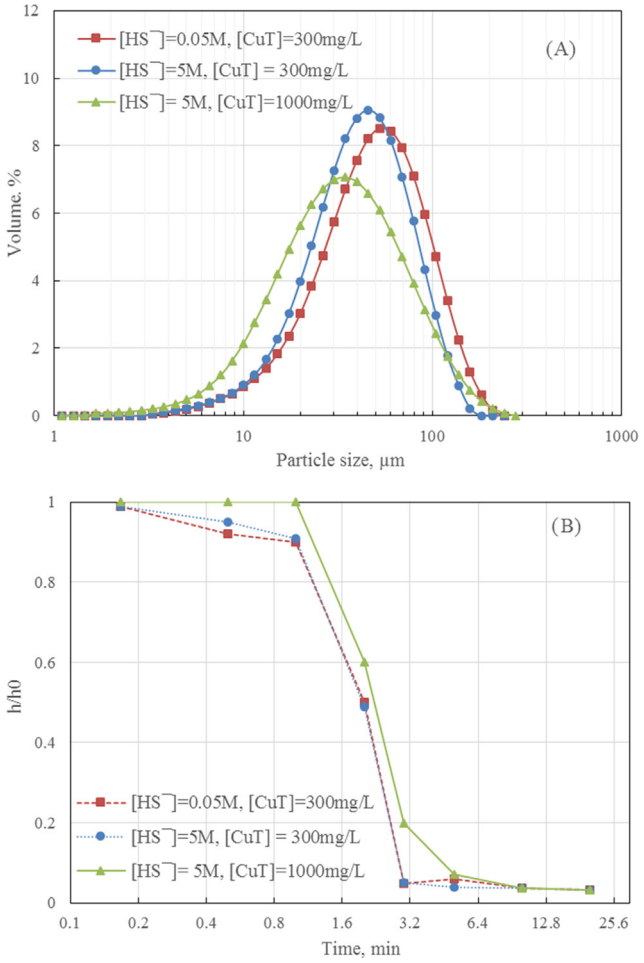

Fig. 6. Effects of different sulfide concentration on (A) PSD and (B) settling rates. Experimental conditions: $[Cu_T]:[CN^-]:[Gly] = 1:1:3$, pH = 10.5, room temperature, Ca^{2+} dosage = 0.5 mM, $[HS]:[Cu_T] = 1.3:1$, reaction time = 5 min, stirring speed = 200 rpm.

decreases, leading to particle coagulation (Lekkerkerker, 2011). Also, based on the salt effect or ionic effect (Moreno & Peinado, 2012), the increase of ionic strength through introducing ions other than those involved in the precipitation equilibrium increases the solubility of the precipitates (i.e. K_{sp}), thus lowing the supersaturation which has potential effect on the particle size enlargement. In this study, the ionic strength of the solutions was adjusted by adding solid NaCl. The effects of different levels of ionic strength on the PSD and settling rate were studied in the absence of Ca^{2+}. Provided in Fig. 7A, the mean particle size increases significantly with the increasing ionic strength from 18.4 μm at 0.1 M to 56.9 μm at 1 M. The PSD become wider as the ionic strength increases, which is probably due to the agglomerated particles are bonded by van der Waal attraction which can be easily broken down.

The PSD result for the test at an ionic strength of 0.01 M is not shown as non-settleable fines were formed, which is mainly because the ionic strength was not high enough to allow the attraction force to be greater than the repulsion force. Settleable particles were generated at the ionic strength of 0.1 M, the settling performance of the tests is shown in Fig. 7B. It can be seen that the precipitates produced at 0.1 M ionic medium have relatively poorer settling rate, but its settling rate is acceptable where the settlement completed at around 5 min. At ionic strengths of 0.2 M and 1 M, their settling characteristics are quite similar, and their settlement completed at about 3 min.

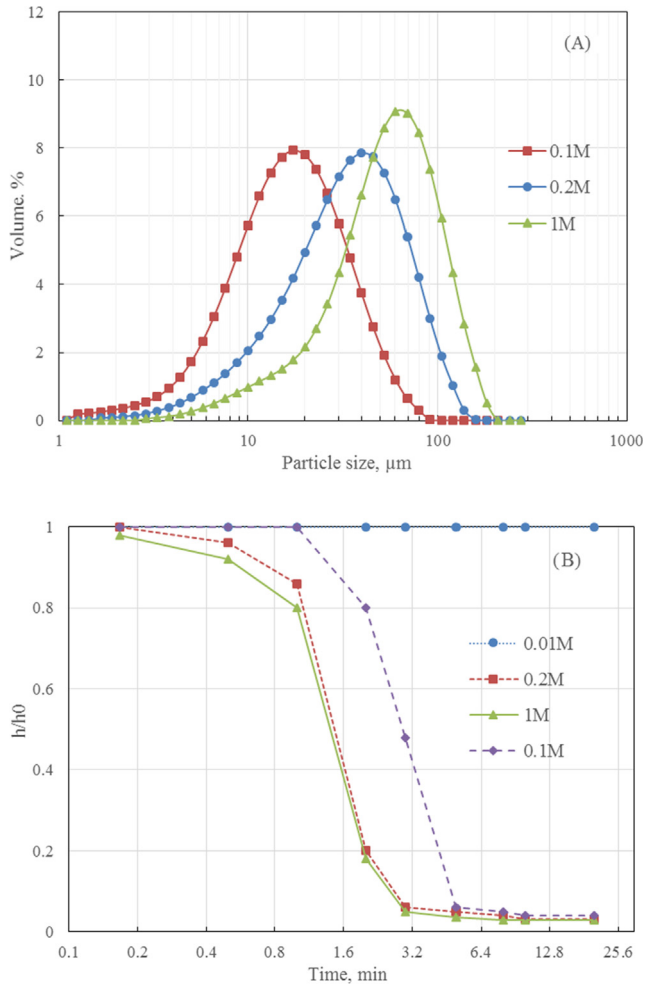

Fig. 7. Effects of different level of ionic strength on (A) PSD and (B) settling performance. Experimental conditions: $[Cu_T]$ = 300 mg/L, $[Cu_T]$:$[CN^-]$:[Gly] = 1:1:3, $[HS^-]$ = 5 M, pH = 10.5, room temperature, [HS]:$[Cu_T]$ = 1.3:1, Sulfide concentrations = 5 M, reaction time = 5 min, stirring speed = 200 rpm.

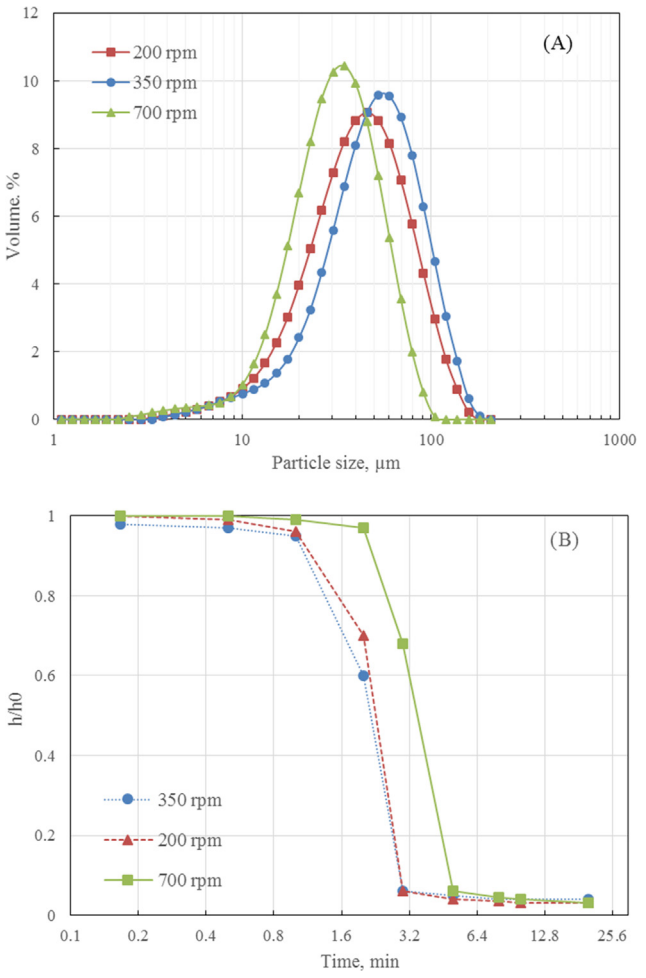

Fig. 8. Effects of stirring speed on the PSD. Experimental conditions: $[Cu_T]$ = 300 mg/L, $[Cu_T]$:$[CN^-]$:[Gly] = 1:1:3, pH = 10.5, room temperature, $[HS^-]$ = 5 M, $[HS^-]$:$[Cu_T]$ = 1.3:1, Ca^{2+} dosage = 0.5 mM, reaction time = 5 min.

3.2. Effects of operational conditions

3.2.1. Effects of stirring speed

The PSD of the precipitates can be significantly influenced by the stirring intensity which has been investigated intensively in the literature (Eksteen et al., 2008; Farahani et al., 2014; Houcine et al., 1997; Marcant & David, 1991; Torbacke & Rasmuson, 2001). Söhnel and Garside (1992) who investigated the basic principles of precipitation, stated that a fast stirring rate can lead to smaller particle size and narrower PSD. Three levels of stirring rates were investigated in this study, and the results are shown in Fig. 8. It can be seen from Fig. 8A that the volume-based mean particle size increased slightly from 44.3 μm to 52.0 μm with an increase the stirring speed from 200 rpm to 350 rpm, further increasing the stirring speed at 700 rpm decreased the mean particle size to 32.2 μm. Similar results were obtained by (Marcant & David, 1991; Torbacke & Rasmuson, 2001). The possible explanation for this phenomenon is that increasing the stirring speed at a certain level minimises the spatial variation and local supersaturation, and increasing the mean particle size. Nevertheless, at a higher level of stirring intensities, the bonds between the agglomerated particles can be broken down, resulting in a decrease in particle size, indicating a medium stirring speed is preferable. Fig. 8B showed that a relatively poor settling characteristics were obtained at 700 rpm with the settlement finishing in 5 min. Good settling performance was observed at both 200 and 350 rpm with the settlement completed in about 3 min. The stirring speed of 350 rpm was selected for the rest of the tests as it produced the largest mean particle size. However, from the industrial point of view, a slower stirring speed of 200 rpm can be preferable considering the energy consumption.

3.2.2. Effects of sulfide addition rate

Semi-batch precipitation tests were performed by adding a diluted NaHS solution (0.25 M) with a pre-calibrated pump at slow (2 ml/min) and fast addition rate (20 ml/min). The purpose of this test is to identify the effects of slow and fast development of supersaturation on the PSD. The results of PSD are shown in Fig. 9. The PSDs are shown in Fig. 9A, the smallest mean particle size (19.3 μm) were obtained from slow sulfide addition, while the largest mean particle size (47.2 μm) obtained from the batch precipitation test where NaHS solution was added all at the beginning of the precipitation tests. Also, it can be seen from the settling rate shown in Fig. 9B, similar settling performance was observed for the fast sulfide addition test and the batch precipitation test. A slower settling characteristic was observed at the sulfide addition rate of 2 ml/min, but its setting rate is still acceptable with the settlement completed in 5 min. It appears that fast addition of sulfide i.e. fast development of supersaturation contributes to a larger particle size and better settling characteristics.

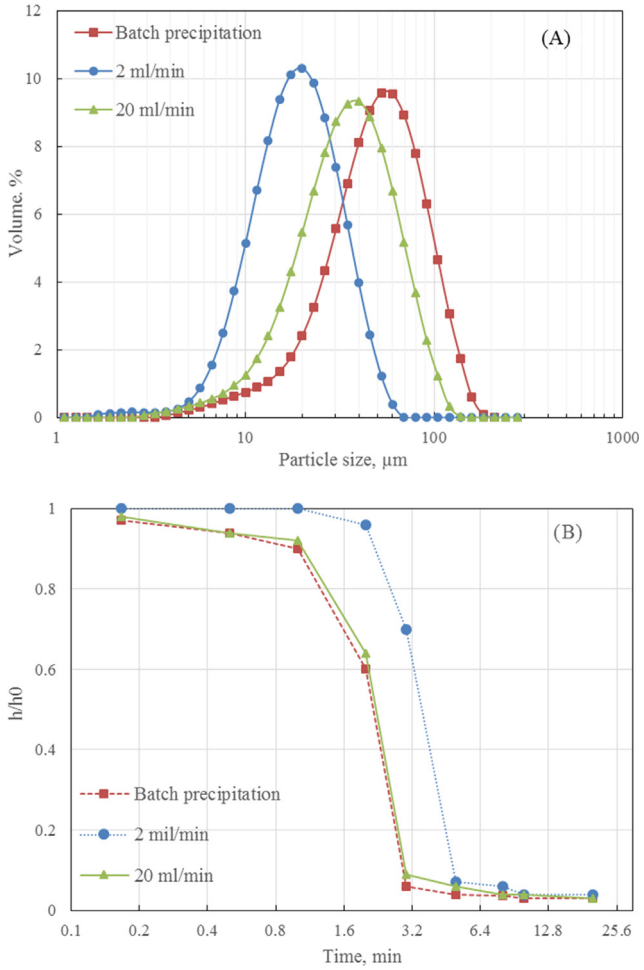

Fig. 9. Effects of sulfide addition rate on the PSD. Experimental conditions: $[Cu_T]$ = 300 mg/L, [CuT]:$[CN^-]$:[Gly] = 1:1:3, pH = 10.5, room temperature, $[HS^-]$ = 0.25 M, [HS]:$[Cu_T]$ = 1.3:1, Ca^{2+} dosage = 0.5 mM, reaction time = 5 min, stirring speed = 350 rpm.

3.2.3. Effects of aging time

If the precipitates were allowed to contact with the mother liquid and stand for a certain time without stirring, the size and the morphology of the precipitates may change, in a process that is referred to as aging. It was found that *meta*-stable polymorph would transform into a more stable form or an amorphous phase can transform into a crystalline phase during aging (Söhnel & Garside, 1992). The effects of aging time on the PSD and particle morphology were studied. As presented in Fig. 10, prolonging the aging time up to 2 h increased the mean particle size from 44.3 μm to 56.1 μm. While the mean particle size at aging time of 24 h is 55.0 μm which is basically the same size at 2 h aging, implying the no further particle agglomeration after 2 h of aging. Although there are slightly differences in PSDs, the settling performance was quite similar with all the cases being settled in 3 min (similar to Fig. 4B).

SEM images for the aged precipitates are illustrated in Fig. 11. A significant morphology evolvement was observed. A high magnification micrograph (Fig. 11A) illustrates that most of the individual particles (30 nm to 50 nm) show granular morphology with a small amount of hexagonal-shaped particles when the precipitates did not undergo aging. The two-hour aged individual particles shown in Fig. 11B consists of mostly hexagonal crystals and a small amount of granular shaped particles (70–150 nm). In Fig. 11C, the twenty-four-hour aged individual particles show well-developed hexagonal morphology and large individual particle size ranging from 160 nm to 220 nm.

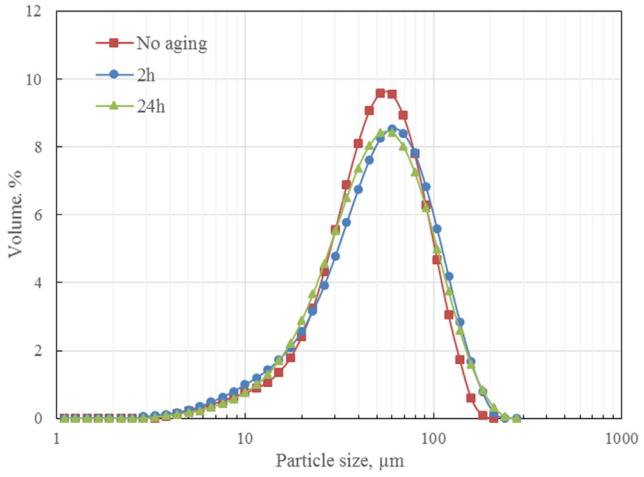

Fig. 10. Effects of aging time on the PSD. Experimental conditions: $[Cu_T]$ = 300 mg/L, $[Cu_T]$:$[CN^-]$:[Gly] = 1:1:3, $[HS^-]$ = 5 M, pH = 10.5, room temperature, Ca^{2+} dosage = 0.5 mM, [HS]:$[Cu_T]$ = 1.3:1, reaction time = 5 min, stirring speed = 350 rpm.

From the above observation, the initial crystals structure seems to be polymorph with small individual crystals. With aging, the size of individual crystals continued to grow, meanwhile, the polymorphous phase slowly transforms into a more mature and crystalline phase. It should be noted that the change in the precipitate morphology has no effect on the final PSDs, mainly because the PSD analysis is a macroscopic technique which is measuring the size of the particle agglomerates.

3.2.4. Effects of temperature

The particle size and morphology of the copper sulfide precipitates can be influenced by the temperature due to crystal growth which is favoured at lower temperature while nucleation becomes predominant at higher temperature (Roy & Srivastava, 2007). They observed rod-shaped CuS precipitates at 105 °C, while hexagonal-shaped nanoparticles were observed at 140 °C. The effects of reaction temperature on the PSD and precipitates morphology were studied. As shown in Fig. 12, the PSDs remained unchanged at higher temperature with the mean particle size slightly decreased from 52.0 μm to 47.2 μm. The slight reduction in the particle size may be attributed to the higher rate of nucleation that gives rise to the increasing number of primary nuclei, which limits the crystal growth.

The SEM images of the morphology of the precipitates after heating are presented in Fig. 13. At 55 °C, hexagonal-shaped individual particles can be observed which are quite similar to the precipitates after aging for 2 h (Fig. 11B). The observation implies that heating can also facilitate the crystal transformation process from polymorphous phase to crystalline phase.

3.2.5. Effects of seeding

The main purpose of adding seed material is to provide surface for the secondary growth of the precipitated particles (Agrawal et al., 2018). Additionally, the use of seed crystals can help control of nucleation step by preventing spontaneous nucleation that limits the number of primary nuclei (Donnet et al., 2005; Linga, 2017). In a typical SART (sulfidisation, acidification, recycle and thickening) process, a portion of the thickener underflow served as seeds are recycled into the precipitation tank for increasing the particle size of the Cu_2S precipitates (Estay, 2018). However, it should be noted that the effect of seeding on the PSDs and morphology of the copper sulfide precipitates was barely studied.

Predetermined concentrations (1 g/L and 5 g/L) of pure covellite (Sigma-Aldrich, 99.99%) were used as seed sources. The results of the

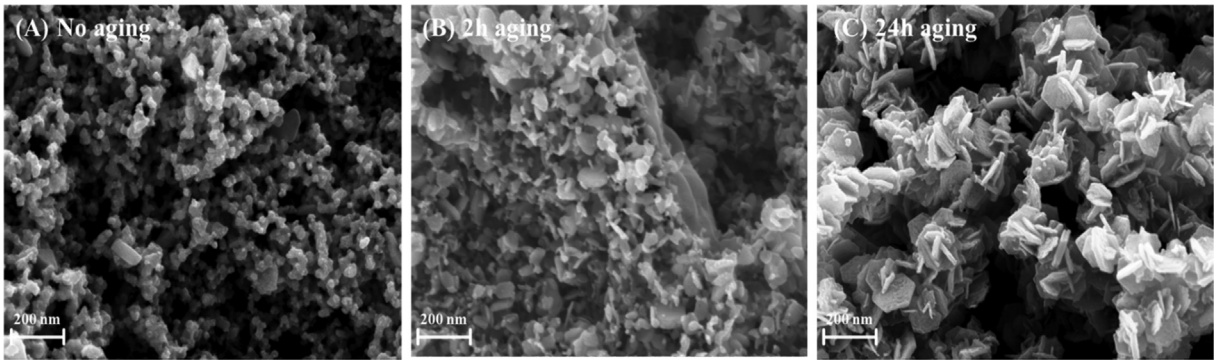

Fig. 11. SEM images of the precipitates produced from different aging time (A) no aging, (B) 2 h aging and (C) 24 h aging. Other experimental conditions: $[Cu_T]$ = 300 mg/L, $[Cu_T]$:$[CN^-]$:[Gly] = 1:1:3, pH = 10.5, room temperature, $[HS^-]$ = 5 M, [HS]:$[Cu_T]$ = 1.3:1, Ca^{2+} dosage = 0.5 mM, reaction time = 5 min, stirring speed = 350 rpm.

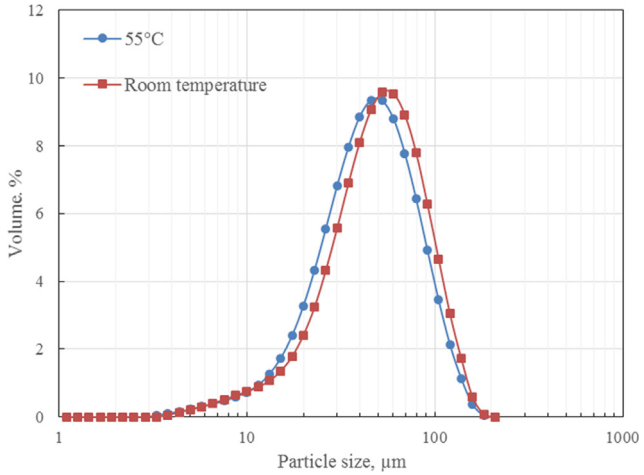

Fig. 12. Effects of reaction temperature on the PSD. Experimental conditions: $[Cu_T]$ = 300 mg/L, $[Cu_T]$:$[CN^-]$:[Gly] = 1:1:3, $[HS^-]$ = 5 M, pH = 10.5, room temperature, Ca^{2+} dosage = 0.5 mM, [HS]:$[Cu_T]$ = 1.3:1, reaction time = 5 min, no aging, stirring speed = 350 rpm.

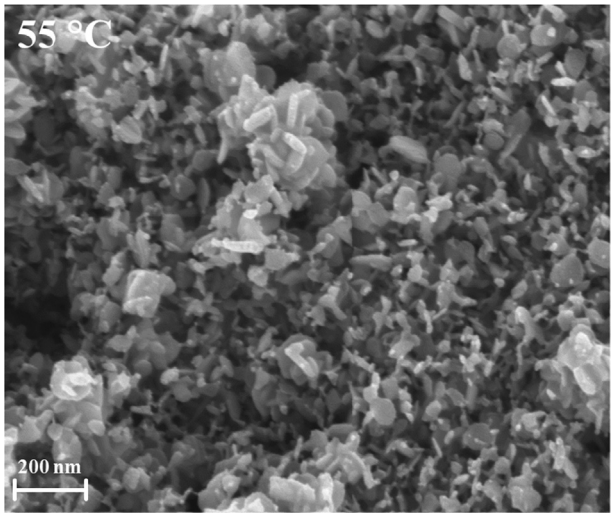

Fig. 13. SEM images of the precipitates produced at 55 °C. Other experimental conditions: $[Cu_T]$ = 300 mg/L, $[Cu_T]$:$[CN^-]$:[Gly] = 1:1:3, pH = 10.5, Ca^{2+} dosage = 0.5 mM, $[HS^-]$ = 5 M, [HS]:$[Cu_T]$ = 1.3:1, reaction time = 5 min, stirring speed = 350 rpm.

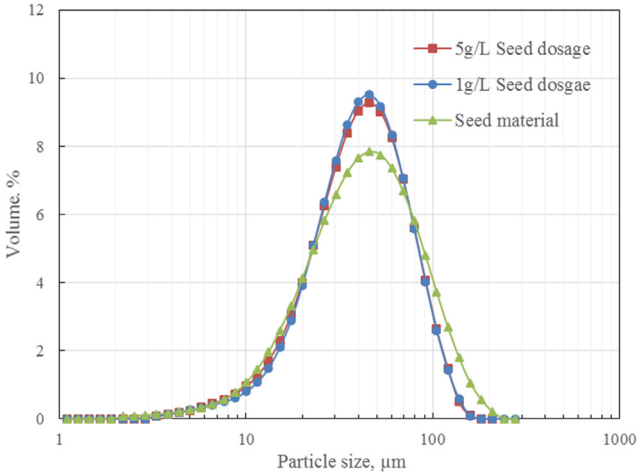

Fig. 14. Effects of using CuS as seed material on the PSD. Experimental conditions: $[Cu_T]$ = 300 mg/L, $[Cu_T]$:$[CN^-]$:[Gly] = 1:1:3, pH = 10.5, room temperature, Ca^{2+} concentrations = 0.5 mM, [HS]:$[Cu_T]$ = 1.3:1, reaction time = 5 min, stirring speed = 350 rpm.

PSDs of the seed material and the PSDs after seeding are presented in Fig. 14. Adding seed and increasing the dosage of seed materials have no effect on the PSDs with a mean particle size of about 39 μm, which implies the PSD of the original seed particles may overshadow any observable growth.

Fig. 15 illustrates SEM images of pure covellite and the seeded precipitations. A stratiform morphology can be seen in Fig. 15A. As for the seeded precipitation (1 g/L seed loading), the surface of the agglomerates shows a flower-like morphology (Fig. 15B), which is very distinctive compared to the morphology obtained at the same conditions but without adding seed (Fig. 11A). It may because the precipitated particles grew on the surface of the seed materials. It can be concluded that adding seed materials has little effect on the enlargement of the precipitations, but it can significantly change the morphology of the precipitates.

3.3. XRD analysis

The XRD analysis of the precipitates obtained from different conditions was conducted to understand the change of crystal structure and phase purity with different morphologies. The XRD analysis of the pure covellite was also undertaken for comparison. The experimental conditions of the tests are summarised in Table 1.

All the XRD patterns ranged from 20° to 100° are presented in Fig. 16. It can be noted that the precipitates generated at the conditions of 0.5 mM Ca^{2+} (test a) and 1 M ionic strength (test b) have very similar

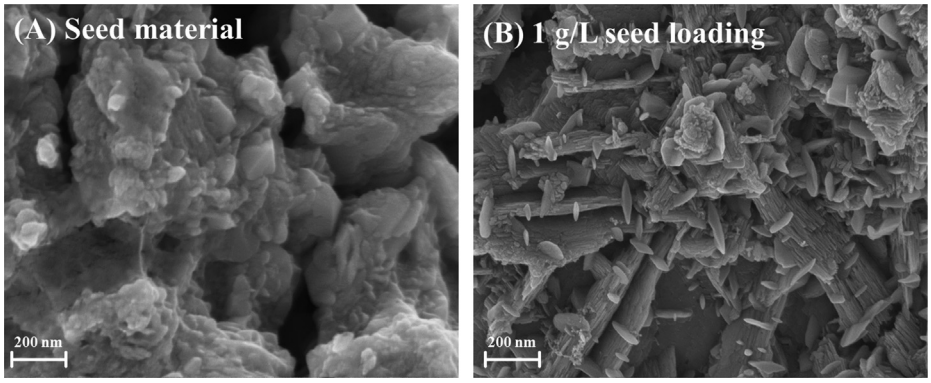

Fig. 15. SEM images of the seed material (A) and the precipitates produced with 1 g/L seed (B). Other experimental conditions: [Cu_T] = 300 mg/L, [CuT]:[CN^-]:[Gly] = 1:1:3, pH = 10.5, Ca^{2+} dosage = 0.5 mM, [HS^-] = 5 M, [HS]:[Cu_T] = 1.3:1, reaction time = 5 min, stirring speed = 350 rpm.

diffraction patterns, where the detected peaks are relatively broad and not intensive, implying small size of crystals and polymorphous crystal structure (Bruce et al., 2013). Qualitative XRD analysis shows their diffraction patterns match with the PDF card no. 00-003-1090, indexed by DIFFRAC.SUIT as copper sulfide. To further estimate the percentage of the mixed phases of copper sulfide, quantitative XRD analysis was conducted using Rietveld refinement technique with TOPAS software, the results are shown in Table 2. The results indicate that mixed phases of CuS (covellite) and $Cu_{1.81}S$ (digenite) were found, consisting of around 55% to 60% of covellite and 40% to 45% of digenite. The morphology of the produced precipitates without aging, heating and seeding (Fig. 11A) also confirms polymorphous structure with granular and hexagonal-shaped crystals.

The other diffraction patterns produced from 24 h aging, 55 °C and 1 g/L seed loading (test c, d, e) are found to match with the diffraction patterns of the pure covellite and the PDF card no. 00-006-0464, indexed as hexagonal phase as covellite (space group $P6_3/mmc$) with lattice parameters a = 3.792 Å and c = 16.344 Å. The quantitative XRD analysis indicates a highly crystalline hexagonal structure that the copper sulfide precipitates produced from those tests are presents as 100% of covellite. Also, the SEM images (Fig. 11C and Fig. 13B) showed a hexagonal crystal structure which are in line with the XRD results that indicate hexagonal crystal structures were formed during the aging and heating tests. It is observed that the morphologies of the seed material and the precipitates from 1 g/L seed loading are not hexagonal phases (Fig. 15), but the XRD analysis indicates they are highly crystalline hexagonal phase. The variations in the peak intensities may be attributed to the procedure of sample preparation where preferred orientation can happen (Bruce et al., 2013).

Based on the XRD results and the SEM images, it seems that a significant morphology evolvement and a crystal phase transformation from polymorph to crystalline copper sulfide precipitates can occur during aging, heating or seeding.

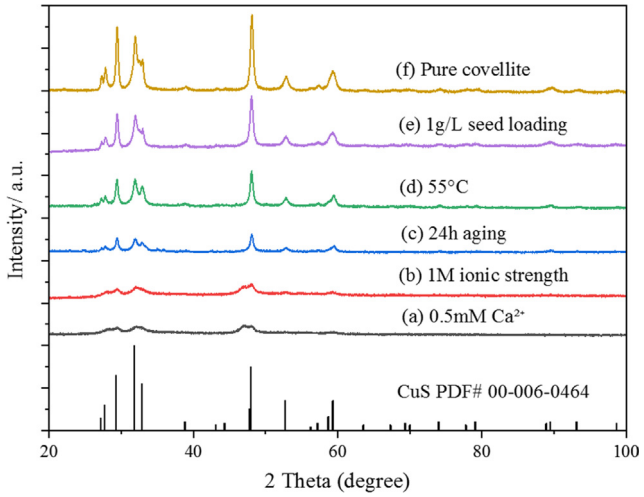

Fig. 16. XRD spectra of CuS from (a) 0.5 mM Ca^{2+}, (b) 1 M ionic strength, (c) 24 h aging, (d) 55 °C, (e) 1 g/L Seed dosage, (f) pure covellite.

Table 2
Quantitative XRD analysis data of the copper sulfide precipitates from (a) 0.5 mM Ca^{2+}, (b) 1 M ionic strength, (c) 24 h aging, (d) 55 °C, (e) 1 g/L Seed dosage.

Test No.	Phases	Name	% of phases	Crystal structure	Space group
a	CuS	Covellite	55.3	Hexagonal	P63/mmc
	$Cu_{1.81}S$	Digenite	44.7	Cubic	Fm-3 m(225)
b	CuS	Covellite	60.19	Hexagonal	P63/mmc
	$Cu_{1.81}S$	Digenite	39.81	Cubic	Fm-3 m(225)
c	CuS	Covellite	100	Hexagonal	P63/mmc
d	CuS	Covellite	100	Hexagonal	P63/mmc
e	CuS	Covellite	100	Hexagonal	P63/mmc

4. Conclusion

The research study investigated the effects of different chemical and operational conditions on the copper sulfide precipitate characteristics from an alkaline glycine-cyanide solutions. An acceptable level of settling performance was achieved for most of the conducted tests with a mean particle size of the copper sulfide precipitate ranging from about

Table 1
Experimental conditions for tests a, b, c, d, e. Other experimental conditions: [Cu_T] = 300 mg/L, [CuT]:[CN^-]:[Gly] = 1:1:3, pH = 10.5, [HS^-] = 5 M, [HS]:[Cu_T] = 1.3:1, reaction time = 5 min, stirring speed = 350 rpm.

Test No.	Ca^{2+} dosage	Ionic strength	Aging time	temperature	Seeding
a	0.5 mM	no control	no aging	room temperature	no seeding
b	0	1M	no aging	room temperature	no seeding
c	0.5 mM	no control	24 h	room temperature	no seeding
d	0.5 mM	no control	no aging	55°C	no seeding
e	0.5 mM	no control	no aging	room temperature	1 g/L seed loading

18–62 μm. Divalent cations, particularly Ca^{2+}, significantly affect the formation of large and settleable precipitates probably due to the cross-linking effect. The increasing dosage of Ca^{2+} slightly increased in the mean particle size but has insignificant effect on settling performances. It will be advantageous for a process plant where lime is usually used as pH modifier, implying no extra Ca^{2+} addition is required. A high initial supersaturation level has little effect on the size of the precipitates, which is beneficial for a process plant when treating high copper concentration solutions. Large and settleable precipitates can be produced by increasing the solution ionic strength

A medium stirring speed (200–350 rpm) with a fast sulfide addition rate were preferable in generating larger particles. While aging, heating or seeding has insignificant impacts on the PSD, however, either of these factors can result in a morphology and crystal phase change. A transformation from polymorph to crystalline crystal structure was observed according to the SEM and XRD results. To produce a more mature and crystalline copper sulfide precipitates, adding seed may be a better option than aging and heating, considering the simplicity of the process and energy consumption.

Declaration of Competing Interest

The authors declare that they have no known competing financial interests or personal relationships that could have appeared to influence the work reported in this paper.

Acknowledgment

The authors would like to acknowledge the financial support from Curtin University, Newcrest Mining, Mining and Process Solutions Ltd and Australian Research Council (ARC) Grant No. LP160101121.

Appendix A. Supplementary material

Supplementary data to this article can be found online at https://doi.org/10.1016/j.mineng.2019.106102.

References

Agrawal, S., Guest, J.S., Cusick, R.D., 2018. Elucidating the impacts of initial supersaturation and seed crystal loading on struvite precipitation kinetics, fines production, and crystal growth. Water Res. 132, 252–259. https://doi.org/10.1016/j.watres.2018.01.002.

Al-Tarazi, M., Heesink, A.B.M., Versteeg, G.F., Azzam, M.O.J., Azzam, K., 2005. Precipitation of CuS and ZnS in a bubble column reactor. AIChE J. 51 (1), 235–246. https://doi.org/10.1002/aic.10310.

Bruce, D.W., O'Hare, D., Walton, R.I., 2013. Inorganic Materials Series Preface. Structure from Diffraction Methods: Inorganic Materials Series, pp. xi–xii.

Chung, J., Jeong, E., Choi, J.W., Yun, S.T., Maeng, S.K., Hong, S.W., 2015. Factors affecting crystallization of copper sulfide in fed-batch fluidized bed reactor. Hydrometallurgy 152, 107–112. https://doi.org/10.1016/j.hydromet.2014.12.014.

Dean, J.A., 1990. Lange's handbook of chemistry. Mater. Manuf. Process. 5 (4), 687–688. https://doi.org/10.1080/10426919008953291.

Deng, Z., Oraby, E.A., Eksteen, J.J., 2019. The sulfide precipitation behaviour of Cu and Au from their aqueous alkaline glycinate and cyanide complexes. Sep. Purif. Technol. 218, 181–190. https://doi.org/10.1016/j.seppur.2019.02.056.

Donnet, M., Bowen, P., Jongen, N., Lemaître, J., Hofmann, H., 2005. Use of seeds to control precipitation of calcium carbonate and determination of seed nature. Langmuir 21 (1), 100–108. https://doi.org/10.1021/la048525i.

Eksteen, J.J., Pelser, M., Onyango, M.S., Lorenzen, L., Aldrich, C., Georgalli, G.A., 2008. Effects of residence time and mixing regimes on the precipitation characteristics of CaF 2 and MgF 2 from high ionic strength sulphate solutions. Hydrometallurgy 91 (1), 104–112. https://doi.org/10.1016/j.hydromet.2007.12.002.

Eksteen, J.J., Pelser, M., Onyango, M.S., Lorenzen, L., Aldrich, C., Gerogalli, G.A., 2008. Effects of Residence Time and Mixing Regimes on the Precipitation Characteristics of CaF_2 and MgF_2 from High Ionic Strength Sulphate Solutions. Hydrometallurgy 91 (1–4), 104–112. https://doi.org/10.1016/j.hydromet.2007.12.002.

Estay, H., 2018. Designing the SART process – a review. Hydrometallurgy 176, 147–165. https://doi.org/10.1016/j.hydromet.2018.01.011.

Farahani, B.V., Rajabi, F.H., Bahmani, M., Ghelichkhani, M., Sahebdelfar, S., 2014. Influence of precipitation conditions on precursor particle size distribution and activity of Cu/ZnO methanol synthesis catalyst. Appl. Catal. A 482, 237–244. https://doi.org/10.1016/j.apcata.2014.05.034.

Houcine, I., Plasari, E., David, R., Villermaux, J., 1997. Influence of mixing characteristics on the quality and size of precipitated calcium oxalate in a pilot scale reactor. Chem. Eng. Res. Des. 75 (2), 252–256. https://doi.org/10.1205/026387697523534.

Lekkerkerker, H.N.W., 2011. Colloids and the Depletion Interaction/by Henk N.W. Lekkerkerker, Remco Tuinier. Dordrecht: Dordrecht : Springer Netherlands.

Lewis, A., van Hille, R., 2006. An exploration into the sulphide precipitation method and its effect on metal sulphide removal. Hydrometallurgy 81 (3), 197–204. https://doi.org/10.1016/j.hydromet.2005.12.009.

Linga, Å., 2017. Effects of Seeding on the Crystallization Behaviour and Filtration Abilities of an Aromatic Amine. NTNU.

Marcant, B., David, R., 1991. Experimental evidence for and prediction of micromixing effects in precipitation. AIChE J. 37 (11), 1698–1710. https://doi.org/10.1002/aic.690371113.

Mokone, T.P., van Hille, R.P., Lewis, A.E., 2010. Effect of solution chemistry on particle characteristics during metal sulfide precipitation. J. Colloid Interface Sci. 351 (1), 10–18. https://doi.org/10.1016/j.jcis.2010.06.027.

Moreno, J., Peinado, R., 2012. Chapter 15 – precipitation equilibria in wine. In: Moreno, J., Peinado, R. (Eds.), Enological Chemistry. Academic Press, San Diego, pp. 253–269.

Oraby, E.A., Eksteen, J.J., 2015. Gold leaching in cyanide-starved copper solutions in the presence of glycine. Hydrometallurgy 156, 81–88. https://doi.org/10.1016/j.hydromet.2015.05.012.

Oraby, E.A., Eksteen, J.J., Tanda, B.C., 2017. Gold and copper leaching from gold-copper ores and concentrates using a synergistic lixiviant mixture of glycine and cyanide. Hydrometallurgy 169, 339–345. https://doi.org/10.1016/j.hydromet.2017.02.019.

Park, S., Lee, K.-S., Bozoklu, G., Cai, W., Nguyen, S.T., Ruoff, R.S., 2008. Graphene oxide papers modified by divalent ions-enhancing mechanical properties via chemical cross-linking. ACS Nano 2 (3), 572. https://doi.org/10.1021/nn700349a.

Roy, P., Srivastava, S.K., 2007. Low-temperature synthesis of CuS nanorods by simple wet chemical method. Mater. Lett. 61 (8), 1693–1697. https://doi.org/10.1016/j.matlet.2006.07.101.

Sampaio, R.M.M., Timmers, R.A., Kocks, N., André, V., Duarte, M.T., Van Hullebusch, E.D., Farges, F., Lens, P.N.L., 2010. Zn–Ni sulfide selective precipitation: the role of supersaturation. Sep. Purif. Technol. 74 (1), 108–118. https://doi.org/10.1016/j.seppur.2010.05.013.

Sampaio, R.M.M., Timmers, R.A., Xu, Y., Keesman, K.J., Lens, P.N.L., 2009. Selective precipitation of Cu from Zn in a pS controlled continuously stirred tank reactor. J. Hazard. Mater. 165 (1), 256–265. https://doi.org/10.1016/j.jhazmat.2008.09.117.

Söhnel, O., Garside, J., 1992. Precipitation : basic principles and industrial applications/Otakar Söhnel and John Garside. Oxford [England].

Seaman, B., Newton, T., Oraby, E.A., 2019. Development of a glycine-cyanide leach process for gold-copper concentrate. Proceedings of ALTA 2019. ALTA, Australia, pp. 1–12.

Söhnel, O., Garside, J., 1992. Precipitation: Basic Principles and Industrial Applications. Butterworth-Heinemann, Oxford, UK.

Tauetsile, P.J., Oraby, E.A., Eksteen, J.J., 2019a. Activated carbon adsorption of gold from cyanide-starved glycine solutions containing copper. Part 1: Isotherms. Sep. Purif. Technol. 211, 594–601. https://doi.org/10.1016/j.seppur.2018.09.024.

Tauetsile, P.J., Oraby, E.A., Eksteen, J.J., 2019b. Activated carbon adsorption of gold from cyanide-starved glycine solutions containing copper. Part 2: Kinetics. Sep. Purif. Technol. 211, 290–297. https://doi.org/10.1016/j.seppur.2018.09.022.

Torbacke, M., Rasmuson, Å.C., 2001. Influence of different scales of mixing in reaction crystallization. Chem. Eng. Sci. 56 (7), 2459–2473. https://doi.org/10.1016/S0009-2509(00)00452-8.

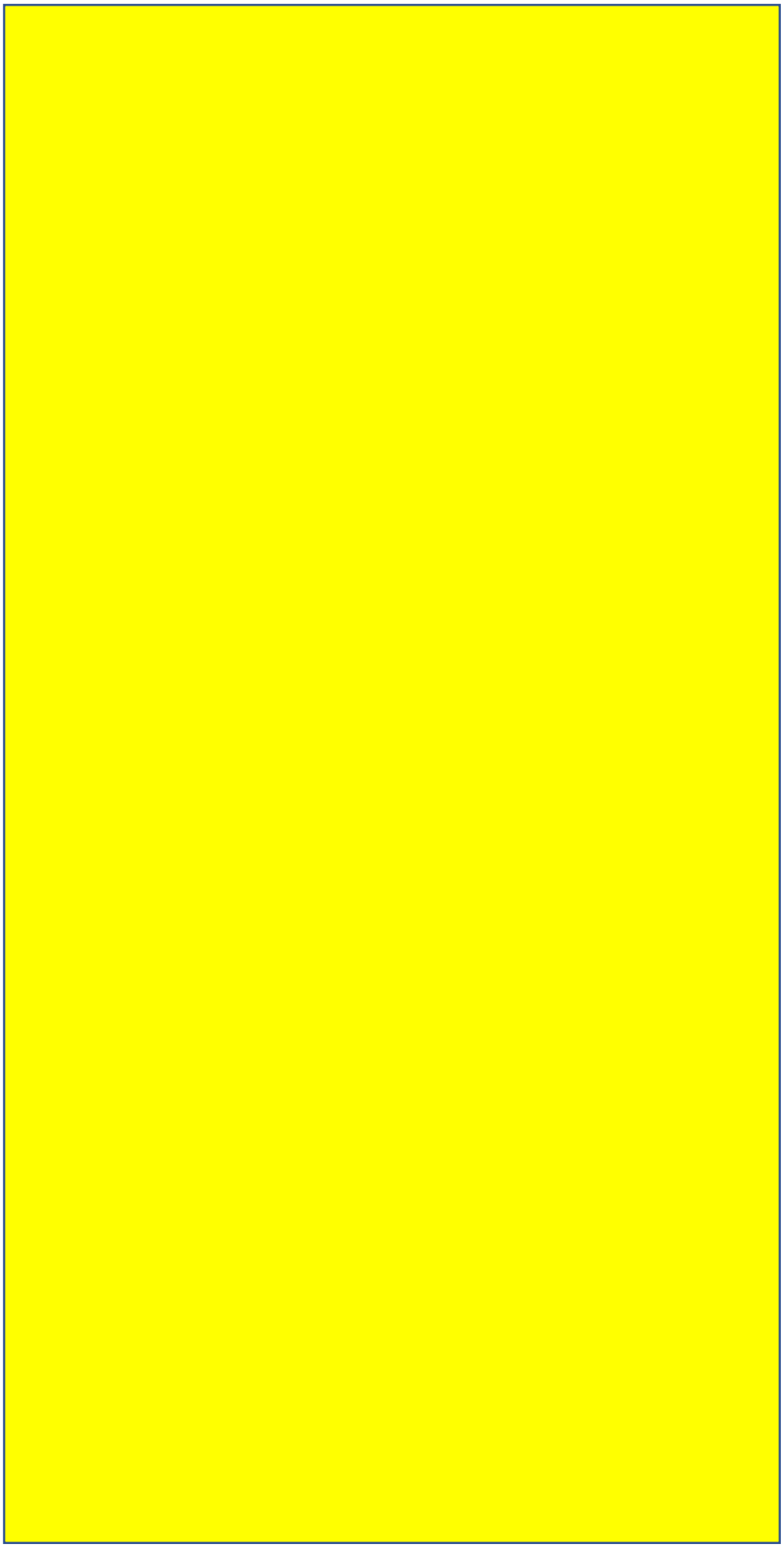

Chapter 5: Cu Adsorption behaviour on chelating resins from cyanide-starved glycine solutions

Submitted for publication as:

Cu adsorption behaviours onto chelating resins from glycine-cyanide
solutions: Isotherms, kinetics and regeneration studies

Deng, Z. Oraby, E.A. and Eksteen, J.J., 2020.
Separation and Purification Technology, 236, 116280.

Accepted for publication on 2 November 2019.

© 2019 Elsevier Ltd.
Reprinted with permission from the publisher.
DOI: https://doi.org/10.1016/j.seppur.2019.116280

Separation and Purification Technology 236 (2020) 116280

Contents lists available at ScienceDirect

Separation and Purification Technology

journal homepage: www.elsevier.com/locate/seppur

Cu adsorption behaviours onto chelating resins from glycine-cyanide solutions: Isotherms, kinetics and regeneration studies

Z. Deng[a], E.A. Oraby[a,b], J.J. Eksteen[a,*]

[a] Western Australian School of Mines: Minerals Energy and Chemical Engineering, Curtin University, GPO Box U1987, Perth, Western Australia 6845, Australia
[b] Faculty of Engineering, Assiut University, Egypt

ARTICLE INFO

Keywords:
Glycine
Copper
Chelating ion-exchange resin
Adsorption
Regeneration

ABSTRACT

A method is presented to remove and recover copper from copper-gold glycinate solutions using an iminodiacetic functionalized resin with subsequent regeneration. The adsorption/desorption approach was evaluated for a glycine leaching process which was shown to be effective for the dissolution of gold and copper from different gold-copper ores and concentrates. In this process, glycine is the lixiviant in the presence of very low cyanide concentration as a synergistic reagent. The copper species in glycine-cyanide process are mainly present as cupric glycinate and a low concentration of cuprous dicyanide and no free cyanide. While cupric glycinate does not load well onto activated carbon, cuprous dicyanide is problematic due to its high carbon affinity and co-loading with gold onto activated carbon, thereby requiring the removal of most of the copper prior to the gold recovery. In this study, the use of ion-exchange resins as one of the possible downstream recovery processes for gold and copper from glycine-cyanide solutions was tested. The isotherms and kinetics of gold and copper (cupric copper (Cu^{2+})) adsorb onto the chelating resin (Puromet MTS9300) from their alkaline glycinate and cyanide complexes were studied. Results show that the [CN_T^-]: [Cu_T] molar ratio has significant effects on the adsorption of Cu_T, due to the change in Cu^{2+}/Cu^+ ratio in the solutions, where [CN_T^-] is the total cyanide in the system (free cyanide being zero). The results show that the chelating resin is selectively adsorbed cupric (Cu^{2+}) over cuprous (Cu^+) ions. The adsorption results were fitted to both the Freundlich and Langmuir isotherm models, while the Langmuir model shows a better correlation. The adsorption kinetic data of Cu^{2+} is well fitted to the pseudo-second-order model. Alkaline glycine solutions in the presence of NaCl was selected as the main eluent for the resin elution study. The multi-cycle adsorption/desorption tests showed that the resin adsorption and regeneration efficiencies are not significantly changed after five cycles of adsorption/desorption. Microscopic visual analysis by using scanning electron microscopy (SEM) showed that there is no significant change in shape and size of the resins, although more cracks were observed after the 5 cycles of adsorption/desorption.

1. Introduction

An innovative leaching method using either glycine on its own [8,9,25,28,36,38–39], or a synergetic mixture lixiviant of glycine and cyanide at starvation levels to extract gold and copper has been presented in a number of research papers [10,26,27]. A two-stage process for the recovery of copper and gold and other metals from waste printed circuit boards have been introduced by Oraby et al. [29] which utilises a two-stage process using initially glycine only followed by a glycine leach with starved cyanide. According to Oraby et al. [27], this synergetic mixture of glycine and small amount of cyanide can be beneficial by (1) reducing the consumption of cyanide by at least 75%, although cyanide reductions > 90% is most frequently observed; (2) forming cupric glycinate which provides extra oxidant (Cu^{2+}) to the leaching system; (3) accelerating the gold dissolution rate by almost three time faster than that in the traditional cyanidation process; (4) yielding zero free cyanide with most of the copper species as cupric glycinate in the final leachates; (5) maintaining weak acid dissoluble (WAD) cyanide at low levels. It should be noted that cyanide which is present as cuprous cyanide runs at starvation levels, which means the cyanide is insufficient for the dissolution of any further cyanide soluble copper minerals [42–43]and that no free cyanide is present as either HCN or the cyanide anion.

To recover copper and gold (together or individually) from the glycine only or cyanide-starved glycine solutions, fundamental studies focused on carbon adsorption[25,40–43] and sulfide precipitation [6]

* Corresponding author.
E-mail address: jacques.eksteen@curtin.edu.au (J.J. Eksteen).

https://doi.org/10.1016/j.seppur.2019.116280
Received 15 September 2019; Received in revised form 26 October 2019; Accepted 2 November 2019
Available online 04 November 2019
1383-5866/ © 2019 Elsevier B.V. All rights reserved.

have been carried out, as well as copper removal by solvent extraction [37]. It was shown that activated carbon can adsorb gold effectively with around 99% of gold recovery in 6 h. However, copper co-adsorption on carbon cannot be avoided with significant copper being co-adsorbed, unless removed beforehand by precipitation, cementation, solvent extraction or ion exchange. The competing nature between the glycine and cyanide to form complexes with the copper and gold creates a dynamic complex system that competes with complex-forming nature of active groups in ion exchange resins and solvent extractants. Recent work conducted by the authors [6] proposed using sulfide precipitation to remove copper prior to the carbon adsorption process and the results indicate that Cu^{2+} complexed with glycine can be precipitated effectively by NaHS precipitation without any gold being precipitated. While the remaining Cu^{+} complexed with cyanide in solutions can be oxidized to Cu^{2+} by hydrogen peroxide so that all copper can be precipitated. The oxidation of cuprous cyanide to cupric glycinate can be optional. That is because copper cyanide species can be recovered during the carbon adsorption process and recycled during leaching, diminishing the loss of cyanide in the circuit.

Using ion-exchange resins to remove copper from the cyanide-starved glycine solutions in the presence of gold before the carbon adsorption step may be another feasible option. Ion-exchange resins are commonly for resin-in-pulp (RIP), resin-in-leach (RIL) and resin-in-column (RIC) systems in hydrometallurgical and environmental applications [14,21,32–33]. Due to the insoluble, spherical and large particulate nature of ion exchange resin beads, it is easy to separate them from solution, pulps and slurries (where the ore/concentrate particle sizes are typically an order of magnitude smaller than the resin size simplifying separation through inter-stage screening) and recycle them for use for significantly longer durations than activated carbon.

The adsorption mechanism of conventional cationic or anionic exchange is via electrostatic interaction. These resins are characterized as low selectivity towards most ions which usually used in purification. To selectively remove heavy metal ions, chelating resins are often required. Chelating resins are developed and designed for selective adsorption of transitional metal ions from solutions [22]. The adsorption of chelating resins is achieved based on the complexation of metal ions through covalent bonding between the ligands of the resin and metals in solutions [3]. The effectiveness of adsorption of metal ions from solutions to adsorbents usually depends on the functional group on the surface of the adsorbents [31]. The most frequently used functional group in these resins include nitrogen form (e.g. N presents in amines, iminos, azo groups, amides, nitriles), sulphur forms (e.g. S presents in thiocarbamates, thioethers, and thiols), and oxygen forms (e.g. O presents in hydroxyl, phenolic, carboxylic) [11].

The adsorption behaviour using chelating resins to recover copper/gold in the recently developed glycine-cyanide leaching system has not been reported to date. Therefore, a fundamental study on gold and copper adsorption onto resin is necessary as an alternative metals recovery option from glycine-cyanide leaching system. In this study, the adsorption behaviour of three commercially available chelating ion-exchange resins (Puromet MTS9300, MTS9600, MTS9850) was studied and evaluated. These resins were selected on the basis of their properties (the grafted functional groups) and availability. The Puromet MTS9300 resin contains iminodiacetic acid (IDA) functional groups in a polystyrene-divinylbenzene (DVB) matrix. It was selected as previous studies revealed that a similar chelating resin (Chelax 100) developed by a different supplier with the same functional IDA groups has high selectivity on the adsorption of divalent transition metal ions, particularly copper and nickel [15,16]. IDA provides a tridentate ligand to form stronger metal complexes than the bidentate ligand glycine, implying the dominant Cu species (cupric glycinate) in the cyanide-starved glycine solutions can be effectively adsorbed by the selected chelating resins. The Puromet MTS9600 resin with the bis-picolylamine functional group has three nitrogen donor atoms and two of them are in the aromatic pyridyl groups (tertiary amine). Some research studies indicated that the bis-picolylamine functionalised resin (DowexTM M4195) showed a very high Cu affinity (99% recovery) compared to other metals such as Al, Fe, Pb, Sn, Ni, Zn, Au and Ag in an acidic environment [23,30,47]. The Puromet MTS9850 chelating resin with polyamine functional groups is expected to selectively remove Cu^{2+} [12].

It should be noted that very few of studies have investigated the copper adsorption onto ion-exchange resins at alkaline condition as the $Cu(OH)_2$ precipitation can be the dominant species in the precursor aqueous system, while the Cu^{2+} coordinated with glycine in the glycine-cyanide solutions is stable over a wide pH-Eh range [8,9]. In this study, the main objective is to evaluate and compare the potential of different types of chelating resins to selectively remove copper from alkaline cyanide-starved glycine solutions in the presence of gold. Copper and gold adsorption on different chelating resins were studied and the adsorption isotherms and kinetics of the most appropriate resin were investigated. The adsorption mechanism i.e. the rate-controlling step was also discussed. The surface morphology of the raw and treated resins was also visualised using the scanning electron microscope (SEM) technique. Multiple locked cycle tests on actual leachates (to evaluate the robustness of capacity and kinetics response in the presence of foulants after multiple adsorption elution cycles) is outside of the scope of the current paper but is being covered in further research by the authors.

2. Experimental design

2.1. Adsorbents

The Puromet MTS9300, MTS9600 and MTS9850 chelating resins

Table 1
Physical and chemical characteristics of different types of chelating resins.

Properties	Type of resin		
	Puromet MTS9300	Puromet MTS9600	Puromet MTS9850
Structure	Macroporous	Macroporous	Macroporous
Matrix	Polystyrene-DVB	Polystyrene-DVB	Polyacrylic-DVB
Functional group	Iminodiacetic 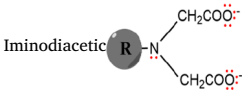	Bis-picolylamine 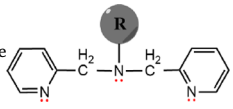	Polyamine 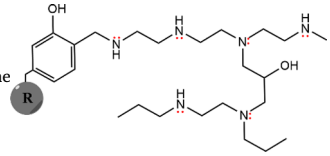
Ionic Form	Na^{+} form	FB*/SO^{4-} form	FB form
Moisture	52% −60% (Na^{+} form)	50% − 60% (SO^{4-} form)	52% − 57% (Cl^{-} form)
Particle size range	425–1000 μm	425–1000 μm	300–1200 μm

*FB: Free-base, the deprotonated form of an amine.

used in this study were purchased from Purolite®. As per the guidelines of the manufacturer, their physical and chemical properties were indicated in Table 1. Prior to the adsorption, a certain mass of resins was pre-conditioned, if required, by 0.1 M HCl solution and washed by deionised water and then mixed with 1 M NaOH solution for 24 h. The pre-conditioned resins were then rinsed by deionised water before its use during the adsorption tests.

2.2. Cyanide-starved glycine solutions

All tests in this study were conducted using synthetic cyanide-starved glycine solutions, where analytical grade reagents and deionized water were being used throughout the tests. A stock cyanide-starved glycine solution containing gold and copper was first prepared. Gold powders (99.998%, spherical, −200 mesh, Alfa Aesar – Thermo Fisher Scientific) were dissolved in deionized water contained glycine (> 99%, Sigma-Aldrich) and CuCN (95%, Ajax, Finechem). The initial pH of all the tests was 10.5, which is at the optimal pH range for the glycine-cyanide leaching system [26]. The solutions were adjusted using sodium hydroxide (NaOH) with a pH meter (Model AQUA-PH Meter). The solution was agitated with a magnetic stirrer and Teflon magnetic stirrer bars at 350 rpm. The solution was filtered by a Supor® 0.45 μm membrane disc filter (Pall Corporation) prior to the tests. Typically, in the synthetic alkaline glycine-cyanide solutions, copper species mainly present as cupric glycinate ($Cu(NH_2CH_2COO)_2$), and cuprous diacyano-complex ($Cu(CN)_2^-$), triacyano- and tetracyano-complexes ($Cu(CN)_3^{2-}$ and $Cu(CN)_4^{3-}$)) may exist depending on the $[Cu_T]$:$[CN_T^-]$:$[Gly_T]$ molar ratios. The overall complexation reactions for copper and gold species in a synthetic glycine-cyanide solution are presented in Eqs. (1) to (3):

$$8CuCN + 8NH_2CH_2COOH + O_2 + 4OH^- \rightarrow 4Cu(NH_2CH_2COO)_2 + 4Cu(CN)_2^- + 6H_2O \quad (1)$$

$$4Au + 8CN^- + O2 + 2H_2O \rightarrow 4Au(CN)_2^- + 4OH^- \quad (2)$$

$$4Au + 8NH_2CH_2COOH + O_2 + 4OH^- \rightarrow 4Au(NH_2CH_2COO)_2^- + 6H_2O \quad (3)$$

Unless specified, the standard solutions containing 300 mg/L Cu_T and 2 mg/L Au at $[Cu_T]$:$[CN_T]$:$[Gly_T]$ molar ratio of 1:1:3 were used for most of the adsorption/desorption tests, where the subscript "T" refers to the total copper, cyanide and glycine concentrations present and not their "free" species in solution. From this point on we will use $[CN^-]$ to represent total cyanide, $[CN_T^-]$, and [Gly] to represent total glycine concentration, $[Gly_T]$. However, $[Cu_T]$ will be retained to distinguish it from the concentrations of Cu^{2+} and Cu^+.

2.3. Adsorption behaviour of different types of resins

Batch adsorption tests were undertaken using a bottle-on-rolls method at room temperature. Certain mass (4.125 g, wet weight) of different types of resins were added in 250 ml synthetic cyanide-starved glycine solutions. The resins and solution mixture were rolled in 2.5 L Winchester bottles for 24 h at 300 rpm and room temperature with 5 ml of kinetic samples taken up at 0.5, 1, 2, 4, 6, 24 h. Each solution sample was filtered by a Supor® 0.45 μm membrane disc filter (Pall Corporation) to remove any fine resins and prevent further adsorption. Only one type of resin was chosen for further investigation based on its selectivity of copper over gold. The metal recovery was calculated by Eq. (4):

$$\text{Metal Recovery } \% = \frac{C_0 - C_t}{C_0} \times 100\% \quad (4)$$

where C_o is the initial metal concentration and C_t is the metal concentration at time t. The effects of different $[CN^-]$: $[Cu_T]$ and [Gly]: $[Cu_T]$ molar ratios were studied. The effects of resin to metal mass ratio on the metal recoveries and metal adsorption capacities was also investigated in this study.

2.4. Adsorption isotherms and kinetics studies

The equilibrium adsorption isotherms were obtained by contacting five different masses of resins with 250 ml synthetic cyanide-starved glycine solutions for 24 h. The amount of metal adsorbed onto the resin (Q_e, mg/g) at equilibrium was calculated by Eq (5):

$$Q_e = \frac{(C_o - C_e)V}{W} \quad (5)$$

where C_e is the metal concentration at equilibrium (mg/L), V is solution volume (L) and W and the mass of dry resin (g). The experimental data at different $[CN^-]$:$[Cu_T]$ molar ratios were fitted to Freundlich and Langmuir isotherm models.

The kinetic samples were taken at different time intervals for analysing the metal ions concentration (mg/L), and the amount of metal adsorbed on to the resin at time t (Q_t) is calculated. The kinetic process at different $[CN^-]$:$[Cu_T]$ molar ratios were described by the pseudo-first-order, pseudo-second-order and intra-particle model using linear regression.

2.5. Desorption and resin reuse

Batch desorption tests were carried out for the selected resin using different concentrations of alkaline glycine solutions with salt and hydrochloride acid as eluants. A 5 ml of eluted resins were previously loaded by contacting a 250 ml Cu-Au-glycine-cyanide solution containing 1500 mg/L of Cu_T at a $[Cu_T]$:$[CN^-]$:[Gly] molar ratio of 1:1:3 for 24 h. The purpose of using a high concentration of Cu_T is to allow the loaded resin to reach its equilibrium state. The fully loaded resins were then transferred to a 250 ml beaker and agitated with a 100 ml of eluent by a magnetic stirrer at 250 rpm at room temperature or mildly elevated temperature (55 °C) for 2 h. The best eluent was selected for reuse according to their desorption efficiency (D%) which was calculated by Eq. (6) [5].

$$D\% = \frac{\text{Mass of metal ions desorbed to HCl solution, mg}}{\text{Mass of metal ions adsorbed onto the resin, mg}} \quad (6)$$

After determining the optimum eluent, 5 cycles of adsorption/desorption tests were carried out for estimating the change of adsorption capacity and regeneration efficiency (RE%), with the same Cu-Au-glycine-cyanide solution used for adsorption. The regeneration efficiency of the adsorbent was calculated as shown in Eq. (7) [35].

$$RE\% = \frac{Q_r}{Q_o} \times 100 \quad (7)$$

where Q_o and Q_r (mg/g) is the adsorption capacities before and after regeneration.

2.6. Analytical methods

The total concentration of copper and gold before and after adsorption and desorption were analysed by an atomic adsorption spectrometer (AAS, Agilent 55B AAS model). The concentration of Cu^{2+} was determined by a UV–Vis Spectrophotometer (Agilent Cary 60 UV–Vis). The concentration of Cu^+ was calculated by the differences between $[Cu_T]$ and $[Cu^{2+}]$.

After adsorption and desorption, the resins were screened, washed by deionised water and dried in an oven at 70 °C. The dried resin samples were sprinkled on the carbon tapes and stuck on an aluminium stub with Pt coated (3 nm). Then the surface morphologies of the dry original, loaded, stripped and regenerated resins were visualised by SEM with a ZEISS Neon 40EsB cross-beam Field Emission Scanning Electron Microscope (FESEM) model.

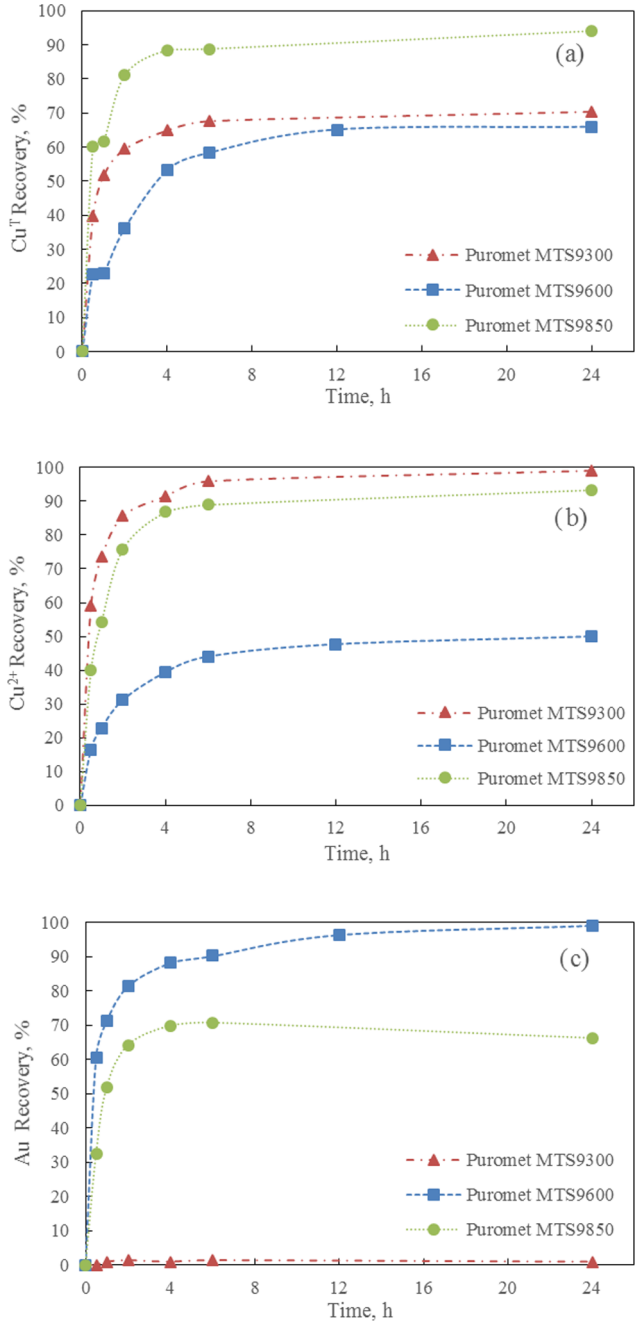

Fig. 1. Recovery of (a) Cu_T, (b) Cu^{2+} and (c) Au onto different types of chelating resins. Experimental conditions: $[Cu_T]$ = 300 mg/L, $[Cu_T]$:$[CN^-]$:[Gly] = 1:1:3, pH = 10.5, resin dosage = 7.5 g/L, room temperature.

3. Results and discussions

3.1. Adsorption behaviour of different types of chelating resins

The adsorption performance of Cu_T, Cu^{2+} and Au from the cyanide-starved glycine solutions onto different types of chelating resins was investigated. The experimental conditions are shown in the caption of Fig. 1. As it can be observed from Fig. 1a, the Puromet MTS9850 resins show the highest total Cu recovery (94.0%) after 24 h, followed by MTS9300 at 70.5% and MTS9600 at 65.8%. Fig. 1b demonstrates that the Cu^{2+} recovery of MTS9300 and MTS9850 resins increase remarkably in the first 2 h and then increase gradually to 99.1% and 93.4% respectively after 24 h. While the MTS9600 resins show relatively poorer Cu^{2+} affinity with only 41.7% of Cu^{2+} being adsorbed after 24 h. As for gold adsorption, it is apparent from Fig. 1c that high Au adsorption (99.0%) was observed when using MTS9600 chelating resins, while very low Au co-adsorption (0.81%) was obtained using MTS9300 chelating resins. The Au adsorption peaked at 70.7% in 6 h and declined slightly at 66.2% in 24 h when using MTS9850 resins. The Cu_T, Cu^{2+}, Cu^+ and Au concentrations during the adsorption period (0, 1, 6, 24 h) using different types of resins are presented in Table 2. It can be seen that the concentrations of Cu^+ stay constant between 88 and 90 mg/L when MTS9300 chelating resins were used as an adsorbent, while both MTS9600 and MTS9850 resins show relatively high Cu^+ affinity that low Cu^+ concentration can be seen after 24 h adsorption. The MTS9600 resin adsorbs almost all the gold in solutions with around 58% of total copper recovery which is similar to the adsorption behaviour of the traditional activated carbon in the same glycine-cyanide system [42–43]. The MTS9850 resin shows high Cu recovery (94%) with about 66% Au recovery which indicates a complete of Cu and Au adsorption onto resins is possible if the resin dosage increases. However, both MTS9600 and MTS9850 resins showed the adsorption of both Cu and Au, showing poor selectivity.

Table 2
Concentrations of Cu_T, Cu^{2+}, Cu^+ and Au during adsorption using different types of resins.

Resin type	Time	Cu_T	Cu^{2+}	Cu^+	Au
	h	mg/L	mg/L	mg/L	mg/L
Puromet MTS9300	0	308	220	88	2.16
	1	149	61	88	2.15
	6	99	9	90	2.15
	24	91	2	89	2.15
Puromet MTS9600	0	308	218	90	2.18
	1	266	193	73	0.63
	6	175	150	25	0.21
	24	128	127	1	0.02
Puromet MTS9850	0	300	228	72	2.01
	1	115	54	61	0.97
	6	33	25	8	0.59
	24	18	15	3	0.68

The different adsorption behaviour of resins can be attributed to the difference in their functional groups and cation-anion characteristics. The MTS9300 resins have iminodiacetic functional group which is classified as weak acid cation resins. While both MTS9600 and MTS9850 are weak base anion resins with amine functional groups. Anion exchangers are normally used in the cyanidation for the adsorption of anionic $Au(CN)_2^-$ [14]. That is because the gold species are presented as very stable $Au(CN)_2^-$, where the concentration of free Au^{3+} ions will be zero or very low in the solutions, thus, the cation exchangers, MTS9300 resins, with negatively charged functional groups, can barely adsorb the $Au(CN)_2^-$ and $Cu(CN)_2^-$ from the glycine-cyanide solutions due to the Donnan co-ions exclusion effect [34]. According to Oraby and Eksteen [24], cupric ions can be dissociated from the neutral cupric glycinate from a simultaneous equilibrium reaction (Eq. (8)), the iminodiacetic functionalised MTS9300 resins can, therefore, adsorb the dissociated Cu^{2+}, where its complexation reaction was through a cation exchange accompanied by chelation [47]. The proposed overall adsorption equation is shown in Eq. (9). That is probably the reason why the MTS9300 resins can selectively adsorb Cu^{2+} over Cu^+ and Au. On the other hand, as anion exchangers, the other two types of resins may adsorb the anionic species by electrostatic bonds and complex the cations (Cu^{2+}) by chelation with the nitrogen donor atoms through coordinate bonds.

The MTS9300 resins show very high selectivity toward Cu^{2+} and a

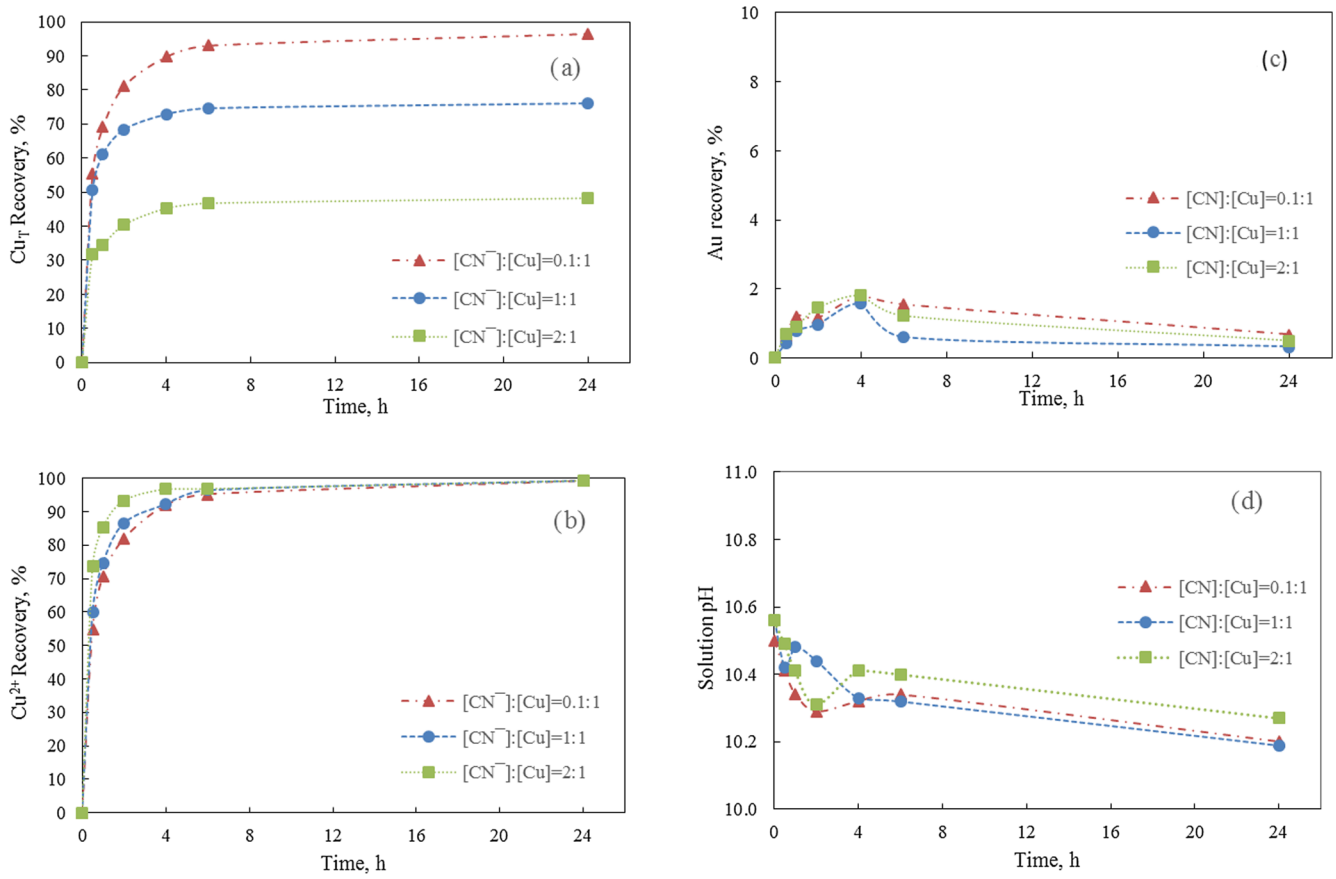

Fig. 2. The Effects of [CN$^-$]: [Cu$_T$] molar ratio on (a) total Cu adsorption, (b) Cu2 + adsorption, (c) Au adsorption, (d) solution pH. Experimental conditions: [Cu$_T$] = 300 mg/L, [Cu$_T$]:[Gly] = 1:3, pH = 10.5, resin dosage = 7.5 g/L, room temperature.

significant low adsorption of Cu^+ and Au, therefore, it was chosen as the best resin for further investigation of its adsorption behaviour in terms of adsorption isotherms and kinetics.

$$Cu(NH_2CH_2COO)_2 \leftrightarrow Cu^{2+} + 2(NH_2CH_2COO^-) \quad (8)$$

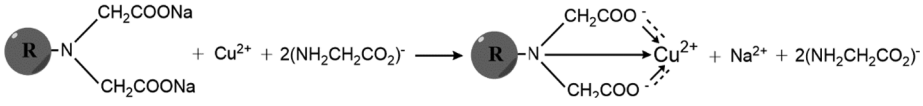

(9)

3.2. Effects of [CN$^-$]: [Cu$_T$] molar ratio

A previous study by the authors [6] focused on the sulfide precipitation from the same leach system showed that the change in [CN$^-$]: [Cu$_T$] molar ratio at a constant glycine concentration significantly affect the [Cu^{2+}]:[Cu$^+$] molar ratio which has a significant influence on the copper precipitation. It was observed that while Cu^{2+} ions precipitated quantitatively, the Cu^+ complexed with cyanide remained in the solution. A similar separation phenomenon was observed when using the Puromet MTS9300 resin. As it can be seen in Fig. 2a, the total copper recovery increases from 43.3% to 96.1% as the [CN$^-$]: [Cu$_T$] molar ratio decreases from 2 to 0.1. That is mainly because at constant glycine concentration, lower [CN$^-$]: [Cu$_T$] molar ratio results in higher [Cu^{2+}]/[Cu$^+$] ratio where more copper glycinate and low cuprous cyanide were presents. Fig. 2b shows the Cu^{2+} recovery reached above 99% after 24 h at any [CN$^-$]: [Cu$_T$] molar ratio. As it can be observed from the data shown in Table 3, the Cu^+ concentration remains constant during the adsorption at any [CN$^-$]: [Cu$_T$] molar ratio, further confirming the remaining cuprous cyanide in solutions was not adsorbed by the MTS9300 chelating resin. Both Fig. 2c and Table 3 indicate that the adsorption of gold was insignificant and only less than 1% of gold was adsorbed at any [CN$^-$]: [Cu$_T$] molar ratio. The pH of solutions during the adsorption was measured during the sampling times, as shown in Fig. 2d. The pH change of the solution was not very significant and the pH slightly decreases from around pH 10.5 to 10.2 during the whole 24 h adsorption. Based on the above observations, the tested MTS9300 chelating resin appears to selectively adsorb Cu^{2+} , over Cu^+ cyanide and Au.

3.3. Effects of [Gly]: [Cu$_T$] molar ratio

A study focused on the same system using activated carbon as the adsorbent illustrated that increasing the free glycine concentration has a significant negative impact on the rate of copper adsorption and copper recovery [42]). The free glycine concentration can affect the ratio between Cu^+ and Cu^{2+} during leaching in a cyanide-starved

Table 3
Concentration of Cu_T, Cu^{2+}, Cu^+ and Au during adsorption at different [CN^-]:[Cu_T] ratios.

[CN]:[Cu] ratio	Time	Cu_T	Cu^{2+}	Cu^+	Au
	h	mg/L	mg/L	mg/L	mg/L
0.1:1	0	300	294	6	2.07
	1	96	90	6	2.04
	6	23	16	7	2.04
	24	11	3	8	2.04
1:1	0	302	223	79	2.17
	1	133	59	74	2.15
	6	84	9	75	2.15
	24	81	2	79	2.15
2:1	0	298	120	178	2.19
	1	196	17	179	2.17
	6	180	4	176	2.16
	24	179	1	178	2.16

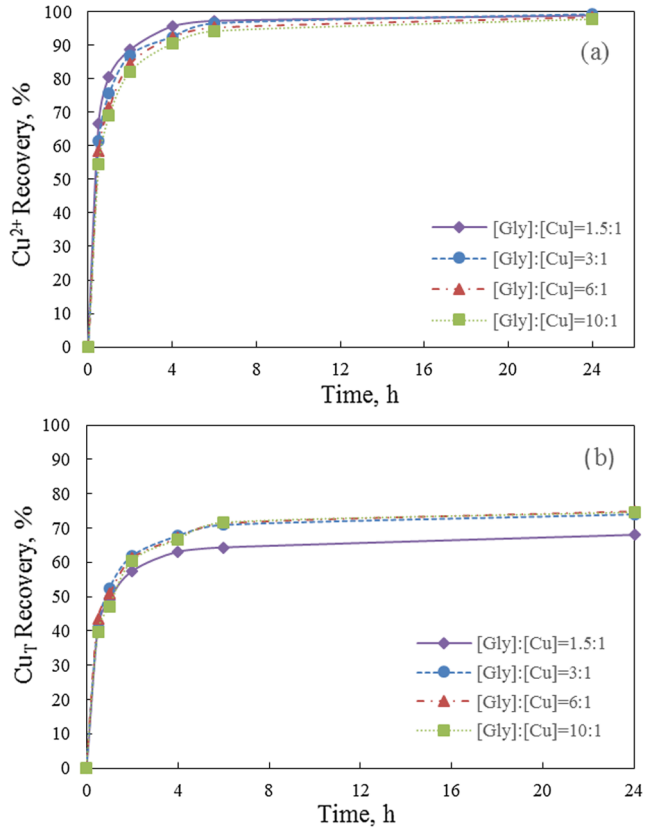

Fig. 3. Effects of [Gly]:[Cu_T] molar ratio on (a) total copper and (b) Cu^{2+} recovery. Experimental conditions: [Cu_T] = 300 mg/L, [Cu_T]:[CN^-] = 1:1, pH = 10.5, room temperature.

glycine system [27]. Different masses of glycine were added accordingly in the synthetic system to investigate the effects of [Gly]:[Cu_T] molar ratios at a fixed [Cu_T]:[CN^-] molar ratio of 1:1 and the results are presented in Fig. 3. It is observed in Fig. 3a that there is no obvious effect on the adsorption regarding the recoveries and the rate of adsorption for Cu^{2+} at any [Gly]:[Cu_T] molar ratios. Whereas, at the lowest [Gly]:[Cu_T] molar ratio of 1.5:1, it is clear that the recovery of total copper is slightly lower due to higher Cu^+ in the system. When insufficient glycine was added in the solutions, less copper was complexed with glycine to form cupric glycinate i.e. $Cu(NH_2CH_2COO)_2$, resulting in relatively lower Cu^{2+} but higher Cu^+ in the glycine-cyanide system. The increasing [Gly]:[Cu_T] molar ratios from 3:1 to 10:1

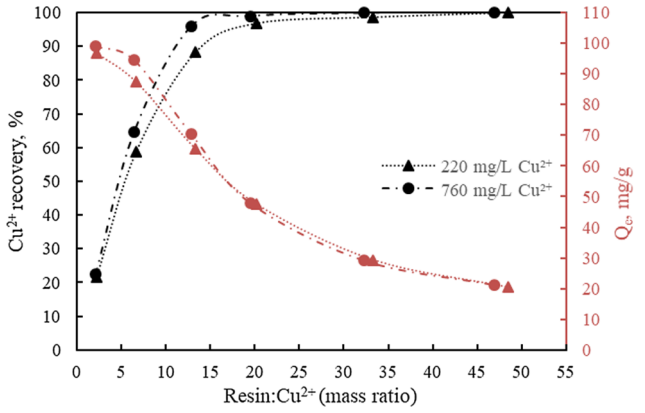

Fig. 4. The Cu^{2+} recovery and the Cu adsorption capacity (Q_e) at different Cu^{2+} concentrations as the function of resin:Cu^{2+} mass ratio. Experimental conditions: [Cu_T]:[CN^-]:[Gly] = 1:1:3, pH = 10.5, room temperature.

have insignificant effects on Cu^{2+}/Cu^+ ratio in the synthetic glycine-cyanide system. This is not a surprising result as only 2 mol of glycine is required to complex one mole of cupric ions as shown in Eq (7). Although the glycine additions were more than the stoichiometric requirement, further conversion/oxidation of Cu^+ to Cu^{2+} requires sufficient oxidants such as peroxide or oxygen.

3.4. Resin dosage and Cu^{2+} concentration

Typically, the required resin dosage is determined by the metal concentrations. The adsorption behaviours of two levels of Cu_T concentrations (300 and 1000 mg/L) at [Cu_T]:[CN^-]:[Gly] molar ratio of 1:1:3, where the initial [Cu^{2+}] were 220 mg/L and 760 mg/L, respectively, were investigated. Resin dosage at a range between 0.5 and 10.8 g of dry resin per litre was used for 220 mg/L of Cu^{2+}; the resin dosage increased proportionally for the adsorption of 767 mg/L Cu^{2+}, ranging from 1.65 to 35.64 g of dry resin per litre. From the previous sections, it can be concluded that the MTS9300 resins only adsorb Cu^{2+}, from this point forward, the adsorption of Cu_T, and Au will not be discussed. The Cu^{2+} recovery and the resin adsorption capacity (Q_e) at different Cu^{2+} concentrations as a function of resin:Cu^{2+} mass ratio are shown in Fig. 4. From the graph, the initial adsorption of Cu^{2+} increased rapidly with increasing the resin dosage as more active sites were available for adsorption with higher resin concentrations. The maximum Cu^{2+} recoveries (around 1 mg/L Cu^{2+} in the barren solutions) were obtained at 7.5 g/L and 24.75 g/L resins for 220 mg/L and 760 mg/L Cu^{2+}, respectively (at a resin:Cu^{2+} mass ratio of 33). Also, it can be seen from the graph that the Cu adsorption capacity of resin remained similar, indicating that when Cu^{2+} concentration increases, increasing the resin dosage proportionally can achieve a similar adsorption performance.

3.5. Equilibrium adsorption isotherms

Freundlich and Langmuir models are commonly used to describe the adsorption process at the equilibrium state [4,20,21,44,46,48]. Linear regression method was used to determine the best-fit model. The model parameters regressed for the models may be suitable for engineering purposes that may be used to predict the amount of metal ions adsorbed on the resins at equilibrium (Q_e).

The Freundlich isotherm model and its linear form can be mathematically expressed by Eqs. (10) and (11) [4,44]:

$$Q_e = K_f C_e^{1/n} \tag{10}$$

$$\log Q_e = \log K_f + \frac{1}{n}\log C_e \tag{11}$$

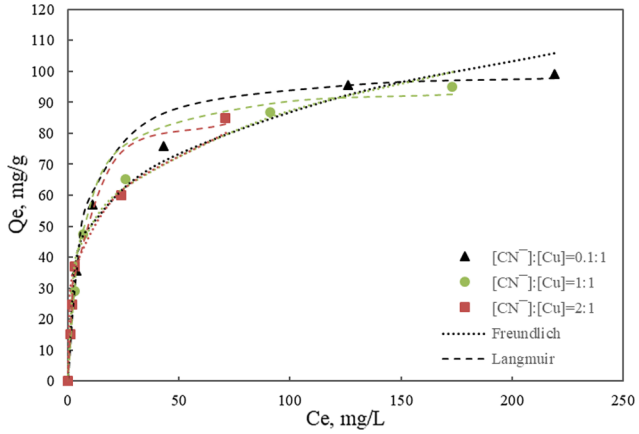

Fig. 5. Experimental adsorption isotherm fitted with Freundlich and Langmuir isotherm at different $[CN^-]$: $[Cu_T]$ molar ratios. Experimental conditions: $[Cu_T]$ = 300 mg/L, pH = 10.5, resin dosage = 0.5 – 7.5 g/L, room temperature.

where K_f is the Freundlich equilibrium adsorption capacity and n is the Freundlich equation constant representing the deviation from linearity of adsorption.

The Langmuir isotherm model and its linear form are presented as shown in Eqs. (12) and (13) [20,46]:

$$\frac{C_e}{Q_e} = \frac{C_e}{Q_m} + \frac{1}{K_L Q_m} \tag{12}$$

$$\frac{1}{Q_e} = \left(\frac{1}{Q_m}\right) + \left(\frac{1}{K_L Q_m}\right)\left(\frac{1}{C_e}\right) \tag{13}$$

where Q_m represents the maximum adsorption capacity (mg/g), K_L represents the energy constant relevant to the heat adsorption (L/mg). An important characteristic of Langmuir isotherm parameter 'R_L', can be used to predict the affinity of the adsorbate and adsorbent. The adsorption is irreversible if $R_L = 0$, favourable if $0 < R_L$ less than 1; linear if $R_L = 1$, or unfavourable if $R_L > 1$. R_L can be calculated by Eq. (14) [20]:

$$R_L = \frac{1}{1 + K_L C_o} \tag{14}$$

The experimental data fitted with both isotherms at different $[CN^-]$:$[Cu_T]$ ratios, (i.e. different initial $[Cu^{2+}]$:$[Cu^+]$ at constant $[Cu_T]$) were presented in Fig. 5. The calculated Freundlich and Langmuir isotherm parameters are shown in Table 4.

As can be seen from Table 4, the values of correlation coefficient (R^2) of the Freundlich model (0.95–0.96) are lower than those of the Langmuir model (> 0.99), which means that Langmuir model represents a better fitting of the experimental data. Fig. 5 showed that both Freundlich and Langmuir models can be used to predict the Q_e according to the value of C_e, while the Langmuir model provides a prediction of the maximum capacity of the resin at different Cu^{2+} concentrations. Based on the Langmuir model, the maximum uptake capacities (Q_m) at different $[CN^-]$: $[Cu_T]$ molar ratios are ranged from 88.50 to 101.01 mg/g (1.39 – 1.59 mmol/g) which have a good agreement of the Cu^{2+} uptake capacities obtained from previous studies [17,18]where similar resins containing iminodiacetic functional groups were used. The maximum adsorption capacity (Q_m) decreased with higher $[CN^-]$: $[Cu_T]$ molar ratio (lower Cu^{2+} concentration). That is probably because the resins did not reach the equilibrium state. At low resin dosage and low initial $[Cu^{2+}]$,a necessary driving force to overcome the resistance of the mass transfer of metal ions from the aqueous phase to the solid phase is not enough [18], thus lowering the Q_m values. The values of R_L are between 0 and 1, indicating favourable adsorption for the initial concentrations and temperature studied [46].

Table 5
Statistical parameters for pseudo-first-order and pseudo-second-order model at different $[CN^-]$: $[Cu_T]$ molar ratio.

Kinetic model	Parameters	$[CN^-]$:[Cu] molar ratio		
		0.1:1	1:1	2:1
Pseudo-first-order	K_1 (h^{-1})	0.144	0.142	0.124
	Q_e, Cal (mg/g)	10.26	6.48	2.12
	R^2	0.864	0.844	0.836
Pseudo-Second-order	K_2 (g/mg/h)	0.059	0.102	0.412
	Q_e, Cal	39.68	30.12	14.90
	Q_e, Exp	39.60	30.03	14.95
	R^2	0.999	0.999	0.999

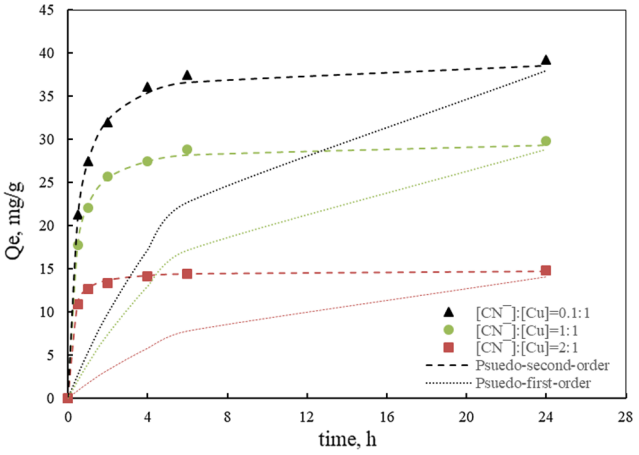

Fig. 6. Adsorption kinetics data fitted with pseudo-first-order and pseudo-second-order models at different $[CN^-]$: $[Cu_T]$ molar ratios. Experimental conditions: $[Cu_T]$ = 300 mg/L, pH = 10.5, resin dosage = 7.5 g/L, room temperature.

3.6. Adsorption kinetics

3.6.1. Pseudo-first-order and pseudo-second-order models

Two reaction-based kinetics models i.e. pseudo-first-order and pseudo-second-order equations were usually used in many adsorption kinetics studies to explain the solid/liquid adsorption with regard to the order of rate constant [2,13,19].

The non-linear and linear form of pseudo-first-order and pseudo-second-order-kinetic models are expressed as shown in Eqs. (15) to (18) [13,19]:

Table 4
Freundlich and Langmuir parameters for Cu^{2+} adsorption at different $[CN^-]$: $[Cu_T]$ molar ratio.

		Freundlich			Langmuir			
$[CN^-]$: $[Cu_T]$	Initial $[Cu^{2+}]$	K_f , (mg/g)/(mg/L)$^{1/n}$	n	R^2	K_L,(L/mg)	R_L	Q_m, (mg/g)	R^2
0.1:1	268	28.13	4.07	0.95	0.15	0.02	101.01	0.99
1:1	223	24.55	3.61	0.95	0.16	0.03	96.15	0.99
2:1	113	17.93	2.71	0.96	0.22	0.04	88.50	0.99

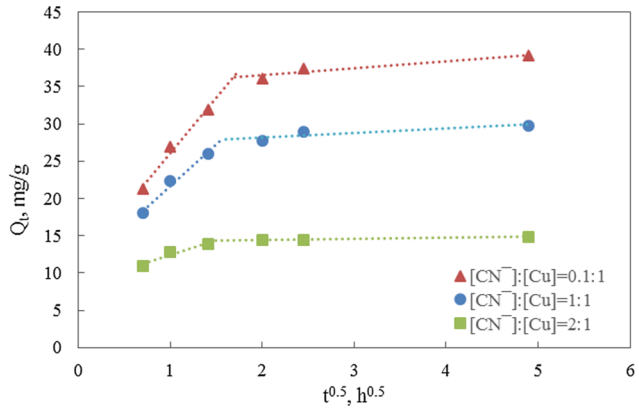

Fig. 7. Intra-particle diffusion model for the adsorption of Cu^{2+} on resin at different $[CN^-]$: $[Cu_T]$ molar ratios.

The Pseudo-first-order kinetic model:

$$Q_t = Q_e\left(1 - e^{-K_1 t}\right) \tag{15}$$

$$\log(Q_e - Q_t) = \log Q_e - \frac{K_1}{2.303}t \tag{16}$$

The Pseudo-second-order kinetic model:

$$Q_t = \frac{Q_e^2 K_2 t}{1 + Q_e K_2 t} \tag{17}$$

$$\frac{t}{Q_t} = \frac{1}{K_2 Q_e^2} + \frac{t}{Q_e} \tag{18}$$

where Q_t is the amount of adsorbate on the surface of the adsorbent at the time, t (mg/g); K_1 is the equilibrium constant of the pseudo-first-order adsorption (min^{-1}), K_2 is the pseudo-second-order rate constant (g/mg/h).

According to the values of R^2 presented in Table 5 and as its visual observation of the model fitting shown in Fig. 6, the pseudo-second-order model shows better applicability ($R^2 > 0.99$) than the pseudo-first-order model (R^2 in a range from 0.75 to 0.86) at different $[CN^-]$: $[Cu_T]$ molar ratios. The calculated Q_e was also in line with the experimental Q_e in the case of the pseudo-second-order model. The calculated pseudo-second-order rate constant K_2 increased with the increasing of $[CN^-]$: $[Cu_T]$ molar ratio (decreasing initial $[Cu^{2+}]$ in solutions). That can be explained by a lower competition for the adsorption of active sites at lower Cu^{2+} concentration, thus increasing the adsorption rate. Based on the high correlation coefficient and the agreement of the calculated Q_e with the experimental data, the adsorption process can be described by the pseudo-second-order kinetic model, which also suggests that the adsorption may be controlled dominantly by chemical processes that especially involved ion-exchange [18,35].

3.6.2. Intra-particle diffusion models

Proposed by Weber and Morris [45], the intra-particle diffusion model is commonly applied for characterizing the diffusion mechanism, the empirical equation in its linear form is presented by Eq. (19):

$$Q_t = K_p t^{\frac{1}{2}} + C \tag{19}$$

where K_p ($mg/g/h^{0.5}$) represents the constant rate of the intra-particle diffusion model, C (mg/g) is a constant. Regarding intercept C, it is proportional to the extent of the boundary layer thickness, a larger value of C means greater boundary layer effect. If the value of C corresponds to a negative value, it indicates the thickness of the boundary layer retards the intra-particle diffusion, while a positive value of the intercept C indicates the adsorption is rapid [7].

A plot of Qt against $t^{1/2}$ was employed, as presented in Fig. 7. It was proposed that if the plot gives a straight line, it suggests the rate-controlling step is intra-particle diffusion; if the plot shows a multi-linearity, it implies the adsorption was affected by two or more steps [2]; Poots et al. 1976; [50]. From Fig. 7, it is clear that the curves exhibit multi-linear plots, indicating intra-particle diffusion is not the only rate-limiting step. Similar trends were observed from carbon adsorption of lead from wastewater by Acharya et al. [1] and resin adsorption of Zn from polluted water by Zhang et al. [49]. Both of Acharya and Zhang's studies believed the initial stage was a film diffusion stage, whereas, in the later stage was due to the intra-particle diffusion effects.

3.7. Desorption and regeneration

3.7.1. Eluent selection

Batch desorption tests for stripping Cu from the fully loaded resins (~100 mg/g Cu) using hydrochloric acid or alkaline glycine solutions as eluents were conducted. Alkaline glycine solutions in the presence of NaCl were proposed to be used as the main eluent in this study. The effects of different concentrations of glycine, sodium hydroxide, and sodium chloride on the resin desorption efficiency were studied.

Also, acidic solutions as the widely used eluent to desorb the heavy metal ions from the resins [44], the desorption tests using HCl as an eluent at different concentrations were carried out. The results are summarised in Fig. 8.

The main observations are presented as follows:

- Alkaline glycine solutions in the presence of salt can effectively strip Cu from the tested resin, the highest stripping efficiency (84.3%) was achieved using 3 M glycine, 3 M NaOH, and 3 M NaCl.
- Desorption efficiency increases with increasing glycine concentration.
- The presence of NaCl enhances desorption efficiency.
- The desorption performance using glycine as the eluent is not sensible at alkaline conditions, according to Test 5 at pH 12 (84.3%) and Test 7 at pH 10 (83.0%).
- At alkaline conditions, higher desorption efficiency can be achieved with increasing the concentration of NaCl.
- Heating the solutions to 55 °C did not increase the desorption efficiency.
- Hydrochloric acid is feasible to strip Cu from the tested resin, the highest desorption efficiency of Cu (93.9%) was achieved when using 4 M HCl and its desorption efficiency decreases with decreasing the concentration of acid.

Although HCl can effectively strip the Cu from the resins, the resins have to be regenerated by high concentrations of NaOH before reuse, otherwise it may cause serious health and safety risks if the resins (H^+ form) contact with glycine-cyanide solutions, toxic hydrogen cyanide (HCN) gases can be evolved. Also, HCl cannot be regenerated and recycled. The merits of using alkaline glycine solutions over acid as the eluents are as follow: (1) the stripped resins can be directly reused for the adsorption without neutralisation; (2) the glycine can be regenerated and (3) the Cu can be recovered as a saleable product (CuS) by sulfide precipitation [6]. Based on the above observations, 3 M glycine with 3 M NaCl and 2 M NaOH (pH 10) was selected as the optimum condition for the resin ruse experiments.

3.7.2. Adsorption/desorption study.

The multi-cycle adsorption/desorption tests on the fully loaded resins were conducted to estimate the change of adsorption capacity and the regeneration efficiency after reuse. The results of the adsorption/desorption tests using 3 M glycine, 2 M NaOH and 3 M NaCl as eluent are shown in Table 6. It can be clearly seen that the Cu adsorption capacity decreases to 15 mg/g after the first cycle. After the first cycle, the Cu adsorption remains stable at about 85% of its original adsorption capacity at around 85 mg/g. Except for the first cycle, the regeneration

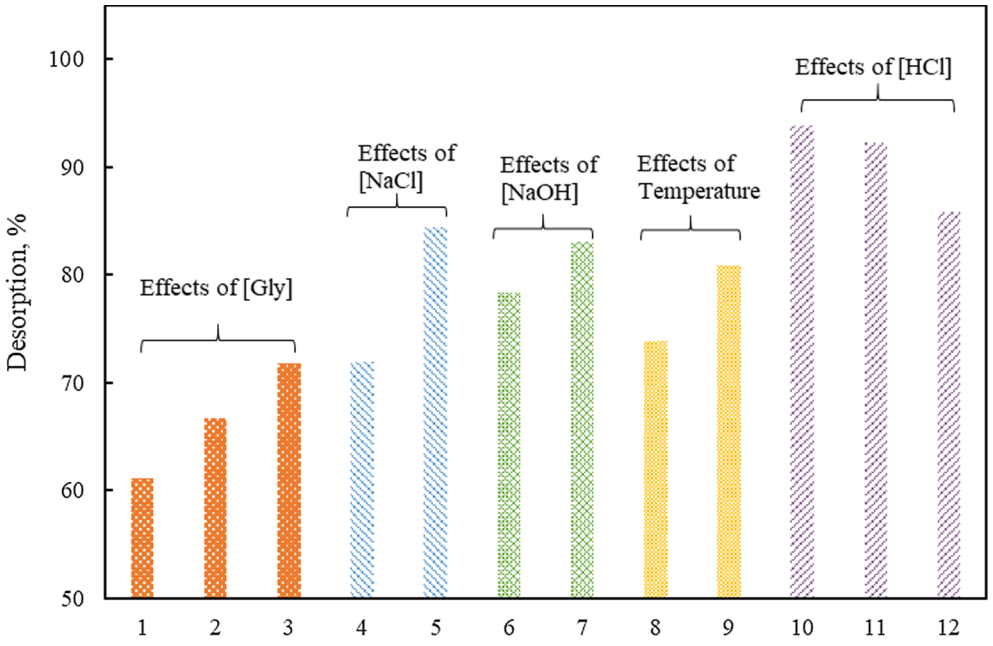

Fig. 8. Desorption efficiency with different eluent agent at different concentration (1 – 1 M glycine, 1 M NaOH; 2 – 2 M glycine, 2 M NaOH; 3 – 3 M glycine, 3 M NaOH; 4 – 2 M glycine, 2 M NaOH, 2 M NaCl; 5 – 3 M glycine, 3 M NaOH, 3 M NaCl; 6 – 3 M glycine, 2 M NaOH, 2 M NaCl; 7 – 3 M glycine, 2 M NaOH, 3 M NaCl; 8 – 3 M glycine, 2 M NaOH, 2 M NaCl, 55 °C; 9 – 3 M glycine, 2 M NaOH, 3 M NaCl, 55 °C; 10 – 3 M HCl; 11 – 2 M HCl; 12 – 1 M HCl).

Table 6
Adsorption/desorption process parameters for five cycles. Adsorption conditions: 1500 mg/L Cu_T, $[Cu_T]:[CN^-]:[Gly] = 1:1:3$, pH = 10, room temperature.

Adsorption/ Desorption	Cycle	Cu adsorption capacity, mg/g	Regeneration efficiecy, %
Adsorption	1	99.77	–
	2	84.30	83.55
	3	85.41	101.97
	4	85.29	99.86
	5	84.20	99.36
	Cycle	Desorption efficiency, %	Residual Cu, mg/g
Desorption	1	83.13	16.83
	2	84.49	15.70
	3	83.87	16.32
	4	82.92	17.37
	5	81.10	19.21

efficiencies are close to 100%. The change of Cu adsorption capacity and regeneration efficiency may due to the small portion of Cu left on the resin was strongly chelated with the iminodiacetic functional group which cannot be stripped easily.

The desorption efficiencies of the eluents are quite stable during the 5 cycles of regeneration, ranging from about 81% to 84%. Also, the accumulation of the calculated residual Cu on the resins (assuming a constant weight of the resins) is not evident, where the accumulation increases only ~2 mg/g Cu after the fifth cycle. The decrease of adsorption capacity, desorption efficiency and the accumulation of Cu over 5 adsorption/desorption cycles can be attributed to the degradation of the resins chemically as the loss of functional groups but also physically that a small number of resins can be broken down during agitation and then flushed away during washing.

3.8. SEM analysis

Each type of ion-exchange resin has its service life, it is inevitable to see the degradation of resins both chemically and physically. If the resin has reached the end of its service life, then the resin needs to be replaced. SEM analysis was conducted to investigate the level of damage during the adsorption/desorption process. Low magnification (15 times magnification) SEM images of the Purolite MTS9300 chelating resins before and after adsorption, and the resin after desorption and regeneration are shown in Fig. 9. It is clearly seen from Fig. 9a and b that, no significant change of resin shape, and damage (e.g. crack and rift) after the first adsorption. Similar results were obtained by Meenakshi and Viswanathan [20].

The SEM images for the resins after desorption at alkaline condition (3 M glycine, 2 M NaOH and 3 M NaCl) and after 5 cycles of adsorption/desorption are shown in Fig. 9c and 9d. Some crakes can be easily observed, and it appears that the number of damaged resins increases after 5 cycles of adsorption/desorption (i.e. more cracks can be seen). These damages can result in a decrease in adsorption capacity and an increase in the accumulation of residual Cu. The damages may be mainly caused by agitation during the adsorption/desorption process and attrition between the resins. Although, it can be noticed that the change in resin shape and size is not significant, a further study on the physical robustness of the resins with extended cycles of adsorption/desorption is required.

4. Conclusion

Leaching gold-copper ores by cyanide-starved solutions is an innovative process at which the leach solutions contain gold, cupric glycinate and cuprous cyanide. A fundamental study on the adsorption behaviours of Cu^{2+} over gold and Cu^+ cyanide species on Purolite MTS9300 chelating resin from synthetic glycinate-cyanide solutions and the desorption and regeneration study using alkaline glycine solutions with salt as the eluents was conducted. The results can be summarized as follows:

- The Purolite MTS9300 resin shows high selectivity of Cu^{2+} over Au and Cu^+.
- The adsorption of copper was found to be dominated by the $[CN^-]:[Cu_T]$ molar ratio (i.e. the Cu^+/Cu^{2+} ratio) that over 99% Cu^{2+} were adsorbed at any ratio.
- The effect of $[Gly]:[Cu_T]$ molar ratio was not significant where the additions of glycine exceeded the stoichiometric requirement; insufficient glycine additions led to higher Cu^+ in the system, lowering the total Cu recovery by resin.
- None or a very small amount of gold was adsorbed in all cases.
- Similar adsorption performance was obtained at higher Cu^{2+}

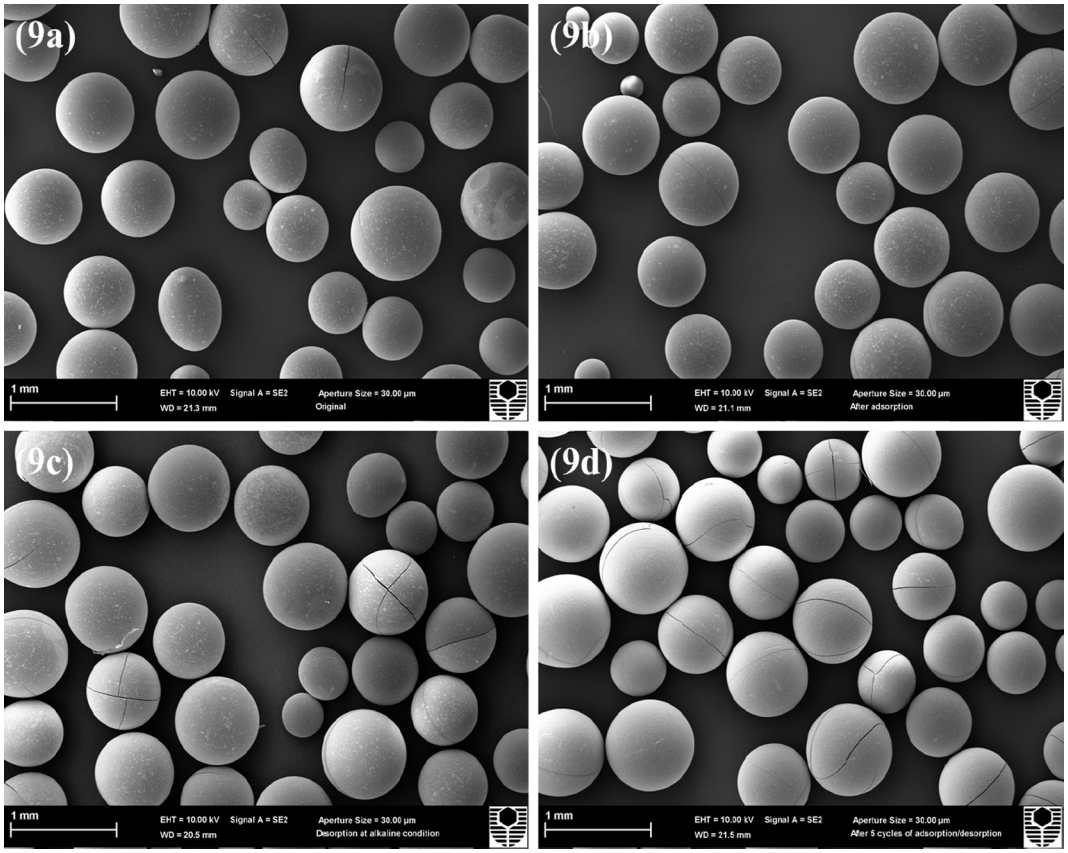

Fig. 9. SEM images at low magnification for (a) raw resins, (b) resins after adsorption (saturated) (c) resins after desorption using 3 M glycine, 3 M NaCl and 2 M NaOH (d) resins after 5 cycles of adsorption/desorption.

concentration by increasing the resin dosage proportionally.

- Both the Freundlich and Langmuir models fit the experimental data, while the Langmuir model represents a better goodness-of-fit.
- The adsorption kinetics of Cu^{2+} followed the pseudo-second-order model.
- The Intra-particle model demonstrated that intra-particle diffusion was not the only rate-controlling step, the initial stage might be controlled by film diffusion while the later stage was limited by intra-particle diffusion.
- The Cu loaded on the MTS9300 resin can be effectively stripped by either glycine solutions at alkaline conditions in the presence of salt or in acidic solutions using HCl.
- The use of alkaline glycine solution with salt as eluent was recommended as the stripped resin can be reused directly without neutralisation, and the glycine and Cu can be regenerated and recovered by sulfide precipitation, respectively.
- The regeneration study demonstrates that the Cu adsorption capacity and regeneration efficiency remain constant after the first cycle of adsorption/desorption.
- The desorption efficiencies were stable over the 5 cycles of adsorption/desorption process with insignificant accumulations of residual Cu on the resins.
- No significant change in resin shape and damage after adsorption was visualised by SEM analysis.
- The degradation of Puromet MTS9300 resin was not significant chemically and it can be effectively regenerated and reused.

Acknowledgements

The authors would like to acknowledge the financial support from Curtin University, Newcrest Mining, Mining and Process Solutions Ltd and Australian Research Council (ARC) Grant No. LP160101121.

Appendix A. Supplementary material

Supplementary data to this article can be found online at https://doi.org/10.1016/j.seppur.2019.116280.

References

[1] J. Acharya, J.N. Sahu, C.R. Mohanty, B.C. Meikap, Removal of lead(II) from wastewater by activated carbon developed from Tamarind wood by zinc chloride activation, Chem. Eng. J. 149 (1) (2009) 249–262, https://doi.org/10.1016/j.cej.2008.10.029.
[2] G. Akpen, M. Aho, M. Mamwan, Equilibrium and kinetics of colour adsorption from textile wastewater By a novel adsorbent, Global J. Pure Appl. Sci. 24 (1) (2018) 61–67, https://doi.org/10.4314/gipas.v24i1.7.
[3] S.D. Alexandratos, Ion-Exchange resins: a retrospective from industrial and engineering chemistry research, Ind. Eng. Chem. Res. 48 (1) (2009) 388–398, https://doi.org/10.1021/ie801242v.
[4] Michał Cegłowski, Grzegorz Schroeder, Preparation of porous resin with Schiff base chelating groups for removal of heavy metal ions from aqueous solutions, Chem. Eng. J. 263 (2015) 402–411, https://doi.org/10.1016/j.cej.2014.11.047.
[5] Chuh-Yean Chen, Chen-Li Chiang, Chuh-Rou Chen, Removal of heavy metal ions by a chelating resin containing glycine as chelating groups, Sep. Purif. Technol. 54 (3) (2007) 396–403, https://doi.org/10.1016/j.seppur.2006.10.020.
[6] Z. Deng, E.A. Oraby, J.J. Eksteen, The sulfide precipitation behaviour of Cu and Au from their aqueous alkaline glycinate and cyanide complexes, Sep. Purif. Technol. 218 (2019) 181–190, https://doi.org/10.1016/j.seppur.2019.02.056.
[7] S.U. Din, M. Tahira, M.H. Abdul Naeem, S.S. Noor, Detailed kinetics study of arsenate adsorption by a sequentially precipitated binary oxide of iron and silicon, Environ. Technol. 1–9 (2017), https://doi.org/10.1080/09593330.2017.1385649.
[8] J.J. Eksteen, E.A. Oraby, The leaching and adsorption of gold using low concentration amino acids and hydrogen peroxide: effect of catalytic ions, sulphide minerals and amino acid type, Miner. Eng. 70 (2015) 36–42, https://doi.org/10.1016/j.mineng.2014.08.020.
[9] J.J. Eksteen, E.A. Oraby, B.C. Tanda, A conceptual process for copper extraction from chalcopyrite in alkaline glycinate solutions, Miner. Eng. 108 (2017) 53–66, https://doi.org/10.1016/j.mineng.2017.02.001.
[10] J.J. Eksteen, E.A. Oraby, B.C. Tanda, P.J. Tauetsile, G.A. Bezuidenhout, T. Newton, F. Trask, I. Bryan, Towards industrial implementation of glycine-based leach and adsorption technologies for gold-copper ores, Can. Metall. Q. 57 (4) (2018)

390–398, https://doi.org/10.1080/00084433.2017.1391736.
[11] E. Ertan, G. Mustafa, Separation of gold(III) ions from copper(II) and zinc(II) ions using thiourea–formaldehyde or urea–formaldehyde chelating resins, J. Appl. Polym. Sci. 111 (6) (2009) 2798–2805, https://doi.org/10.1002/app.29330.
[12] J.H. Hodgkin, R. Eibl, Copper selective chelating resins, React. Poly. Ion Exchangers, Sorbents 3 (2) (1985) 83–89, https://doi.org/10.1016/0167-6989(85)90051-0.
[13] Q. Hu, Y. Meng, T. Sun, M. Qaisar, D. Wu, J. Zhu, G. Lu, Kinetics and equilibrium adsorption studies of dimethylamine (DMA) onto ion-exchange resin, J. Hazard. Mater. 185 (2) (2011) 677–681, https://doi.org/10.1016/j.jhazmat.2010.09.071.
[14] M. Kotze, B. Green, J. Mackenzie, M. Virnig, Resin-in-pulp and resin-in-solution, Develop. Min. Proc. 15 (C) (2005) 603–635, https://doi.org/10.1016/S0167-4528(05)15025-X.
[15] J. Lehto, A. Paajanen, R. Harjula, H. Leinonen, Hydrolysis and H + Na + exchange by Chelex 100 chelating resin, React. Polym. 23 (2) (1994) 135–140, https://doi.org/10.1016/0923-1137(94)90013-2.
[16] H. Leinonen, J. Lehto, Ion-exchange of nickel by iminodiacetic acid chelating resin Chelex 100, React. Funct. Polym. 43 (1) (2000) 1–6, https://doi.org/10.1016/S1381-5148(98)00082-0.
[17] Li-Chun Lin, Ruey-Shin Juang, Ion-exchange equilibria of Cu(II) and Zn(II) from aqueous solutions with Chelex 100 and Amberlite IRC 748 resins, Chem. Eng. J. 112 (1–3) (2005) 211–218, https://doi.org/10.1016/j.cej.2005.07.009.
[18] Fuqiang Liu, Lanjuan Li, Panpan Ling, Xiaosheng Jing, Chenghui Li, Aimin Li, Xiaozeng You, Interaction mechanism of aqueous heavy metals onto a newly synthesized IDA-chelating resin: Isotherms, thermodynamics and kinetics, Chem. Eng. J. 173 (1) (2011) 106–114, https://doi.org/10.1016/j.cej.2011.07.044.
[19] Shihabudheen M. Maliyekkal, Sanjay Shukla, Ligy Philip, Indumathi M. Nambi, Enhanced fluoride removal from drinking water by magnesia-amended activated alumina granules, Chem. Eng. J. 140 (1) (2008) 183–192, https://doi.org/10.1016/j.cej.2007.09.049.
[20] S. Meenakshi, N. Viswanathan, Identification of selective ion-exchange resin for fluoride sorption, J. Colloid Interface Sci. 308 (2) (2007) 438–450, https://doi.org/10.1016/j.jcis.2006.12.032.
[21] C.N. Mpinga, J.J. Eksteen, C. Aldrich, L. Dyer, A conceptual hybrid process flowsheet for platinum group metals (PGMs) recovery from a chromite-rich Cu-Ni PGM bearing ore in oxidized mineralization through a single-stage leach and adsorption onto ion exchange resin, Hydrometallurgy 178 (2018) 88–96, https://doi.org/10.1016/j.hydromet.2018.03.024.
[22] D. Muraviev, Ion exchange, in: M. Dimitri, V.I. Gorshkov, A. Warshawsky, M. Dekker, New York: New York, 2000.
[23] I.F.F. Neto, A. Cátia, M.S.C.A. Sousa, A.M.F. Brito, M.V.M.S. Helena, A simple and nearly-closed cycle process for recycling copper with high purity from end life printed circuit boards, Separa. Purifi. Technol. 164 (C) (2016) 19–27, https://doi.org/10.1016/j.seppur.2016.03.007.
[24] E.A. Oraby, J.J. Eksteen, The selective leaching of copper from a gold–copper concentrate in glycine solutions, Hydrometallurgy 50 (2014) 14–19, https://doi.org/10.1016/j.hydromet.2014.09.005.
[25] E.A. Oraby, J.J. Eksteen, The leaching and carbon based adsorption behaviour of gold and silver and their alloys in alkaline glycine-peroxide solutions, Hydrometallurgy 152 (2015) 199–203, https://doi.org/10.1016/j.hydromet.2014.12.015.
[26] E.A. Oraby, J.J. Eksteen, Gold leaching in cyanide-starved copper solutions in the presence of glycine, Hydrometallurgy 156 (2015) 81–88, https://doi.org/10.1016/j.hydromet.2015.05.012.
[27] E.A. Oraby, J.J. Eksteen, B.C. Tanda, Gold and copper leaching from gold-copper ores and concentrates using a synergistic lixiviant mixture of glycine and cyanide, Hydrometallurgy 169 (2017) 339–345, https://doi.org/10.1016/j.hydromet.2017.02.019.
[28] E.A. Oraby, J.J. Eksteen, A. Karrech, M. Attar, Gold extraction from paleochannel ores using an aerated alkaline glycine lixiviant for consideration in heap and in-situ leaching applications, Eng. Min. Eng. 138 (2019) 112–118, https://doi.org/10.1016/j.mineng.2019.04.023.
[29] E.A. Oraby, H. Li, J.J. Eksteen, An alkaline glycine-based leach process of base and precious metals from powdered waste printed circuit boards, Waste Bio. Valorization (2019), https://doi.org/10.1007/s12649-019-00780-0.
[30] A.L. Riley, E. Sarah, A.J. Pepper, S.F.B. Canner, D.O. Mark, Metal recovery from jarosite waste – A resin screening study, Sep. Sci. Technol. 53 (1) (2018) 22–35, https://doi.org/10.1080/01496395.2017.1378679.
[31] S. Saçmaci, M. Saçmaci, C. Soykan, Ş. Kartal, Synthesis and Characterization of New Chelating Resin: Adsorption Study of Copper(II) and Chromium (III) Ions, J. Macromol. Sci. Part A 47 (6) (2010) 552–557, https://doi.org/10.1080/10601321003742055.
[32] E. Schoeman, S.M. Bradshaw, G. Akdogan, C.A. Snyders, J.J. Eksteen, The elution of platinum and palladium cyanide from strong base anion exchange resins, Int. J. Miner. Process. 162 (2017) 19–26.
[33] E. Schoeman, S.M. Bradshaw, G. Akdogan, C.A. Snyders, J.J. Eksteen, The extraction of platinum and palladium from a synthetic cyanide heap leach solution with strong base anion exchange resins, Int. J. Miner. Process. 162 (2017) 27–35.
[34] A.K. Sengupta, Yuewei Zhu, D. Hauze, Metal (II) ion binding onto chelating exchangers with nitrogen donor atoms: Some new observations and related implications, Environ. Sci. Technol. 25 (3) (1991) 481–488, https://doi.org/10.1021/es00015a016.
[35] Wen Song, Baoyu Gao, Xu. Xing, Lulu Xing, Shuang Han, Pijun Duan, Wuchang Song, Ruibao Jia, Adsorption–desorption behavior of magnetic amine/Fe3O4 functionalized biopolymer resin towards anionic dyes from wastewater, Bioresour. Technol. 210 (2016) 123–130, https://doi.org/10.1016/j.biortech.2016.01.078.
[36] B.C. Tanda, J.J. Eksteen, E.A. Oraby, An investigation into the leaching behaviour of copper oxide minerals in aqueous alkaline glycine solutions, Hydrometallurgy 167 (2017) 153–162, https://doi.org/10.1016/j.hydromet.2016.11.011.
[37] B.C. Tanda, E.A. Oraby, J.J. Eksteen, Recovery of copper from alkaline glycine leach solution using solvent extraction, Sep. Purif. Technol. 187 (2017) 389–396, https://doi.org/10.1016/j.seppur.2017.06.075.
[38] B.C. Tanda, E.A. Oraby, J.J. Eksteen, Kinetics of Chalcocite Leaching in Oxygenated Alkaline Glycine Solutions, Hydrometallurgy 178 (2018) 264–273, https://doi.org/10.1016/j.hydromet.2018.05.005.
[39] B.C. Tanda, E.A. Oraby, J.J. Eksteen, Kinetics of Malachite Leaching in Alkaline Glycine Solution, Min. Proc. Extrac. Metall. (TIMM C) (2018), https://doi.org/10.1080/25726641.2018.1505211.
[40] P.J. Tauetsile, E.A. Oraby, J.J. Eksteen, Adsorption behaviour of copper and gold glycinates in alkaline media onto activated carbon. Part 1: isotherms, Hydrometallurgy 178 (2018) 202–208, https://doi.org/10.1016/j.hydromet.2018.04.015.
[41] P. Tauetsile, E.A. Oraby, J.J. Eksteen, Adsorption behaviour of copper and gold Glycinates in alkaline media onto activated carbon. Part 2: kinetics, Hydrometallurgy 178 (2018) 195–201, https://doi.org/10.1016/j.hydromet.2018.04.016.
[42] P.J. Tauetsile, E.A. Oraby, J.J. Eksteen, Activated carbon adsorption of gold from cyanide-starved glycine solutions containing copper. Part 1: isotherms, Sep. Purif. Technol. 211 (2019) 594–601, https://doi.org/10.1016/j.seppur.2018.09.024.
[43] P.J. Tauetsile, E.A. Oraby, J.J. Eksteen, Activated carbon adsorption of gold from cyanide-starved glycine solutions containing copper. Part 2: kinetics, Sep. Purif. Technol. 211 (2019) 290–297, https://doi.org/10.1016/j.seppur.2018.09.022.
[44] Jinnan Wang, Xu. Li, Cheng Cheng, Ying Meng, Aimin Li, Preparation of new chelating fiber with waste PET as adsorbent for fast removal of Cu^{2+} and Ni^{2+} from water: Kinetic and equilibrium adsorption studies, Chem. Eng. J. 193–194 (2012) 31–38, https://doi.org/10.1016/j.cej.2012.03.070.
[45] J. Weber, J. Morris, Kinetics of adsorption on carbon from solution, J. Sanit. Eng. Div. 89 (2) (1963) 31–60.
[46] A. Wołowicz, Z. Hubicki, Investigation of macroporous weakly basic anion exchangers applicability in palladium(II) removal from acidic solutions – batch and column studies, Chem. Eng. J. 174 (2) (2011) 510–521, https://doi.org/10.1016/j.cej.2011.08.075.
[47] A. Wołowicz, Z. Hubicki, The use of the chelating resin of a new generation Lewatit MonoPlus TP-220 with the bis-picolylamine functional groups in the removal of selected metal ions from acidic solutions, Chem. Eng. J. 197 (2012) 493–508, https://doi.org/10.1016/j.cej.2012.05.047.
[48] Zaimawati Zainol, Michael J. Nicol, Ion-exchange equilibria of Ni 2+, Co 2+, Mn 2+ and Mg 2+ with iminodiacetic acid chelating resin Amberlite IRC 748, Hydrometallurgy 99 (3–4) (2009) 175–180, https://doi.org/10.1016/j.hydromet.2009.08.004.
[49] Y. Zhang, Y. Li, L. Yang, X. Ma, L. Wang, Z. Ye, Characterization and adsorption mechanism of Zn2+ removal by PVA/EDTA resin in polluted water, J. Hazard. Mater. 178 (1) (2010) 1046–1054, https://doi.org/10.1016/j.jhazmat.2010.02.046.
[50] W. Zhu, J. Liu, M. Li, Fundamental studies of novel zwitterionic hybrid membranes: kinetic model and mechanism insights into strontium removal, Sci. World J. 2014 (2014), https://doi.org/10.1155/2014/485820.

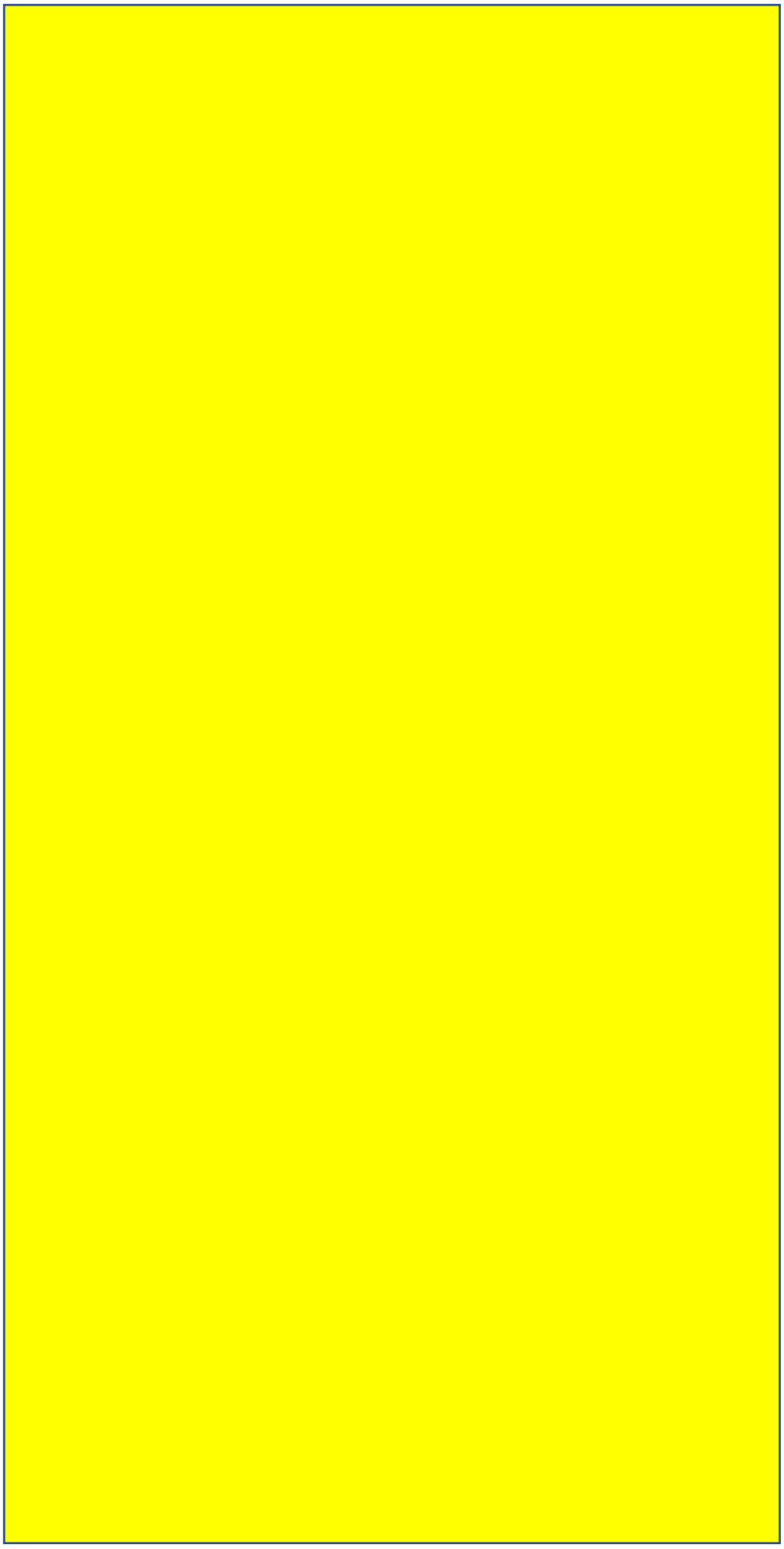

Chapter 6: Au adsorption behaviours on gold-selective resins from cyanide-starved glycine solutions

Submitted for publication as:

Gold recovery from cyanide-starved glycine solutions in the presence of Cu using a molecularly imprinted resin (IXOS-AuC)

Deng, Z. Oraby, E.A. and Eksteen, J.J., 2020.
Hydrometallurgy

Accepted for publication on 22 July 2020

© 2020 Elsevier Ltd.
Reprinted with permission from the publisher.
DOI: https://doi.org/10.1016/j.hydromet.2020.105425

Hydrometallurgy 196 (2020) 105425

Contents lists available at ScienceDirect

Hydrometallurgy

journal homepage: www.elsevier.com/locate/hydromet

Gold recovery from cyanide-starved glycine solutions in the presence of Cu using a molecularly imprinted resin (IXOS-AuC)

Z. Deng[a], E.A. Oraby[a,b], J.J. Eksteen[a,*]

[a] Western Australian School of Mines: Minerals Energy and Chemical Engineering, Curtin University, GPO Box U1987, Perth, Western Australia 6845, Australia
[b] Faculty of Engineering, Assiut University, Egypt

ARTICLE INFO

Keywords:
Glycine
Gold
Molecularly imprinted resin
Adsorption equilibrium and kinetics
Elution and regeneration

ABSTRACT

The synergistic leaching system using glycine as the main lixiviant with low levels of cyanide as a catalyst has been shown to be an effective approach to leach gold-copper ores and concentrates, allowing the consumption of cyanide to be remarkably reduced. The recovery of gold from the synthetic cyanide-starved glycine leachate in the presence of copper has been investigated using. It was found that the adsorbed copper was mostly cuprous cyanide. The effects of $[CN^-]$:$[Cu_T]$ and [Gly]: $[Cu_T]$ molar ratios were not significant on the adsorption of gold and copper using IXOS-AuC resin. The gold recovery increased, while the copper recovery decreased with the increasing initial gold concentration. The equilibrium and kinetics studies were undertaken, and the experimental adsorption equilibrium and rate data showed an excellent fit using the Freundlich isotherm and pseudo-second-order models respectively. Elution tests showed that the loaded copper can be selectively pre-eluted over gold by 0.4 M NaCN at pH 11.5. Gold can be effectively eluted by either acidic thiourea or alkaline thiocyanate. The multi-cycle adsorption/elution tests showed that the resin can be effectively regenerated by both acidic thiourea and alkaline thiocyanate, with an insignificant decrease in adsorption and elution efficiency over 3 adsorption/elution cycles. From SEM analysis, the change of surface morphology of the resin was not significant after adsorption and the adsorption/elution cycles.

1. Introduction

According to the data from 2011, free-milling (easily extracted through cyanidation/CIP(CIL) gold ores are nearly exhausted, occupying only 18% of the global gold deposits (Adams, 2016). Nowadays, most of the gold is produced from the refractory gold ores, many of which were accompanied by reactive copper minerals. Extracting gold from gold-copper ores is usually problematic and uneconomic due to the extra cyanide consumption by the reactive copper minerals, where a high $[CN^-]$: [Cu] molar ratio of 4:1 is required to maintain an acceptable gold leaching rate (Sceresini and Breuer, 2016). An innovative leaching method for gold-copper ores was developed and patented using a synergistic lixiviant mixture of glycine and cyanide which has attracted interest from both industry and academia (Eksteen et al., 2018). The leaching method shows high effectiveness in leaching gold from gold-copper ores and concentrates with a reduction of cyanide consumption by at least 75% (Oraby and Eksteen, 2015; Oraby et al., 2017), although cyanide reductions of more than 90% are often seen, depending on ore mineralogy. While cyanide free (i.e. glycine-only) dissolution is possible and can be considered for heap and in situ leaching (Oraby et al., 2019), the kinetics remain too slow for agitated tank leaching for an alkaline glycine-oxygen leach system without catalysts (Eksteen and Oraby, 2015). The final leachate derived from Cu-Au ores with cyanide-starved glycine solutions normally contains mostly cupric glycinate, small amount of cuprous cyanide and zero free cyanide. The term “cyanide-starved” refers to the cyanide present as cuprous cyanide runs at starvation levels and it is insufficient for the dissolution of any cyanide soluble copper minerals and that no free cyanide is present as either HCN or the CN^- anion. Carbon adsorption has proved to be effective in recovering gold in the presence of Cu from a cyanide-starved glycine synthetic solution (Tauetsile et al., 2019a, 2019b) and glycine only leaching system (Tauetsile et al., 2018a, 2018b). Copper, on the other hand, can be recovered by sulfide precipitation prior to the carbon adsorption to mitigate the competitive copper adsorption on the activated carbon (Deng et al., 2019, 2020b), or by solvent extraction (Tanda et al., 2017). Deng et al. (2020a) also investigated the adsorption/desorption behaviour of gold and copper using cation chelating resin, where the resin shows a high affinity to Cu^{2+} from the synthetic cyanide-starved glycine leachates, leaving anion gold cyanide and copper cyanide species in the solutions, and the

* Corresponding author.
E-mail address: jacques.eksteen@curtin.edu.au (J.J. Eksteen).

https://doi.org/10.1016/j.hydromet.2020.105425
Received 2 March 2020; Received in revised form 6 June 2020; Accepted 21 July 2020
Available online 25 July 2020
0304-386X/ © 2020 Elsevier B.V. All rights reserved.

resin can be effectively eluted and regenerated by using alkaline glycine solutions.

Although the application of activated carbon remains dominant in the Western World (compared to Russia), the use of resins has its advantages over carbon. For examples, it does not require an energy-intensive thermal regeneration process, which is expensive; it is suitable to treat pre-robbing ores as it is less prone to be poisoned by organics such as diesel and kerosene used to deactivate carbonaceous gold ores and concentrates; and it has a better selectivity towards gold over base metals (Van et al., 2012; Pilśniak-Rabiega and Trochimczuk, 2014). In the past decades, many gold-selective resins have been developed and are commercially available in the markets. Some of these resins have been successfully implemented in the resin-in-pulp (RIP) and resin-in-leach (RIL) plants, including Penjom Gold Mine in Malaysia, Golden Jubilee Mine and Barbrook Gold Mine in South Africa (Kotze et al., 2005; Pilśniak-Rabiega and Trochimczuk, 2014; van Deventer, 2011). Given that the advantages of resins and their availability and successful commercial implementation of RIL/RIP process in the gold mining industry, resin has great potential to be implemented in the glycine-cyanide leaching system.

A new type of resin (IXOS-AuC, marketed by 6th Wave Innovation Corp.) using a molecular recognition technology is developed based on a “lock and key” chemistry. This type of resin is a type of molecularly imprinted polymer (MIP) and a branch of nanotechnology which is specifically targeting aurocyanide. MIPs generate cavities in a polymer matrix using the target molecule or a proxy molecule to create a polymer with an imprint and affinity (charge complex) for a target molecule. According to Ritz et al. (2018), the IXOS-AuC resin is different from the regular ion-exchange resins, where its adsorption of gold cyanide is through a complementary charge and a physical imprint for aurocyanide, allowing the co-adsorption of other metals to be minimised. Unlike the typical ion-exchange resins which are merely functionalised to allow metal ions to exchange with a donor ion, this kind of resin is synthesised using a combination of polystyrene and other monomers bound together by a functionalised ligand (proprietary) that imprints the shape of the $Au(CN)_2^-$ molecule during the polymerisation stage (Ritz et al., 2018). Fig. 1 demonstrated the MIP process for IXOS-AuC generation, where a void with the same size and shape as the aurocyanide left in the final polymer matrix. The physical imprint for aurocyanide which mitigates the formation of strong bonds between other metal cyanide complexes allows the target aurocyanide to be adsorbed preferentially and to displace the less boned metal cyanide during the adsorption.

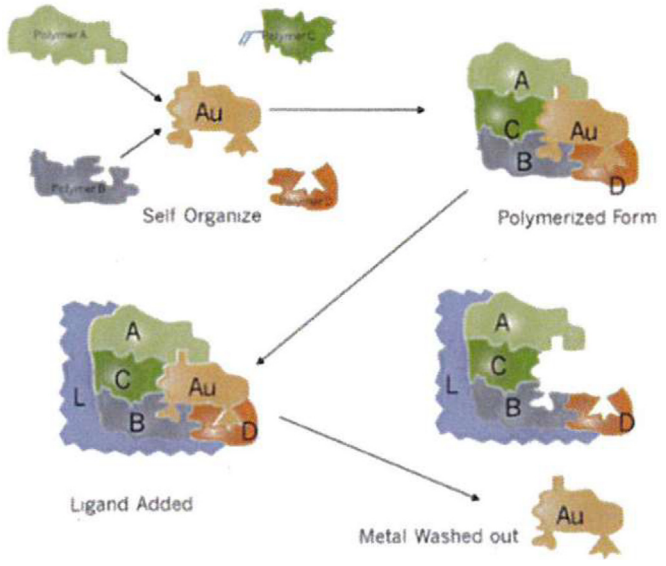

Fig. 1. The generation process of IXOS-AuC resin. (Ritz et al., 2018).

The current study aims to study a selective method of gold recovery from the cyanide-starved glycine leaching system containing gold and copper. The effects of $[CN^-]$:$[Cu_T]$, [Gly]: $[Cu_T]$ ratios and initial Au concentration on the adsorption of the IXOS-AuC resin were studied, where $[Cu_T]$ is the molar concentration of total copper, i.e. cuprous and cupric copper. Equilibrium isotherms and kinetics studies were undertaken. Elution and regeneration studies were also carried out to ensure the resin can be effectively reused.

2. Experimental design

2.1. Adsorbents

The adsorption behaviours of the IXOS-AuC resin were studied. In this research, the mass of the resin was presented as dry weight. Their moisture contents of the resins were calculated by subtracting the resin after drying in an oven at 70 °C for 24 h. The resins were pre-conditioned before the adsorption tests, by contacting 1 M NaOH solution for 2 h and then washing by deionised water before its use. The characteristic properties of the IXOS-AuC resin provided by the manufacturer are shown in Table 1.

2.2. Synthetic cyanide-starved glycine solution

Analytical grade reagents and deionised water were used for all the tests in this study. The synthetic cyanide-starved glycine solutions were used throughout the adsorption tests. A stock cyanide-starved glycine solution containing gold and copper was first prepared. Gold powders (99.998%, spherical, −200 mesh, Alfa Aesar – Thermo Fisher Scientific) were dissolved in deionised water contained glycine (> 99%, Sigma-Aldrich) and CuCN (95%, Ajax, Finechem) and NaOH (CuCN was first dissolved in glycine) for 24 h. Unless specified, the initial pH of all the tests was 10.5, which is a suitable pH for the cyanide-starved glycine leaching system (Oraby and Eksteen, 2015), although pH's from 9 to 12.5 can be employed in leaching. The solutions pH were adjusted using sodium hydroxide (NaOH) (Chem-Supply Pty Ltd) with a pH meter (Model AQUA-PH Meter). The solution was agitated with a magnetic stirrer and Teflon magnetic stirrer bars at 350 rpm. The solution was filtered by a Supor® 0.45 μm membrane disc filter (Pall Corporation) and stored in a 1 L container with lids. Different gold concentrations were achieved by diluting the stock solution accordingly in a cyanide-starved glycine solutions containing the same amount of Cu and at the same $[Cu_T]$:$[CN_T]$:$[Gly_T]$ molar ratio. Unless specified, the standard solutions contain about 1000 mg/L Cu_T and about 6 mg/L of Au at $[Cu_T]$:$[CN_T]$:$[Gly_T]$ molar ratio of 1:1:3. The

Table 1
Chemical and physcial characteristics of the IXOS-AuC resin

Resin name	IXOS-AuC
Matrix	polystyrene-co-divinyl benzene
Functional group	Bis (N-(4-vinylbenzyl)-N-decyl-N N-dimethylammonium)
Moisture	55%
Wet density	0.36 g/mL
Particle size range	850–1400 μm

subscript "T" refers to the total copper, cyanide and glycine concentrations present and not their "free" species in solution. From this point on we will use [CN^-] to represent total cyanide, [CN_T^-], and [Gly] to represent total glycine concentration, [Gly_T]. However, [Cu_T] will be retained to distinguish it from the concentrations of Cu^{2+} and Cu^+. Typically, in the synthetic alkaline cyanide-starved glycine solutions, copper species mainly present as cupric glycinate ($Cu(NH_2CH_2COO)_2$), and cuprous diacyano-complex ($Cu(CN)_2^-$), triacyano- ($Cu(CN)_3^{2-}$) and tetracyano- complexes ($Cu(CN)_4^{3-}$) may exist depending on the [Cu_T]:[CN_T^-]:[Gly_T] molar ratios, where the subscript "T" refers to the total amount of copper, cyanide, and glycine present, respectively. Gold species are presented as gold cyanide ($Au(CN)_2^-$) and gold glycinate ($Au(Gly)_2^-$).

2.3. Adsorption behaviours of IXOS-AuC resin

The adsorption behaviours of the IXOS-AuC resin were studied through batch tests. An exact dry mass of resin beads (1.5 g) was stirred with 250 mL of the standard solutions in 500 mL flasks. The flasks were completely sealed and shaken in a 400 × 400 mm square orbital incubator shaker for 24 h at 250 rpm and room temperature with 5 mL of kinetic samples taken up at 0.5, 1, 2, 4, 6, 24 h. Each solution sample was filtered by 0.22 μm syringe filters to remove any fine resins and avoid further adsorption. The most selective resin was chosen for further investigation based on their gold and copper recovery. The metal recovery was calculated by Eq. (1):

$$\text{Metal Recovery\%} = \frac{C_0 - C_t}{C_0} \times 100\% \quad (1)$$

Where C_0 is the initial metal concentration and C_t is the metal concentration at time t. The effects of different [CN^-]: [Cu_T] and [Gly]: [Cu_T] molar ratios and initial gold concentrations on the resin were studied.

2.4. Equilibrium tests

The equilibrium adsorption tests were performed at different gold concentrations. The equilibrium isotherms were obtained by contacting five different dosages of resins (0.1, 1, 3, 6, 12 g/L) with 250 mL synthetic cyanide-starved glycine solutions in a 400 × 400 mm square orbital incubator shaker at room temperature for 24 h. The amount of metal adsorbed onto the resin (Q_e, mg/g) at equilibrium was calculated by Eq. (2):

$$Q_e = \frac{(C_o - C_e)V}{W} \quad (2)$$

Where C_e is the metal concentration at equilibrium (mg/L), V is solution volume (L) and W is the mass of dry resin (g). The experimental data at different [CN^-]:[Cu_T] molar ratios were fitted to Freundlich and Langmuir isotherm models and compared using linear regression of the linearized forms of the isotherms.

2.5. Adsorption kinetics

Kinetic studies were carried out at different gold concentrations. A fixed dosage of resin (6 g/L) and 250 mL of synthetic solutions were mixed in a 400 × 400 mm square orbital incubator shaker at room temperature for 24 h with 5 mL of the kinetic samples taken at different time intervals for analysing the metal ions concentration (mg/L), and the amount of metals adsorbed on the resin at time t (Q_t) is calculated. The kinetic process at different conditions was described by the pseudo-first-order, pseudo-second-order using linear regression.

2.6. Elution and regeneration tests

Two-stage batch elution tests were conducted in 250 mL flasks, stirring by a shaker box. Certain mass of resin (1.5 g) was pre-loaded in a 250 mL cyanide-starved glycine solution containing 1000 mg/L Cu_T, 12 mg/L Au with a [Cu]:[CN-]:[Gly] molar ratio of 1:1:3 at room temperature for 24 h. The resins were then collected using a 200 μm screen and washed gently by DI water.

The 1st stage elution tests aim to pre-elute the copper. The tests were conducted using 100 mL (40BV) sodium cyanide at alkaline condition (pH = 11.5) and room temperature for 6 h. The effects of different concentrations of NaCN were studied. The elution efficiency (E %) was calculated by Eq. (3) (Chen et al., 2007)

$$E\% = \frac{\text{Mass of metal ions desorbed in the solutions,mg}}{\text{Mass of metal ions adsorbed onto the resin,mg}} \quad (3)$$

After the 1st stage of elution, the resin was collected by a 200 μm screen and gently washed by ~200 mL DI water. For the 2nd stage of elution, two types of eluents were selected (i.e. alkaline sodium thiocyanate and acidic thiourea). The resins were agitated with 100 mL (40BV) of different concentrations of the eluents at 55 °C for 6 h. The optimum concentrations were selected for the regeneration tests.

The reusability of the resin was investigated by repeating the above adsorption/elution cycle for 3 times, based on the change of loading capacity and regeneration efficiency (RE%). The regeneration efficiency of the adsorbent was calculated as shown in Eq. (4) (Song et al., 2016).

$$RE\% = \frac{Q_r}{Q_o} \times 100 \quad (4)$$

where Q_o and Q_r (mg/g) are the adsorption capacities before and after regeneration.

2.7. Analytical methods

The total concentration of copper and gold before and after adsorption and desorption were analysed by an atomic absorption spectrometer (AAS, Agilent 55B AAS model). The concentration of Cu^{2+} was determined by a UV–Vis Spectrophotometer (Agilent Cary 60 UV–Vis). The concentration of Cu^+ was calculated by subtracting the measured [Cu^{2+}] from the measured [Cu_T]. After adsorption and desorption, the resins were screened, washed thoroughly by deionised water and dried in an oven at 70 °C. The dried resin samples were sprinkled on the carbon tapes and stuck on an aluminium stub with Pt coated (3 nm). Then the surface morphologies of the dry original, loaded, stripped and regenerated resins were visualised by SEM with a MIRA3 XMU model.

3. Results and discussions

3.1. Adsorption behaviours of IXOS-AuC resin

Batch tests were carried out to investigate the adsorption behaviours of the IXOS-AuC resin. Fig. 2 summarised the results of Au, Cu_T, Cu^{2+} and Cu^+ recoveries and Table 2 shows the metal concentrations and solution pH during the adsorption at different time intervals. As can be seen from Fig. 2, the gold recovery of the IXOS was 97.2% at resin dosage of 6 g/L. About 7.4% of total copper was adsorbed by the IXOS-AuC resin with only 1.6% of Cu^{2+} and 24.2% of Cu^+ being adsorbed. The solution pH was barely changed with insignificant pH reduction from 10.50 to 10.37 after 24 h adsorption.

The IXOS-AuC resin shows a good recovery of gold with a fairly low affinity to Cu^{2+} and relatively low affinity to Cu^+. This can be attributed that the resin provides complementary positive charge on its functional group which tends to complex with the anionic ions i.e. gold cyanide, gold glycinate and cuprous cyanide in the cyanide-starved glycine solutions. The co-adsorption of Cu^{2+} was very low as neutral cupric glycinate and the dissociated Cu^{2+} from the cupric glycinate do not interact with the cationic functional group. The adsorption of cuprous cyanide is not very significant, this can be attributed to the

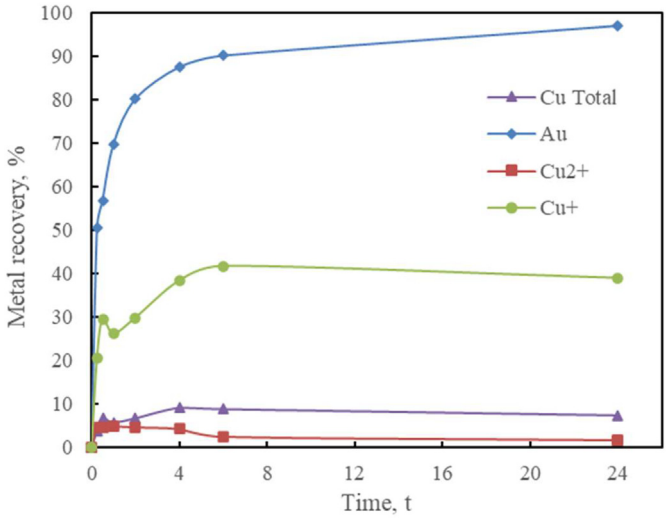

Fig. 2. Au, Cu_T, Cu^{2+} and Cu^+ recoveries as a function of time. Experimental conditions: [Au] =6 mg/L, [Cu_T] = 1000 mg/L, [Cu_T]:[CN^-]:[Gly] = 1:1:3, pH = 10.5, resin dosage = 6 g/L, room temperature.

Table 2
Concentrations of Cu_T, Cu^{2+}, Cu^+ and Au during the adsorption period.

Time, h	pH	Cu_T, mg/L	Cu^{2+}, mg/L	Cu^+, mg/L	Au, mg/L
0	10.50	1040	776	264	6.33
0.25	10.47	1000	740	260	2.81
0.50	10.45	970	739	231	2.45
1	10.43	980	738	242	1.71
2	10.44	970	740	230	1.12
4	10.42	945	743	202	0.70
6	10.39	948	757	191	0.55
24	10.37	963	763	200	0.16

physical imprint does not fit the cuprous cyanide species.

3.2. Effect of [CN^-]:[Cu_T]

Based on the above adsorption behaviours of IXOS-AuC, it appears that this type of resin only adsorbs the gold and cuprous cyanide species from the synthetic cyanide-starved glycine leachate.

In a cyanide-starved glycine system, the Cu^{2+}/Cu^+ ratio can be significantly affected by the [CN^-]:[Cu_T] molar ratio at fixed glycine concentration. When the [CN^-]:[Cu_T] molar ratio increases, the concentration of Cu^+ will increase due to more Cu tends to complex with cyanide in the presence of Cu^{2+} and dissolved oxygen in solutions. Fig. 3 shows the speciation diagram of cupric glycinate and cuprous cyanide at different [CN^-]:[Cu_T] molar ratios.

In this test, the initial Cu^+ concentrations were 129, 305 and 598 mg/L at the [CN^-]:[Cu_T] molar ratios of 0.5:1, 1:1, 2:1, respectively. The effects of different levels of [CN^-]:[Cu_T] molar ratios at a fixed level of glycine concentration were investigated and the results are summarised in Fig. 3. From the results shown in Fig. 4a, similar gold recovery was obtained at different [CN^-]:[Cu_T] molar ratios, where the final gold recovery is ranged from 97 to 98%. This implies that the gold adsorption is not significantly influenced by [Cu^+] concentration. The recoveries of the total Cu are shown in Fig. 4b, it can be seen that the final Cu_T recovery increases slightly from 7.3% at 0.5:1 to 10.0% at 2:1. This phenomenon implies that the increasing concentration of Cu^+ has insignificant effects on the Cu recovery.

3.3. Effect of [Gly]:[Cu_T]

In order to verify whether the free anion glycinate in the cyanide-

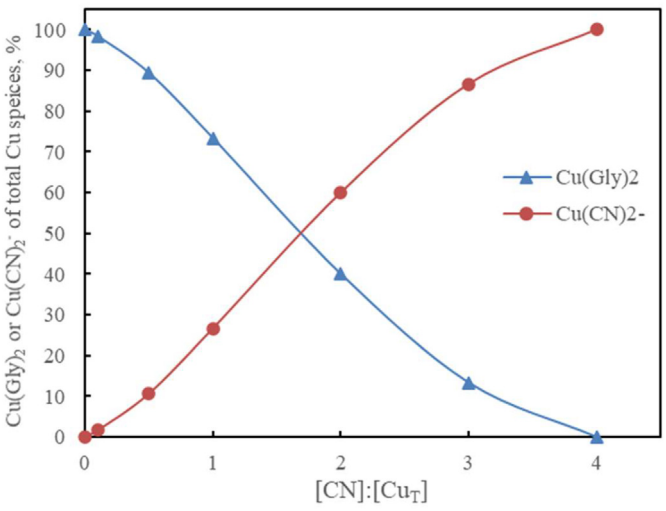

Fig. 3. Speciation diagram of cupric glycinate and cuprous cyanide at different [CN^-]:[Cu_T] molar ratios.

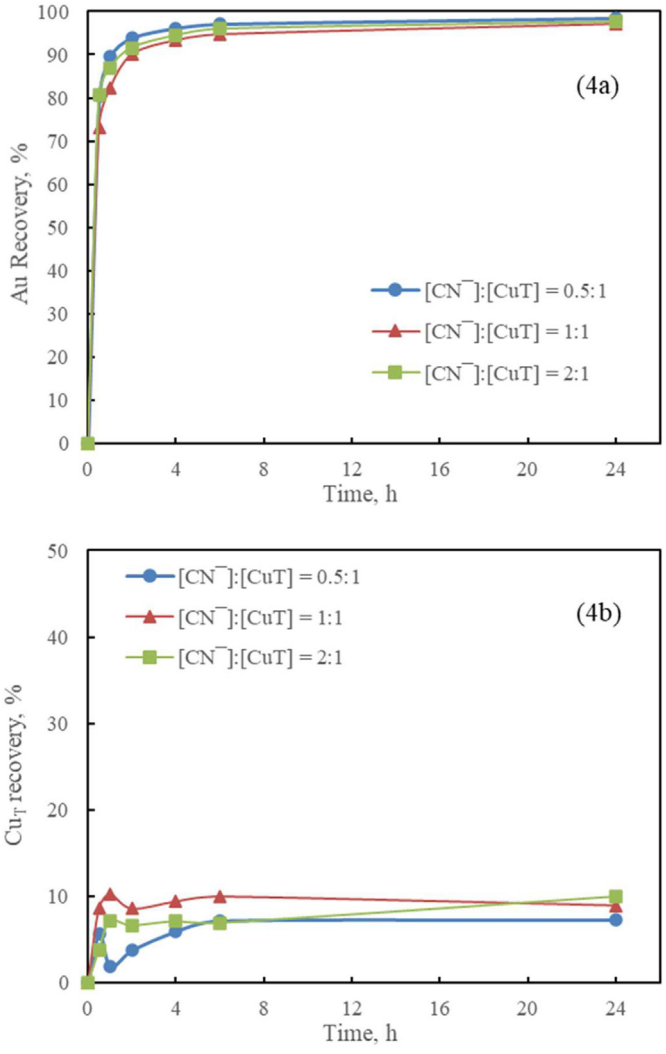

Fig. 4. Metal recoveries as a function of time at different [CN^-]:[Cu_T] molar ratios. Experimental conditions: [Au] = 6 mg/L, [Cu_T] = 1000 mg/L, [Gly]:[Cu_T] = 3:1, pH = 10.5, resin dosage = 6 g/L, room temperature.

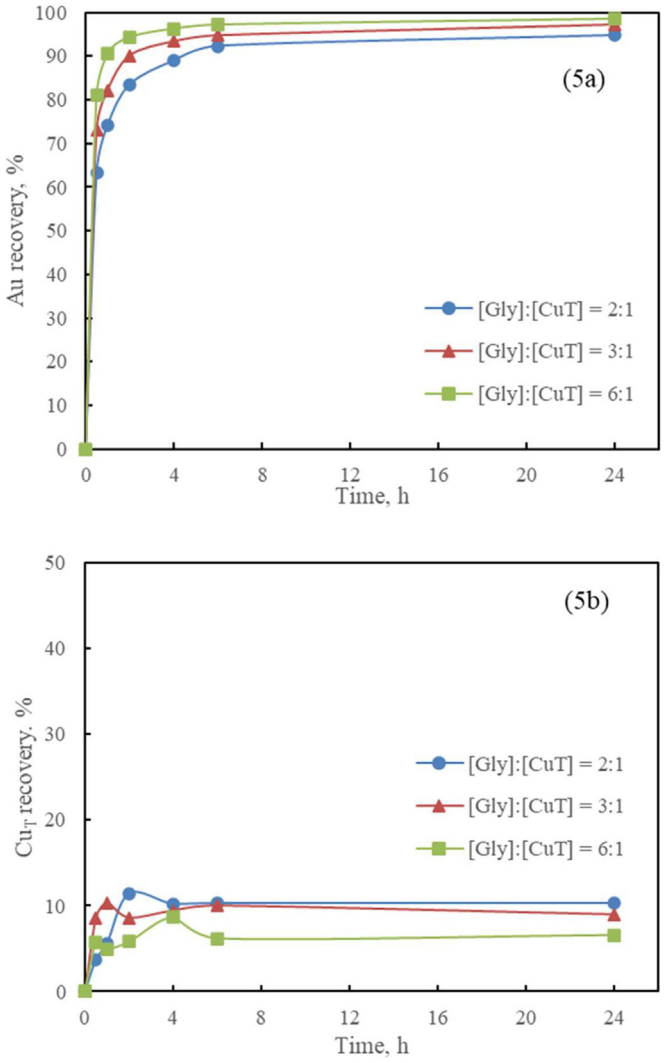

Fig. 5. Au and Cu_T recoveries as a function of time at different [Gly]:[Cu_T] molar ratios. Experimental conditions: [Au] = 6 mg/L, [Cu_T] = 1000 mg/L, [CN^-]:[Cu_T] = 1:1, pH = 10.5, resin dosage = 6 g/L, room temperature.

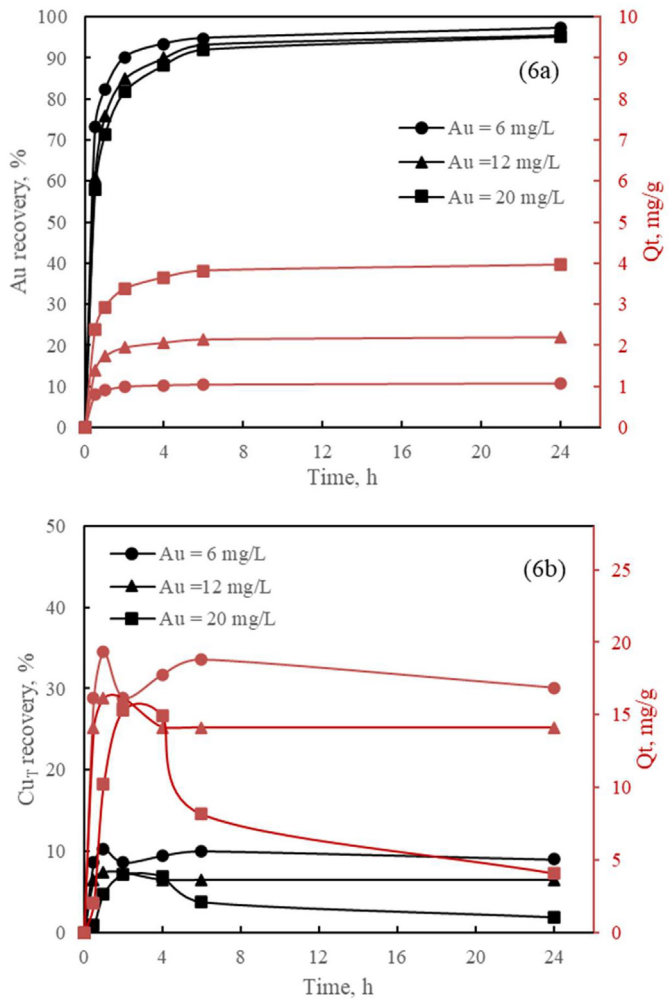

Fig. 6. Au and Cu_T recoveries and adsorption capacities as a function of time at different initial gold concentrations. Experimental conditions: [Cu_T] = 1000 mg/L, [Cu_T]:[CN^-]:[Gly] = 1:1:3, pH = 10.5, resin dosage = 6 g/L, room temperature. (For interpretation of the references to colour in this figure legend, the reader is referred to the web version of this article.)

starved glycine solutions can be adsorbed by the IXOS-AuC resin. The effects of different levels of [Gly]:[Cu_T] molar ratios were investigated. Fig. 5 shows the kinetic graphs of gold and copper recoveries at different [Gly]:[Cu_T] molar ratios. From Fig. 5a, the final gold recovery decreased from 98.5% at [Gly]:[Cu_T] of 6:1 to 94.8% at [Gly]:[Cu_T] of 2:1; whereas the final copper adsorption decreased from 10.3% to 6.5% with increasing the [Gly]:[Cu_T] molar ratio (Fig. 4b). At a high [Gly]:[Cu_T] molar ratio of 6:1, a higher gold recovery and a lower copper co-adsorption were obtained, implying the excess amount of free anion glycinate has no competitive effect. It appears that the increasing [Gly] improves the adsorption of gold and depresses the co-adsorption of copper due to more Cu complexed with glycine to form cupric glycinate.

3.4. Effect of initial gold concentration

The effects of initial gold concentration in the synthetic solutions on the gold and copper adsorption behaviours in terms of recovery and the amount of metal adsorbed on the resin at time, t (Q_t) were summarised in Fig. 6a. As can be seen, the gold recovery decreased slightly from 97.2% to 95.2% with the increasing initial gold concentration in solutions. While the gold loading capacity increased from 1.1 mg/g at 6 mg/L of initial [Au] to 3.5 mg/g at 20 mg/L of initial [Au]. From Fig. 6b, the copper adsorption fluctuated during the whole period at different gold concentrations. An obvious drop of copper adsorption can be observed at Au concentration of 20 mg/L. The final total copper recovery decreased significantly from 9.0% to 1.9% with the final copper adsorption capacity decreased from 16.9 mg/g at 6 mg/L Au to 4.1 mg/g at 20 mg/L Au. These results indicate that the IXOS-AuC resin has promising selectivity towards gold which adsorbed more gold and less copper at higher initial gold concentration. That is probably the resin adsorbed the gold preferentially, leaving less space for Cu co-adsorption.

3.5. Equilibrium isotherm study

The adsorption equilibrium tests of gold from the cyanide-starved glycine solutions in the presence of copper at different initial gold concentrations were conducted. The experimental data of gold adsorption were fitted with two common adsorption isotherm models, Langmuir model and Freundlich model, by a linear regression method.

The Freundlich isotherm model and its linear form can be mathematically expressed by Eqs. (5) and (6) (Cegłowski and Schroeder, 2015; Wang et al., 2012).

$$Q_e = K_f C_e^{1/n} \quad (5)$$

Table 3
Freundlich and Langmuir parameters for Au adsorption at different initial gold concentrations.

Equilibrium model	Freundlich			Langmuir		
Initial [Au], mg/L	K_f, (mg/g)/(mg/L)$^{1/n}$	n	R^2	K_L, (L/mg)	Q_m, (mg/g)	R^2
6	2.71	1.53	0.9970	1.42	4.79	0.9836
12	2.81	1.40	0.9997	0.50	9.57	0.9855
20	2.51	1.57	0.9989	0.38	10.44	0.9812

$$\log Q_e = \log K_f + \frac{1}{n}\log C_e \quad (6)$$

Where K_f is the Freundlich equilibrium adsorption capacity and n is the Freundlich equation constant representing the deviation from linearity of adsorption.

The Langmuir isotherm model and its linear form are presented as shown in Eqs. (7) and (8) (Meenakshi, S., & Viswanathan, N., 2007; Wołowicz & Hubicki, 2011):

$$\frac{C_e}{Q_e} = \frac{C_e}{Q_m} + \frac{1}{K_L Q_m} \quad (7)$$

$$\frac{1}{Q_e} = \left(\frac{1}{Q_m}\right) + \left(\frac{1}{K_L Q_m}\right)\left(\frac{1}{C_e}\right) \quad (8)$$

Where Q_m represents the maximum adsorption capacity (mg/g), K_L represents the energy constant relevant to the heat adsorption (L/mg).

Fig. 6 shows the experimental data fitted with both Langmuir and Freundlich isotherm models at different gold concentrations. Table 3 shows the calculated Langmuir and Freundlich isotherms parameters. As can be seen, the regression correlation coefficients (R^2) of the Langmuir model (0.980–0.985) were relatively lower compared with the ones obtained by the Freundlich model (0.997–0.999). From the results shown in Fig. 7, it is clear that the Freundlich model presents a better fitting to the experimental data which means it provides a better prediction of its gold adsorption (Q_e). This does not prove that the adsorption mechanism of the Freundlich model is the dominant mechanism, only that the Freundlich isotherm is a useful model and sufficiently accurate fit of the data. Based on the Freundlich model, the gold adsorption capacity of IXOS-AuC resin is about 15 mg/g. The adsorption capacity increased with increasing the gold concentration, which is probably related to increasing the driving force at a higher gold concentration to overcome the resistance of the mass transfer of metal ions from the aqueous phase to the solid phase.

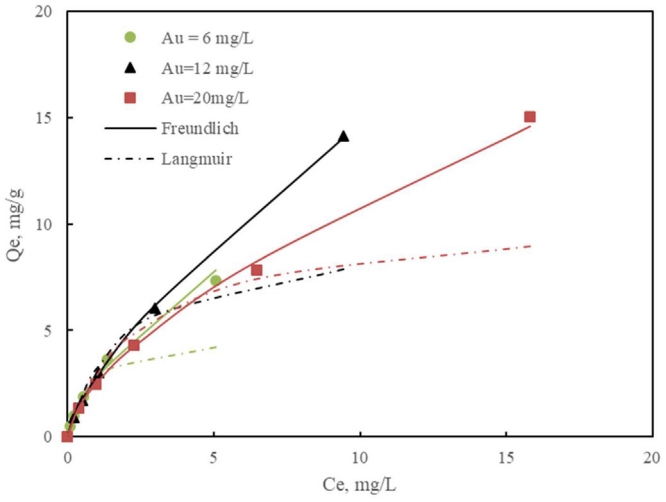

Fig. 7. Experimental adsorption isotherms fitted with Freundlich and Langmuir isotherms at different gold concentrations. Experimental conditions: [Cu_T] = 1000 mg/L, pH = 10.5, room temperature. (For interpretation of the references to colour in this figure legend, the reader is referred to the web version of this article.)

3.6. Kinetics study

The adsorption kinetics of gold from the cyanide-starved glycine solutions have been studied at different initial gold concentrations. The experimental data were fitted with two common reaction-based kinetic models i.e. pseudo-first-order and pseudo-second-order model.

The non-linear and linear form of pseudo-first-order and pseudo-second-order-kinetic models are expressed as shown in Eqs. (9)–(12) (Hu et al., 2011; Maliyekkal et al., 2008)

The Pseudo-first-order kinetic model:

$$Q_t = Q_e(1 - e^{-K_1 t}) \quad (9)$$

$$\log(Q_e - Q_t) = \log Q_e - \frac{K_1}{2.303}t \quad (10)$$

The Pseudo-second-order kinetic model:

$$Q_t = \frac{Q_e^2 K_2 t}{1 + Q_e K_2 t} \quad (11)$$

$$\frac{t}{Q_t} = \frac{1}{K_2 Q_e^2} + \frac{t}{Q_e} \quad (12)$$

where Q_t is the amount of adsorbate on the surface of the adsorbent at the time, t (mg/g); K_1 is the equilibrium constant of the pseudo-first-order adsorption (min^{-1}), K_2 is the pseudo-second-order rate constant (g/mg/h).

As can be seen in Table 4 and by visual observation of the model fitting shown in Fig. 8, the pseudo-second-order model shows better applicability ($R^2 > 0.999$) than the pseudo-first-order model (R^2 in a range from 0.59 to 0.95) at different initial gold concentrations. The calculated Q_e was also consistent with the experimental Q_e in the case of the pseudo-second-order model. The calculated pseudo-second-order rate constant K_2 decreased with the increasing initial gold concentration, which is probably due to lower competition for the adsorption of active sites at lower Au concentration, thus increasing the absorption rate. The adsorption process can be described by the pseudo-second-order kinetic model according to the high correlation coefficient. Also, this suggests that the adsorption may be dominantly controlled by chemical processes especially involved in ion-exchange (Liu et al., 2011; Song et al., 2016)

3.7. Elution and resin reuse

3.7.1. Pre-elution of Cu

Typically, high solutions concentration are applied as an eluent for achieving a rapid and efficient elution (Oliveira et al., 2008). Different concentrations of sodium cyanide (0–0.8 M) were applied for the 1st

Table 4
Statistical parameters for pseudo-first-order and pseudo-second-order model at different initial gold concentrations.

Kinetic model	Parameters	Initial [Au], mg/L		
		6	12	20
Pseudo-first-order	K_1 (h^{-1})	0.1222	0.216	0.285
	Q_e, Cal (mg/g)	0.22	0.61	1.47
	R^2	0.5938	0.8500	0.9519
Pseudo-Second-order	K_2 (g/mg/h)	5.965	2.025	0.891
	Q_e, Cal	1.08	2.22	4.00
	Q_e, Exp	1.09	2.21	3.96
	R^2	0.9999	0.9998	0.9998

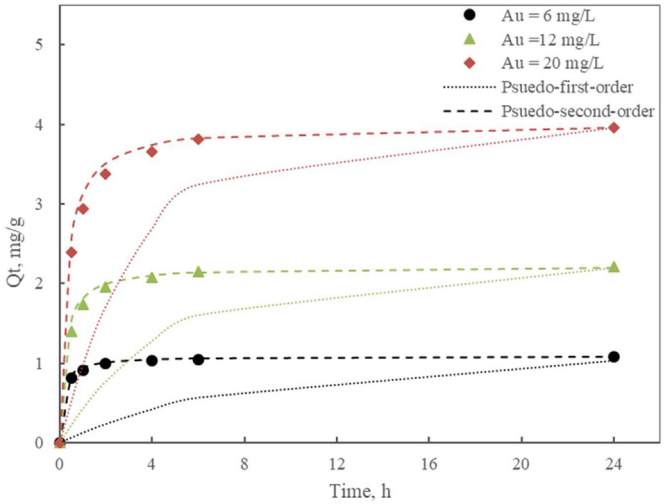

Fig. 8. Experimental data fitted with pseudo-first-order and pseudo-second-order at different gold concentrations. Experimental conditions: [Cu_T] = 1000 mg/L, pH = 10.5, resin dosage = 6 g/L, room temperature. (For interpretation of the references to colour in this figure legend, the reader is referred to the web version of this article.)

Table 5
Elution efficiency of Au and Cu at different NaCN concentrations. Experimental conditions: NaOH = 1.5 g/L, pH: ~11.5, room temperature, Resin loadings: ~20,000 g/t Cu, ~2000 g/t Au.

Eluent concentration	Elution efficiency	
[NaCN], M	Au, %	Cu, %
0	0.00	1.79
0.2	0.00	69.27
0.4	0.00	80.98
0.8	0.00	80.49

stage of elution of Cu from the resin at alkaline conditions (pH = 11.5) and room temperature. The results were summarised in Table 5. As can be seen, no gold and very little copper was eluted at pH 11 without any cyanide. And about 80% of the Cu elution efficiency was achieved at 0.4 M and 0.8 M of NaCN, indicating a concentration of 0.4 M NaCN is sufficient. No gold was detected in the solutions after the pre-elution, indicating a good separation between gold and copper. That is probably because CN^- has less affinity to replace the gold cyanide and gold glycinate, while the cuprous cyanide was not well loaded on the resin due to physical repulsion of the imprinted void. Thus, 0.4 M of NaCN was used for the following tests.

3.7.2. Elution of Au

According to Ritz et al. (2018){Ritz, 2018 #201}, gold can be eluted by thiourea or thiocyanate at 60 °C from the IXOS-AuC resin. However, the concentration of the eluents and the pH conditions were not mentioned. In this study, both acidic thiourea and alkaline thiocyanate elution systems were tested. The effects of different concentrations of thiourea ($CS(NH_2)_2$) and thiocyanate (SCN^-) were studied. All the resins were pre-eluted by 0.4 M NaCN solutions and thoroughly washed by DI water before the 2nd stage of elution where the Cu elution efficiency was ~80%. Table 6 showed that no gold was eluted without thiourea or thiocyanate at acidic or alkaline conditions. The Au elution efficiency increased slightly and then levelled off at about 99% with increasing concentration of thiourea. The residual gold on the resin was round 15–50 g/t. The accumulated Cu elution efficiencies were also similar, ranging from 97 to 98% with the residual copper left on the resin being at about 40–110 g/t.

Table 6
Elution efficiency of Au and Cu at different NaCN concentrations. Experimental conditions: pH = 11.5, 60 °C; Resin loadings: ~4000 g/t Cu, ~2000 g/t Au.

Eluent concentration		Elution efficiency	
[$CS(NH_2)_2$], M	H_2SO_4, M	Au, %	*Cu_a, %
0	0.5	0.00	89.20
0.2	0.5	97.47	98.56
0.5	0.5	99.22	99.02
1	0.5	99.05	99.25
[SCN^-], M	NaOH, g/L	Au, %	*Cu_a,%
0	1.5	0.00	81.04
1	1.5	87.44	97.25
2.5	1.5	96.44	99.28
5	1.5	96.97	98.99

* Cu_a E% —— accumulated Cu elution efficiency from the 1st and 2nd stage of elution.

For the thiocyanate elution system, the elution efficiency of Au increased with the thiocyanate concentration up to 2.5 M with a residual gold on the resin at about 70 g/t; no significant improvement in gold elution was achieved at 5 M thiocyanate. The highest copper elution efficiency (99.2%) was achieved at 2.5 M thiocyanate where the residual copper is about 100 g/t.

3.7.3. Resin reuse

Further adsorption/elution tests were carried out to investigate the reusability of IXAC-AuC resin. After the adsorption from the alkaline cyanide-starved glycine solutions in the presence of 12 mg/L Au and 1000 mg/L Cu_T, the resin was pre-eluted by 0.4 M NaCN solutions followed by water wash and then eluted by 2.5 M thiocyanate (pH = 11.5) and 0.5 M thiourea/0.5 M H_2SO_4 at 60 °C, respectively. Then, the resin was washed by deionised water and reused for subsequent adsorption/elution cycle.

Table 7 shows the results after three cycles of adsorption/elution using 0.5 M thiourea/0.5 M H_2SO_4 as eluents. It can be observed that the gold adsorption capacity slightly increased from 1840 to 2100 g/t, with high regeneration efficiency, while the copper adsorption capacity decreased from 10,360 to 5250 g/t after three adsorption/elution cycles. The Cu adsorption capacity remained the same after the second cycle. During the 1st elution cycles, the copper elution efficiency slightly drops from 80.7% to 75.5%; no gold was eluted after the three cycles. The gold and copper elution efficiency remain stable at about 97% - 98% using 0.5 M thiourea/0.5 M H_2SO_4 as the eluents. About 40 g/t of both gold and copper remained on the resin. The results indicate that the resin can be effectively regenerated by acidic thiourea.

Table 8 shows the results of the multi-cycle tests using alkaline thiocyanate in the 2nd stage elution. It can be seen that the gold adsorption capacity increased after the first cycle and it keeps constant at about 2200 g/t at the second and the third adsorption cycle. The copper adsorption capacity decreased after the three adsorption cycles from about 12,000 g/t to 9600 g/t. Compared to the first group using thiourea as eluent, the reduction in copper adsorption capacity is less significant. For the 1st stage of elution, the copper elution was slightly less efficient than the first group, where the copper elution efficiency decreased from about 77% to 70%. The gold elution efficiency was stable at 97–98% and the accumulated copper efficiency remains constant at about 99%. After the three adsorption/elution cycles, the final residual gold and copper was about 167 and 198 g/t, respectively. The decrease in adsorption capacity and the increase in the residual metal on the resin can be resulted from the degradation of resins coatings due to the loss of functional groups, but also physically that a small number of resins were broken down and screened out during the washing process.

It appears that gold elution is more effective by using acidic thiourea where the gold elution efficiency is relatively stable after the

Table 7
Adsorption/elution process for three cycles using thiourea as the eluent. Adsorption conditions: 12 ppm [Au], 1000 mg/L [Cu_T],[Cu_T]:[CN^-]:[Gly] = 1:1:3, pH = 10.5, resin dosage = 6 g/L, room temperature. Elution conditions: 1st stage elution with 0.4 M NaCN at pH 11.5 and room temperature; 2nd stage elution with 0.5 M Thiourea/0.5 M H_2SO_4, at 55 °C.

Adsorption cycle	Au adsorption capacity, g/t	RE, %	Cu adsorption capacity, g/t	RE, %
1	1840	–	10,360	–
2	1820	98.91	5470	52.80
3	2100	115.38	5250	95.98
1st stage elution cycle	Au E %	Residual Au, g/t	Cu E%	Residual Cu, g/t
1	0.00	1840	80.70	1998.69
2	0.00	1820	80.00	1697.99
3	0.00	2100	75.53	1584.16
2nd stage elution cycle	Au E %	Residual Au, g/t	Cu E%	Residual Cu, g/t
1	98.61	25.44	98.95	109.02
2	97.72	41.51	99.11	75.47
3	97.86	43.41	99.29	45.70

Table 8
Adsorption/elution process for three cycles using thiocyanate as the eluent. Adsorption conditions: 12 ppm [Au], 1000 mg/L [Cu_T],[Cu_T]:[CN^-]:[Gly] = 1:1:3, pH = 10.5, resin dosage = 6 g/L, room temperature. Elution conditions: 1st stage elution with 0.4 M NaCN at pH 11.5 and room temperature; 2nd stage elution with 2.5 M Thiocyanate at pH 11.5 and 55 °C.

Adsorption cycle	Au adsorption capacity, g/t	RE, %	Cu adsorption capacity, g/t	RE, %
1	1760	–	12,140	–
2	2230	127.02	12,610	103.89
3	2220	99.29	9610	76.23
1st stage elution	Au E%	Residual Au, g/t	Cu E%	Residual Cu, g/t
1	0.00	1760	77.71	2705.52
2	0.00	2230	74.30	3240.92
3	0.00	2300	69.96	2888.34
2nd stage elution	Au E%	Residual Au, g/t	Cu E%	Residual Cu, g/t
1	96.71	57.75	96.15	104.06
2	94.46	123.58	93.98	195.24
3	92.73	166.77	93.15	197.83

adsorption/elution cycle with less residual gold and copper left on the resin. However, it should be noted that the evolvement of toxic HCN gases can occur by contacting the resin which is loaded with gold and copper cyanide species at acidic condition, thus additional gas extraction and scrubbing system is needed to minimize the health and safety issues. Also, high resin losses may happen as the results of the osmotic shock generated by repeated elution in acidic environment and adsorption in alkaline conditions. Alkaline thiocyanate can also be an alternative eluent for the elution process, although it is less effective. Thiocyanate may also be adsorbed by the resin during the elution, thus a further investigation is needed to verify whether the thiocyanate can impose adverse effects on the leaching circuit.

3.8. SEM analysis

The purpose of SEM analysis is to investigate whether there is a significant degradation (i.e. breakage, cracks and rift) in the resin after adsorption and the multiple adsorption/elution tests. Low magnification SEM images of the IXOS-AuC resin before and after adsorption and the resin after the multiple cycle tests using thiourea and thiocyanate were shown in Fig. 9. It can be clearly seen from Fig. 8a, b and d that no evident change of resin shape and damage was observed after the adsorption and the adsorption/elution cycle using thiocyanate as the eluent. A small breakage of resin is noticed in the centre of Fig. 8c, which is obtained after the adsorption/elution cycle using acidic thiourea as the eluent. That is probably due to the osmotic shock generated by repeated the elution in acidic environment and adsorption in alkaline conditions. In general, the damages were negligible and insignificant, but a further study on the physical robustness of the resin with extended adsorption/elution cycles is required.

4. Conclusions

The adsorption behaviours of four different types of gold-selective resins including a novel molecularly imprinted resin (IXOS-AuC) and three standard ion-exchange resins from the synthetic cyanide-starved glycine leachates containing gold and copper were investigated. Elution and multiple adsorption/elution tests on the selected resin were also conducted. The following conclusions are drawn from the conducted research:

- The IXOS-AuC resin shows the best selectivity towards gold over copper with only about 7.4% of Cu_T being adsorbed on the resin, where the adsorbed copper was mostly cuprous cyanide species.
- The effects of [CN^-]:[Cu_T] and [Gly]: [Cu_T] molar ratios were insignificant on the adsorption of gold and copper using the IXOS-AuC resin.
- From the adsorption equilibrium tests, the Freundlich isotherm model showed a better correlation than in the case of the Langmuir model with the experimental data.
- Kinetics study showed the Pseudo-second-order fits very well the experimental data.
- Copper on the IXOS-AuC resin can be pre-eluted by 0.4 M NaCN solutions at pH 11.5, where no gold was eluted.
- Gold on the IXOS-AuC resin can be effectively stripped by either acidic thiourea (0.5 M Thiourea/0.5 M H_2SO_4) or alkaline thiocyanate (2.5 M Thiocyanate/1.5 g/L NaOH).
- The adsorption/elution tests showed that the IXOS-AuC resin can be effectively regenerated and reused using both acidic thiourea and alkaline thiocyanate.
- SEM images showed that the change of surface morphology of the resin was not significant after adsorption and the adsorption/elution cycle, although resin breakage occurred when using acidic thiourea as the eluent.
- The resin can be applied for RIL/RIP process.

Author statement

All authors/co-authors participated actively in the preparation of this research manuscript and has seen the final manuscript prior to submission and approved it for submission.

Mr. Zixian Deng is a Ph.D. student under the supervision of Prof Jacques Eksteen and the co-supervision of Dr. Elsayed Oraby, all affiliated with the WA School of Mines, Minerals, Energy and Chemical Engineering at Curtin University.

The work credits are as follows:

Mr Zixian Deng is the lead author who curated the data, performed

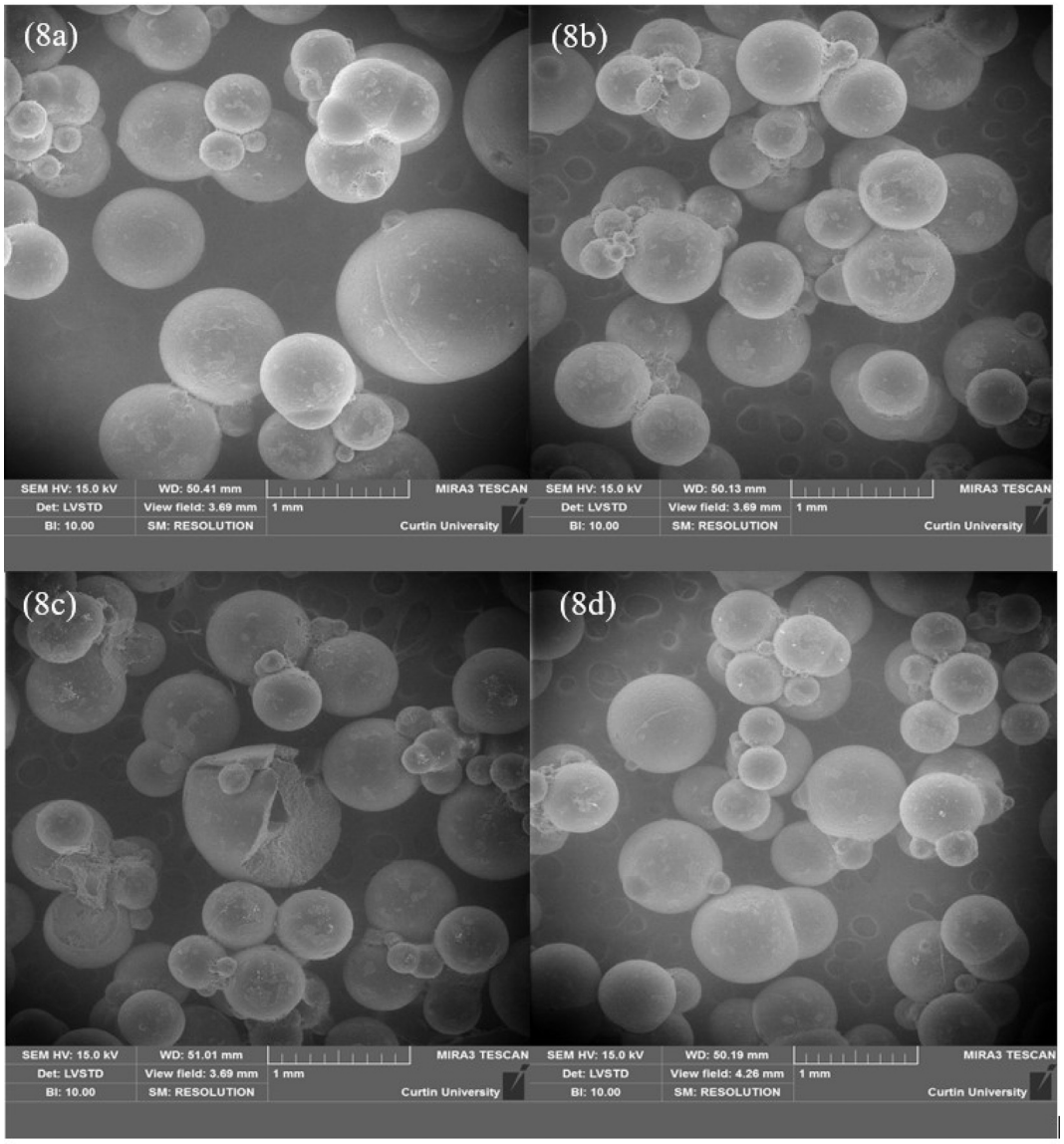

Fig. 9. SEM images at low magnification for (a) raw resins, (b) resins after adsorption (c) resins after 3 cycles of adsorption/elution (acidic thiourea) (d) resins after 3 cycles of adsorption/elution (alkaline thiocyanate).

the experiments under supervision and did the formal data analysis for this paper as part of his PhD research.

The conceptualisation was a joint effort.

Dr Elsayed Oraby is the investigation lead and co-supervisor of Mr. Deng. He is also the joint Chief Investigator with Prof Jacques Eksteen on the ARC Linkage Grant that funded this research. He participated in the checking and reviewing of the paper.

Prof Jacques (given names: Jacobus Johannes) Eksteen is the main supervisor of Mr. Deng. He performed the project administration and wrote the original proposal for the ARC Linkage funding grant (LP160101121) which was awarded and is the lead Chief Investigator on this project. Prof Eksteen also arranged for the provision of all the resources and facilities and manages the overall project delivery. Prof Eksteen reviewed the paper, checked all corrections and responses made by the student and prepared the overall package of documents for submission. Prof Eksteen is the corresponding author.

Dr. Oraby and Prof Eksteen are joint and listed inventors on a group of patented processes that utilises amino acids, and glycine in particular in alkaline environments to leach and selectively extract precious metals and base metals from ores, concentrates, tailings and waste materials such as electronic scrap, and subsequently recover the metals from solution with recycling of the reagents, where appropriate.

Declaration of Competing Interest

The authors hereby declare:

1. Zixian Deng, the lead author, has no conflict of interest and is a PhD student supported by Curtin University, Newcrest and an Australian Research Council grant.
2. Dr. Elsayed Oraby and Prof Jacques Eksteen are the supervisors of Mr. Zixian Deng.
3. Messrs. Oraby and Eksteen are the listed inventors of a number of patents that utilises glycine as a lixiviant for numerous precious and base metals from various materials such as ores, wastes, concentrates, etc., and which is background Intellectual Property to the research presented in this paper.
4. Should processes be commercialised that utilises the patents mentioned in Point no. 3 above, Messrs. Oraby and Eksteen may be eligible to receive royalty income.

Acknowledgements

The authors would like to acknowledge the financial support from Curtin University, Newcrest Mining, Mining and Process Solutions Ltd. and Australian Research Council (ARC) Grant No. LP160101121.

References

Adams, M.D., 2016. Gold Ore Processing: Project Development and Operations/Edited by Mike D. Adams, Second edition. Elsevier, Amsterdam, [Netherlands].

Cegłowski, M., Schroeder, G., 2015. Preparation of porous resin with Schiff base chelating groups for removal of heavy metal ions from aqueous solutions. Chem. Eng. J. 263, 402–411. https://doi.org/10.1016/j.cej.2014.11.047.

Chen, C.-Y., Chiang, C.-L., Chen, C.-R., 2007. Removal of heavy metal ions by a chelating resin containing glycine as chelating groups. Sep. Purif. Technol. 54 (3), 396–403. https://doi.org/10.1016/j.seppur.2006.10.020.

Deng, Z., Oraby, E.A., Eksteen, J.J., 2019. The sulfide precipitation behaviour of Cu and Au from their aqueous alkaline glycinate and cyanide complexes. Sep. Purif. Technol. 218, 181–190. https://doi.org/10.1016/j.seppur.2019.02.056.

Deng, Z., Oraby, E.A., Eksteen, J.J., 2020a. Cu adsorption behaviours onto chelating resins from glycine-cyanide solutions: isotherms, kinetics and regeneration studies. Sep. Purif. Technol. 236, 116280. https://doi.org/10.1016/j.seppur.2019.116280.

Deng, Z., Oraby, E.A., Eksteen, J.J., 2020b. Sulfide precipitation of copper from alkaline glycine-cyanide solutions: precipitate characterisation. Miner. Eng. 145, 106102. https://doi.org/10.1016/j.mineng.2019.106102.

Eksteen, J.J., Oraby, E.A., 2015. The leaching and adsorption of gold using low concentration amino acids and hydrogen peroxide: effect of catalytic ions, sulphide minerals and amino acid type. Miner. Eng. 70, 36–42. https://doi.org/10.1016/j.mineng.2014.08.020.

Eksteen, J.J., Oraby, E.A., Tanda, B.C., Tauetsile, P.J., Bezuidenhout, G.A., Newton, T., Trask, F., Bryan, I., 2018. Towards industrial implementation of glycine-based leach and adsorption technologies for gold-copper ores. Can. Metall. Q. 57 (4), 390–398. https://doi.org/10.1080/00084433.2017.1391736.

Hu, Q., Meng, Y., Sun, T., Mahmood, Q., Wu, D., Zhu, J., Lu, G., 2011. Kinetics and equilibrium adsorption studies of dimethylamine (DMA) onto ion-exchange resin. J. Hazard. Mater. 185 (2), 677–681. https://doi.org/10.1016/j.jhazmat.2010.09.071.

Kotze, M., Green, B., Mackenzie, J., Virnig, M., 2005. Resin-in-pulp and resin-in-solution. Dev. Miner. Process. 15 (C), 603–635. https://doi.org/10.1016/S0167-4528(05)15025-X.

Liu, F., Li, L., Ling, P., Jing, X., Li, C., Li, A., You, X., 2011. Interaction mechanism of aqueous heavy metals onto a newly synthesized IDA-chelating resin: isotherms, thermodynamics and kinetics. Chem. Eng. J. 173 (1), 106–114. https://doi.org/10.1016/j.cej.2011.07.044.

Maliyekkal, S.M., Shukla, S., Philip, L., Nambi, I.M., 2008. Enhanced fluoride removal from drinking water by magnesia-amended activated alumina granules. Chem. Eng. J. 140 (1), 183–192. https://doi.org/10.1016/j.cej.2007.09.049.

Meenakshi, S., Viswanathan, N., 2007. Identification of selective ion-exchange resin for fluoride sorption. Journal of Colloid And Interface Science 308 (2), 438–450. https://doi.org/10.1016/j.jcis.2006.12.032.

Oliveira, A.M., Leão, V.A., Da Silva, C.A., 2008. A proposed mechanism for nitrate and thiocyanate elution of strong-base ion exchange resins loaded with copper and gold cyanocomplexes. React. Funct. Polym. 68 (1), 141–152. https://doi.org/10.1016/j.reactfunctpolym.2007.10.002.

Oraby, E.A., Eksteen, J.J., 2015. Gold leaching in cyanide-starved copper solutions in the presence of glycine. Hydrometallurgy 156, 81–88. https://doi.org/10.1016/j.hydromet.2015.05.012.

Oraby, E.A., Eksteen, J.J., Tanda, B.C., 2017. Gold and copper leaching from gold-copper ores and concentrates using a synergistic lixiviant mixture of glycine and cyanide. Hydrometallurgy 169, 339–345. https://doi.org/10.1016/j.hydromet.2017.02.019.

Oraby, E.A., Eksteen, J.J., Karrech, A., Attar, M., 2019. Gold extraction from paleochannel ores using an aerated alkaline glycine lixiviant for consideration in heap and in-situ leaching applications. Miner. Eng. 138, 112–118. https://doi.org/10.1016/j.mineng.2019.04.023.

Pilśniak-Rabiega, M., Trochimczuk, A.W., 2014. Selective recovery of gold on functionalized resins. Hydrometallurgy 146, 111–118. https://doi.org/10.1016/j.hydromet.2014.03.016.

Ritz, S., Gluckman, J., Southard, G., Maull, B., Kim, D.J., 2018. Imprinted resin—the 21st century adsorbent, in the Gordon Ritcey symposium: advances in hydrometallurgical solution purification separations. In: Davis, B.R. (Ed.), Extraction 2018, pp. 1943–1960. https://doi.org/10.1007/978-3-319-95022-8_161. Ottowa.

Sceresini, B., Breuer, P., 2016. Chapter 43 - gold-copper ores. In: Adams, M.D. (Ed.), Gold Ore Processing, Second edition. Elsevier, pp. 771–801.

Song, W., Gao, B., Xu, X., Xing, L., Han, S., Duan, P., ... Jia, R., 2016. Adsorption–desorption behavior of magnetic amine/Fe3O4 functionalized biopolymer resin towards anionic dyes from wastewater. Bioresource Technology 210, 123–130. https://doi.org/10.1016/j.biortech.2016.01.078.

Tanda, B.C., Oraby, E.A., Eksteen, J.J., 2017. Recovery of copper from alkaline glycine leach solution using solvent extraction. Sep. Purif. Technol. 187, 389–396. https://doi.org/10.1016/j.seppur.2017.06.075.

Tauetsile, P., Oraby, E., Eksteen, J., 2018b. Adsorption behaviour of copper and gold glycinates in alkaline media onto activated carbon. Part 2: kinetics. Hydrometallurgy 178, 195–201. https://doi.org/10.1016/j.hydromet.2018.04.016.

Tauetsile, P.J., Oraby, E.A., Eksteen, J.J., 2018a. Adsorption behaviour of copper and gold glycinates in alkaline media onto activated carbon. Part 1: isotherms. Hydrometallurgy 178, 202–208. https://doi.org/10.1016/j.hydromet.2018.04.015.

Tauetsile, P.J., Oraby, E.A., Eksteen, J.J., 2019a. Activated carbon adsorption of gold from cyanide-starved glycine solutions containing copper. Part 1: isotherms. Sep. Purif. Technol. 211, 594–601. https://doi.org/10.1016/j.seppur.2018.09.024.

Tauetsile, P.J., Oraby, E.A., Eksteen, J.J., 2019b. Activated carbon adsorption of gold from cyanide-starved glycine solutions containing copper. Part 2: kinetics. Sep. Purif. Technol. 211, 290–297. https://doi.org/10.1016/j.seppur.2018.09.022.

Van, D., Yahorava, V., Kotze, M., 2012. Gold Recovery from Copper-Rich Ores Employing the Purolite S992 Gold Selective Ion Exchange Resin. Mintek.

van Deventer, J., 2011. Selected ion exchange applications in the hydrometallurgical industry. Solvent Extraction Ion Exch. 29 (5–6), 695–718. https://doi.org/10.1080/07366299.2011.595626.

Wang, J., Xu, L., Cheng, C., Meng, Y., Li, A., 2012. Preparation of new chelating fiber with waste PET as adsorbent for fast removal of Cu2+ and Ni2+ from water: kinetic and equilibrium adsorption studies. Chem. Eng. J. 193–194, 31–38. https://doi.org/10.1016/j.cej.2012.03.070.

Wołowicz, A., Hubicki, Z., 2011. Investigation of macroporous weakly basic anion exchangers applicability in palladium(II) removal from acidic solutions – batch and column studies. Chemical Engineering Journal 174 (2), 510–521. https://doi.org/10.1016/j.cej.2011.08.075.

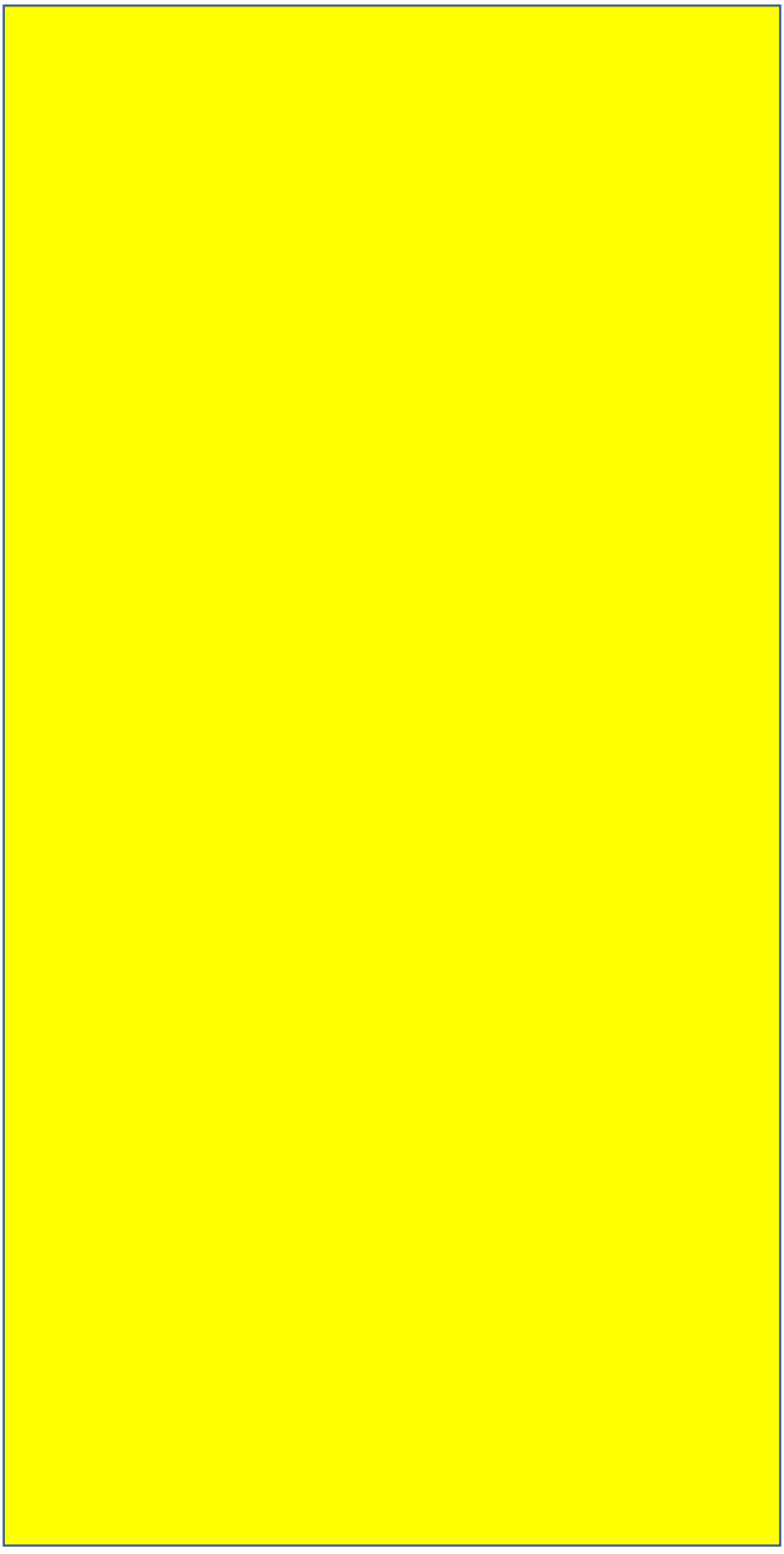

Chapter 7: Conclusions and Recommendations

This study can be divided into three main sections i.e. a literature review providing the context for the further research, a sulfide precipitation study (precipitation chemistry and precipitate characteristics) and ion-exchange resins adsorption study (for Cu and Au). The sulfide precipitation study first gained insight into the chemistry of sulfide precipitation in cyanide-starved glycine solutions by investigating the effects of different process conditions on copper recovery. The main finding is that the total copper recovery is determined by the $[Cu^{+}]$:$[Cu^{2+}]$ ratios or [CN]:$[Cu_T]$ ratio, where all the Cu^{2+} was precipitated by adding NaHS while Cu^{+} complexed with cyanide was not precipitated from the alkaline glycine-cyanide solutions. Sulfide precipitation particularly the size of precipitates was found be difficult to control, and this was addressed by an investigation of how different process conditions affecting the sulfide precipitate characteristics. The study suggested that coarse and easy settable and filterable size of precipitates can be generated by either adding divalent cations, particularly Ca^{2+}, or increasing the ionic strength of the solutions. It was also found that ageing, heating and seeding appear to mature the copper sulfide precipitates to form a more crystalline CuS product.

The second part of this study investigated the Cu adsorption behaviours using different types of commercially available resins from the synergetic glycine-cyanide system. A type of chelating resin, Puromet MTS9300, was chosen based on its superior selectivity towards Cu^{2+} over other species in the cyanide-starved glycine solutions. The separation phenomenon of using this resin is similar to that of using sulfide precipitation, where the Cu^{2+} recovery is also determined by the Cu^{2+}/Cu^{+} ratio. It is indicated that resin adsorption can be an alternative method to sulfide precipitation for Cu removal, depending on the economic. Elution of copper can be achieved by using either HCl or alkaline glycine solutions with NaCl present, and the resin can be effectively regenerated using the alkaline glycine as the eluent. A gold adsorption study using different types of commercial gold-selective resin were also undertaken. The results indicated that a recent developed molecularly imprinted polymer, IXOS-AuC resin, exhibited a good selectivity towards gold against Cu with no Cu^{2+} adsorption and a smaller amount of Cu^{+} being adsorbed compared with those commercial resins tested. The Cu can be pre-eluted by a cyanide solution and then the gold can be eluted by either acidic thiourea or alkaline

thiocyanate. Regeneration study suggested that both elution systems can potentially regenerate the IXOS-AuC resin.

7.1 Enumerated Conclusions

7.1.1 Sulfide precipitation

7.1.1.1 Sulfide precipitation chemistry

A summary of the copper sulfide precipitation behaviours by addition of NaHS to the cyanide-starved glycine solutions at different conditions are presented as follows:

- Process conditions such as $[HS^-]$:$[Cu_T]$, [Gly]:$[Cu_T]$, pH and reaction time have insignificant effects on the copper recovery.
- Total copper recovery was improved slightly from 65.8% to 75.9% by heating the solutions to 55°C.
- The $[Cu^+]$:$[Cu^{2+}]$ molar ratio determined by $[CN^-]$:$[Cu_T]$ molar ratio controls the copper recovery and higher total copper recovery was obtained in the presence of a higher amount of Cu^{2+}.
- The reaction is rapid and can be finished in 5 minutes of reaction
- Insignificant gold co-precipitation was observed with a small portion of gold precipitated (2.2%) at 60 min of reaction time, which may be ascribed to surface adsorption of gold onto CuS.
- Pre-oxidation of Cu^+ to Cu^{2+} was studied, and it was found that the optimum addition of peroxide varied depending on optimal $[H_2O_2]$:$[Cu^+]$ molar ratios. When the $[CN^-]$:$[Cu_T]$ molar ratios were 1:1 and 2:1, the optimum $[H_2O_2]$:$[Cu^+]$ molar ratios were 4:1 and 5:1, respectively.
- Total copper removal increased significantly after pre-oxidation from about 70% to over 96%.
- Lower the DO level can increase the copper recovery, which may be due to a copper sulfide redissolution in the presence of oxygen/peroxide and glycine.
- No obvious effects of pre-oxidation on gold precipitation that gold remained in solutions at different initial gold concentrations.
- Through a glycine titration method, it is concluded that the total glycine concentration was not significantly impacted by pre-oxidation, and more glycine was released from the cupric glycinate complex after precipitation.

7.1.1.2 Copper sulfide precipitate characteristics

Different factors affecting the copper sulfide precipitate characteristics were investigated from alkaline glycine-cyanide solutions. Conclusions are drawn in the following:

- Divalent cations, particularly Ca^{2+}, tend to enhance the formation of large and settleable precipitates, owing to a cross-linking effect.
- Increasing the dosage of Ca^{2+} can slightly increase in the mean particle size, but it does not affect settling performances. This will be an advantage for process plants where usually use lime as a pH modifier, thus no extra Ca^{2+} addition is required.
- Lowering the initial supersaturation level by reducing the solution concentrations has an insignificant effect on enlarging the size of the precipitates. This may be beneficial for process plants that no dilution of concentrated leachates is needed.
- Increasing the solution ionic strength can significantly enhance the formation of coarse and settleable precipitates even without Ca^{2+} addition.
- The optimum range of stirring speed of this study is 200 – 350 rpm
- A fast addition rate appears to be preferable in forming coarser particles.
- Ageing, heating or seeding have insignificant impacts on the PSD, but either of these measures can result in a morphology and crystal phase change.
- Based on the SEM and XRD results, a transformation from polymorph to crystalline crystal structure was observed after ageing, heating or seeding, implying the production of more mature and crystalline CuS.

7.1.2 Ion-exchange resin adsorption

7.1.2.1 Cu adsorption behaviours on resins

The adsorption behaviours using different types of chelating resins from synthetic glycinate-cyanide solutions containing Au and Cu were studied. A summary of the results are shown as follows:

- Compared with other chelating resin tested, Puromet MTS9300 resin exhibits high selectivity of Cu^{2+} against the Au and Cu^{+} cyanide species, due to the cation affinity of the resin.
- Similar to the sulfide precipitation, the adsorption of copper is controlled by the Cu^{+}/Cu^{2+} ratio determined by the $[CN^{-}]$: $[Cu_T]$ molar ratio.

- Over 99% of Cu^{2+} was recovered at any [CN^-]: [Cu_T] molar ratio.
- The [Gly]:[Cu_T] molar ratio does not significantly influence the adsorption behaviours of the resin if the additions of glycine exceeded the stoichiometric requirement; insufficient glycine additions i.e [Gly]:[Cu_T] = 1.5:1, can result in higher Cu^+ in the system, thus lowering the total Cu recovery.
- None or a very small amount of gold (< 1%) was co-adsorbed at all conditions tested.
- Similar adsorption performance was observed at different initial Cu^{2+} concentrations by maintaining the same resin:Cu^{2+} mass rato.
- The experimental data fit both the Freundlich and Langmuir models, while the Langmuir model represents a better fitting with a higher correlation coefficient.
- The adsorption kinetics of Cu^{2+} followed the pseudo-second-order model.
- Based on the curve fitted with the Intra-particle model, intra-particle diffusion was not the only rate-controlling step.
- The effective elution of Cu from the Puromet MTS9300 resin can be achieved by using either alkaline glycine solutions with salt (3M glycine, 3M NaCl and 2 – 3 M NaOH) or 2 – 3M HCl.
- Alkaline glycine solution with salt as eluent was recommended and was used in regeneration study, as the barren resin can be reused directly without neutralisation.
- The Cu adsorption capacity and regeneration efficiency dropped and then remain constant after the first cycle.
- The desorption efficiency remained constant during the multi-cycle tests with insignificant accumulations of residual Cu on the resin.
- No obvious change in resin shape and damage on resin surface was visualised by the SEM images after adsorption/regeneration.

7.1.2.2 Gold adsorption behaviours on resins

The adsorption behaviours of a novel molecularly imprinted polymer (IXOS-AuC) from the synthetic cyanide-starved glycine leachates containing gold and copper were investigated. The following conclusions are drawn:

- Four types of resins were compared (not presented in the published paper, (See Appendix C4.1) and they show good recovery of gold with low copper co-adsorption, insignificant Cu^{2+} co-adsorption was observed for most of the tested resins, excluding S992 resin
- The IXOS-AuC resin was selected for further investigations since it exhibits the best selectivity towards gold over copper with only about 7.4% of Cu_T being adsorbed.
- Factors such as $[CN^-]$:$[Cu_T]$ and [Gly]: $[Cu_T]$ molar ratios have insignificant influences on the adsorption of gold and copper.
- Higher initial gold concentration tends to decrease the copper co-adsorption on the resin.
- From an adsorption equilibrium test, experimental data fit the Freundlich isotherm model better than the Langmuir model with a higher regression coefficient.
- The Kinetics study showed the experimental data fit well with the Pseudo-second-order model.
- Copper can be pre-eluted by 0.4M NaCN solutions at pH 11.5 from the IXOS-AuC resin, while gold was not eluted at such conditions.
- Gold can be effectively stripped by either using acidic thiourea (0.5M Thiourea/0.5M H_2SO_4) or alkaline thiocyanate (2.5M Thiocyanate/1.5g/L NaOH) from the resin.
- The multi-cycle tests revealed that the IXOS-AuC resin can be effectively regenerated and reused in both acidic thiourea and alkaline thiocyanate elution system.
- The change of surface morphology of the resin was generally not significant after adsorption/regeneration.

7.2 Recommendation and Potential Opportunities for Future Study

The following recommendations were proposed for a continuous study based on the identified research gap:

- Sulfide precipitation tests in a cyanide-starved glycine solution containing Au and Cu with other metals with Ag, Zn, Ni, Co, Pd, etc. How do the other metals behave as well as gold and copper?

- Ion-exchange resin adsorption study in a cyanide-starved glycine solution containing Au and Cu with other metals. To what extent do the other metals affect the adsorption of gold? And what types of resin can purify the solutions?
- Sulfide precipitation test for a glycine-only system containing copper and gold. How does the gold glycinate behave, will it be co-precipitated with copper or remain in solutions?
- Ion-exchange resin adsorption study for a glycine-only system containing copper and gold. Do the previously selected resins still perform well with good selectivity towards the desired metals? Will other types of resins give better results? What kinds of eluent would be suitable?
- Lock-cycle tests incorporated with leaching, sulfide precipitation and resin adsorption to recover copper and gold from a real copper-gold ore in either cyanide-starved glycine system or glycine-only systems. Can these recovery methods work well in the presence of other impurities? What are the optimum operational conditions?
- Construct conceptual flowsheet integrated with leaching and recovery based on the glycine-cyanide and synergetic glycine cyanide system and conduct a high-level cost evaluation and environmental impact estimation. Which leach system and what types of recovery techniques would be more economic and environmental friendly?
- Pilot the process in a mini-scale pilot plant with a continuous process using the optimum conditions obtained from the bench-scale lock-cycle tests and the cost and environmental impact estimations.
- A full techno-economic analysis is still required to evaluate the profitability of the metal recovery circuit (which would include leaching).
- It is foreseen that this technology may have applications in the following areas:
    - Recovery of copper and gold from leachates from copper-gold ores and tailings.
    - Recovery of copper and gold from flotation and gravity concentrates

- Recovery of copper and gold from copper anode slimes during copper refining
- Recovery of copper and gold from electronic and electrical waste
- Recovery and copper and gold from acid mine drainage solutions from old copper-gold mine sites effluents after pH adjustment

It is therefore clear that the technology and outcomes derived in this thesis should be of use across a broad range of streams from diverse gold-copper operations.

Appendices

Appendix A Signed Statement of contribution of co-authors

Appendix B Example calculation for synthetic solution preparation

Appendix C Tabulation of experimental data

Appendix D Copyright Permission

Appendix A Signed Statement of contribution of co-authors

Curtin University

STATEMENT OF CONTRIBUTION OF CO-AUTHORS

To whom it may concern

I, **Zixian Deng**, contributed with the conception, design, analysis and interpretation of experimental data and wrote all four papers reported in this thesis. These are:

- **Deng, Z.**, Oraby, E. A., & Eksteen, J. J. (2019). The sulfide precipitation behaviour of Cu and Au from their aqueous alkaline glycinate and cyanide complexes. Separation and Purification Technology, 218, 181-190. https://doi.org/10.1016/j.seppur.2019.02.056

- **Deng, Z.**, Oraby, E. A., & Eksteen, J. J. (2020). Sulfide precipitation of copper from alkaline glycine-cyanide solutions: Precipitate characterisation. Minerals Engineering, 145, 106102. https://doi.org/10.1016/j.mineng.2019.106102

- **Deng, Z.**, Oraby, E. A., & Eksteen, J. J. (2020). Cu adsorption behaviours onto chelating resins from glycine-cyanide solutions: Isotherms, kinetics and regeneration studies. Separation and Purification Technology, 236, 116280. https://doi.org/10.1016/j.seppur.2019.116280

- **Deng, Z.**, Oraby, E. A., & Eksteen, J. J. (2020). Gold recovery from cyanide-starved glycine solutions in the presence of Cu using a molecularly imprinted resin (IXOS-AuC). Hydrometallurgy, 196, 105425. https://doi.org/10.1016/j.hydromet.2020.105425

Signature of Candidate:

I, as a co-author, endorse that this level of contribution by the candidate indicated above is appropriate.

Prof. Jacques Ekteen

Signature:

Dr Elsayed Oraby

Signature:

Appendix B Example calculation for synthetic solution preparation

Stock Au Cyanide-starved glycine solution

Prepare a 1L Au stock solution by dissolving gold powders (99.998%) in a solution containing CuCN and glycine at [Cu]:[CN]:[Gly] molar ratio =1:1:3 and pH = 10.5 for 24h (300 mg/L Cu).

Mass of Au powders: 0.2 g

Mass of CuCN:

Molar mass of CuCN = 89.56 g/mol

Molar mass of Cu = 63.55 g/mol

To obtain a 300 mg/L (0.3 g/L) Cu in solution, the required mass of solid CuCN (purity = 95%):

$$m_{CuCN} = \frac{0.3 \times 89.56}{63.55 \times 0.95} = 0.445 \text{ g}$$

Mass of glycine:

Molar mass of Glycine = 75.07 g/mol

To achieve a [Cu]:[CN]:[Gly] molar ratio of 1:1:3, the required mass of glycine (purity =99%):

$$m_{Gly} = \frac{0.3 \times 75.07 \times 3}{63.55 * 0.99} = 1.063 \text{ g}$$

Adjust pH to 10.5 using NaOH

After 24h of reaction, filter the solution by a Supor® 0.45 μm membrane disc filter paper. The Au concentration is determined by AAS.

Cyanide-starved glycine solution ([Cu]:[CN]:[Gly] =1:1:3)

To prepare the a synthetic cyanide-starved glycine solution containing 300 mg/L Cu and 2 mg/L Au at [Cu]:[CN]:[Gly] molar ratio =1:1:3 and pH = 10.5:

Prepare a 1L cyanide-starved glycine solution by diluting the Au stock solution in a solution with the same Cu concentration at the same [Cu]:[CN]:[Gly] molar ratio and pH conditions, targeting 300 mg/L Cu and 2 mg/L Au in solutions.

[Au] of the Au stock solution = 134 mg/L

To obtain a target [Au] of 2 mg/L, according to $C_1V_1=C_2V_2$, the required volume of Au stock solution :

$$V_{Au\ stock} = \frac{2\times1}{134} = 0.0149\ L$$

Dilute the Au stock solution in a 1L volumetric flask with CuCN and glycine using 0.9851L of DI Water.

To obtain 300 mg/L Cu and a [Cu]:[CN]:[Gly] molar ratio of 1:1:3, the required mass of CuCN and glycine:

$$m_{CuCN} = 0.445 \times 0.9851 = 0.438\ g$$

$$m_{Gly} = 1.063 \times 0.9851 = 1.047\ g$$

Adjust pH to 10.5 using NaOH and/or $Ca(OH)_2$, and then filter the solution by a Supor® 0.45 μm membrane disc filter paper.

Cyanide-starved glycine solution ([Cu]:[CN]:[Gly] =1:2:3)

To prepare the a synthetic cyanide-starved glycine solution containing 300 mg/L Cu and 2 mg/L Au at [Cu]:[CN]:[Gly] molar ratio =1:2:3 and pH = 10.5:

In this case, cyanide is sourced from the same mole of CuCN and NaCN. The required mass of CuCN and glycine are the same as the above section, 0.438g and 1.047g, respectively. The extra CN^- was sourced from NaCN addition.

Molar mass of NaCN = 49.01 g/L

The required mass of NaCN (purity = 95 %):

$$m_{NaCN} = \frac{0.3\times49.01}{63.55\times0.95} = 0.244\ g$$

Cyanide-starved glycine solution ([Cu]:[CN]:[Gly] =1:0.5:3)

To prepare the a synthetic cyanide-starved glycine solution containing 300 mg/L Cu and 2 mg/L Au at [Cu]:[CN]:[Gly] molar ratio =1:0.5:3 and pH = 10.5:

In this case, Cu is sourced from the same mole of CuCN and $CuSO_4$. The required mass of CuCN is 50% of the above section, which is 0.438/2 = 0.219 g.

Molar mass of $CuSO_4 \cdot H_2O$ = 249.72 g/mol

The required mass of $CuSO_4 \cdot H_2O$ (putity = 98%):

$$m_{CuSO_4} = \frac{0.15 \times 249.72}{63.55 \times 0.98} = 0.382 \text{ g}$$

The required mass of glycine is the same, which is 1.047 g.

Appendix C Tabulation of experimental data

Appendix C1 - Sulfide precipitation behaviour study

C1.1 Effects of $[HS^-]$:$[Cu_T]$

Experimental condition: 300mg/L Cu_T, 1 mg/L Au, $[Cu_T]$:$[CN^-]$:[Gly] molar ratio = 1:1:3 , room temeperature pH =10.5 and 5 min reaction time

S:Cu	pH	Eh	Cu_T, ppm	Au,ppm	Cu^{2+}, ppm	Cu_T Removal, %	Au Removal, %
Original	10.52	115	303.6	1.209	200		
1:1	10.41	-36	120.3	1.323	30	62.75	-2.86
1.1:1	10.21	-193	103.2	1.265	0	68.05	1.65
1.3:1	10.25	-250	99.75	1.352	0	69.12	-5.12
1.6:1	10.34	-287	102.15	1.358	0	68.04	-6.71
2:1	10.31	-440	109.35	1.371	0	66.14	-6.60
3:1	10.31	-453	104.55	1.355	0	68.32	-3.11

C1.2 Effects of reaction time

Experimental condition: 300mg/L Cu_T, 1 mg/L Au, $[Cu_T]$:$[CN^-]$:[Gly] molar ratio = 1:1:3, room temeperature pH = 10.5 and $[HS^-]$:$[Cu_T]$ = 1.3:1

Time, min	Cu_T, ppm	Au, ppm	Cu^{2+}, ppm	pH	Eh	Cu_T Removal, %	Au Removal, %
0	303.6	1.209	200	10.53	116	0	
5	99.75	1.352	0	10.25	-250	69.12	-5.12
10	98.35	1.338	0	10.31	-193	69.23	-5.14
20	96.05	1.335	0	10.28	-159	69.63	-6.00
30	87.95	1.299	4	10.18	-103	72.77	-1.00
60	95.05	1.258	27	9.38	88	70.57	2.19

C1.3 Effects of [Gly]:[CuT] molar ratio

Experimental condition: 300mg/L Cu_T, 1 mg/L Au, $[CN^-]$:$[Cu_T]$ =1:1, pH =10.5, $[HS^-]$:$[Cu_T]$=1.3:1, room temeperature and 5 min reaction time.

Before precipitation					After precipitation					
Cu:Gly	Cu_T, ppm	Au,ppm	pH	Eh	Cu_T, ppm	Au,ppm	pH	Eh	Cu_T Removal, %	Au Removal, %
1:3	302.8	1.213	10.56	102	99.75	1.352	10.25	-250	68.80	-4.77
1:4	270.5	1.257	10.53	49	97.8	1.421	10.57	-398	69.41	-6.26
1:6	296.9	0.952	10.57	-10	97.95	1.274	10.45	-305	69.36	-25.79
1:8	298.1	1.095	10.51	40	96.25	1.444	10.25	-306	69.89	-23.96

C1.4 Effects of $[CN^-]:[Cu_T]$ molar ratio

Experimental condition: 300mg/L Cu_T, 1 mg/L Au, $[Gly]:[Cu_T]$ = 3:1, pH = 10.5, $[HS^-]:[Cu_T]$= 1.3:1, room temeperature and 5 min reaction time

Before precipitation					**After precipitation**					
Cu:CN	**Cu_T, ppm**	**Au, ppm**	**pH**	**Eh**	**Cu_T, ppm**	**Au, ppm**	**pH**	**Eh**	**Cu_T Removal, %**	**Au Removal, %**
1:0.1	275.1	1.276	10.55	43	20.15	1.511	10.18	91	92.68	-18.42
1:0.5	263.3	1.38	10.49	89	57.35	1.502	10.34	-140	78.22	-8.84
1:1	302.8	1.213	10.56	98	99.75	1.357	10.26	-263	67.12	-11.87
1:2	298.8	1.238	10.47	93	176.9	1.28	10.16	-329	40.80	-3.39

C.1.5 Effects of pH

Experimental condition: 300mg/L Cu_T, 1 mg/L Au, $[Cu_T]:[CN^-]:[Gly]$ molar ratio =1:1:3, $[HS^-]:[Cu_T]$= 1.3:1, room temeperature and5 min reaction time,

Before precipitation				**After precipitation**					
pH	**Cu_T, ppm**	**Au, ppm**	**Eh**	**Cu_T, ppm**	**Au, ppm**	**pH**	**Eh**	**Cu_T Removal, %**	**Au Removal, %**
8.10	244.4	1.156	200	110.75	1.287	9.5	-24	65.30	-11.33
9.04	275.3	1.056	107	99.1	1.348	9.58	-236	68.95	-27.65
10.55	282.8	0.967	59	103.35	1.002	10.38	-247	67.62	-3.62
12.00	272.8	0.987	104	99.55	1.102	11.79	-341	68.81	-11.65

C.1.6 Effects of Temperature

Experimental condition: 300mg/L Cu_T, 1 mg/L Au, $[Cu_T]:[CN^-]:[Gly]$ molar ratio =1:1:3, pH = 10.5, $[HS^-]:[Cu_T]$= 1.3:1 and 5 min reaction time

Temperature	**Cu_T, ppm**	**Cu2+**	**Au, ppm**	**pH**	**Eh**	**Cu_T Removal, %**
original	303.6	226	1.209	10.81	106	
25	103.7	2	1.362	10.29	-334	65.84
35	93.6	0	1.352	10.22	-256	69.17
55	73.1	0	1.395	10.12	-293	75.92

C1.7 Pre-oxidation of Cu^{+} to Cu^{2+} at different $[H_2O_2]$:$[Cu^{+}]$ molar ratio

1. $[H_2O_2]$:$[Cu^{+}]$ = 5:1

Experimental conditions: 300mg/L Cu_T, 1 mg/L Au, $[Cu_T]$:$[CN^-]$:[Gly] =1:2:3, pH = 10.5, and room temperature.

Time, min	Cu^{2+}, ppm	DO, ppm	% oxidation from Cu^{+} to Cu^{2+}
0	101	2.5	0.00
5	295	21.6	97.49
15	291	15.6	95.48
30	286	11.5	92.96
60	285	5.6	92.46
120	283	4.3	91.46
240	281	4.1	90.45

2. $[H_2O_2]$:$[Cu^{+}]$ = 4:1

Experimental conditions: 300mg/L Cu_T, 1 mg/L Au, $[Cu_T]$:$[CN^-]$:[Gly] =1:2:3, pH = 10.5, and room temperature.

Time, min	Cu^{2+}, ppm	DO, ppm	% oxidation from Cu^{+} to Cu^{2+}
0	101	2.5	0.00
5	219	20.5	59.30
15	218	10.8	58.79
30	215	8.5	57.29
60	214	4.8	56.78
120	215	4.3	57.29
240	216	3.8	57.79

3. $[H_2O_2]$:$[Cu^{+}]$ = 3:1

Experimental conditions: 300mg/L Cu_T, 1 mg/L Au, $[Cu_T]$:$[CN^-]$:[Gly] =1:2:3, pH = 10.5, and room temperature.

Time, min	Cu^{2+}, ppm	DO, ppm	% oxidation from Cu^{+} to Cu^{2+}
0	110	2.4	0.00
5	191	18.5	42.63
15	197	9.1	45.79
30	197	5.4	45.79
60	198	3.5	46.32
120	197	3.6	45.79
240	203	3.2	48.95

4. $[H_2O_2]$:$[Cu^{+}]$ = 1:1

Experimental conditions: 300mg/L Cu_T, 1 mg/L Au, $[Cu_T]$:$[CN^-]$:[Gly] =1:2:3, pH = 10.5, and room temperature.

Time, min	Cu^{2+}, ppm	DO, ppm	% oxidation from Cu^{+} to Cu^{2+}
0	110	3	0.00%
5	117	11.5	3.68
15	121	7.7	5.79
30	126	5	8.42
60	126	3.9	8.42
120	133	3.3	12.11
240	139	3.5	15.26

C1.8 Effects of $[CN]^-$:$[Cu_T]$ molar ratio on H_2O_2 dosage

1. $[H_2O_2]$:$[Cu^+]$ = 5:1

Experimental conditions: 300mg/L Cu_T, 1 mg/L Au, $[Cu_T]$:$[CN^-]$:[Gly] =1:1:3, pH = 10.5, and room temperature.

Time, min	Cu^{2+}, ppm	DO, ppm	% oxidation from Cu^+ to Cu^{2+}
0	204	2.5	0.00
5	324	20.5	99.55
15	324	16.2	99.55
30	324	12.3	99.55
60	323	4.5	99.11
120	322	4.2	98.66
240	319	3.9	97.32

2. $[H_2O_2]$:$[Cu^+]$ = 4:1

Experimental conditions: 300mg/L Cu_T, 1 mg/L Au, $[Cu_T]$:$[CN^-]$:[Gly] =1:1:3, pH = 10.5, and room temperature.

Time, min	Cu^{2+}, ppm	DO, ppm	% oxidation from Cu^+ to Cu^{2+}
0	204	2.5	0.00
5	321	20.6	98.21
15	322	15.6	98.66
30	323	11.5	99.11
60	320	5.6	97.77
120	321	4.5	98.21
240	318	4.1	96.88

3. $[H_2O_2]$:$[Cu^+]$ = 3:1

Experimental conditions: 300mg/L Cu_T, 1 mg/L Au, $[Cu_T]$:$[CN^-]$:[Gly] =1:1:3, pH = 10.5, and room temperature.

Time, min	Cu^{2+}, ppm	DO, ppm	% oxidation from Cu^+ to Cu^{2+}
0	204	2.4	0.00
5	277	17.8	78.57
15	278	10.2	79.02
30	279	5.3	79.46
60	278	3.5	79.02
120	276	3.1	78.13
240	274	3.2	77.23

C.1.9 Effects of dissolved oxygen (after pre-oxidation)

Experimental conditions: 300mg/L Cu_T, 1 mg/L Au, 300mg/L Cu_T, 1 mg/L Au, $[Cu_T]$:$[CN^-]$:[Gly] =1:2:3, and pH = 10.5, $[HS^-]$:$[Cu_T]$ =1.3:1, 5 min reaction time.

Before		After	
Do, ppm	Cu_T, ppm	Cu_T, ppm	Cu removal, %
21.6	303	41.9	86.17
4.3	303	28	90.76
0	303	26.9	91.12

C1.10 Effects of $[HS^-]$:$[Cu_T]$ molar ratio (after pre-oxidation)

Experimental conditions: 300mg/L Cu_T, 1 mg/L Au, $[Cu_T]$:$[CN^-]$:[Gly] =1:2:3, and pH = 10.5, 0 ppm Do, 5 min reaction time.

[HS]:[Cu_T]	Cu_T, ppm	Au, ppm	Cu^{2+}, ppm	pH	Eh	DO, ppm	Au Removal, %	Cu_T Removal, %
Orignial	300.2	1.213	298	10.56	110	0		
1:1	86	1.202	81	10.31	-33	0.3	0.91	71.2
1:1.3	28.4	1.273	37	10.49	-2	1.3	-4.95	91.10
1:1.4	11.25	1.421	5	10.36	-68	1.1	-17.15	96.48
1:1.6	26.15	1.328	0	10.13	-355	0	-9.48	91.81

C1. 11 Effects of contact time during precipitation (after pre-oxidation)

Experimental conditions: 300mg/L Cu_T, 1 mg/L Au, $[Cu_T]$:$[CN^-]$:[Gly] =1:2:3, and pH = 10.5, 0 ppm Do, $[HS^-]$:$[Cu_T]$ =1.4:1 and 5 min reaction time.

Time, min	Cu_T, ppm	Au, ppm	Cu^{2+}, ppm	pH	Eh	DO, ppm	Au Removal, %	Cu_T Removal, %
0	300.5	1.352	296	10.61	78	0		
5	11.25	1.421	5	10.36	-68	1.1	-5.10	96.48
10	14.7	1.44	0	10.45	-73	0.5	-6.51	95.39
20	20.35	1.42	15	10.52	-12	0.5	-5.03	93.62
30	23.05	1.417	40	10.54	-16	0.5	-4.81	92.78
60	32.65	1.073	29	10.56	40	2.3	22.67	89.77

C1. 12 Effects of pre-oxidation on gold precipitation

Experimental conditions: 300mg/L Cu_T, $[Cu_T]$:$[CN^-]$:[Gly] =1:2:3, and pH = 10.5, 0 ppm Do, $[HS^-]$:$[Cu_T]$ =1.4:1 and 5 min reaction time.

Conditions	Before precipitation		After precipitation			
	Cu_T, ppm	Au, ppm	Cu_T, ppm	Au, ppm	Cu_T Removal, %	Au Removal, %
4 mg/L Au (with pre-oxidation)	301.5	4.375	9.52	4.456	96.07	-1.85
1 mg/L Au (with pre-oxidation)	300.5	1.215	6.16	1.278	96.40	-5.19
4 mg/L Au (without pre-oxidation)	301.5	4.375	178.49	4.561	40.80	-4.25

Appendix C2 - Sulfide precipitate characteristics study

C2.1 Effects of cation addition

Experimental condition: $[Cu_T]$ = 300mg/L, $[Cu_T]$:$[CN^-]$:[Gly]=1:1:3, pH = 10.5, room temperature, $[HS^-]$ = 5M, $[HS^-]$:[Cu] = 1.3:1, reaction time = 5min, stirring speed =200 rpm.

Cation concentration	0.5mM Ca^{2+}	0.5mM Mg^{2+}
Specific Surface Area, m2/g:	0.0751	0.326
Surface Weighted Mean D[3,2], µm	29.596	6.812
Vol. Weighted Mean D[4,3], µm	44.34	24.734
d10, µm	16.312	10.244
d50, µm	39.226	21.934
d80, µm	63.712	34.787

PSD data at 0.5mM Ca^{2+}

Size (µm)	Vol Under %	Size (µm)	Vol Under %	Size (µm)	Vol Under %	Size (µm)	Vol Under %
1.096	0	11.482	1.22	120.226	5.9	1258.925	0
1.259	0	13.183	1.35	138.038	4.46	1445.44	0
1.445	0	15.136	1.48	158.489	3	1659.587	0
1.66	0.01	17.378	1.63	181.97	1.77	1905.461	0
1.905	0.06	19.953	1.83	208.93	0.76	2187.762	0
2.188	0.08	22.909	2.13	239.883	0.16	2511.886	0
2.512	0.09	26.303	2.6	275.423	0	2884.032	0
2.884	0.12	30.2	3.25	316.228	0	3311.311	0
3.311	0.15	34.674	4.11	363.078	0	3801.894	0
3.802	0.2	39.811	5.13	416.869	0	4365.158	0
4.365	0.26	45.709	6.22	478.63	0	5011.872	0
5.012	0.35	52.481	7.28	549.541	0	5754.399	0
5.754	0.45	60.256	8.11	630.957	0	6606.934	0
6.607	0.6	69.183	8.6	724.436	0	7585.776	0
7.586	0.74	79.433	8.62	831.764	0	8709.636	0
8.71	0.9	91.201	8.13	954.993	0	10000	0
10	1.06	104.713	7.19	1096.478	0		

PSD data at 0.5mM Mg^{2+}

Size (µm)	Vol Under %	Size (µm)	Vol Under %	Size (µm)	Vol Under %	Size (µm)	Vol Under %
1.096	0	11.482	1.37	120.226	1.76	1258.925	0
1.259	0	13.183	1.78	138.038	0.92	1445.44	0
1.445	0	15.136	2.36	158.489	0.3	1659.587	0
1.66	0	17.378	3.07	181.97	0.05	1905.461	0
1.905	0	19.953	3.98	208.93	0	2187.762	0
2.188	0	22.909	5.01	239.883	0	2511.886	0
2.512	0	26.303	6.1	275.423	0	2884.032	0
2.884	0.05	30.2	7.16	316.228	0	3311.311	0
3.311	0.09	34.674	8.07	363.078	0	3801.894	0
3.802	0.15	39.811	8.68	416.869	0	4365.158	0
4.365	0.21	45.709	8.91	478.63	0	5011.872	0
5.012	0.3	52.481	8.66	549.541	0	5754.399	0
5.754	0.4	60.256	7.97	630.957	0	6606.934	0
6.607	0.52	69.183	6.91	724.436	0	7585.776	0

7.586	0.65	79.433	5.6	831.764	0	8709.636	0
8.71	0.83	91.201	4.2	954.993	0	10000	0
10	1.05	104.713	2.89	1096.478	0		

Experimental data of settling tests (Effects of cation addition)

	h			**h/h_0**		
time, min	**0.5mM Ca^{2+}**	**0.5mM Mg^{2+}**	**0.5mM Al^{3+}**	**0.5mM Ca^{2+}**	**0.5mM Mg^{2+}**	**0.5mM Al^{3+}**
0	500	500	500	1	1	1
0.15	490	500	500	0.98	1	1
0.5	475	500	500	0.95	1	1
1	455	500	500	0.91	1	1
2	245	300	500	0.49	0.6	1
3	25	100	500	0.05	0.2	1
5	20	40	500	0.04	0.08	1
8	18	30	500	0.036	0.06	1
10	16	25	500	0.032	0.05	1
20	15	25	500	0.03	0.05	1

C2. 2 Effects of Ca^{2+} dosage

Experimental conditions: $[Cu_T]$ = 300mg/L, $[Cu_T]$:$[CN^-]$:[Gly]=1:1:3, pH = 10.5, room temperature, $[HS^-]$ = 5M, $[HS^-]$:$[Cu_T]$ = 1.3:1, reaction time =5min, stirring speed =200 rpm.

Ca^{2+} concentration, mM	0.25	0.5	1.25
Specific Surface Area, m2/g:	0.0876	0.0751	0.0589
Surface Weighted Mean D[3,2], μm	25.378	29.596	37.699
Vol. Weighted Mean D[4,3], μm	37.11	44.34	62.109
d10, μm	14.338	16.312	19.561
d50, μm	33.124	39.226	54.992
d80, μm	52.922	63.712	90.909

PSD data at 0.25mM Ca^{2+}

Size (μm)	**Vol Under %**	**Size (μm)**	**Vol Under %**	**Size (μm)**	**Vol Under %**	**Size (μm)**	**Vol Under %**
1.096	0	11.482	1.63	120.226	0.42	1258.925	0
1.259	0	13.183	2.27	138.038	0.08	1445.44	0
1.445	0	15.136	3.13	158.489	0	1659.587	0
1.66	0	17.378	4.17	181.97	0	1905.461	0
1.905	0	19.953	5.35	208.93	0	2187.762	0
2.188	0	22.909	6.58	239.883	0	2511.886	0
2.512	0	26.303	7.74	275.423	0	2884.032	0
2.884	0.07	30.2	8.67	316.228	0	3311.311	0
3.311	0.12	34.674	9.25	363.078	0	3801.894	0
3.802	0.17	39.811	9.36	416.869	0	4365.158	0
4.365	0.23	45.709	8.98	478.63	0	5011.872	0

5.012	0.29	52.481	8.1	549.541	0	5754.399	0
5.754	0.37	60.256	6.86	630.957	0	6606.934	0
6.607	0.47	69.183	5.39	724.436	0	7585.776	0
7.586	0.61	79.433	3.87	831.764	0	8709.636	0
8.71	0.83	91.201	2.47	954.993	0	10000	0
10	1.15	104.713	1.37	1096.478	0		

PSD data at 0.125mM Ca^{2+}

Size (μm)	**Vol Under %**	**Size (μm)**	**Vol Under %**	**Size (μm)**	**Vol Under %**	**Size (μm)**	**Vol Under %**
1.096	0	11.482	1.18	120.226	5.78	1258.925	0
1.259	0	13.183	1.42	138.038	4.89	1445.44	0
1.445	0	15.136	1.72	158.489	3.89	1659.587	0
1.66	0	17.378	2.03	181.97	2.9	1905.461	0
1.905	0	19.953	2.39	208.93	1.98	2187.762	0
2.188	0	22.909	2.81	239.883	1.21	2511.886	0
2.512	0.06	26.303	3.28	275.423	0.64	2884.032	0
2.884	0.09	30.2	3.81	316.228	0.24	3311.311	0
3.311	0.12	34.674	4.4	363.078	0.01	3801.894	0
3.802	0.15	39.811	5.03	416.869	0	4365.158	0
4.365	0.2	45.709	5.67	478.63	0	5011.872	0
5.012	0.27	52.481	6.27	549.541	0	5754.399	0
5.754	0.35	60.256	6.76	630.957	0	6606.934	0
6.607	0.46	69.183	7.07	724.436	0	7585.776	0
7.586	0.59	79.433	7.16	831.764	0	8709.636	0
8.71	0.76	91.201	6.96	954.993	0	10000	0
10	0.95	104.713	6.5	1096.478	0		

Experimental data of settling tests (Effects of Ca^{2+} dosage)

	h			**h/h0**		
time, min	**0.5mM Ca^{2+}**	**0.25mM Ca^{2+}**	**5mM Ca^{2+}**	**0.5mM Ca^{2+}**	**0.25mM Ca^{2+}**	**1.25mM Ca^{2+}**
0	500	500	500	1	1	1
0.15	490	500	485	0.98	1	0.97
0.5	475	495	480	0.95	0.99	0.96
1	455	490	400	0.91	0.98	0.8
2	245	300	200	0.49	0.6	0.4
3	25	30	24	0.05	0.06	0.048
5	20	25	20	0.04	0.05	0.04
8	18	20	15	0.036	0.04	0.03
10	16	20	15	0.032	0.04	0.03
20	15	20	15	0.03	0.04	0.03

C2.3 Effects of supersaturation

Experimental conditions: $[Cu_T]:[CN^-]:[Gly]=1:1:3$, pH = 10.5, room temperature, Ca^{2+} dosage =0.5mM, $[HS]:[Cu_T]$ = 1.3:1, reaction time =5min, stirring speed =200 rpm.

Concentrations	$[HS^-]$=5M, $[Cu_T]$ = 300mg/L	$[HS^-]$= 5M, [CuT]=1000mg/L	$[HS^-]$=0.05M, [CuT]=300mg/L
Specific Surface Area, m2/g:	0.0751	0.0763	0.0671
Surface Weighted Mean D[3,2], µm	29.596	29.108	33.137
Vol. Weighted Mean D[4,3], µm	44.34	47.393	52.793
d10, µm	16.312	15.095	17.569
d50, µm	39.226	41.806	46.006
d80, µm	63.712	69.343	76.863

PSD data at $[HS^-]$=5M, $[Cu_T]$ = 300mg/L (Same as as the PSD data at 0.5mM Ca^{2+})

PSD data at $[HS^-]$= 5M, [CuT]=1000mg/L

Size (µm)	**Vol Under %**	**Size (µm)**	**Vol Under %**	**Size (µm)**	**Vol Under %**	**Size (µm)**	**Vol Under %**
1.096	0	11.482	1.44	120.226	2.49	1258.925	0
1.259	0	13.183	1.79	138.038	1.45	1445.44	0
1.445	0	15.136	2.22	158.489	0.67	1659.587	0
1.66	0	17.378	2.77	181.97	0.16	1905.461	0
1.905	0	19.953	3.45	208.93	0	2187.762	0
2.188	0	22.909	4.28	239.883	0	2511.886	0
2.512	0	26.303	5.21	275.423	0	2884.032	0
2.884	0.05	30.2	6.2	316.228	0	3311.311	0
3.311	0.09	34.674	7.15	363.078	0	3801.894	0
3.802	0.13	39.811	7.94	416.869	0	4365.158	0
4.365	0.21	45.709	8.45	478.63	0	5011.872	0
5.012	0.3	52.481	8.58	549.541	0	5754.399	0
5.754	0.42	60.256	8.27	630.957	0	6606.934	0
6.607	0.57	69.183	7.53	724.436	0	7585.776	0
7.586	0.73	79.433	6.45	831.764	0	8709.636	0
8.71	0.93	91.201	5.13	954.993	0	10000	0
10	1.17	104.713	3.77	1096.478	0		

PSD data at $[HS^-]$=0.05M, [CuT]=300mg/L

Size (µm)	**Vol Under %**	**Size (µm)**	**Vol Under %**	**Size (µm)**	**Vol Under %**	**Size (µm)**	**Vol Under %**
1.096	0	11.482	1.1	120.226	3.41	1258.925	0
1.259	0	13.183	1.41	138.038	2.25	1445.44	0
1.445	0	15.136	1.83	158.489	1.3	1659.587	0
1.66	0	17.378	2.36	181.97	0.62	1905.461	0
1.905	0	19.953	3.02	208.93	0.16	2187.762	0

2.188	0	22.909	3.83	239.883	0	2511.886	0
2.512	0	26.303	4.75	275.423	0	2884.032	0
2.884	0	30.2	5.74	316.228	0	3311.311	0
3.311	0.04	34.674	6.71	363.078	0	3801.894	0
3.802	0.08	39.811	7.56	416.869	0	4365.158	0
4.365	0.13	45.709	8.2	478.63	0	5011.872	0
5.012	0.19	52.481	8.52	549.541	0	5754.399	0
5.754	0.27	60.256	8.43	630.957	0	6606.934	0
6.607	0.38	69.183	7.95	724.436	0	7585.776	0
7.586	0.5	79.433	7.1	831.764	0	8709.636	0
8.71	0.65	91.201	5.96	954.993	0	10000	0
10	0.85	104.713	4.7	1096.478	0		

Experimental data of settling tests (Effects of supersaturation)

	h			**h/h0**		
time, min	**$[HS^-]$=5 M, $[Cu_T]$ = 300 mg/L**	**$[HS^-]$=0.05 M, [CuT]=300 mg/L**	**$[HS^-]$= 5M, [CuT]=1000 mg/L**	**$[HS^-]$=5M, $[Cu_T]$ = 300 mg/L**	**$[HS^-]$=0.05 M, [CuT]=300 mg/L**	**$[HS^-]$= 5M, [CuT]=1000 mg/L**
0	500	500	500	1	1	1
0.15	495	495	490	0.99	0.99	0.98
0.5	475	460	465	0.95	0.92	0.93
1	455	450	445	0.91	0.9	0.89
2	245	250	225	0.49	0.5	0.45
3	25	24	25	0.05	0.048	0.05
5	20	30	22.5	0.04	0.06	0.045
8	18	18	16	0.036	0.036	0.032
10	16	17	16	0.032	0.033	0.032
20	16	17	16	0.032	0.033	0.032

C2.4 Effects of ionic strength

Experimental conditions: $[Cu_T]$:$[CN^-]$:[Gly]=1:1:3, pH = 10.5, room temperature, Ca^{2+} dosage =0.5mM, [HS]:$[Cu_T]$ = 1.3:1, reaction time =5min, stirring speed =200 rpm.

Ionic strength, M	0.1M	0.2M	1M
Specific Surface Area, m2/g:	0.22	0.108	0.0653
Surface Weighted Mean D[3,2], μm	10.121	20.54	34.015
Vol. Weighted Mean D[4,3], μm	18.44	36.719	56.867
d10, μm	5.776	10.232	17.627
d50, μm	15.397	31.837	51.783
d80, μm	27.014	55.064	83.147

PSD data at 0.1M of ionic strength

Size (µm)	Vol Under %	Size (µm)	Vol Under %	Size (µm)	Vol Under %	Size (µm)	Vol Under %
1.096	0	11.482	6.58	120.226	0	1258.925	0
1.259	0.18	13.183	7.27	138.038	0	1445.44	0
1.445	0.21	15.136	7.74	158.489	0	1659.587	0
1.66	0.25	17.378	7.93	181.97	0	1905.461	0
1.905	0.31	19.953	7.8	208.93	0	2187.762	0
2.188	0.36	22.909	7.38	239.883	0	2511.886	0
2.512	0.44	26.303	6.68	275.423	0	2884.032	0
2.884	0.55	30.2	5.79	316.228	0	3311.311	0
3.311	0.7	34.674	4.79	363.078	0	3801.894	0
3.802	0.94	39.811	3.75	416.869	0	4365.158	0
4.365	1.27	45.709	2.77	478.63	0	5011.872	0
5.012	1.73	52.481	1.91	549.541	0	5754.399	0
5.754	2.33	60.256	1.2	630.957	0	6606.934	0
6.607	3.06	69.183	0.65	724.436	0	7585.776	0
7.586	3.9	79.433	0.3	831.764	0	8709.636	0
8.71	4.81	91.201	0.03	954.993	0	10000	0
10	5.73	104.713	0	1096.478	0		

PSD data at 0.2M of ionic strength

Size (µm)	Vol Under %	Size (µm)	Vol Under %	Size (µm)	Vol Under %	Size (µm)	Vol Under %
1.096	0	11.482	2.48	120.226	1.03	1258.925	0
1.259	0	13.183	2.97	138.038	0.3	1445.44	0
1.445	0.01	15.136	3.55	158.489	0.04	1659.587	0
1.66	0.07	17.378	4.2	181.97	0	1905.461	0
1.905	0.09	19.953	4.95	208.93	0	2187.762	0
2.188	0.11	22.909	5.72	239.883	0	2511.886	0
2.512	0.15	26.303	6.48	275.423	0	2884.032	0
2.884	0.2	30.2	7.16	316.228	0	3311.311	0
3.311	0.28	34.674	7.64	363.078	0	3801.894	0
3.802	0.38	39.811	7.85	416.869	0	4365.158	0
4.365	0.51	45.709	7.75	478.63	0	5011.872	0
5.012	0.68	52.481	7.27	549.541	0	5754.399	0
5.754	0.88	60.256	6.48	630.957	0	6606.934	0
6.607	1.12	69.183	5.41	724.436	0	7585.776	0
7.586	1.38	79.433	4.21	831.764	0	8709.636	0
8.71	1.7	91.201	2.99	954.993	0	10000	0
10	2.06	104.713	1.9	1096.478	0		

PSD data at 1M of ionic strength

Size (µm)	Vol Under %	Size (µm)	Vol Under %	Size (µm)	Vol Under %	Size (µm)	Vol Under %
1.096	0	11.482	1.15	120.226	4.36	1258.925	0
1.259	0	13.183	1.32	138.038	2.83	1445.44	0
1.445	0	15.136	1.52	158.489	1.57	1659.587	0
1.66	0	17.378	1.78	181.97	0.51	1905.461	0
1.905	0	19.953	2.15	208.93	0	2187.762	0
2.188	0	22.909	2.7	239.883	0	2511.886	0
2.512	0	26.303	3.42	275.423	0	2884.032	0
2.884	0.05	30.2	4.36	316.228	0	3311.311	0
3.311	0.09	34.674	5.46	363.078	0	3801.894	0
3.802	0.12	39.811	6.63	416.869	0	4365.158	0
4.365	0.18	45.709	7.74	478.63	0	5011.872	0
5.012	0.26	52.481	8.6	549.541	0	5754.399	0
5.754	0.37	60.256	9.08	630.957	0	6606.934	0
6.607	0.5	69.183	9.03	724.436	0	7585.776	0
7.586	0.66	79.433	8.45	831.764	0	8709.636	0
8.71	0.82	91.201	7.37	954.993	0	10000	0
10	0.98	104.713	5.94	1096.478	0		

Experimental data of settling tests (Effects of ionic strength)

	h				h/h0			
time, min	1M	0.2M	0.1M	0.01M	1M	0.2M	0.1M	0.01M
0	500	500	500	500	1	1	1	1
0.15	490	500	500	500	1	1	1	1
0.5	460	480	500	500	0.96	1	1	1
1	400	430	500	500	0.86	1	1	1
2	90	100	400	500	0.2	0.8	0.8	1
3	25	30	240	500	0.06	0.48	0.48	1
5	18	25	30	500	0.05	0.06	0.06	1
8	14	20	25	500	0.04	0.05	0.05	1
10	14	16	20	500	0.032	0.04	0.04	1
20	14	16	20	500	0.032	0.04	0.04	1

C2. 5 Effects of stirring speed

Experimental conditions: [Cu_T] = 300mg/L, [Cu_T]:[CN^-]:[Gly]=1:1:3, pH = 10.5, room temperature, [HS^-] = 5M, [HS^-]:[Cu_T] = 1.3:1, Ca^{2+} dosage = 0.5mM, reaction time =5min.

Stirring speed, rpm	200	350	700
Specific Surface Area, m2/g:	0.0751	0.0645	0.0962
Surface Weighted Mean D[3,2], µm	29.596	34.443	23.103
Vol. Weighted Mean D[4,3], µm	44.34	52	32.206
d10, µm	16.312	19.404	14.051
d50, µm	39.226	47.24	29.458
d80, µm	63.712	74.331	44.917

PSD data at 200 rpm of stirring speed (Same as the PSD data at 0.5mM Ca^{2+})

PSD data at 350 rpm of stirring speed

Size (µm)	**Vol Under %**	**Size (µm)**	**Vol Under %**	**Size (µm)**	**Vol Under %**	**Size (µm)**	**Vol Under %**
1.096	0	11.482	0.89	120.226	3.05	1258.925	0
1.259	0	13.183	1.07	138.038	1.73	1445.44	0
1.445	0	15.136	1.36	158.489	0.6	1659.587	0
1.66	0	17.378	1.78	181.97	0.09	1905.461	0
1.905	0	19.953	2.41	208.93	0	2187.762	0
2.188	0	22.909	3.24	239.883	0	2511.886	0
2.512	0	26.303	4.33	275.423	0	2884.032	0
2.884	0	30.2	5.57	316.228	0	3311.311	0
3.311	0	34.674	6.89	363.078	0	3801.894	0
3.802	0.06	39.811	8.1	416.869	0	4365.158	0
4.365	0.14	45.709	9.06	478.63	0	5011.872	0
5.012	0.22	52.481	9.58	549.541	0	5754.399	0
5.754	0.3	60.256	9.54	630.957	0	6606.934	0
6.607	0.41	69.183	8.92	724.436	0	7585.776	0
7.586	0.52	79.433	7.8	831.764	0	8709.636	0
8.71	0.64	91.201	6.29	954.993	0	10000	0
10	0.75	104.713	4.66	1096.478	0		

PSD data at 700 rpm of stirring speed

Size (µm)	**Vol Under %**	**Size (µm)**	**Vol Under %**	**Size (µm)**	**Vol Under %**	**Size (µm)**	**Vol Under %**
1.096	0	11.482	1.63	120.226	0	1258.925	0
1.259	0	13.183	2.5	138.038	0	1445.44	0
1.445	0	15.136	3.69	158.489	0	1659.587	0
1.66	0	17.378	5.11	181.97	0	1905.461	0
1.905	0	19.953	6.69	208.93	0	2187.762	0
2.188	0	22.909	8.2	239.883	0	2511.886	0
2.512	0.08	26.303	9.47	275.423	0	2884.032	0

2.884	0.13	30.2	10.26	316.228	0	3311.311	0
3.311	0.2	34.674	10.44	363.078	0	3801.894	0
3.802	0.26	39.811	9.92	416.869	0	4365.158	0
4.365	0.31	45.709	8.79	478.63	0	5011.872	0
5.012	0.35	52.481	7.19	549.541	0	5754.399	0
5.754	0.38	60.256	5.36	630.957	0	6606.934	0
6.607	0.42	69.183	3.56	724.436	0	7585.776	0
7.586	0.49	79.433	1.99	831.764	0	8709.636	0
8.71	0.68	91.201	0.79	954.993	0	10000	0
10	1.03	104.713	0.08	1096.478	0		

Experimental data of settling tests (Effects of supersaturation)

	h			**h/h0**		
time, min	**200 rpm**	**350 rpm**	**700 rpm**	**200 rpm**	**350 rpm**	**700 rpm**
0	500	500	500	1	1	1
0.15	500	490	500	1	0.98	1
0.5	495	485	500	0.99	0.97	1
1	480	475	495	0.96	0.95	0.99
2	350	300	485	0.7	0.6	0.97
3	30	30	340	0.06	0.06	0.68
5	20	25	30	0.04	0.05	0.06
8	18	20	22	0.036	0.04	0.044
10	16	20	20	0.032	0.04	0.04
20	15	20	15	0.03	0.04	0.03

C2.6 Effects of sulfide addition rate

Experimental conditions: [Cu_T] = 300mg/L, [CuT]:[CN^-]:[Gly]=1:1:3, pH = 10.5, room temperature, [HS^-] = 0.25M, [HS]:[Cu_T] = 1.3:1, Ca^{2+} dosage = 0.5mM, reaction time =5min, stirring speed =350 rpm.

Sulfide addition rate, ml/min	Batch test	2	20
Specific Surface Area, m2/g:	0.0645	0.155	0.0902
Surface Weighted Mean D[3,2], μm	34.443	14.351	24.633
Vol. Weighted Mean D[4,3], μm	52	19.3	36.292
d10, μm	19.404	8.599	13.8
d50, μm	47.24	17.394	32.442
d80, μm	74.331	26.792	51.865

PSD data for batch test

Size (μm)	**Vol Under %**	**Size (μm)**	**Vol Under %**	**Size (μm)**	**Vol Under %**	**Size (μm)**	**Vol Under %**

1.096	0	11.482	0.89	120.226	3.05	1258.925	0
1.259	0	13.183	1.07	138.038	1.73	1445.44	0
1.445	0	15.136	1.36	158.489	0.6	1659.587	0
1.66	0	17.378	1.78	181.97	0.09	1905.461	0
1.905	0	19.953	2.41	208.93	0	2187.762	0
2.188	0	22.909	3.24	239.883	0	2511.886	0
2.512	0	26.303	4.33	275.423	0	2884.032	0
2.884	0	30.2	5.57	316.228	0	3311.311	0
3.311	0	34.674	6.89	363.078	0	3801.894	0
3.802	0.06	39.811	8.1	416.869	0	4365.158	0
4.365	0.14	45.709	9.06	478.63	0	5011.872	0
5.012	0.22	52.481	9.58	549.541	0	5754.399	0
5.754	0.3	60.256	9.54	630.957	0	6606.934	0
6.607	0.41	69.183	8.92	724.436	0	7585.776	0
7.586	0.52	79.433	7.8	831.764	0	8709.636	0
8.71	0.64	91.201	6.29	954.993	0	10000	0
10	0.75	104.713	4.66	1096.478	0		

PSD data at 2ml/min adding rate

Size (µm)	**Vol Under %**	**Size (µm)**	**Vol Under %**	**Size (µm)**	**Vol Under %**	**Size (µm)**	**Vol Under %**
1.096	0	11.482	6.71	120.226	0	1258.925	0
1.259	0	13.183	8.16	138.038	0	1445.44	0
1.445	0.01	15.136	9.38	158.489	0	1659.587	0
1.66	0.1	17.378	10.12	181.97	0	1905.461	0
1.905	0.13	19.953	10.3	208.93	0	2187.762	0
2.188	0.15	22.909	9.86	239.883	0	2511.886	0
2.512	0.16	26.303	8.83	275.423	0	2884.032	0
2.884	0.15	30.2	7.37	316.228	0	3311.311	0
3.311	0.15	34.674	5.68	363.078	0	3801.894	0
3.802	0.17	39.811	3.97	416.869	0	4365.158	0
4.365	0.26	45.709	2.44	478.63	0	5011.872	0
5.012	0.48	52.481	1.22	549.541	0	5754.399	0
5.754	0.88	60.256	0.39	630.957	0	6606.934	0
6.607	1.55	69.183	0.01	724.436	0	7585.776	0
7.586	2.49	79.433	0	831.764	0	8709.636	0
8.71	3.73	91.201	0	954.993	0	10000	0
10	5.15	104.713	0	1096.478	0		

PSD data at 20ml/min adding rate

Size (µm)	**Vol Under %**	**Size (µm)**	**Vol Under %**	**Size (µm)**	**Vol Under %**	**Size (µm)**	**Vol Under %**
1.096	0	11.482	1.75	120.226	0.33	1258.925	0
1.259	0	13.183	2.4	138.038	0.04	1445.44	0

1.445	0	15.136	3.26	158.489	0	1659.587	0
1.66	0	17.378	4.29	181.97	0	1905.461	0
1.905	0	19.953	5.46	208.93	0	2187.762	0
2.188	0	22.909	6.68	239.883	0	2511.886	0
2.512	0	26.303	7.81	275.423	0	2884.032	0
2.884	0.07	30.2	8.72	316.228	0	3311.311	0
3.311	0.13	34.674	9.25	363.078	0	3801.894	0
3.802	0.18	39.811	9.32	416.869	0	4365.158	0
4.365	0.26	45.709	8.87	478.63	0	5011.872	0
5.012	0.33	52.481	7.95	549.541	0	5754.399	0
5.754	0.43	60.256	6.67	630.957	0	6606.934	0
6.607	0.55	69.183	5.16	724.436	0	7585.776	0
7.586	0.71	79.433	3.67	831.764	0	8709.636	0
8.71	0.95	91.201	2.28	954.993	0	10000	0
10	1.26	104.713	1.22	1096.478	0		

Experimental data of settling tests (Effects of sulfide addition)

	h			**h/h0**		
time, min	Batch test	2 mil/min	20 ml/min	Batch test	2 mil/min	20 ml/min
0	500	500	500	1	1	1
0.15	485	500	490	0.97	1	0.98
0.5	470	500	470	0.94	1	0.94
1	450	500	460	0.9	1	0.92
2	300	480	320	0.6	0.96	0.64
3	30	350	45	0.06	0.7	0.09
5	20	35	30	0.04	0.07	0.06
8	18	30	20	0.036	0.06	0.04
10	15	20	20	0.03	0.04	0.04
20	15	20	15	0.03	0.04	0.03

C2. 7 Effects of aging time

Experimental conditions: [Cu_T] = 300mg/L, [Cu_T]:[CN^-]:[Gly]=1:1:3, [HS^-] = 5M , pH = 10.5, room temperature, Ca^{2+} dosage = 0.5mM, [HS]:[Cu_T] = 1.3:1, reaction time =5min, stirring speed =350 rpm.

Aging time, h	0	2	24
Specific Surface Area, m2/g:	0.0751	0.067	0.0645
Surface Weighted Mean D[3,2], µm	29.596	33.167	34.453
Vol. Weighted Mean D[4,3], µm	44.34	56.089	55.048
d10, µm	16.312	16.984	18.35
d50, µm	39.226	49.809	47.63
d80, µm	63.712	82.659	80.069

PSD data without aging (Same as the PSD data at 0.5mM Ca^{2+})

PSD data at 2h of aging

Size (µm)	Vol Under %	Size (µm)	Vol Under %	Size (µm)	Vol Under %	Size (µm)	Vol Under %
1.096	0	11.482	1.2	120.226	4.19	1258.925	0
1.259	0	13.183	1.43	138.038	2.85	1445.44	0
1.445	0	15.136	1.73	158.489	1.68	1659.587	0
1.66	0	17.378	2.09	181.97	0.78	1905.461	0
1.905	0	19.953	2.56	208.93	0.17	2187.762	0
2.188	0	22.909	3.16	239.883	0	2511.886	0
2.512	0	26.303	3.91	275.423	0	2884.032	0
2.884	0.05	30.2	4.79	316.228	0	3311.311	0
3.311	0.09	34.674	5.77	363.078	0	3801.894	0
3.802	0.12	39.811	6.74	416.869	0	4365.158	0
4.365	0.17	45.709	7.61	478.63	0	5011.872	0
5.012	0.25	52.481	8.25	549.541	0	5754.399	0
5.754	0.35	60.256	8.54	630.957	0	6606.934	0
6.607	0.48	69.183	8.39	724.436	0	7585.776	0
7.586	0.63	79.433	7.82	831.764	0	8709.636	0
8.71	0.8	91.201	6.83	954.993	0	10000	0
10	0.99	104.713	5.58	1096.478	0		

PSD data at 24h of aging

Size (µm)	Vol Under %	Size (µm)	Vol Under %	Size (µm)	Vol Under %	Size (µm)	Vol Under %
1.096	0	11.482	0.99	120.226	3.75	1258.925	0
1.259	0	13.183	1.29	138.038	2.59	1445.44	0
1.445	0	15.136	1.71	158.489	1.59	1659.587	0
1.66	0	17.378	2.21	181.97	0.85	1905.461	0
1.905	0	19.953	2.88	208.93	0.33	2187.762	0
2.188	0	22.909	3.66	239.883	0.06	2511.886	0
2.512	0	26.303	4.57	275.423	0	2884.032	0
2.884	0	30.2	5.53	316.228	0	3311.311	0
3.311	0.04	34.674	6.51	363.078	0	3801.894	0
3.802	0.08	39.811	7.38	416.869	0	4365.158	0
4.365	0.12	45.709	8.04	478.63	0	5011.872	0
5.012	0.17	52.481	8.41	549.541	0	5754.399	0
5.754	0.23	60.256	8.41	630.957	0	6606.934	0
6.607	0.33	69.183	8.01	724.436	0	7585.776	0
7.586	0.44	79.433	7.26	831.764	0	8709.636	0
8.71	0.58	91.201	6.22	954.993	0	10000	0
10	0.76	104.713	5	1096.478	0		

C2. 8 4 Effects of temperature

Experimental conditions: [CuT] = 300mg/L, [CuT]:[CN-]:[Gly]=1:1:3, [HS-] = 5M, pH = 10.5, room temperature, Ca2+ dosage = 0.5mM, [HS]:[CuT] = 1.3:1, reaction time =5min, no aging, stirring speed =350 rpm.

Temperature, ℃	Room temperature	55
Specific Surface Area, m2/g:	0.0751	0.067
Surface Weighted Mean D[3,2], μm	29.596	33.167
Vol. Weighted Mean D[4,3], μm	44.34	56.089
d10, μm	16.312	16.984
d50, μm	39.226	49.809
d80, μm	63.712	82.659

PSD data at room temperature (Same as the PSD data obtained from the batch test)

PSD data at 55 ℃

Size (μm)	**Vol Under %**	**Size (μm)**	**Vol Under %**	**Size (μm)**	**Vol Under %**	**Size (μm)**	**Vol Under %**
1.096	0	11.482	0.94	120.226	2.14	1258.925	0
1.259	0	13.183	1.27	138.038	1.14	1445.44	0
1.445	0	15.136	1.74	158.489	0.38	1659.587	0
1.66	0	17.378	2.4	181.97	0.05	1905.461	0
1.905	0	19.953	3.27	208.93	0	2187.762	0
2.188	0	22.909	4.34	239.883	0	2511.886	0
2.512	0	26.303	5.56	275.423	0	2884.032	0
2.884	0	30.2	6.82	316.228	0	3311.311	0
3.311	0.05	34.674	7.96	363.078	0	3801.894	0
3.802	0.11	39.811	8.86	416.869	0	4365.158	0
4.365	0.16	45.709	9.35	478.63	0	5011.872	0
5.012	0.23	52.481	9.33	549.541	0	5754.399	0
5.754	0.31	60.256	8.8	630.957	0	6606.934	0
6.607	0.39	69.183	7.78	724.436	0	7585.776	0
7.586	0.47	79.433	6.44	831.764	0	8709.636	0
8.71	0.59	91.201	4.93	954.993	0	10000	0
10	0.74	104.713	3.45	1096.478	0		

C2.9 Effects of seeding

Experimental conditions: [Cu_T] = 300mg/L, [Cu_T]:[CN^-]:[Gly]=1:1:3, [HS^-] = 5M , pH = 10.5, room temperature, Ca^{2+} dosage = 0.5mM, [HS]:[Cu_T] = 1.3:1, reaction time =5min, stirring speed =350 rpm.

Seed addition, g/L	Original seed material	1	5
Specific Surface Area, m2/g:	0.0786	0.0752	0.0767
Surface Weighted Mean D[3,2], μm	28.255	29.553	28.965
Vol. Weighted Mean D[4,3], μm	47.681	43.409	43.118

d10, µm	15.053	16.83	16.03
d50, µm	39.964	38.867	38.603
d80, µm	70.1	61.732	61.833

PSD data for the seed material

Size (µm)	**Vol Under %**	**Size (µm)**	**Vol Under %**	**Size (µm)**	**Vol Under %**	**Size (µm)**	**Vol Under %**
1.096	0	11.482	1.46	120.226	2.69	1258.925	0
1.259	0	13.183	1.96	138.038	1.79	1445.44	0
1.445	0	15.136	2.59	158.489	1.05	1659.587	0
1.66	0	17.378	3.3	181.97	0.55	1905.461	0
1.905	0	19.953	4.12	208.93	0.2	2187.762	0
2.188	0.06	22.909	4.97	239.883	0	2511.886	0
2.512	0.08	26.303	5.82	275.423	0	2884.032	0
2.884	0.1	30.2	6.58	316.228	0	3311.311	0
3.311	0.13	34.674	7.22	363.078	0	3801.894	0
3.802	0.16	39.811	7.65	416.869	0	4365.158	0
4.365	0.2	45.709	7.84	478.63	0	5011.872	0
5.012	0.25	52.481	7.75	549.541	0	5754.399	0
5.754	0.32	60.256	7.35	630.957	0	6606.934	0
6.607	0.42	69.183	6.68	724.436	0	7585.776	0
7.586	0.56	79.433	5.81	831.764	0	8709.636	0
8.71	0.77	91.201	4.79	954.993	0	10000	0
10	1.06	104.713	3.72	1096.478	0		

PSD data at 1g/L seed addition

Size (µm)	**Vol Under %**	**Size (µm)**	**Vol Under %**	**Size (µm)**	**Vol Under %**	**Size (µm)**	**Vol Under %**
1.096	0	11.482	1.07	120.226	1.43	1258.925	0
1.259	0	13.183	1.48	138.038	0.58	1445.44	0
1.445	0	15.136	2.09	158.489	0.08	1659.587	0
1.66	0	17.378	2.88	181.97	0	1905.461	0
1.905	0	19.953	3.91	208.93	0	2187.762	0
2.188	0	22.909	5.09	239.883	0	2511.886	0
2.512	0	26.303	6.37	275.423	0	2884.032	0
2.884	0	30.2	7.59	316.228	0	3311.311	0
3.311	0.07	34.674	8.63	363.078	0	3801.894	0
3.802	0.13	39.811	9.3	416.869	0	4365.158	0
4.365	0.19	45.709	9.51	478.63	0	5011.872	0
5.012	0.25	52.481	9.18	549.541	0	5754.399	0
5.754	0.31	60.256	8.33	630.957	0	6606.934	0
6.607	0.4	69.183	7.07	724.436	0	7585.776	0
7.586	0.49	79.433	5.57	831.764	0	8709.636	0
8.71	0.6	91.201	4.02	954.993	0	10000	0
10	0.79	104.713	2.59	1096.478	0		

PSD data at 5g/L seed addition

Size (µm)	Vol Under %	Size (µm)	Vol Under %	Size (µm)	Vol Under %	Size (µm)	Vol Under %
1.096	0	11.482	1.26	120.226	1.48	1258.925	0
1.259	0	13.183	1.7	138.038	0.49	1445.44	0
1.445	0	15.136	2.28	158.489	0.09	1659.587	0
1.66	0	17.378	3.04	181.97	0	1905.461	0
1.905	0	19.953	3.99	208.93	0	2187.762	0
2.188	0	22.909	5.09	239.883	0	2511.886	0
2.512	0	26.303	6.26	275.423	0	2884.032	0
2.884	0	30.2	7.4	316.228	0	3311.311	0
3.311	0.06	34.674	8.39	363.078	0	3801.894	0
3.802	0.12	39.811	9.04	416.869	0	4365.158	0
4.365	0.17	45.709	9.28	478.63	0	5011.872	0
5.012	0.24	52.481	9.01	549.541	0	5754.399	0
5.754	0.33	60.256	8.24	630.957	0	6606.934	0
6.607	0.44	69.183	7.05	724.436	0	7585.776	0
7.586	0.56	79.433	5.61	831.764	0	8709.636	0
8.71	0.73	91.201	4.07	954.993	0	10000	0
10	0.95	104.713	2.63	1096.478	0		

Appendix C3 - Cu adsorption behaviours using resin

C3.1 Adsorption behaviour of different types of chelating resins

Experimental conditions: [Cu_T] = 300 mg/L, [Au]=2 mg/L, [Cu_T]:[CN^-]:[Gly]=1:1:3, pH = 10.5, resin dosage = 7.5 g/L, room temperature.

Resin type	Time, h	Cu_T, mg/L	Cu^{2+}, mg/L	Au, mg/L	Cu_T recovery, %	Cu^{2+} recovery, %	Au recovery, %
Puromet MTS9300	0	308.0	223	2.169	0.00	0.00	0.00
	0.5	186.0	91	2.164	39.61	59.19	0.23
	1	149.0	59	2.152	51.62	73.54	0.78
	2	125.0	32	2.142	59.42	85.65	1.24
	4	108.0	19	2.158	64.94	91.48	0.51
	6	99.5	9	2.156	67.69	95.96	0.60
	24	91.0	2	2.162	70.45	99.10	0.32
Puromet MTS9600	0	294.1	218	2.177	0.00	0.00	0.00
	0.5	228.0	182	0.858	22.48	16.51	60.59
	1	226.7	168	0.629	22.92	22.94	71.11
	2	187.9	150	0.407	36.11	31.19	81.30
	4	137.9	132	0.258	53.11	39.45	88.15
	6	122.8	122	0.214	58.25	44.04	90.17
	24	100.5	109	0.02	65.83	50.00	99.08
	0	300.3	228	2.007	0.00	0.00	0.00

Puromet MTS9850	0.5	119.3	137	1.355	60.26	39.91	32.49
	1	115.3	104	0.966	61.60	54.39	51.87
	2	56.8	55	0.72	81.07	75.88	64.13
	4	34.9	30	0.606	88.38	86.84	69.81
	6	33.8	25	0.588	88.75	89.04	70.70
	24	18.0	15	0.678	94.00	93.42	66.22

C3. 2 Effects of $[CN^-]$: $[Cu_T]$ molar ratio

Experimental conditions: $[Cu_T]$ = 300 mg/L, [Au]=2 mg/L, $[Cu_T]$:[Gly]=1:3, pH = 10.5, resin dosage = 7.5 g/L, room temperature.

[CN]:[Cu_T]	**Time, h**	**Cu_T, mg/L**	**Cu^{2+}, mg/L**	**Au, mg/L**	**Cu_T recovery, %**	**Cu^{2+} recovery, %**	**Au recovery, %**
0.1:1	0	300.0	294	2.07	0.00	0.00	0.00
	0.5	136.0	136	2.05	55.57	54.67	0.97
	1	96.3	94	2.04	69.18	69.31	1.45
	2	60.1	57	2.03	81.17	81.78	1.93
	4	33.2	26	2.05	89.82	91.86	0.97
	6	23.0	16	2.04	93.10	95.10	1.45
	24	11.7	3	2.04	96.57	99.10	1.45
1:1	0	308.0	223	2.17	0.00	0.00	0.00
	0.5	186.0	91	2.16	40.82	73.51	0.46
	1	153.0	59	2.15	52.31	85.30	0.92
	2	125.0	32	2.14	61.85	93.23	1.38
	4	108.0	19	2.15	67.74	96.68	0.92
	6	99.5	9	2.15	70.93	96.76	0.92
	24	91.0	2	2.15	74.00	99.21	0.92
2:1	0	287.0	111	2.19	0.00	0.00	0.00
	0.5	200.0	30	2.19	31.71	60.01	0.00
	1	196.0	17	2.17	34.44	74.60	0.91
	2	182.0	8	2.18	40.39	86.51	0.46
	4	171.0	4	2.16	45.18	92.16	1.37
	6	170.0	4	2.16	46.69	96.37	1.37
	24	169.0	1	2.16	48.18	99.21	1.37

C3. 3 Effects of [Gly]: [Cu_T] molar ratio

Experimental conditions: [Cu_T] = 300 mg/L, [Au]=2 mg/L, [Cu_T]:[CN^-]=1:1, pH = 10.5, resin dosage = 7.5g/L, room temperature.

[Gly]:[Cu_T]	Time, h	Cu_T, mg/L	Cu^{2+}, mg/L	Au, mg/L	Cu_T recovery, %	Cu^{2+} recovery, %	Au recovery, %
1.5:1	0	301.5	186	2.18	0.00	0.00	0.00
	0.5	177.1	62	2.16	41.26	66.67	0.46
	1	153.0	36	2.15	49.26	80.65	0.92
	2	128.3	21	2.14	57.47	88.71	1.38
	4	111.3	8	2.15	63.10	95.70	0.92
	6	107.5	5	2.15	64.35	97.31	0.92
	24	96.4	2	2.16	68.04	98.92	0.46
3:1	0	308.0	223	2.07	0.00	0.00	0.00
	0.5	186.0	91	2.05	40.82	61.56	0.74
	1	153.0	59	2.04	52.31	75.59	1.11
	2	125.0	32	2.03	61.85	87.03	1.48
	4	108.0	19	2.05	67.74	92.47	0.74
	6	99.5	9	2.04	70.93	96.51	1.11
	24	91.0	2	2.04	74.00	99.24	1.11
6:1	0	308.0	232	2.10	0.00	0.00	0.00
	0.5	178.0	98	2.08	43.36	58.60	1.16
	1	158.0	69	2.08	50.75	71.45	1.16
	2	127.0	38	2.03	61.24	84.60	3.16
	4	110.0	19	1.99	67.14	92.47	5.16
	6	97.5	12	2.05	71.51	95.34	2.36
	24	87.5	4	2.08	75.00	98.48	1.16
10:1	0	308.0	244	2.08	0.00	0.00	0.00
	0.5	190.0	108	2.03	39.55	54.38	2.24
	1	170.0	75	2.01	47.01	68.97	3.45
	2	130.0	44	2.04	60.32	82.17	1.84
	4	112.0	24	1.99	66.55	90.48	4.25
	6	97.5	15	2.02	71.51	94.18	3.04
	24	89.5	6	2.03	74.43	97.72	2.24

C3.4 Resin dosage and Cu^{2+} concentration

Experimental conditions: $[Cu_T]:[CN^-]:[Gly]=1:1:3$, [Au]=2 mg/L, pH = 10.5, room temperature.

Cu^{2+} concentration mg/L	**Resin dosage, g/L**	**Resin:Cu**	**Cu^{2+}, mg/L**	**Cu^{2+} recovery, %**	**Qe, mg/g**
220	0.50	2.25	173	21.72	96.97
	1.49	6.75	91	58.82	87.54
	2.97	13.50	26	88.24	65.66
	4.50	20.45	7	96.83	47.56
	7.50	33.75	3	98.64	29.36
	10.80	49.09	0	100.00	20.46
760	1.65	2.25	589	22.50	99.09
	4.95	6.75	270	64.47	94.65
	9.90	13.50	31	95.92	70.40
	15.00	20.45	8	98.95	47.93
	24.75	33.75	1	99.87	29.32
	36.00	49.09	0	100.00	21.32

C3.5 Equilibrium adsorption isotherms at different $[CN^-]:[Cu_T]$ molar ratios

Experimental conditions: $[Cu_T]$ = 300 mg/L, [Au]=2 mg/L, pH = 10.5, resin dosage = 0.5 – 7.5 g/L, room temperature.

					Freundlich parameters			**Langmuir parameters**		
$[CN^-]:[Cu_T]$	**Resin, g**	**Resin, g/L**	**Cu^{2+}, mg/L**	**Qe, mg/L**	**Log Q**	**Log C**	**Qe (F)**	**1/Q**	**1/C**	**Qe (L)**
0.1:1	0.00	0.00	268.00	0.00	0.00	0.00	0.00	0.00	0.00	0.00
	0.12	0.50	219.00	98.99	2.00	2.34	0.01	0.00	105.77	97.78
	0.37	1.49	126.00	95.62	1.98	2.10	0.01	0.01	92.34	95.53
	0.74	2.97	43.00	75.76	1.88	1.63	0.01	0.02	70.89	86.47
	1.13	4.50	11.00	57.11	1.76	1.04	0.02	0.09	50.71	60.94
	1.86	7.50	4.00	35.56	1.55	0.60	0.03	0.25	39.54	35.97
1:1	0.00	0.00	220.00	0.00	0.00	0.00	0.00	0.00	0.00	0.00
	0.12	0.50	173.00	94.95	1.98	2.24	0.01	0.01	99.82	92.57
	0.37	1.49	91.00	86.87	1.94	1.96	0.01	0.01	85.24	89.56
	0.74	2.97	26.00	65.32	1.82	1.41	0.02	0.04	62.65	76.45
	1.13	4.50	7.00	47.33	1.68	0.85	0.02	0.14	45.38	49.12
	1.86	7.50	3.00	29.23	1.47	0.48	0.03	0.33	36.84	29.73
2:1	0.00	0.00	113.00	0.00	0.00	0.00	0.00	0.00	0.00	0.00
	0.12	0.50	71.00	84.85	1.93	1.85	0.01	0.01	80.19	82.91
	0.37	1.49	24.00	59.93	1.78	1.38	0.02	0.04	61.43	73.78
	0.74	2.97	3.00	37.04	1.57	0.48	0.03	0.33	36.84	34.09
	1.13	4.50	2.00	24.67	1.39	0.30	0.04	0.50	33.35	26.08
	1.86	7.50	1.00	15.08	1.18	0.00	0.07	1.00	28.13	15.29

C3.6 Pseudo-first-order and pseudo-second-order models

Experimental conditions: [Cu_T] = 300 mg/L, [Au]=2 mg/L, pH = 10.5, resin dosage = 7.5 g/L, room temperature.

				Psuedo-first-order		**Psuedo-second-order**	
[CN^-]:[Cu_T]	**Time, h**	**Cu^{2+}, mg/L**	**Qt, mg/g**	**log Qe - Qt**	**Qt, mg/g (1st)**	**t/Qt**	**Qt, mg/g (2nd)**
0.1:1	0	294	0.00	1.60	0.00	0.00	0.00
	0.5	136	21.28	1.26	2.73	0.02	20.99
	1	90	27.47	1.08	5.27	0.04	27.33
	2	57	31.92	0.89	9.83	0.06	32.21
	4	26	36.09	0.54	17.19	0.11	35.36
	6	16	37.44	0.33	22.71	0.16	36.55
	24	3	39.19	-0.39	37.97	0.61	38.49
1:1	0	223	0.00	1.17	0.00	0.00	0.00
	0.5	91	17.78	0.61	0.89	0.05	11.15
	1	59	22.09	0.36	1.73	0.08	12.72
	2	32	25.72	0.21	3.25	0.15	13.69
	4	19	27.47	-0.09	5.79	0.28	14.23
	6	9	28.82	-0.27	7.77	0.42	14.42
	24	2	29.76	-0.87	14.05	1.62	14.71
2:1	0	111	0.00	1.48	0.00	0.00	0.00
	0.5	30	10.91	1.09	2.05	0.03	17.94
	1	17	12.66	0.90	3.96	0.05	22.39
	2	12	13.33	0.63	7.39	0.08	25.55
	4	6	14.14	0.41	12.95	0.15	27.50
	6	4	14.41	0.08	17.13	0.21	28.21
	24	1	14.81	-0.57	28.79	0.81	29.36

C3.7 Intra-particle diffusion models

Experimental conditions: [Cu_T] = 300 mg/L, [Au]=2 mg/L, pH = 10.5, resin dosage = 0.5 – 7.5 g/L, room temperature.

[CN]:[Cu_T]	**Time, h**	**$t^{1/2}$, $h^{1/2}$**	**Cu^{2+}, mg/L**	**Qt, mg/g**
0.1:1	0	0.00	294	0.00
	0.5	0.71	136	9.58
	1	1.00	94	12.12
	2	1.41	57	14.36
	4	2.00	26	16.24
	6	2.45	16	16.85
	24	4.90	3	17.64
1:1	0	0.00	223	0.00
	0.5	0.71	91	8.11
	1	1.00	59	10.08
	2	1.41	32	11.69
	4	2.00	19	12.46
	6	2.45	9	13.02

	24	4.90	2	13.41
2:1	0	0.00	111	0.00
	0.5	0.71	30	4.95
	1	1.00	17	5.74
	2	1.41	8	6.27
	4	2.00	4	6.50
	6	2.45	4	6.51
	24	4.90	1	6.67

C3.8 Eluent selection

No.	Conditions	Desorption efficiency, %
1	1M Gly, 1M NaOH	61.07
2	2M Gly, 2M NaOH	71.74
3	3M Gly, 3M NaOH	75.93
4	2M Gly, 2M NaCl, 2M NaOH	78.18
5	3M Gly, 3M NaCl, 3M NaOH	84.35
6	3M Gly, 2M NaCl, 2M NaOH	82.65
7	3M Gly, 3M NaCl, 2M NaOH	83.01
8	2M Gly, 3M NaCl, 2M NaOH, 55°C	73.86
9	3M Gly, 3M NaCl, 2M NaOH, 55°C	80.89
10	3M HCl	93.85
11	2M HCl	92.27
12	1M HCl	85.79

C3.9 Adsorption/desorption study

Adsorption conditions: 1500 mg/L Cu_T, $[Cu_T]:[CN^-]:[Gly]$ =1:1:3, pH =10, room temperature.

Cycle	1	2	3	4	5
Cu^{2+} at 0h, mg/L	1127	1180	1204	1236	1180
Cu^{+} at 0h, mg/L	373	320	296	264	320
Cu^{2+} at 24h, mg/L	386	473	505	525	488
Cu^{+} at 24h, mg/L	397	385	353	333	370
Cu on resin, mg	185.25	155.75	157.00	156.00	153.23
Adsorption Capacity, mg/g	99.77	84.30	85.41	85.29	84.20
Cu^{2+} recovery, %	65.75	59.92	58.06	57.52	58.64

Desorption condition: 100 ml solution containing 3M Gly, NaCl, 2M NaOH, room temperature

Cycle	1	2	3	4	5
dry weight	1.86	1.85	1.84	1.83	1.82
Cu^{2+} on resin, mg	185.25	187.00	186.00	186.00	185.00
Q, mg/g	99.77	101.22	101.18	101.69	101.65
Cu^{2+} at 2h, mg/L	1540.00	1580.00	1560.00	1542.33	1500.33
Desorption, %	83.13	84.49	83.87	82.92	81.10
Cu left on resin, mg	31.25	29.00	30.00	31.77	34.97
Cu left on the resin, mg/g	16.83	15.70	16.32	17.37	19.21

Appendix C4 - Au adsorption behaviours using resins

C4. 1 Resin screening (not presented in the published paper 4)

Experimental conditions: [Au] =6 mg/L, [CuT] = 1000 mg/L, [Cu_T]:[CN-]:[Gly]=1:1:3, pH =10.5, resin dosage = 6 g/L, room temperature.

Resin type	Time, h	Cu_T, mg/L	Cu^{2+}, mg/L	Au, mg/L	Cu_T recovery, %	Cu^{2+} recovery, %	Au recovery, %
Aurix 100	0	1000	782	5.61	0.00	0.00	0.00
	0.25	919	737	1.97	8.10	5.75	64.88
	0.5	904	739	1.38	9.60	5.50	75.40
	1	843	732	0.87	15.70	6.39	84.49
	2	814	730	0.55	15.70	6.65	90.20
	4	781	733	0.37	18.60	6.27	93.40
	6	804	745	0.301	21.90	4.73	94.63
	24	794	754	0.17	19.60	3.58	96.97
Minix	0	1040	753	5.68	0.00	0.00	0.00
	0.25	920	753	1.78	11.54	0.00	68.66
	0.5	876	753	1.22	15.77	0.00	78.52
	1	868	752	0.76	16.54	0.13	86.62
	2	861	752	0.52	17.21	0.13	90.85
	4	908	756	0.34	12.69	-0.40	94.01
	6	843	756	0.3	18.94	-0.40	94.72
	24	864	754	0.18	16.92	-0.13	96.83
S992	0	1070	742	5.71	0.00	0.00	0.00
	0.25	958	699	2.91	7.88	7.17	48.77
	0.5	949	686	2.53	8.75	8.90	55.46
	1	881	669	1.66	15.29	11.16	70.77
	2	806	645	1.04	22.50	14.34	81.69
	4	772	622	0.653	25.77	17.40	88.50
	6	747	619	0.507	28.17	17.80	91.07
	24	673	563	0.235	35.29	25.23	95.86
IXOS-AuC	0	1040	776	6.33	0.00	0.00	0.00
	0.25	1000	740	2.81	3.85	4.64	50.53
	0.5	970	739.00	2.45	6.73	4.77	56.87
	1	980	738.00	1.71	5.77	4.90	69.89

	2	970	740.00	1.12	6.73	4.64	80.28
	4	945	743.00	0.701	9.13	4.25	87.66
	6	948	757.00	0.551	8.85	2.45	90.30
	24	18	763.00	0.261	7.40	1.68	95.40

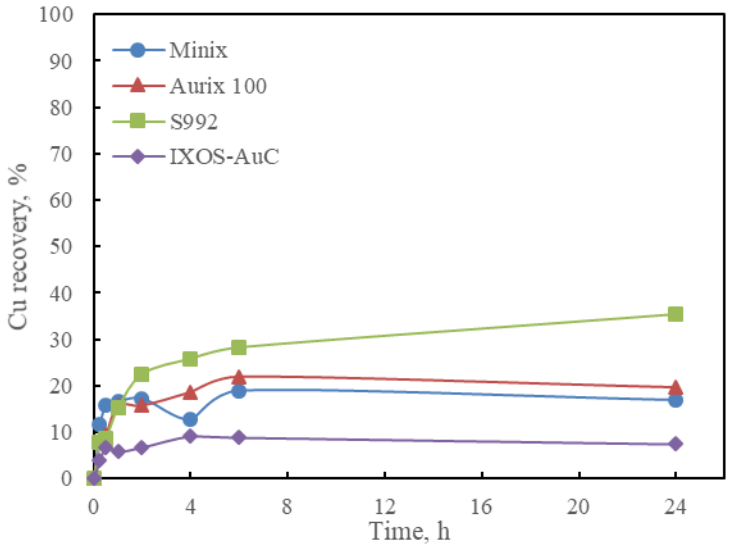

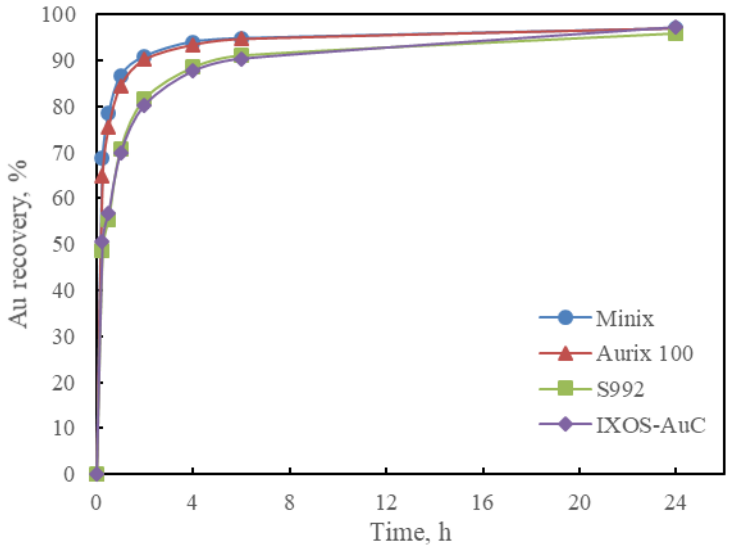

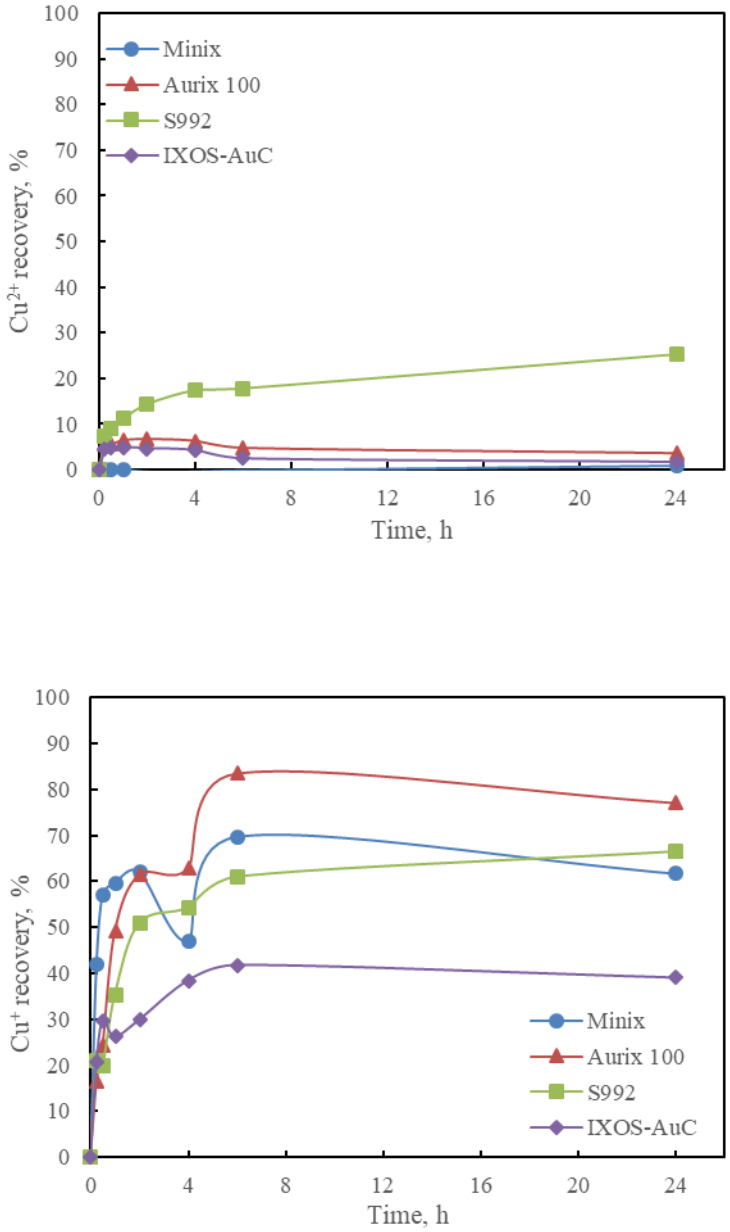

Figure C4.1 Au, Cu_T, Cu^{2+} and Cu^{+} recoveries as a function of time for different types of resins.

C4.2 Effect of $[CN^-]$:$[Cu_T]$

Experimental conditions: [Au] =6 mg/L, [CuT] = 1000 mg/L, [Gly]: $[Cu_T]$ =3:1, pH =10.5, resin dosage = 6 g/L, room temperature.

[CN]:[Cu_T]	**Time, h**	**Cu_T, mg/L**	**Cu^{2+}, mg/L**	**Au, mg/L**	**Cu_T recovery, %**	**Cu^{2+} recovery, %**	**Au recovery, %**
0.5:1	0	1060	949	6.38	0.00	0.00	0.00
	0.5	1000	946	1.28	5.66	0.32	80.34
	1	1040	952	0.695	1.89	-0.32	89.54
	2	1020	947	0.413	3.77	0.21	93.92
	4	997	950	0.265	5.94	-0.11	96.18

	6	984	952	0.204	7.17	-0.32	97.12
	24	983	937	0.11	7.26	1.26	98.48
1:1	0	1070	770	6.33	0.00	0.00	0.00
	0.5	978	760	1.73	8.60	1.15	73.22
	1	960	750	1.17	10.28	2.30	82.26
	2	978	743	0.662	8.60	3.10	90.17
	4	969	768	0.452	9.44	0.23	93.43
	6	963	765	0.366	10.00	0.57	94.80
	24	974	764	0.2	8.97	0.69	97.22
2:1	0	1050	482	6.47	0.00	0.00	0.00
	0.5	1010	484	1.28	3.81	-0.41	80.61
	1	975	481	0.884	7.14	0.21	86.88
	2	980	483	0.579	6.67	-0.21	91.59
	4	975	484	0.392	7.14	-0.41	94.43
	6	977	486	0.293	6.95	-0.83	95.92
	24	945	475	0.178	10.00	1.45	97.58

C4.3 Effect of [Gly]:[Cu_T]

Experimental conditions: [Au] =6 mg/L, [CuT] = 1000 mg/L, [Gly]: [Cu_T] =3:1, pH =10.5, resin dosage = 6 g/L, room temperature.

[Gly]:[Cu_T]	**Time, h**	**Cu_T, mg/L**	**Cu^{2+}, mg/L**	**Au, mg/L**	**Cu_T recovery, %**	**Cu^{2+} recovery, %**	**Au recovery, %**
2:1	0	1070	770	6.33	0.00	0.00	0.00
	0.5	1030	742	2.37	3.74	0.00	63.31
	1	1010	749	1.7	5.61	3.22	74.22
	2	948	750	1.11	11.40	2.41	83.52
	4	961	757	0.758	10.19	2.30	88.98
	6	960	765	0.54	10.28	1.49	92.32
	24	960	766	0.375	10.28	0.57	94.79
3:1	0	1070	770	6.33	0.00	0.00	0.00
	0.5	978	756	1.73	8.60	1.61	73.22
	1	960	745	1.17	10.28	2.87	82.26
	2	978	752	0.662	8.60	2.07	90.17
	4	969	758	0.452	9.44	1.38	93.43
	6	963	763	0.366	10.00	0.80	94.80
	24	974	764	0.2	8.97	0.69	97.22
6:1	0	1050	770	6.33	0.00	0.00	0.00
	0.5	990	742	1.22	5.71	3.22	81.11
	1	998	755	0.624	4.95	1.72	90.54
	2	989	752	0.379	5.81	2.07	94.37

	4	959	762	0.254	8.67	0.92	96.31
	6	985	761	0.196	6.19	1.03	97.21
	24	981	763	0.106	6.57	0.80	98.53

C4.4 Effect of initial gold concentration

Experimental conditions: [Cu_T] = 1000 mg/L, [Cu_T]:[CN^-]:[Gly]=1:1:3, pH =10.5, resin dosage = 6 g/L, room temperature.

Initial [Au], mg/L	**Time, h**	**Cu_T, mg/L**	**Cu^{2+}, mg/L**	**Au, mg/L**	**Cu_T recovery, %**	**Cu^{2+} recovery, %**	**Au recovery, %**
6	0	1070	776	6.33	0.00	0.00	0.00
	0.5	978	740	1.73	8.60	4.64	73.22
	1	960	745	1.17	10.28	3.99	82.26
	2	978	745	0.662	8.60	3.99	90.17
	4	969	757	0.452	9.44	2.45	93.43
	6	963	769	0.366	10.00	0.90	94.80
	24	974	770	0.2	8.97	0.77	97.22
12	0	1080	765	11.5	0.00	0.00	0.00
	0.5	1010	752	4.59	6.48	1.70	60.89
	1	1000	740	2.9	7.41	3.27	75.79
	2	1000	746	1.84	7.41	2.48	84.96
	4	1010	752	1.24	6.48	1.70	90.08
	6	1010	762	0.85	6.48	0.39	93.35
	24	1010	762	0.575	6.48	0.39	95.60
20	0	1060	772	20.5	0.00	0.00	0.00
	0.5	1050	765	8.81	0.94	0.91	57.88
	1	1010	760	6.13	4.72	1.55	71.29
	2	985	754	3.97	7.08	2.33	81.80
	4	987	763	2.61	6.89	1.17	88.29
	6	1020	768	1.81	3.77	0.52	92.05
	24	1040	766	1.11	1.89	0.78	95.24

C4.5 Equilibrium isotherm study

Experimental conditions: [Cu_T] = 1000 mg/L, [Cu_T]:[CN^-]:[Gly]=1:1:3, pH = 10.5, room temperature.

					Freundlich parameters			**Langmuir parameters**		
Initial [Au]	**Resin, g**	**Resin, g/L**	**Au, mg/L**	**Qe, mg/L**	**LogQ**	**LogC**	**Qe (F)**	**1/Q**	**1/C**	**Qe (L)**
6	0.00	0	6.33	0.00	0.00	0.00	0.00	0.00	0.00	0.00
	0.01	0	5.08	7.35	0.87	0.71	7.86	0.14	0.20	4.21
	0.11	1	1.37	3.62	0.56	0.14	3.33	0.28	0.73	3.17
	0.31	3	0.55	1.88	0.27	-0.26	1.83	0.53	1.82	2.10

	0.60	6	0.23	1.01	0.01	-0.64	1.03	0.99	4.37	1.18
	1.20	12	0.08	0.50	-0.30	-1.10	0.52	1.99	12.50	0.49
12	0.00	0	11.20	0.00	0.00	0.00	0.00	0.00	0.00	0.00
	0.01	0	9.43	14.16	1.15	0.97	14.06	0.07	0.11	7.88
	0.11	1	2.98	6.04	0.78	0.47	6.16	0.17	0.34	5.71
	0.32	3	1.06	3.01	0.48	0.03	2.93	0.33	0.94	3.30
	0.60	6	0.51	1.69	0.23	-0.30	1.72	0.59	1.98	1.92
	1.20	12	0.21	0.91	-0.04	-0.69	0.91	1.10	4.85	0.89
20	0.00	0	18.10	0.00	0.00	0.00	0.00	0.00	0.00	0.00
	0.01	0	15.80	15.03	1.18	1.20	14.61	0.07	0.06	8.95
	0.11	1	6.45	7.82	0.89	0.81	8.24	0.13	0.16	7.41
	0.31	3	2.26	4.31	0.63	0.35	4.22	0.23	0.44	4.82
	0.60	6	0.98	2.48	0.39	-0.01	2.47	0.40	1.02	2.83
	1.20	12	0.38	1.34	0.13	-0.43	1.34	0.75	2.67	1.30

C4.6 Kinetics study

Experimental conditions: [Cu_T] = 1000 mg/L, pH = 10.5, [Cu_T]:[CN^-]:[Gly]=1:1:3, resin dosage = 6 g/L, room temperature.

				Psuedo-first-order		**Psuedo-second-order**	
Initial [Au], mg/L	**Time, h**	**Au, mg/L**	**Qt, mg/g**	**log Qe - Qt**	**Qt, mg/g (1st)**	**t/Qt**	**Qt, mg/g (2nd)**
6	0	6.33	0.00	0.00	0.00	0.00	0.00
	0.5	1.73	0.81	-0.54	0.06	0.62	73.22
	1	1.17	0.91	-0.73	0.13	1.10	82.26
	2	0.662	1.00	-1.01	0.24	2.01	90.17
	4	0.452	1.03	-1.21	0.42	3.87	93.43
	6	0.366	1.05	-1.33	0.57	5.73	94.80
	24	0.2	1.08	-1.76	1.04	22.29	97.22
12	0	11.5	0.00	0.00	0.00	0.00	0.00
	0.5	4.59	1.39	-0.09	0.23	0.36	60.89
	1	2.9	1.74	-0.32	0.43	0.58	75.79
	2	1.84	1.95	-0.58	0.77	1.03	84.96
	4	1.24	2.07	-0.86	1.28	1.93	90.08
	6	0.85	2.15	-1.22	1.60	2.79	93.35
	24	0.575	2.20	-2.30	2.20	10.88	95.60
20	0	20.5	0.00	0.00	0.00	0.00	0.00
	0.5	8.81	2.39	0.20	0.53	0.21	57.88
	1	6.13	2.93	0.01	0.98	0.34	71.29

	2	3.97	3.37	-0.23	1.72	0.59	81.80
	4	2.61	3.65	-0.51	2.69	1.10	88.29
	6	1.81	3.82	-0.84	3.24	1.57	92.05
	24	1.11	3.96	-2.69	3.96	6.06	95.24

C4.7 Pre-elution of Cu

Experimental conditions: NaOH = 1.5g/L, pH : ~11.5, room temperature, Resin loadings: 14,790 g/t Cu, 2160 g/t Au, resin mass = 1.38g, 100 ml of eluent.

NaCN, M	Au, mg/L	Cu, mg/L	Au Elution, %	Cu Elution, %
0	0	3.57	0	1.79
0.2	0	138	0	69.27
0.4	0	166	0	80.98
0.8	0	165	0	80.49

C4.8 Elution of Au

Experimental conditions: pH = 11.5, 60°C; Resin loadings: ~3900 g/t Cu, 2,160 g/t Au, resin mass = 1.38g, 100 ml of eluent

$[CS(NH_2)_2]$, M	H_2SO_4, M	Au, mg/L	Cu, mg/L	Au Elution, %	Cu_a Elution, %
0	0.5	0	16.86	0	89.2
0.2	0.5	29.14	36.048	97.47	98.56
0.5	0.5	29.67	36.991	99.22	99.02
1	0.5	29.61	37.4625	99.05	99.25
$[SCN^-]$, M	**NaOH, g/L**	**Au, mg/L**	**Cu, mg/L**	**Au Elution, %**	**Cu_a Elution, %**
0	1.5	0.00	0.13	0	81.04
1	1.5	26.14	33.36	87.44	97.25
2.5	1.5	28.84	37.52	96.44	99.28
5	1.5	28.99	36.93	96.97	98.99

C4.9 Resin reuse

Adsorption conditions: 12 ppm [Au], 1000 mg/L $[Cu_T]$,$[Cu_T]$:$[CN^-]$:[Gly] =1:1:3, pH =10.5, resin dosage = 6 g/L, room temperature. Elution conditions: 1st stage elution with 0.4M NaCN at pH 11.5 and room temperature; 2nd stage elution with 0.5M Thiourea/0.5M H_2SO_4, or 2.5M Thiocyanate at pH 11.5 at 55℃.

Eluent: 0.5M Thiourea/0.5M H_2SO_4				
Adsorption cycle	Au adsorption capacity, mg/g	RE, %	Cu adsorption capacity, mg/g	RE, %
1	1.84		10.36	
2	1.82	98.91	5.47	52.80
3	2.10	115.38	5.25	95.98
Cu pre-elution cycle	Au E%	Residual Au, g/t	Cu E%	Residual Cu, g/t

1	0.00	1.84	80.70	1998.69
2	0.00	1.82	80.00	1697.99
3	0.00	2.10	75.53	1584.16
Au elution cycle	Au E%	Residual Au, g/t	Cu *E%	Residual Cu, g/t
1	98.61	25.44	94.55	109.02
2	97.72	41.51	95.56	75.47
3	97.86	43.41	97.12	45.70

Eluent: 2.5M Thiocyanate/1.5g/L NaOH				
Adsorption cycle	Au adsorption capacity, mg/g	RE, %	Cu adsorption capacity, mg/g	RE, %
1	1.76		12.14	
2	2.23	127.02	12.61	103.89
3	2.22	99.29	9.61	76.23
Cu pre-elution cycle	Au E%	Residual Au, g/t	Cu E%	Residual Cu, g/t
1	0.00	1.84	77.71	2705.52
2	0.00	1.82	74.30	3240.92
3	0.00	2.10	69.96	2888.34
Au elution cycle	Au E%	Residual Au, g/t	Cu *E%	Residual Cu, g/t
1	96.71	25.44	96.15	104.06
2	97.96	41.51	93.98	195.24
3	98.19	43.41	93.15	197.83

Appendix D Copyright Permission

Dear Dr Deng,

Thank you for your e-mail that was forwarded to us and apologies for the delayed response.

We wish to advise that as an author of the article, you have retained the right to include the journal article, in full or in part, in a thesis or dissertation.

As an author, you retain rights for a large number of author uses, including use by your employing institute or company. These rights are retained and permitted without the need to obtain specific permission from Elsevier

These include:
The right to make copies of the article for your own personal use, including for your own classroom teaching use.

The right to make copies and distribute copies (including through e-mail) of the article to research colleagues, for the personal use by such colleagues (but not commercially or systematically, e.g. via an e mail list or list serve).

The right to present the article at a meeting or conference and to distribute copies of such paper or article to the

delegates attending the meeting.

The right to include the article in full or in part in a thesis or dissertation (provided that this is not to be published

commercially).

The right to use the article or any part there of in a printed compilation of works of the author, such as collected writings or lecture notes (subsequent to publication of the article in the journal).

The right to prepare other derivative works, to extend the article into book-length form, or to otherwise re-use portions or excerpts in other works, with full acknowledgement of its original publication in the journal.

For more information, please refer to the author's rights via the link below:
https://service.elsevier.com/app/answers/detail/a_id/565/supporthub/generic/

If I can be any further assistance, please do not hesitate to contact us again.

Kind regards,

Aireen Altiche
Researcher Support
ELSEVIER

Bibliography

Acharya, J., Sahu, J. N., Mohanty, C. R., & Meikap, B. C. (2009). Removal of lead(II) from wastewater by activated carbon developed from Tamarind wood by zinc chloride activation. *Chemical Engineering Journal, 149*(1), 249-262. https://doi.org/10.1016/j.cej.2008.10.029

Adams, M. D. (2016). *Gold ore processing: project development and operations / edited by Mike D. Adams* (2nd ed.): Amsterdam, [Netherlands]: Elsevier.

Adams, M., Lawrence, R., & Bratty, M. (2008). Biogenic sulphide for cyanide recycle and copper recovery in gold–copper ore processing. *Minerals Engineering, 21*(6), 509-517. https://doi.org/10.1016/j.mineng.2008.02.001

Agrawal, S., Guest, J. S., & Cusick, R. D. (2018). Elucidating the impacts of initial supersaturation and seed crystal loading on struvite precipitation kinetics, fines production, and crystal growth. *Water Research, 132*, 252-259. https://doi.org/10.1016/j.watres.2018.01.002

Akpen, G., Aho, M., & Mamwan, M. (2018). Equilibrium and kinetics of colour adsorption from textile wastewater by a novel adsorbent. *Global Journal of Pure and Applied Sciences, 24*(1), 61-67. https://doi.org/10.4314/gipas.v24i1.7

Aksu, S., & Doyle, F. (2001). Electrochemistry of copper in aqueous glycine solutions. *J. Electrochem. Soc., 148*(1), B51-B57.

Al-Tarazi, M., Heesink, A. B. M., Versteeg, G. F., Azzam, M. O. J., & Azzam, K. (2005). Precipitation of CuS and ZnS in a bubble column reactor. *AIChE Journal, 51*(1), 235-246. https://doi.org/10.1002/aic.10310

Alexandratos, S. D. (2009). Ion-Exchange resins: A retrospective from industrial and engineering chemistry research. *Industrial and Engineering Chemistry Research, 48*(1), 388-398. https://doi.org/10.1021/ie801242v

Alodan, M., & Smyrl, W. (1998). Effect of thiourea on copper dissolution and deposition. *Electrochimica Acta, 44*(2), 299-309. https://doi.org/10.1016/S0013-4686(98)00060-7

Alonso-González, O., Nava-Alonso, F., Jimenez-Velasco, C., & Uribe-Salas, A. (2013). Copper cyanide removal by precipitation with quaternary ammonium salts. *Minerals Engineering, 42*, 43-49. doi:10.1016/j.mineng.2012.11.013

Anonymous, 2003. Caledonia shows multi-commodity promise. Mining Mirror September, 10-15.

Anonymous. (2016). Green vehicles could drive copper boom; Electric vehicles require more copper. *Mining Engineering, 68*(12), 18.

Aylmore, M. (2016a). Alternative lixiviants to cyanide for leaching gold ores. In M.D Adams (Ed.), *Gold Ore Processing* (2nd ed., pp 447-484). Elsevier B.V.

Aylmore, M. (2016b). Thiosulfate as an alternative lixiviant to cyanide for gold ores. In M.D Adams (Ed.), *Gold Ore Processing* (2nd ed., pp 485-523). Elsevier B.V.

Aylmore, M. G. (2005). Alternative lixiviants to cyanide for leaching gold ores. In M.D Adams (Ed.), *Gold Ore Processing* (1st ed., pp 501-539). Elsevier B.V.

Aylmore, M. G., & Muir, D. M. (2001). Thiosulfate leaching of gold—A review. *Minerals Engineering, 14*(2), 135-174. https://doi.org/10.1016/S0892-6875(00)00172-2

Bailey, P. R. (1987). Application of Activated Carbon to Gold Recovery. (Retroactive Coverage). *South African Institute of Mining and Metallurgy, The Extractive Metallurgy of Gold in South Africa. Vol. 1, pp. 379-614, 1987*, 379-614.

Bansal, R. C., & Goyal, M. (2005). Activated carbon adsorption / Roop Chand Bansal, Meenakshi Goyal: Boca Raton : Taylor & Francis.

Beckmann, W. (2013). Crystallization: Basic Concepts and Industrial Applications (1. Aufl.1st ed.). Weinheim: Weinheim: Wiley-VCH.

Ben, S., Jeff, B., & Stephen, L., Brooy. (2017). Gold recovery via ion exchange resins. In ALTA 2017, Gold-PM Proceedings, Perth, Australia.

Bleam, W. (2017). Chapter 5 - Water Chemistry. In W. Bleam (Ed.), *Soil and Environmental Chemistry (2nd Edition)* (pp. 189-251): Academic Press.

Breuer, P. L., & Jeffrey, M. I. (2000). Thiosulfate leaching kinetics of gold in the presence of copper and ammonia. *Minerals Engineering, 13*(10), 1071-1081. https://doi.org/10.1016/S0892-6875(00)00091-1

Bruce, D. W., O'Hare, D., & Walton, R. I. (2013). Inorganic Materials Series Preface. *Structure from Diffraction Methods: Inorganic Materials Series*, xi-xii.

Cegłowski, M., & Schroeder, G. (2015). Preparation of porous resin with Schiff base chelating groups for removal of heavy metal ions from aqueous solutions. *Chemical Engineering Journal, 263*, 402-411. https://doi.org/10.1016/j.cej.2014.11.047

Chen, C.-Y., Chiang, C.-L., & Chen, C.-R. (2007). Removal of heavy metal ions by a chelating resin containing glycine as chelating groups. *Separation and Purification Technology, 54*(3), 396-403. https://doi.org/10.1016/j.seppur.2006.10.020

Chen, F., Zhao, X., Liu, H., & Qu, J. (2014). Reaction of $Cu(CN)_3^{2-}$ with H_2O_2 in water under alkaline conditions: Cyanide oxidation, Cu^+/Cu^{2+} catalysis and H_2O_2 decomposition. *Applied Catalysis B: Environmental, 158-159*(C), 85-90. https://doi.org/10.1016/j.apcatb.2014.04.010

Cheong, W. J., Yang, S. H., & Ali, F. (2013). Molecular imprinted polymers for separation science: A review of reviews. *Journal of Separation Science, 36*(3), 609-628. https://doi.org/10.1002/jssc.201200784

Chung, J., Jeong, E., Choi, J. W., Yun, S. T., Maeng, S. K., & Hong, S. W. (2015). Factors affecting crystallization of copper sulfide in fed-batch fluidized bed reactor. *Hydrometallurgy, 152*, 107-112. https://doi.org/10.1016/j.hydromet.2014.12.014

Ciglenečki, I., Krznarić, D., & Helz, G. R. (2005). Voltammetry of copper sulfide particles and nanoparticles: Investigation of the cluster hypothesis. *Environmental Science and Technology, 39*(19), 7492-7498. https://doi.org/10.1021/es050586v

Claflin, J.K., La Brooy, S.R., Preedy, D.R., Slater, A., Urutia, F., 2015. Fast payback reactivation of carbon from a flotation tails CIL circuit. In: Proceedings of the World Gold Conference 2015 (SAIMM Symposium Series S85). SAIMM, Johannesburg, pp. 337-348.

Conradie, P. J., Johns, M. W., & Fowles, R. J. (1995). Elution and electrowinning of gold from gold-selective strong-base resins. *Hydrometallurgy, 37*(3), 349-366. https://doi.org/10.1016/0304-386X(94)00032-X

Costello, M. (2016). Chapter 33 - Electrowinning. In M. D. Adams (Ed.), *Gold Ore Processing (2nd Edition)* (pp. 585-594): Elsevier.

Costello, M. C., Ritchie, I. C., & Lunt, D. J. (1992). Use of the ammonia cyanide leach system for gold copper ores with reference to the retreatment of the torco tailings. *Minerals Engineering, 5*(10), 1421-1429. https://doi.org/10.1016/0892-6875(92)90176-A

Dai, X., Breuer, P., Hewitt, D., & Bergamin, A. (2013). *Thiosulfate process for treating gold concentrates*. Paper presented at the World Gold 2013, Brisbane, Queensland, Australia.

Dai, X., Simons, A., & Breuer, P. (2011a). A review of copper cyanide recovery technologies for the cyanidation of copper containing gold ores. *Minerals Engineering*. https://doi.org/10.1016/j.mineng.2011.10.002

Dai, X., Simons, A., & Breuer, P. (2011b). A review of copper cyanide recovery technologies for the cyanidation of copper containing gold ores. *Minerals Engineering, 25*(1). https://doi.org/10.1016/j.mineng.2011.10.002

Davidson, R. J. (1974). The mechanism of gold adsorption on activated charcoal. Journal of the South African Institute of Mining and Metallurgy, 75(4), 67-76.

Davis, M., Sole, K., Mackenzie, J., & Virnig, M. (1998). *A proposed solvent extraction route for the treatment of copper cyanide solutions produced in leaching of gold ores.* ALTA 1998, Copper Hydrometallurgy Forum Proceedings, Perth, Australia.

Dean, J. A. (1990). Lange's handbook of chemistry. *Materials and Manufacturing Processes*, *5*(4), 687-688. https://doi.org/10.1080/10426919008953291

Deng, Z., Oraby, E. A., & Eksteen, J. J. (2019). The sulfide precipitation behaviour of Cu and Au from their aqueous alkaline glycinate and cyanide complexes. *Separation and Purification Technology, 218*, 181-190. https://doi.org/10.1016/j.seppur.2019.02.056

Deng, Z., Oraby, E. A., & Eksteen, J. J. (2020a). Cu adsorption behaviours onto chelating resins from glycine-cyanide solutions: Isotherms, kinetics and regeneration studies. *Separation and Purification Technology, 236*, 116280. https://doi.org/10.1016/j.seppur.2019.116280

Deng, Z., Oraby, E. A., & Eksteen, J. J. (2020b). Sulfide precipitation of copper from alkaline glycine-cyanide solutions: Precipitate characterisation. *Minerals Engineering, 145*, 106102. https://doi.org/10.1016/j.mineng.2019.106102

Deng, Z., Oraby, E. A., & Eksteen, J. J. (2020c). Gold recovery from cyanide-starved glycine solutions in the presence of Cu using a molecularly imprinted resin (IXOS-AuC). Hydrometallurgy, 196, 105425. https://doi.org/10.1016/j.hydromet.2020.105425

Din, S. U., Mahmood, T., Naeem, A., Hamayun, M., & Shah, N. S. (2017). Detailed kinetics study of arsenate adsorption by a sequentially precipitated binary oxide of iron and silicon. *Environmental Technology*, 1-9. https://doi.org/10.1080/09593330.2017.1385649

Diniz, C. V., Ciminelli, V. S. T., & Doyle, F. M. (2005). The use of the chelating resin Dowex M-4195 in the adsorption of selected heavy metal ions from manganese solutions. *Hydrometallurgy, 78*(3), 147-155. https://doi.org/10.1016/j.hydromet.2004.12.007

Donnet, M., Bowen, P., Jongen, N., Lemaître, J., & Hofmann, H. (2005). Use of seeds to control precipitation of calcium carbonate and determination of seed nature. *Langmuir, 21*(1), 100-108. https://doi.org/10.1021/la048525i

Dreisinger, D., Ji, J., & Wassink, B. (1995). The solvent extraction and electrowinning recovery of copper and cyanide using XI7950 extractant and membrane cell electrolysis. *Randol Gold Forum '95*, 239-244.

Dreisinger, D., Vaughan, J., Lu, J., Wassink, B., & West-Sells, P. (2008). Treatment of the Carmacks copper-gold ore by acid leaching and cyanide leaching with sart recovery of copper and cyanide from barren cyanide solution. Hydormetallurgy 2008, Proceedings of the 6th International Symposium, 740-749.

Du, T., Vijayakumar, A., & Desai, V. (2004). Effect of hydrogen peroxide on oxidation of copper in CMP slurries containing glycine and Cu ions. *Electrochimica Acta, 49*(25), 4505-4512. doi:10.1016/j.electacta.2004.05.008

Eksteen, J. J., & Oraby, E. A. (2015). The leaching and adsorption of gold using low concentration amino acids and hydrogen peroxide: Effect of catalytic ions, sulphide minerals and amino acid type. *Minerals Engineering, 70*, 36-42. https://doi.org/10.1016/j.mineng.2014.08.020

Eksteen, J. J., Oraby, E. A., & Tanda, B. C. (2017). A conceptual process for copper extraction from chalcopyrite in alkaline glycinate solutions. *Minerals Engineering, 108*, 53-66. https://doi.org/10.1016/j.mineng.2017.02.001

Eksteen, J. J., Oraby, E. A., Tanda, B. C., Tauetsile, P. J., Bezuidenhout, G. A., Newton, T., Bryan, I. (2018). Towards industrial implementation of glycine-based leach and adsorption technologies for gold-copper ores. *Canadian Metallurgical Quarterly, 57*(4), 390-398. https://doi.org/10.1080/00084433.2017.1391736

Eksteen, J. J., Pelser, M., Onyango, M. S., Lorenzen, L., Aldrich, C., & Georgalli, G. A. (2008). Effects of residence time and mixing regimes on the precipitation characteristics of CaF 2 and MgF 2 from high ionic strength sulphate solutions. *Hydrometallurgy, 91*(1), 104-112. https://doi.org/10.1016/j.hydromet.2007.12.002

Ertan, E., & Gülfen, M. (2009). Separation of gold(III) ions from copper(II) and zinc(II) ions using thiourea–formaldehyde or urea–formaldehyde chelating resins. *Journal of Applied Polymer Science, 111*(6), 2798-2805. https://doi.org/10.1002/app.29330

Estay, H. (2018). Designing the SART process – A review. *Hydrometallurgy, 176*, 147-165. https://doi.org/10.1016/j.hydromet.2018.01.011

Fang, Z., & Muhammed, M. (1992). Leaching of Precious Metals from Complex Sulphide Ores. On the Chemistry of Gold Lixiviation by Thiourea. *Mineral Processing and Extractive Metallurgy Review, 11*(1-2), 39-60. https://doi.org/10.1080/08827509208914213

Farahani, B. V., Rajabi, F. H., Bahmani, M., Ghelichkhani, M., & Sahebdelfar, S. (2014). Influence of precipitation conditions on precursor particle size distribution and activity of Cu/ZnO methanol synthesis catalyst. *Applied Catalysis A, General, 482*, 237-244. https://doi.org/10.1016/j.apcata.2014.05.034

Fisher, G.T., Lewis, R.G., Virnig, M.J., Mackenzie, J.M.W., Davis, M.R., 2000. Cognis AuRIX 100 resin for gold extraction, engineering cost study and pilot plant investigations. In: ALTA 2000 SX/IX-1. ALTA Metallurgical Services, Melbourne.

Fleming, C. A. (1998). *The potential role of anion exchange resins in the gold industry*. In EPD Congress 1998 (pp. 95-117).

Fleming, C. A., & Hancock, R. D. (1979). The mechanism in the poisoning of anion-exchange resins by cobalt cyanide. *Journal of the South African Institute of Mining and Metallurgy, 79*(11), 334-341.

Freitas, L. R., Trindade, R. B. E., & Carageorgos, T. (2001). *Thiosulfate leaching of gold-copper ores from Igarape Bahia mine (CVRD).* Paper presented at the Proceedings of the Sixth Southern Hemisphere Meeting on Mineral Technology.

Godfrey, J. C., & Slater, M. J. (1994). *Liquid-liquid extraction equipment / edited by J.C. Godfrey and M.J. Slater*. Chichester. New York: John Wiley & Sons.

González-López, J., Rodelas, B., Pozo, C., Salmerón-López, V., Martínez-Toledo, M. V., & Salmerón, V. (2005). Liberation of amino acids by heterotrophic nitrogen fixing bacteria. *Amino Acids, 28*(4), 363-367. https://doi.org/10.1007/s00726-005-0178-9

Gray, A., Hughes, T., & Abols, J. (2005). The use of AURIX®100 resin for the selective recovery of gold and silver from copper, gold and silver solutions. *Australasian Institute of Mining and Metallurgy Publication Series*.

Gray, S., Katsikaros, N., & Fallon, P. (1999). *Gold recovery from gold-copper gravity concentrates using the InLine Leach Reactor and weak-base resin.* Oretest Colloquium 1999; Scarborough, Western Australia; Australia, 67-79.

Groudev, S. N., Ivanov, I. M., Spasova, I. I., & Groudeva, V. I. (1995). Pilot scale microbial leaching of gold and silver from an oxide ore in Elshitza Mine, Bulgaria. Minerals Bioprocessing II; Snowbird, Utah; USA, 135-144.

Gylienė, O. (2001). Insoluble compounds of heavy metal complexes. Paper presented at the XVI-th ARS SEPARATORIA, Borówno, Poland.

Harland, C. E. (1994). *Ion-exchange: theory and practice / C. E. Harland* (2nd ed.). London: Royal Society of Chemistry.

Hilson, G., & Monhemius, A. J. (2006). Alternatives to cyanide in the gold mining industry: what prospects for the future? *Journal of Cleaner Production, 14*(12-13), 1158-1167. https://doi.org/10.1016/j.jclepro.2004.09.005

Hiskey, J. B., & Qi, P. H. (1991). *Leaching behaviour of gold in iodide solutions*. Paper presented at the World Gold '91, Melbourne.

Hodgkin, J. H., & Eibl, R. (1985). Copper selective chelating resins. *Reactive Polymers, Ion Exchangers, Sorbents, 3*(2), 83-89. https://doi.org/10.1016/0167-6989(85)90051-0

Horie, K., Barón, M., Fox, R., Hess, M., Kahovec, J., Kitayama, T., Work, W. (2010). Definitions of terms relating to reactions of polymers and to functional polymeric materials (IUPAC Recommendations 2003). *Pure and*

Applied Chemistry. Chimie Pure et Appliquee, 76(4), 889-906. https://doi.org/10.1351/pac200476040889

Houcine, I., Plasari, E., David, R., & Villermaux, J. (1997). Influence of Mixing Characteristics on the Quality and Size of Precipitated Calcium Oxalate in a Pilot Scale Reactor. *Chemical Engineering Research and Design, 75*(2), 252-256. https://doi.org/10.1205/026387697523534

Hu, Q., Meng, Y., Sun, T., Mahmood, Q., Wu, D., Zhu, J., & Lu, G. (2011). Kinetics and equilibrium adsorption studies of dimethylamine (DMA) onto ion-exchange resin. *Journal of Hazardous Materials, 185*(2), 677-681. https://doi.org/10.1016/j.jhazmat.2010.09.071

Hunt, B., 1901. U.S. Patent 689190.

Ilievski, D., & White, E. T. (1994). Agglomeration during precipitation: agglomeration mechanism identification for Al(OH) 3 crystals in stirred caustic aluminate solutions. *Chemical Engineering Science, 49*(19), 3227-3239. https://doi.org/10.1016/0009-2509(94)E0060-4

Jia, Y. F., Steele, C. J., Hayward, I. P., & Thomas, K. M. (1998). Mechanism of adsorption of gold and silver species on activated carbons. *Carbon, 36*(9), 1299-1308. https://doi.org/10.1016/S0008-6223(98)00091-8

Jiang, T., Zhang, Y.-z., Yang, Y.-b., & Huang, Z.-c. (2001). Influence of copper minerals on cyanide leaching of gold. *Science & Technology of Mining and Metallurgy, 8*(1), 24-28. https://doi.org/10.1007/s11771-001-0019-2

Kesler, S. E., Chryssoulis, S. L., & Simon, G. (2002). Gold in porphyry copper deposits: its abundance and fate. *Ore Geology Reviews, 21*(1), 103-124. https://doi.org/10.1016/S0169-1368(02)00084-7

Kharaka, Y. K., Law, L. M., Carothers, W. W., & Goerlitz, D. F. (1986). Role of organic species dissolved in formation waters from sedimentary basins in mineral diagenesis. In D. L. Gautier (Ed.), *Roles of organic matter in sediment diagenesis* (pp. 111-122), SEPM Society for Sedimentary Geology。

Kim, H., G. Eggert, R., W. Carlsen, B., & W. Dixon, B. (2016). Potential uranium supply from phosphoric acid: A U.S. analysis comparing solvent extraction and Ion exchange recovery. *Resources Policy, 49*(C), 222-231. https://doi.org/10.1016/j.resourpol.2016.06.004

Kononova, O., Kuznetsova, M., Mel'nikov, A., Karplyakova, N., & Kononov, Y. (2014). Sorption recovery of copper (II) and zinc (II) from chloride aqueous solutions. *Journal of the Serbian Chemical Society, 79*, 1037-1049. https://doi.org/10.2298/JSC130911033K

Kotze, M., Green, B., Mackenzie, J., & Virnig, M. (2005). Resin-in-pulp and resin-in-solution. *Developments in Mineral Processing, 15*(C), 603-635. https://doi.org/10.1016/S0167-4528(05)15025-X

Kotze, M., Green, B., Mackenzie, J., & Virnig, M. (2016). Chapter 32 - Resin-in-Pulp and Resin-in-Solution. In M. D. Adams (Ed.), *Gold Ore Processing (2nd Edition)* (pp. 561-583): Elsevier.

Krishnamurthy, G. T. (2009). *Nuclear Hepatology: A Textbook of Hepatobiliary Diseases / by Gerbail T. Krishnamurthy, S. Krishnamurthy*. Berlin, Heidelberg: Berlin, Heidelberg: Springer Berlin Heidelberg.

La Brooy, S. R., Komosa, T., & Muir, D. M. (1991). *Selective leaching of gold from copper-gold ores using ammonia-cyanide mixtures*. AusIMM, the 5th Extractive Metallurgy Conference, Perth, Australia.

La Brooy, S. R., Linge, H. G., & Walker, G. S. (1994). Review of gold extraction from ores. *Minerals Engineering, 7*(10), 1213-1241. https://doi.org/10.1016/0892-6875(94)90114-7

Lacoste-Bouchet, P., Deschênes, G., & Ghali, E. (1998). Thiourea leaching of a copper-gold ore using statistical design. *Hydrometallurgy, 47*(2), 189-203. https://doi.org/10.1016/S0304-386X(97)00043-1

Lakshmanan, V. I. e., Roy, R. e., & Ramachandran, V. e. (2016). *Innovative Process Development in Metallurgical Industry: Concept to Commission / edited by Vaikuntam Iyer Lakshmanan, Raja Roy, V. Ramachandran* (1st ed. 2016.. ed.): Cham : Springer International Publishing : Imprint: Springer.

Langhans, J. W., Lei, K. P. V., & Carnahan, T. G. (1992). Copper-catalyzed thiosulfate leaching of low-grade gold ores. *Hydrometallurgy, 29*(1-3), 191-203. https://doi.org/10.1016/0304-386X(92)90013-P

Lehto, J., Paajanen, A., Harjula, R., & Leinonen, H. (1994). Hydrolysis and H^+ Na^+ exchange by Chelex 100 chelating resin. *Reactive Polymers, 23*(2), 135-140. https://doi.org/10.1016/0923-1137(94)90013-2

Leinonen, H., & Lehto, J. (2000). Ion-exchange of nickel by iminodiacetic acid chelating resin Chelex 100. *Reactive and Functional Polymers, 43*(1), 1-6. https://doi.org/10.1016/S1381-5148(98)00082-0

Lekkerkerker, H. N. W. (2011). *Colloids and the Depletion Interaction / by Henk N.W. Lekkerkerker, Remco Tuinier*. Dordrecht: Dordrecht : Springer Netherlands.

Lewis, G.V., (2000). *"The Penjom Process" an innovative approach to extracting gold from carbonaceous ore.* Gold Processing in the 21st Century, An International Forum. AJ Parker Cooperative Research Centre for Hydrometallurgy, Perth, Australia.

Lewis, A., & van Hille, R. (2006). An exploration into the sulphide precipitation method and its effect on metal sulphide removal. *Hydrometallurgy, 81*(3), 197-204. https://doi.org/10.1016/j.hydromet.2005.12.009

Lewis, A. E. (2010). Review of metal sulphide precipitation. *Hydrometallurgy, 104*(2), 222-234. https://doi.org/10.1016/j.hydromet.2010.06.010

Li, H., Oraby, E., & Eksteen, J. (2020). Extraction of copper and the co-leaching behaviour of other metals from waste printed circuit boards using alkaline glycine solutions. *Resources, Conservation & Recycling, 154*. https://doi.org/10.1016/j.resconrec.2019.104624

Li, W., Zhang, Y., Liu, T., Huang, J., & Wang, Y. (2013). Comparison of ion exchange and solvent extraction in recovering vanadium from sulfuric acid leach solutions of stone coal. *Hydrometallurgy, 131-132*, 1-7. https://doi.org/10.1016/j.hydromet.2012.09.009

Liang, C. J., & Li, J. Y. (2019). Recovery of gold in iodine-iodide system - a review. *Separation Science and Technology, 54*(6), 1055-1066. doi:10.1080/01496395.2018.1523931

Lin, L.-C., & Juang, R.-S. (2005). Ion-exchange equilibria of Cu(II) and Zn(II) from aqueous solutions with Chelex 100 and Amberlite IRC 748 resins. *Chemical Engineering Journal, 112*(1-3), 211-218. https://doi.org/10.1016/j.cej.2005.07.009

Ling, C., Liu, F.-Q., Long, C., Wei, M.-M., & Li, A. (2014). Highly efficient co-removal of copper (II) and phthalic acid with self-synthesized polyamine resin. *Water science and technology: a journal of the International Association on Water Pollution Research, 69*(9), 1879. https://doi.org/10.2166/wst.2014.082

Linga, Å. (2017). Effects of Seeding on the Crystallization Behaviour and Filtration Abilities of an Aromatic Amine. [Master's thesis, NTNU]. https://ntnuopen.ntnu.no/ntnu-xmlui/handle/11250/2461109

Littlejohn, P., Kratochvil, D., & Hall, A. (2013). *Sulfidisation-acidification-recycling-thickening (SART) for complex gold ores*. World Gold 2013, Brisbane, Australia.

Liu, F., Li, L., Ling, P., Jing, X., Li, C., Li, A., & You, X. (2011). Interaction mechanism of aqueous heavy metals onto a newly synthesized IDA-chelating resin: Isotherms, thermodynamics and kinetics. *Chemical Engineering Journal, 173*(1), 106-114. https://doi.org/10.1016/j.cej.2011.07.044

Maliyekkal, S. M., Shukla, S., Philip, L., & Nambi, I. M. (2008). Enhanced fluoride removal from drinking water by magnesia-amended activated alumina granules. *Chemical Engineering Journal, 140*(1), 183-192. https://doi.org/10.1016/j.cej.2007.09.049

Malla, M. E., Alvarez, M. B., & Batistoni, D. A. (2002). Evaluation of sorption and desorption characteristics of cadmium, lead and zinc on Amberlite IRC-718 iminodiacetate chelating ion exchanger. *Talanta, 57*(2), 277-287. https://doi.org/10.1016/S0039-9140(02)00034-6

Marcant, B., & David, R. (1991). Experimental evidence for and prediction of micromixing effects in precipitation. *AIChE Journal, 37*(11), 1698-1710. https://doi.org/10.1002/aic.690371113

Marsden, J. O. (2009). *Chemistry of Gold Extraction* (2nd ed.). Littleton: Littleton: SME.

Marsden, J. O., & House, C. I. (2009). *Chemistry of Gold Extraction* (2nd ed.). Littleton: Littleton: SME.

Marsh, H. (2006). *Activated carbon / Harry Marsh, Francisco Rodríguez-Reinoso* (1st ed.). Amsterdam. London : Elsevier.

McDougall, G. J. H. R. D. N. M. J. W. O. L., & Copperthwaite, R. G. (1980). The mechanism of the adsorption of gold cyanide on activated carbon. *Journal of the South African Institute of Mining and Metallurgy, 80*(9), 344-356.

Meenakshi, S., & Viswanathan, N. (2007). Identification of selective ion-exchange resin for fluoride sorption. *Journal of Colloid And Interface Science, 308*(2), 438-450. https://doi.org/10.1016/j.jcis.2006.12.032

Mersmann, A. (1999). Crystallization and precipitation. *Chemical Engineering & Processing: Process Intensification, 38*(4), 345-353. https://doi.org/10.1016/S0255-2701(99)00025-2

Mokone, T. P., van Hille, R. P., & Lewis, A. E. (2010). Effect of solution chemistry on particle characteristics during metal sulfide precipitation. *Journal of Colloid And Interface Science, 351*(1), 10-18. https://doi.org/10.1016/j.jcis.2010.06.027

Moreno, J., & Peinado, R. (2012). Chapter 15 - Precipitation Equilibria in Wine. In J. Moreno & R. Peinado (Eds.), *Enological Chemistry* (pp. 253-269). San Diego: Academic Press.

Mpinga, C. N., Eksteen, J. J., Aldrich, C., & Dyer, L. (2018). A conceptual hybrid process flowsheet for platinum group metals (PGMs) recovery from a chromite-rich Cu-Ni PGM bearing ore in oxidized mineralization through a single-stage leach and adsorption onto ion exchange resin. *Hydrometallurgy, 178*, 88-96. https://doi.org/10.1016/j.hydromet.2018.03.024

Muir, D. M. (2011). A review of the selective leaching of gold from oxidised copper–gold ores with ammonia–cyanide and new insights for plant control and operation. *Minerals Engineering, 24*(6), 576-582. https://doi.org/10.1016/j.mineng.2010.08.022

Muir, D. M., La Brooy, S. R., & Cao, C. (1989). *Recovery of copper from copper bearing ores*. Paper presented at the World Gold '89, Warrendale.

Muir, D. M., Vukcevic, S., & Shuttleworth, J. (1995). *Optimising the ammonia–cyanide process for copper–gold ores.* Paper presented at the Proceedings Randol Gold Forum, Perth.

Muraviev, D. (2000). *Ion exchange / edited by Dimitri Muraviev, Vladimir Gorshkov, Abraham Warshawsky*. New York: New York : M. Dekker.

Neto, I. F. F., Sousa, C. A., Brito, M. S. C. A., Futuro, A. M., & Soares, H. M. V. M. (2016). A simple and nearly-closed cycle process for recycling copper with high purity from end life printed circuit boards. *Separation and Purification Technology, 164*(C), 19-27. https://doi.org/10.1016/j.seppur.2016.03.007

Nicol, M. J., Fleming, C.A., amp, & Cromberge, G. (1984). The absorption of gold cyanide onto activated carbon. II. Application of the kinetic model to multistage absorption circuits. *Journal of the South African Institute of Mining and Metallurgy, 84*(3), 70-78.

O'Connor, G. M., Lepkova, K., Eksteen, J. J., & Oraby, E. A. (2018). Electrochemical behaviour of copper in alkaline glycine solutions. *Hydrometallurgy, 181*, 221-229. https://doi.org/10.1016/j.hydromet.2018.10.001

Oraby, E. A., & Eksteen, J. J. (2014b). The selective leaching of copper from a gold–copper concentrate in glycine solutions. *Hydrometallurgy, 150*, 14-19. https://doi.org/10.1016/j.hydromet.2014.09.005

Oraby, E. A., & Eksteen, J. J. (2015a). Gold leaching in cyanide-starved copper solutions in the presence of glycine. *Hydrometallurgy, 156*, 81-88. https://doi.org/10.1016/j.hydromet.2015.05.012

Oraby, E. A., & Eksteen, J. J. (2015b). The leaching of gold, silver and their alloys in alkaline glycine–peroxide solutions and their adsorption on carbon. *Hydrometallurgy, 152*(C), 199-203. https://doi.org/10.1016/j.hydromet.2014.12.015

Oraby, E. A., & Eksteen, J. J. (2015c). The leaching of gold, silver and their alloys in alkaline glycine–peroxide solutions and their adsorption on carbon. *Hydrometallurgy, 152*, 199-203. https://doi.org/10.1016/j.hydromet.2014.12.015

Oraby, E. A., Eksteen, J. J., Karrech, A., & Attar, M. (2019). Gold extraction from paleochannel ores using an aerated alkaline glycine lixiviant for consideration in heap and in-situ leaching applications. *Minerals Engineering, 138*, 112-118. https://doi.org/10.1016/j.mineng.2019.04.023

Oraby, E. A., Eksteen, J. J., & Tanda, B. C. (2017). Gold and copper leaching from gold-copper ores and concentrates using a synergistic lixiviant mixture of glycine and cyanide. *Hydrometallurgy, 169*, 339-345. https://doi.org/10.1016/j.hydromet.2017.02.019

Oraby, E. A., Li, H., & Eksteen, J. J. (2019). An Alkaline Glycine-Based Leach Process of Base and Precious Metals from Powdered Waste Printed Circuit Boards. *Waste and Biomass Valorization*. https://doi.org/10.1007/s12649-019-00780-0

Oshita, K., & Motomizu, S. (2008). Development of chelating resins and their ability of collection and separation for metal ions. In *Bunseki Kagaku* (Vol. 57, pp. 291-311).

Pakiari, A. H., & Jamshidi, Z. (2007). Interaction of amino acids with gold and silver clusters. *The journal of physical chemistry. A, 111*(20), 4391-4396. https://doi.org/10.1021/jp070306t

Park, S., Lee, K.-S., Bozoklu, G., Cai, W., Nguyen, S. T., & Ruoff, R. S. (2008). Graphene oxide papers modified by divalent ions-enhancing mechanical properties via chemical cross-linking. *ACS nano, 2*(3), 572. https://doi.org/10.1021/nn700349a

Patel, D. D., & Anderson, B. D. (2013). Maintenance of supersaturation II: Indomethacin crystal growth kinetics versus degree of supersaturation. *Journal of Pharmaceutical Sciences, 102*(5), 1544-1553. https://doi.org/10.1002/jps.23498

Pian, H., & Santosh, M. (2019). Gold deposits of China: Resources, economics, environmental issues, and future perspectives. *Geological Journal*. 1-12. https://doi.org/10.1002/gj.3531

Riley, A. L., Pepper, S. E., Canner, A. J., Brown, S. F., & Ogden, M. D. (2018). Metal recovery from jarosite waste – A resin screening study. *Separation Science and Technology, 53*(1), 22-35. doi:10.1080/01496395.2017.1378679

Ritz, S., Gluckman, J., Southard, G., Maull, B., & Kim, D. J. (2018). *Imprinted Resin—The 21st Century Adsorbent.* Extraction 2018, Proceedings of the 1st Global Conference on Extactive Metallurgy, Ottawa, Canada.

Roy, P., & Srivastava, S. K. (2007). Low-temperature synthesis of CuS nanorods by simple wet chemical method. *Materials Letters, 61*(8), 1693-1697. https://doi.org/10.1016/j.matlet.2006.07.101

Ruane, M. (1991). *Gold recovery from the Paris mine tailings using ammoniacal cyanide leachant*. Processing of Gold–Copper Ores Colloquium, Perth, Australia.

Rydberg, J. (2004). *Solvent extraction principles and practice / edited by Jan Rydberg .[et al.]* (2nd ed.). New York: M. Dekker.

Saçmaci, Ş., Saçmaci, M., Soykan, C., & Kartal, Ş. (2010). Synthesis and Characterization of New Chelating Resin: Adsorption Study of Copper(II) and Chromium (III) Ions. *Journal of Macromolecular Science, Part A, 47*(6), 552-557. https://doi.org/10.1080/10601321003742055

Sampaio, R. M. M., Timmers, R. A., Kocks, N., André, V., Duarte, M. T., van Hullebusch, E. D., Lens, P. N. L. (2010). Zn–Ni sulfide selective precipitation: The role of supersaturation. *Separation and Purification Technology, 74*(1), 108-118. https://doi.org/10.1016/j.seppur.2010.05.013

Sampaio, R. M. M., Timmers, R. A., Xu, Y., Keesman, K. J., & Lens, P. N. L. (2009). Selective precipitation of Cu from Zn in a pS controlled continuously stirred tank reactor. *Journal of Hazardous Materials, 165*(1), 256-265. https://doi.org/10.1016/j.jhazmat.2008.09.117

Sceresini, B. (2005). Gold-Copper Ores. In D. A. M. B. A. Wills (Ed.), *Developments in Mineral Processing* (Vol. 15, pp. 789-824): Elsevier.

Sceresini, B., & Breuer, P. (2016). Chapter 43 - Gold-Copper Ores. In M. D. Adams (Ed.), *Gold Ore Processing (2nd Edition)* (pp. 771-801): Elsevier.

Sceresini, B., & Staunton, W. P. (1991). *Copper/cyanide in the treatment of high copper gold ores.* The 5th AusIMM Extractive Metallurgy Conference, Perth, Australia.

Schwarzenbach, G. (1952). Der Chelateffekt. *35*(7), 2344-2359. https://doi.org/10.1002/hlca.19520350721

Sengupta, A. K., Zhu, Y., & Hauze, D. (1991). Metal (II) ion binding onto chelating exchangers with nitrogen donor atoms: Some new observations and related implications. *Environmental Science and Technology, 25*(3). https://doi.org/10.1021/es00015a016

Shaofeng, L., & Shuixing, F. (2016). A research review of iron oxide copper‐gold deposits. *Acta Geologica Sinica - English Edition, 90*(4), 1341-1352. https://doi.org/10.1111/1755-6724.12773

Sillitoe, R. H., & Meinert, L. D. (2010). Porphyry copper systems. *Economic Geology and the Bulletin of the Society of Economic Geologists, 105*(1), 3-41. https://doi.org/10.2113/gsecongeo.105.1.3

Simons, A., & Breuer, P. (2011). *The effect of process variables on cyanide and copper recovery using SART*. ALTA 2011, Gold Procceedings, Perth, Australia.

Simons, A., Breuer, P., & Browner, R. (2015). *The impact of metal cyanide species on the recovery of cyanide and copper using SART*. Paper presented at the World Gold 2015, Misty Hills, Gauteng, South Africa.

Slund, B. L. Å., & Rasmuson, Å. K. C. (1992). Semibatch reaction crystallization of benzoic acid. *AIChE Journal, 38*(3), 328-342. https://doi.org/10.1002/aic.690380303

Söhnel, O., & Garside, J. (1992). *Precipitation: basic principles and industrial applications / Otakar Söhnel and John Garside*. Oxford [England]. Boston : Butterworth-Heinemann.

Song, W., Gao, B., Xu, X., Xing, L., Han, S., Duan, P., . . . Jia, R. (2016). Adsorption–desorption behavior of magnetic amine/Fe3O4 functionalized biopolymer resin towards anionic dyes from wastewater. *Bioresource Technology, 210*, 123-130. https://doi.org/10.1016/j.biortech.2016.01.078

Sparrow, G. J., & Woodcock, J. T. (1995). Cyanide and Other Lixiviant Leaching Systems for Gold with Some Practical Applications. *Mineral Processing and Extractive Metallurgy Review, 14*(3-4), 193-247. https://doi.org/10.1080/08827509508914125

Stace, C. R. (1984). *Selective Passivation of Sulfides*. Technical report, No R84/043, CRA Services Ltd Research, Cockle Creek.

Staunton, W. P. (2016). Chapter 30 - Carbon-in-Pulp. In M. D. Adams (Ed.), *Gold Ore Processing (2nd Edition)* (pp. 535-552): Elsevier.

Tanda, B., Eksteen, J., & Oraby, E. (2018). Kinetics of chalcocite leaching in oxygenated alkaline glycine solutions. *Hydrometallurgy, 178*, 264-273. https://doi.org/10.1016/j.hydromet.2018.05.005

Tanda, B. C. (2017). *Glycine as a lixiviant for the leaching of low grade copper-gold ores* [Dotoral thesis, Curtin University].

Tanda, B. C., Eksteen, J. J., & Oraby, E. A. (2017). An investigation into the leaching behaviour of copper oxide minerals in aqueous alkaline glycine solutions. *Hydrometallurgy, 167*, 153-162. https://doi.org/10.1016/j.hydromet.2016.11.011

Tanda, B. C., Eksteen, J. J., Oraby, E. A., & O'Connor, G. M. (2019). The kinetics of chalcopyrite leaching in alkaline glycine/glycinate solutions. *Minerals Engineering, 135*, 118-128. https://doi.org/10.1016/j.mineng.2019.02.035

Tanda, B. C., Oraby, E. A., & Eksteen, J. J. (2017). Recovery of copper from alkaline glycine leach solution using solvent extraction. *Separation and Purification Technology, 187*, 389-396. https://doi.org/10.1016/j.seppur.2017.06.075

Tanda, B. C., Oraby, E. A., & Eksteen, J. J. (2018). Kinetics of malachite leaching in alkaline glycine solutions. *Mineral Processing and Extractive Metallurgy: Transactions of the Institute of Mining and Metallurgy*, 128(1). https://doi.org/10.1080/25726641.2018.1505211

Tauetsile, P., Oraby, E., & Eksteen, J. (2018). Adsorption behaviour of copper and gold Glycinates in alkaline media onto activated carbon. Part 2: Kinetics. *Hydrometallurgy, 178*, 195-201. https://doi.org/10.1016/j.hydromet.2018.04.016

Tauetsile, P. J. (2019). *Adsorption of gold and copper from alkaline glycine-based leach solutions using activated carbon* [Dotoral thesis, Curtin University].

Tauetsile, P. J., Oraby, E. A., & Eksteen, J. J. (2018a). Adsorption behaviour of copper and gold glycinates in alkaline media onto activated carbon. Part 1: Isotherms. *Hydrometallurgy, 178*, 202-208. https://doi.org/10.1016/j.hydromet.2018.04.015

Tauetsile, P. J., Oraby, E. A., & Eksteen, J. J. (2018b). Adsorption behaviour of copper and gold Glycinates in alkaline media onto activated carbon. Part 2: Kinetics. *Hydrometallurgy, 178*, 195-201. https://doi.org/10.1016/j.hydromet.2018.04.016

Tauetsile, P. J., Oraby, E. A., & Eksteen, J. J. (2019a). Activated carbon adsorption of gold from cyanide-starved glycine solutions containing copper. Part 1: Isotherms. *Separation and Purification Technology, 211*, 594-601. https://doi.org/10.1016/j.seppur.2018.09.024

Tauetsile, P. J., Oraby, E. A., & Eksteen, J. J. (2019b). Activated carbon adsorption of gold from cyanide-starved glycine solutions containing copper. Part 2: Kinetics. *Separation and Purification Technology, 211*, 290-297. doi:10.1016/j.seppur.2018.09.022

Tauetsilea, P. J., Oraby, E. A., & Eksteen, J. J. (2018). Activated carbon adsorption of gold from cyanide-starved glycine solutions containing copper. Part 1: Isotherms.

Torbacke, M., & Rasmuson, Å. C. (2001). Influence of different scales of mixing in reaction crystallization. *Chemical Engineering Science, 56*(7), 2459-2473. https://doi.org/10.1016/S0009-2509(00)00452-8

Tran, T., Lee, K., & Fernando, K. (2001). Halide as an alternative lixiviant for gold processing - an update. In (pp. 501-508).

Tremblay, L., Deschênes, G., Ghali, E., McMullen, J., & Lanouette, M. (1996). Gold recovery from a sulphide bearing gold ore by percolation leaching with thiourea. *International Journal of Mineral Processing, 48*(3-4), 225-244. https://doi.org/10.1016/S0301-7516(96)00029-4

Van, D., Yahorava, V., & Kotze, M. (2012). *Gold Recovery from Copper-rich Ores Employing the Purolite S992 Gold Selective Ion Exchange Resin*. ALTA 2012, Gold Conference, Perth, Australia.

van Deventer, J. (2011). Selected ion exchange applications in the hydrometallurgical industry. *Solvent Extraction and Ion Exchange, 29*(5-6), 695-718. https://doi.org/10.1080/07366299.2011.595626

van Hille, R. P., A. Peterson, K., & Lewis, A. E. (2005). Copper sulphide precipitation in a fluidised bed reactor. *Chemical Engineering Science, 60*(10), 2571-2578. https://doi.org/10.1016/j.ces.2004.11.052

Veeken, A. H. M., de Vries, S., van Der Mark, A., & Rulkens, W. H. (2003). Selective precipitation of heavy metals as controlled by a sulfide-selective electrode. *Separation Science and Technology, 38*(1), 1-19. https://doi.org/10.1081/SS-120016695

Walton, R. (2016). Chapter 31 - Zinc Cementation. In M. D. Adams (Ed.), *Gold Ore Processing (2nd Edition)* (pp. 553-560): Elsevier.

Wang, J., Xu, L., Cheng, C., Meng, Y., & Li, A. (2012). Preparation of new chelating fiber with waste PET as adsorbent for fast removal of Cu2+ and Ni2+ from water: Kinetic and equilibrium adsorption studies. *Chemical Engineering Journal, 193-194*, 31-38. https://doi.org/10.1016/j.cej.2012.03.070

Wang, X., & Forssberg, K. S. E. (1990). The chemistry of cyanide-metal complexes in relation to hydrometallurgical processes of precious metals. *Mineral Processing and Extractive Metallurgy Review, 6*(1-4), 81-125. https://doi.org/10.1080/08827509008952658

Weber, J., & Morris, J. (1963). Kinetics of adsorption on carbon from solution. *Journal of the Sanitary Engineering Division, 89*(2), 31-60.

Wołowicz, A., & Hubicki, Z. (2010). Selective Adsorption of Palladium(II) Complexes onto the Chelating Ion Exchange Resin Dowex M 4195 - Kinetic Studies. *Solvent Extraction and Ion Exchange, 28*(1), 124-159. https://doi.org/10.1080/07366290903408953

Wołowicz, A., & Hubicki, Z. (2011). Investigation of macroporous weakly basic anion exchangers applicability in palladium(II) removal from acidic solutions – batch and column studies. *Chemical Engineering Journal, 174*(2), 510-521. https://doi.org/10.1016/j.cej.2011.08.075

Wołowicz, A., & Hubicki, Z. (2012). The use of the chelating resin of a new generation Lewatit MonoPlus TP-220 with the bis-picolylamine functional groups in the removal of selected metal ions from acidic solutions. *Chemical Engineering Journal, 197*, 493-508. https://doi.org/10.1016/j.cej.2012.05.047

Wong, S. Y., Myerson, A. S., & Cui, Y. (2013). Contact secondary nucleation as a means of creating seeds for continuous tubular crystallizers. *Crystal Growth and Design, 13*(6), 2514-2521. https://doi.org/10.1021/cg4002303

Xia, C., Yen, W., & Deschenes, G. (2003). Improvement of thiosulfate stability in gold leaching. *An Official International Peer-reviewed Journal of the Society, 20*(2), 68-72. https://doi.org/10.1007/BF03403135

Xiao-Hua, C., & Bing, X. (2013). Recent advances on asymmetric Strecker reactions. *Arkivoc, 2014*(1), 205. https://doi.org/10.3998/ark.5550190.p008.487

Xie, F., & Dreisinger, D. (2009a). Copper Solvent Extraction from Waste Cyanide Solution with LIX 7820. *Solvent Extraction and Ion Exchange, 27*(4), 459-473. doi:10.1080/07366290902966829

Xie, F., & Dreisinger, D. (2009b). Recovery of copper cyanide from waste cyanide solution by LIX 7950. *Minerals Engineering, 22*(2), 190-195. https://doi.org/10.1016/j.mineng.2008.07.001

Yan, M. (2004). *Molecularly Imprinted Materials* (1 ed.).

Zadra, J. B., Engel, A. L., Heinen, H. J., & United States. (1952). *Process for recovering gold and silver from activated carbon by leaching and electrolysis*. Washington, D.C.: U.S. Department of the Interior, Bureau of Mines.

Zainol, Z., & Nicol, M. J. (2009). Ion-exchange equilibria of Ni 2+, Co 2+, Mn 2+ and Mg 2+ with iminodiacetic acid chelating resin Amberlite IRC 748. *Hydrometallurgy, 99*(3), 175-180. https://doi.org/10.1016/j.hydromet.2009.08.004

Zhang, Y., Li, Y., Yang, L.-q., Ma, X.-j., Wang, L.-y., & Ye, Z.-F. (2010). Characterization and adsorption mechanism of Zn^{2+} removal by PVA/EDTA resin in polluted water. *Journal of Hazardous Materials, 178*(1), 1046-1054. https://doi.org/10.1016/j.jhazmat.2010.02.046

Zhu, W., Liu, J., & Li, M. (2014). Fundamental Studies of Novel Zwitterionic Hybrid Membranes: Kinetic Model and Mechanism Insights into Strontium Removal. *The Scientific World Journal, 2014*. https://doi.org/10.1155/2014/485820

Zhu, Z. (2016). Gold in iron oxide copper–gold deposits. *Ore Geology Reviews, 72*(1), 37-42. https://doi.org/10.1016/j.oregeorev.2015.07.001